Regulation of Cardiac Function by Nitric Oxide and Calcium/Calmodulin-dependent protein kinase II

Esther Udo Asamudo

Supervisor: Dr Jeffrey Erickson

A thesis submitted for the degree of Doctor of Philosophy at the University of Otago, Dunedin, New Zealand

April 2021

ABSTRACT

Nitric oxide (NO) is a gaseous signaling molecule that plays a role in cardiac contraction and relaxation. One of the pathways of NO signaling is through S-nitrosylation, which is the covalent attachment of a NO moiety to the thiol side chain of a cysteine residue. One downstream target of NO via S-nitrosylation is the calcium handling protein calcium-calmodulin dependent protein kinase II (CaMKII). There is evidence that the S-nitrosylation of CaMKII promotes calcium mishandling in cardiomyocytes, which is the precursor of cardiac arrhythmias. The role of CaMKII in the whole heart during NO exposure is yet to be understood. Therefore, the aim of this thesis was to determine how CaMKII modification by NO and β-adrenergic stimulation can affect cardiac contractility and arrhythmias.

With the use of echocardiography, cardiac function was compared between wild type (WT) mice and transgenic mice lacking cardiac CaMKIIδ (KO), and loss of CaMKIIδ did not severely alter cardiac structure and function. To determine if NO and CaMKIIδ did affect cardiac function, the hearts were isolated from the mice and treated with different concentrations of a NO donor (GSNO). GSNO reduced contractility measured as left ventricular (LV) developed pressure and increased heart rate in WT mice whereas KO mice showed no response to GSNO treatment. WT mice were susceptible to arrhythmias and the number of arrhythmic events increased with increasing GSNO concentration. There was no change in the number of arrhythmic events in the KO mouse hearts with GSNO treatment compared to baseline. Therefore, CaMKIIδ removal was cardioprotective, as it prevented arrhythmias during acute GSNO treatment.

Having established a role for CaMKII in determining the effects of acute NO treatment on cardiac function, I then focused on a model of chronically elevated NO. Chronic GSNO treatment of WT and KO mice involved a 5-week supplementation with GSNO in drinking water, followed by measurement of cardiac function in isolated hearts from these mice with and without GSNO. Echocardiographic data from WT and KO mice showed no effect of GSNO treatment after 5-week GSNO supplementation. The isolated hearts showed no difference in cardiac function at baseline. Following subsequent GSNO treatment, the LV developed pressure and rates of contraction and relaxation decreased compared to baseline in WT and KO hearts. Both animal models showed a trend towards

increased number of arrhythmic events, suggesting that knocking out CaMKIIδ from the heart did not prevent the KO hearts from developing arrhythmias in the chronic treatment compared to the acute treatment.

β-adrenergic stimulation using the β-adrenergic receptor agonist (ISO) enhanced cardiac contractility and arrhythmias in both WT and KO hearts. However, ISO induced an increase in arrhythmic events in WT hearts, but not in KO hearts, suggesting that the presence of CaMKII enhanced the susceptibility of WT hearts to ISO-induced cardiac stress. To determine the effect of NO treatment and β-adrenergic stimulation on cardiac function, WT hearts were treated with ISO and GSNO. There were two groups, ISO-GSNO (ISO before GSNO treatment) and GSNO-ISO (GSNO before ISO treatment). In both groups, ISO increased contraction and relaxation. GSNO did not alter cardiac contractility compared to baseline except in the ISO-GSNO group. ISO-GSNO induced cardiac arrhythmias, and GSNO treatment prolonged the arrhythmias. Interestingly, in the GSNO-ISO group, there was no increase in arrhythmic events compared to baseline. This finding provided evidence of a differential role of NO in the heart.

Overall, the findings in this thesis show, for the first time, CaMKII plays a role in the development of arrhythmias in the whole heart during NO signaling. Additionally, this thesis highlights the dual role of NO in preventing or prolonging cardiac arrhythmias during β-adrenergic stimulation.

MANUSCRIPT IN PREPARATION

Power, A. S., *Asamudo, E. U., Wallace, R., & J. Erickson. Nitric oxide attenuates spontaneous Ca^{2+} release and ventricular arrhythmias during β-adrenergic signaling in the mouse heart (Chapter 5).

*Work also contained in this thesis

Conference Abstracts

*Asamudo, E., Wallace, R., Power, A., & Erickson, J. (2020). 237 Modulation of CaMKIIδ Activity by Nitric Oxide can Promote or Prevent ß-adrenergic-Induced Cardiac Arrhythmias. *Heart, Lung and Circulation*, 29, S140. Abstract.

*Asamudo, E. U. & Erickson, J. R. (2019). S-Nitrosylation as a Post-Translational Modification of CaMKIIδ and its Effects on Cardiac Function. *Heart, Lung and Circulation*, 28, S228-S229. Abstract

Statement of contributions

I wrote part of the manuscript for the article above and did the presentations below. Data in Chapters 3, 4 and 5 were collected by me. I prepared cardiac tissue samples for S-nitrosylation experiments and biotin switch assay was performed by Dr Oby Ebenebe, Kohr Laboratory of Cardiovascular Redox Signaling, Johns Hopkins University, Baltimore, MD, USA. Statistical analysis was carried out by me.

PRESENTATIONS AND AWARDS

Asamudo, E. U. and Erickson, J. R. (2021) Nitric oxide influences cardiac arrhythmias through CaMKII pathway during stress. Oral presentation delivered at University of Otago Biomedical Science Research Symposium, Dunedin, New Zealand.

Asamudo, E. U. and Erickson, J. R. (2020) Modulation of CaMKII activity by nitric oxide can promote beta-adrenergic-induced cardiac arrhythmias. Oral presentation at CSANZ/ISHR Annual Scientific Meeting.
Conference grant awarded

Asamudo, E. U. and Erickson, J. R. (2020) The dual role of Nitric Oxide-mediated CaMKII activity during beta-adrenergic stimulation in the heart. Oral presentation at New Zealand Medical Sciences Congress.
PSNZ Mary Bullivant prize finalist

Asamudo, E. U. and Erickson, J. R. (2019) S-nitrosylation as a post-translational modification of CaMKIIδ and its effects on cardiac function. Oral presentation delivered at CSANZ/ISHR Annual Scientific Meeting, Adelaide, Australia.
Travel grant awarded

Asamudo, E. U. and Erickson, J. R. (2019) Modulation of cardiac protein kinase, CaMKIIδ by nitric oxide impairs cardiac function in mice. Poster presented at the University of Otago Postgraduate Research Symposium, Otago, New Zealand.

Asamudo, E. U. and Erickson, J. R. (2019) Acute S-nitrosylation of CaMKII and its effect on cardiac function. Poster presented at University of Otago Biomedical Science Research Symposium, Dunedin, New Zealand.

Asamudo, E. U. and Erickson, J. R. (2019) Acute S-nitrosylation of CaMKII and its effect on cardiac function. Oral presentation delivered at University of Otago Biomedical Science Research Symposium, Dunedin, New Zealand.

ACKNOWLEDGEMENTS

This thesis is dedicated to my parents, Udo and Naomi, who have both been a source of inspiration in my life, and contributed greatly towards my education. I am thankful to God for His grace that has kept me throughout this PhD journey, which has been a life changing experience for me and I am sincerely grateful that He blessed me with many people who all contributed in making this a success.

I would like to thank my supervisor, Dr Jeffrey Erickson, for granting me the opportunity to do my PhD in his lab and for the enormous support throughout my PhD study. For being a great mentor, cheerleader, helping me become a better communicator and encouraging me to stay positive through this journey, I am forever grateful. I want to thank my research committee chair, A/Prof Phil Sheard and my advisor, A/Prof Daryl Schwenke for ensuring I was making good progress and providing very valuable feedback on my reports. I thank A/Prof Rajesh Katare, A/Prof Regis Lamberts and Dr Carol Bussey for their training on the various techniques I required for my research work.

I thank Rachel Wallace for helping me in the lab, proof reading my thesis, listening to my Western blotting failure stories, sending me memes to make me smile, always happy to offer great feedback and for always reminding me it is alright to take a break as required. I hope we get to pick a “Rachel Day” just to celebrate your awesomeness and I will buy you a hat. To Dr Zoe Ashley, thank you for all the support, for feedback on my writing, for your help with the nitric oxide sensor. Thank you for making me reminding me to breath and that weekends are for resting. I thank Dr Amelia Power, you have been very helpful with troubleshooting my experimental techniques, proof reading my writing and always being there through my Langendorff experiment adventures. I thank Prof Fiona McDonald for always encouraging me with kind words and always showing concern about my progress. Thank you, Dr Tanya Cully, for sharing your protocol for s-nitrosylation experiments and tips for winging it during PhD, with me.

I also can’t fail to thank Niah Khan for teaching me heart cannulation and celebrating the wins of every working heart in the lab. Thank you, Chris Veitch and Raquel Parackal for chocolates, listening to my rants and your help with my experiments. I also thank all past and present members of the Erickson lab. I do appreciate Puja for encouraging me during

the last days of thesis writing and helping me with formatting. I thank all past and present occupants of Office 150. It has been such a pleasure, great vibes, interesting stories, liquorice, the green atmosphere, chocolates and for obeying the instructions on the back of my chair during my intense writing sessions. Thank you to postgraduate students of Physiology for encouraging me and for always being supportive with words too.

Thank you to Dr Oby Ebenebe for the motivational talks, emotional and academic support. I also thank you for doing the s-nitrosylation experiments and answering all my questions. Thank you, A/Prof Ahmed Oloyo for the support, recommendations and opportunities to excel in my academics. I appreciate you, Khadijah, for your concern and being an amazing sister. I enjoyed working with you both. I thank my academic mentors, Dr Koofreh Davies and Dr Mohammed Meah who have always been concerned and supported me on this academic journey.

What would I have done without you, Dr Chidinma Adanna Levi Okolo? Right from my first email to you, we bonded, became friends and then sisters. You have been a shoulder to lean on, a great support system, you have watched me break down and you have lifted me. You have listened to every rant, adventure and always assured me it was well. Through you, Dr Patrick, Chiamaka, Adimchinobi have become my family too. I can never thank you enough, you have been a great blessing to me.

Thank you to Dr Christian Chukwuka and Dr Chima Robert for being awesome friends to me, for the love you showed me and knowing that you could relate to my constant rants helped a lot. Thank you to Dr Charmaine for making sure I was not stuck in my office too long to forget what the outside looked like. I thank my Equippers Church family, Felicity, Rebecca, Katy, Sharonne, Brittany, Hannah, for listening to my highlights and lowlights, showing me love and care through this journey and being very supportive in kind words and prayers. Thank you, Yann Huey Ng and Angie Greenman for always coming through whenever I needed a hand to hold and for making me realise I was never alone on this journey. To my New Zealand Mum, Veronica and my sisters, Promise and Christiana Osam, thank you for the warmth and for welcoming me as your daughter/sister with open arms. Thank you, Karynmitchelle for always giving off positive vibes and for showing concern towards me. Idara, Inemesid, Amindi, Augusta, Oto-Obong, Timse, Aniekan, Ogumka, Borono, you are the best friends, thank you for holding me up in love and

prayers. Udy and Aidi Basi, you both coloured my world in ways I could never imagine, with Aidi working as my full time shrink without pay. Thank you, Engr (Dr) Mfon Uko, I feel great to be starting and finishing this PhD journey with you, you are a brother indeed. Dr Sinem, thank you for always being there, I hope to see you in Palmy. My sister and brother, Dr Ema and Anietie Ido, thank you for the love and prayers, and sharing the gift of Zoe with me. Yakekpono, thank you for your kindness and therapy in those crazy moments, never being too busy when I needed help and for just always armed with motivation and faith to share with me.

Finally, I would like to thank my family, my reason for being here, you all are the best. I thank Uncle Sam for motivating me. Thank you, Aunty Ema and Aunt Mary for always praying for me and sending gifts. To my siblings, Lydia, Joe and Sam, thank you for being very supportive and loving, for the great conversations and banter, just to ease my stress. I am very grateful to my parents who let their beloved daughter travel 10,000 miles away from home, who were always concerned about me, and did a countdown from day one of PhD. Thank you for a great foundation in life, I can never repay you for all you have done for me over the years, I really hope I make you proud.

CONTENTS

LIST OF FIGURES

APPENDICES

LIST OF TABLES

LIST OF ABBREVIATIONS

AC	Adenylyl cyclase
AF	Atrial fibrillation
AIP	Autocamtide 2-related inhibitory peptide
ANS	Autonomic nervous system
APD	Action potential duration
ATP	Adenosine triphosphate
AV	Atrioventricular
β-AR	Beta-adrenergic receptor
Ca^{2+}	Calcium
CaM	Calmodulin
CaMKIIδ	Calcium calmodulin dependent protein kinase II delta
cAMP	cyclic adenosine-3',5'-cyclic monophosphate
cGMP	cyclic guanosine monophosphate
CICR	Calcium induced calcium release
CO	Cardiac output
COX-2	cyclooxygenase-2
CTRL	Control
Cu^{+}	Cuprous ion
CVD	Cardiovascular diseases
Cys	Cysteine
DADS	Delayed after depolarizations
EADS	Early after depolarizations
ECC	Excitation contraction coupling
EDV	End diastolic volume
EF	Ejection fraction
eNOS	endothelial nitric oxide synthase
ESV	End systolic volume
FS	Fractional shortening
GAPDH	Glyceraldehyde 3-phosphate dehydrogenase
GC	Guanylate cyclase
GSNO	S-nitroso-glutathione
HF	Heart failure

HR	Heart rate
I/R	Ischaemia/Reperfusion
I_{Ca}	Ca^{2+} current
I_{Kr}	delayed rectifier potassium current
I_f	hyperpolarization activated inward current
IL-6	Interleukin-6
iNOS	inducible nitric oxide synthase
ISO	Isoproterenol
IVSd	LV interventricular septal thicknesses at diastole
IVSs	LV interventricular septal thicknesses at systole
K^+	Potassium
KHB	Krebs-Henseleit buffer
KO	Knockout
L-NAME	L-N^G-Nitro arginine methyl ester
LTCC	L-type Ca^{2+} channels
LV	Left ventricle
LVDP	Left ventricular developed pressure
LVESV	Left ventricle end systolic volume
LVIDd	LV internal dimension at diastole
LVIDs	LV internal dimension at systole
LVPWd	Left ventricle posterior wall during diastole
LVPWs	Left ventricle posterior wall during systole
Max dP/dt	Speed of contraction
Met	Methionine
Min dP/dt	Speed or relaxation
MMTS	Methyl methanethiosulfonate
mV	Millivolts
Na^+	Sodium
NADPH	Nicotinamide adenine dinucleotide phosphate
NCX	Na^+/Ca^{2+} exchanger
NLS	Nuclear localisation signaling
nNOS	neuronal nitric oxide synthase
NO	Nitric oxide
NOS	Nitric oxide synthase

O-GlcNAc	O-linked N-acetylglucosamine
O_2	Oxygen
PAGE	Polyacrylamide gel electrophoresis
PBS	Phosphate buffered saline
PDE	Phosphodiesterase
PKA	Protein kinase A
PKG	Protein kinase G
PLN	Phospholamban
PMSF	Phenylmethanesulfonyl fluoride
PNS	Peripheral nervous system
PTI	Pressure-time integral
PTM	Post-translation modification
PVT	Polymorphic ventricular tachycardia
RIPA	Radio Immunoprecipitation Assay
ROS	Reactive oxygen species
RV	Right ventricle
RyR2	Ryanodine receptor
SA	Sinoatrial
SDS	Sodium dodecyl sulphate
SEM	Standard error of the mean
SERCA	Sarco-endoplasmic reticulum Ca^{2+} ATPase
SNAC	S-nitroso-N-acetylcysteine
SNAP	S-nitroso-N-acetylpenicillamine
SNP	Sodium nitroprusside
SR	Sarcoplasmic reticulum
SV	Stroke volume
TdP	Torsades des pointes
TNF-α	Tumour necrosis factor – alpha
VF	Ventricular fibrillation
VPB	Ventricular premature beat

CHAPTER 1: INTRODUCTION

1.1 Regulation of cardiac contraction

1.1.1 Autonomic regulation of the heart

The heart is a vital organ in the body which contracts and relaxes in order to pump deoxygenated blood to the lungs and oxygenated blood to the body through blood vessels. The heart is controlled by the autonomic nervous system (ANS), which consists of the parasympathetic nervous system (PNS) and sympathetic nervous system (SNS), which act complementarily with each other. The SNS has a wide variety of cardiovascular actions which include increase in cardiac contractility, acceleration of heart rate, reduction of venous capacitance and constriction of resistance vessels (Triposkiadis et al., 2009). It is known to be responsible for the "fight or flight" response as it controls the body's reaction to stress. The PNS is required for the rest state and does the contrary by slowing the heart rate (Kishi, 2012; Gordan et al., 2015) and it is also known as "rest and digest". In physiologic conditions, there is always a net balance between the actions of the SNS and PSNS therefore in autonomic dysregulation which is a main feature of CVD, there is an imbalance between both systems. Certain circulating and hormonal factors like angiotensin II, aldosterone, atrial natriuretic peptide, reactive oxygen species (ROS) and nitric oxide (NO) also contribute to the modulation of sympathetic outflow at several sites in the central nervous system (Kishi, 2012). The stimulation of the SNS leads to increase myocardial contractility which is caused elevation of intracellular Ca^{2+} in the cardiomyocytes (Gordan et al., 2015). The autonomic regulation of the heart is usually propagated through cardiac excitation and contraction coupling (ECC). ECC is the process from electrical excitation of the myocyte to contraction of the heart to cause ejection of blood (Bers, 2002). Calcium ion (Ca^{2+}) plays a role in activation of myofilaments to cause contraction.

1.1.2 Action Potential in cardiac cell

The cardiac action potential is the waveform that occurs in response to changes in electrical potential across the cell membrane in the cardiac cell during contraction and relaxation. In cardiac cells, action potential is composed of 5 phases (Figure 1.1). Prior to influx of Ca^{2+} into the cell, there is resting membrane potential of -90 mV, here the Na^{+} and Ca^{2+} channels remain deactivated, as K^{+} leak out of the cell. This is known as Phase 4. Resting membrane potential is the electrical potential difference across the cell membrane under resting conditions. The next phase is Phase 0, which is known as the depolarisation phase. Here, there is rapid transient influx of Na^{+} as the membrane potential rises from -90 mV to approximately +20 mV. As the Na^{+} channels are deactivated, the K^{+} channels open and there is an efflux of K^{+}, this makes up Phase 1, which is a brief phase characterised by a rapid initial repolarisation. This brings the membrane potential to 0 mV. Phase 2 is the plateau phase, a stable period where is a slow opening of voltage-gated L-type calcium channels (LTCCs) and high influx of Ca^{2+} ions. Slow Na^{+} channels are also opened, and the entry of Na^{+} and Ca^{2+} ions allows the membrane potential to remain at 0 mV leading to prolonged depolarisation which forms a plateau. Phase 3 is the final repolarisation phase where there is efflux of K^{+}, and Ca^{2+} channels become inactivated. As the K^{+} exiting the cell exceeds the amount of Ca^{2+} entering the cell, this creates a negative current. This also brings the cell back to its resting potential at -90 mV. In this phase also, excess Ca^{2+} is pumped out through the Na^{+}/Ca^{2+} exchanger (NCX) and the activated Na^{+}/K^{+} pump allows influx of K^{+}. This is to allow for membrane ionic concentrations to return to basal levels.

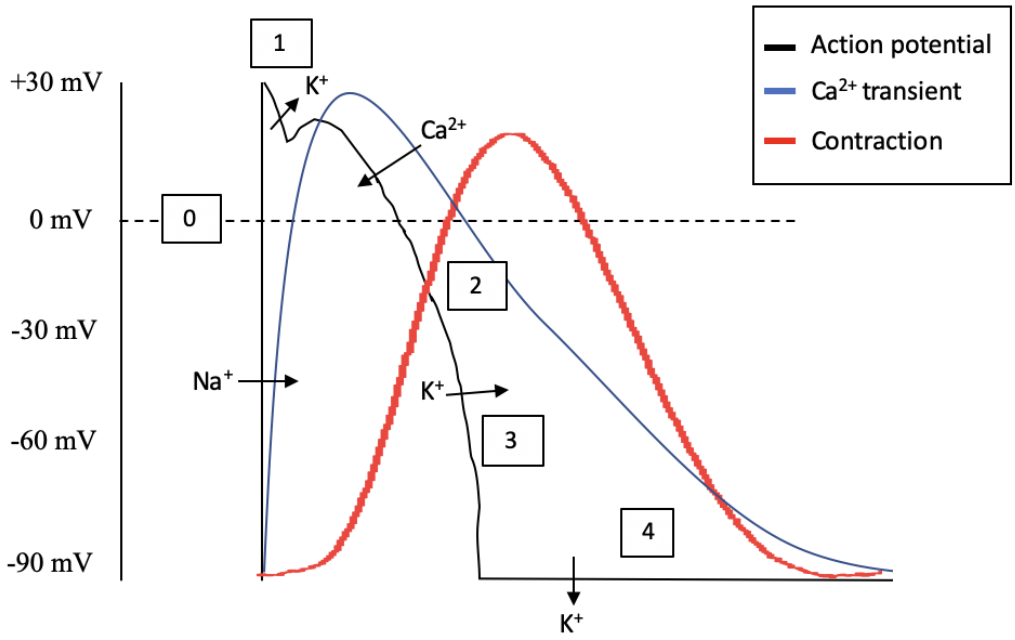

Figure 1.1 Action potential in ventricular myocyte. Time course showing different phases of action potential in ventricular myocyte at 37°C. Phase 0 is rapid depolarisation, Phase 1 is early rapid depolarisation, Phase 2 is plateau, Phase 3 is final rapid depolarisation and phase 4 is resting membrane potential. Black line is action potential. Blue line is Ca^{2+} transient during action potential. Red line is contraction and relaxation in the cardiac cell. Schematic adapted from Bers (2002).

1.1.3 Excitation Contraction Coupling in cardiomyocytes

For the myocardium to contract, there is a series of events that must occur between excitation and contraction (Figure 1.2). Ca^{2+} is critical for ECC because it is the effector that acts on the myofilaments in cardiomyocytes for contraction to occur (Bers, 2002). Action potentials spread over the sarcolemma through the transverse tubules, which have LTCCs. During the plateau phase of action potential, there is Ca^{2+} influx into the cardiomyocyte through LTCCs that triggers the release of Ca^{2+} release from the intracellular stores in sarcoplasmic reticulum (SR) through the ryanodine receptor type 2 (RyR2). This mechanism is known as calcium-induced calcium release (CICR) (Fabiato & Fabiato, 1978). The SR releases Ca^{2+} into the cytosol and increases free intracellular Ca^{2+} concentration. The cytosolic Ca^{2+} transient then activates myofilaments when Ca^{2+} binds to myofilament protein troponin C. A change in position of troponin occurs, pulling the tropomyosin complex away from actin to expose the binding site. Myosin binds to actin, the filaments form a cross-bridge which causes a shortening of the sarcomere and myofilament contraction is initiated (Gordan et al., 2015; Beckendorf et al., 2018). This concept is known as cross-bridge cycle. Relaxation occurs when there is a decline in Ca^{2+} current (I_{ca}) and there is dissociation of Ca^{2+} from troponin C. Ca^{2+} declines as there is re-uptake of Ca^{2+} into the SR through the Phospholamban (PLB)-regulated Sarcoplasmic Reticulum Calcium ATPase 2 (SERCA2a), out of the cytosol. There is also extrusion of Ca^{2+} through the sarcolemmal Na^{+}/Ca^{2+} exchanger (NCX) into the extracellular space (Rokita & Anderson, 2012; Dobrev & Wehrens, 2014). The re-acquired Ca^{2+} are then stored in the SR in preparation for the influx of Ca^{2+} through the LTCCs, for the next cycle (contraction and relaxation) to occur.

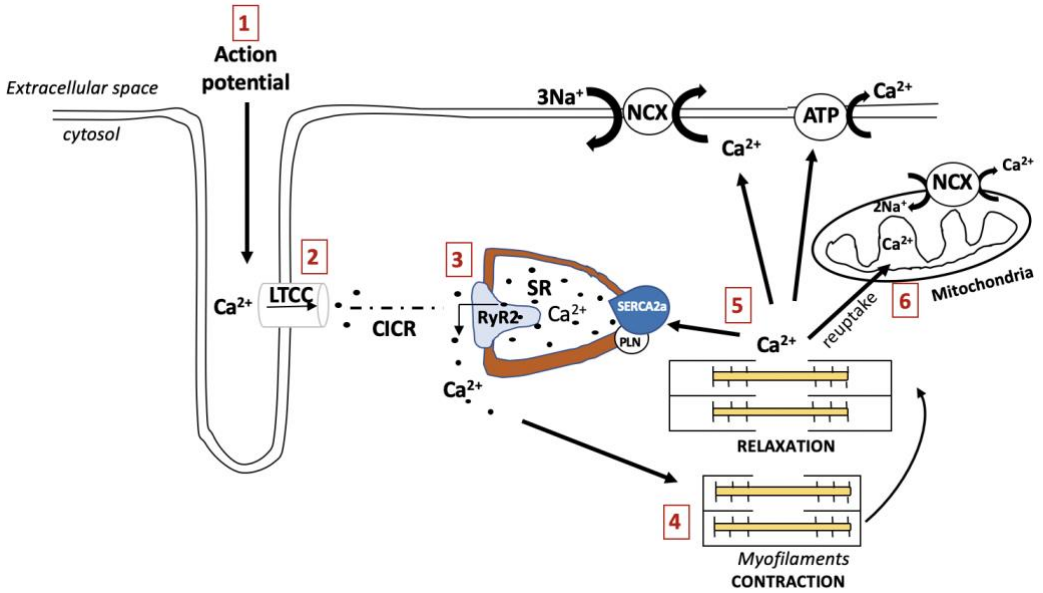

Figure 1.2 Excitation contraction coupling in cardiac cells. Action potential spreads over the sarcolemma through the transverse tubules. (2) LTCCs opens to allow influx of Ca^{2+} into the cell. (3) Calcium-induced calcium release (CICR) mechanism triggers the release of Ca^{2+} release from the sarcoplasmic reticulum (SR) through the ryanodine receptor type 2 (RyR2). The SR releases Ca^{2+} into the intracellular space and increases free intracellular Ca^{2+} concentration. (4) The cytosolic Ca^{2+} transient then activates myofilaments to initiate contraction. Relaxation occurs when there is a decline in Ca^{2+} initiates relaxation. (5) There is re-uptake of Ca^{2+} into the SR through the Phospholamban (PLN)-regulated Sarcoplasmic Reticulum Calcium ATPase 2 (SERCA2a) and extrusion of Ca^{2+} through the sarcolemmal Na^{+}/Ca^{2+} exchanger (NCX) and Ca^{2+} ATPase (6) The mitochondrial Ca^{2+} uniporter takes up the Ca^{2+} and also extrudes Ca^{2+} from the mitochondrial matrix via the NCX. Adapted from Bers (2002).

1.2 Cardiac arrhythmias

Cardiovascular diseases (CVDs) are caused by disorders of the heart and blood vessels, that affect the circulatory system of the body (D'Andrea et al., 2015). They are highly prevalent and include cerebrovascular diseases (stroke), peripheral arterial diseases, rheumatic heart diseases, deep vein thrombosis and pulmonary embolism, congenital diseases, coronary heart diseases (heart attack), cardiomyopathies and arrhythmias (D'Andrea et al., 2015; World Health Organisation, 2017). CVD is the leading cause of death worldwide. In 2015, 17.7 million people died from CVDs (World Health Organisation, 2017) and annually, over 7 million people die from cardiac arrhythmias (Ramanathan et al., 2004). In New Zealand, CVDs account for 32% of deaths annually and approximately 35,000 New Zealanders are known to suffer from a type of cardiac arrhythmia (Ministry of Health, 2017).

Arrhythmia is the deviation of the heart rhythm from the regular sinus rhythm. It is caused by disruptions in the orderly propagation of electrical impulses through the heart muscles (Ramanathan et al., 2004; Tse, 2016). Arrhythmias are often an indication of high-risk cardiovascular diseases such as heart failure, myocardial infarction, coronary artery disease, and valvular heart disease, all of which can lead to cardiac arrest. An alteration in the myocardium or in the autonomic system can lead to arrhythmias. Arrhythmias can be classified according to its effect on heart rate; when the hearts beats too fast (tachycardia) or too slow (bradycardia). They can also be classified based on part of the heart where it originates; the upper part (supraventricular arrhythmias) or the lower part (ventricular arrhythmias) of the heart (Lindberg, 2017). This thesis will focus on ventricular arrhythmias.

In physiological conditions, electrical stimulus from the sinoatrial (SA) node located in the wall of the right atrium depolarises the cardiac cells causing atrial contraction. The electrical impulses are then transmitted to the atrioventricular (AV) node causing the atrioventricular valves to open and fill the ventricles with blood. The impulses from the

AV node travel through the left and right branches of bundle of His into the purkinje fibres located in the muscular walls of the ventricles, which causes the ventricles to contract. Contraction of the ventricles allows the right ventricle to push blood out into the pulmonary system while the left ventricle pushes blood out into the systemic circulation.

One of the known mechanisms of arrhythmia is triggered activity, which results from afterdepolarization during abnormal pulse initiation (Wit & Boyden, 2007). Afterdepolarisations are spontaneous depolarisations which interrupt phases of the action potential in cardiomyocytes. They are of two types; early afterdepolarisation (EAD) and delayed afterdepolarisation (DAD). EAD is defined as the secondary voltage oscillations that occur before full repolarisation of action potential in ventricular cardiomyocytes. They correspond to phase 2 and 3 of the cardiac action potential (Qu et al., 2013; Tse, 2016; Huang et al., 2018). DAD occurs after repolarisation has been completed. They correspond to the phase 4 of the cardiac action potential. Afterdepolarisations are known to be related to increase in diastolic Ca^{2+} (Gaztañaga et al., 2012).

Untreated arrhythmias can lead to serious complications and become life threatening, and as such can lead to sudden cardiac death or damage other body organs. Anti-arrhythmic drug therapies that target electrolyte imbalance and triggered activity are used in clinical settings. Aside from the contribution of autonomic activation to the development of arrhythmias, one of the mechanisms that is known to alter cardiac function and trigger arrhythmias is impaired intracellular Ca^{2+} cycling by cardiac proteins during excitation contraction coupling (ECC) (Qu et al., 2013). The role of impaired Ca^{2+} cycling in triggered rhythm activities is complex. Further understanding of this mechanism at the cellular level is required, in order to design new therapies that target cardiac arrhythmias and can be applied in the clinic.

1.3 Nitric oxide in the heart

Nitric Oxide (NO) is a ubiquitous gasotransmitter molecule involved in many physiological processes throughout the cardiovascular system. It is a well-known vasodilator which plays a role in overall cardiac homeostasis. Aside from the vascular response pathway, it is also involved in neuronal and immune response pathways (Kojda & Kottenberg, 1999; Bishop, 2012). It also regulates blood pressure, as well as myocardial contraction and relaxation, making it a key regulator of ECC (Massion et al., 2003; Houston & Hays, 2014; Vielma et al., 2016). Previous studies focused on NO signaling have provided great insight about its involvement in complex pathophysiological conditions such as myocardial infarction, heart failure, diabetic heart disease and pulmonary hypertension (Katz *et al.*, 1999; Phillips *et al.*, 2009; Liu, 2017; Ling *et al.*, 2018).

1.3.1 Nitric oxide synthesis

NO is produced in the cardiomyocytes from the cleavage of L-arginine into L-citrulline by nitric oxide synthase (NOS) enzyme isoforms. The neuronal (nNOS/NOS1) isoform is localized to the sarcoplasmic reticulum while the endothelial (eNOS/NOS3) isoform is localized to the plasmalemmal caveolae (Ziolo et al., 2008). The NOS1 and NOS3 are expressed constitutively in cardiomyocytes (Lima et al., 2010; Moosavi et al., 2014); (Đorđević et al., 2012). The inducible isoform (iNOS/NOS2) is a cytosolic protein (Ziolo & Bers, 2003) expressed in response to inflammation or injury as seen in heart failure and ischemia-reperfusion injury (Balligand et al., 1994; Wildhirt et al., 1999; Ziolo et al., 2004). The eNOS and nNOS control fluctuating low levels of NO to ensure normal physiological functions in neurons and vascular cells respectively (Hancock et al., 2008).

1.3.2 Nitric oxide donors

The role of NO has been extensively studied in cardiac function using different NO donors, which store NO in a stable form and spontaneously release NO or require enzymatic reaction to generate NO (Ignarro et al., 2002; Herman & Moncada, 2005). Some of the NO-releasing compounds (NO donors) used in studying physiological processes include sodium nitrite, sodium nitroprusside (SNP), S-nitroso-N-acetylpenicillamine (SNAP) and S-nitroso-glutathione (GSNO). For example, NO release from sodium nitrite reduced the number of arrhythmic episodes in anaesthesised dogs after a 25-min period of coronary artery occlusion and reperfusion (Kovács et al., 2015). For measurement of quantitative release of NO, the decomposition of SNAP triggered by Cu^{+} has been used for calibration of electrochemical NO microsensors (Zhang et al., 2000). SNP exhibited direct positive chronotropic effect by increasing heart rate of rabbits in vivo and in vitro (Hogan et al., 1999). In a study by Poluektov et al. (2019), GSNO was found to accelerate recovery of contractility of isolated perfused rat hearts after ischaemia-reperfusion. Exposure of cardiomyocytes to GSNO has also been found to induce positive inotropic response in cardiomyocytes (Sarkar et al., 2000).

1.3.3 Nitric oxide signaling

NO signaling in the heart involves two pathways (Figure 1.3). One is the guanylate cyclase (GC) pathway which is dependent on cyclic guanosine monophosphate (cGMP) where NO activates GC and leads to formation of cGMP and the activation of protein kinase G (PKG). This causes inhibition of phosphoinositide hydrolysis and reduction of intracellular Ca^{2+} concentration. Another signaling pathway for NO is through S-nitrosylation, which is the covalent attachment of NO to cysteine sulphyldryls on the thiol side chain of a protein. S-nitrosylation leads to further activation of downstream protein targets such as LTCC, RyR2 and PLN. This affects Ca^{2+} handling in cardiomyocytes, which makes NO a key regulator of ECC (Vielma et al., 2016). NO can also activate adenylate cyclase to mediate myocardial contractility (Vila-Petroff et al., 1999).

Superoxide radicals can also react with NO to form reactive nitrogen species such as peroxynitrite, which also influence cardiac contractility (Ziolo et al., 2008; Kruzliak et al., 2014).

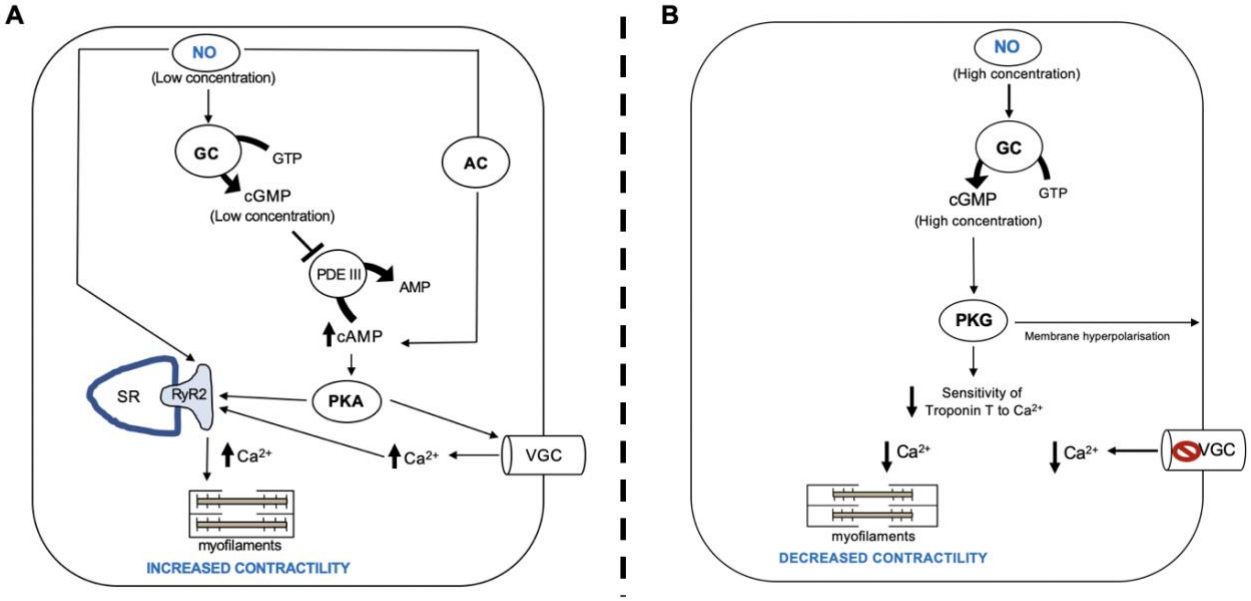

Figure 1.3 NO signaling pathways and the biphasic effect in cardiomyocytes. A, Low concentration of NO activates guanylate cyclase (GC) which leads to increase production of cyclic guanosine monophosphate (cGMP) and inhibits phosphodiesterase III (PDE III) which prevents cyclic adenosine-3',5'-cyclic monophosphate (cAMP) hydrolysis. Low NO concentration also activates adenylyl cyclase (AC) which leads to increase in cAMP. Activation of protein kinase A (PKA) fosters the opening of voltage gated Ca^{2+} channels (VGC) and RyR2, which allows increase in Ca^{2+} and results in increased contractility. B, High concentration of NO leads to increase in cGMP, activation of protein kinase G (PKG) which decreases sensitivity of Troponin T to Ca^{2+} and results in decreased contractility. Schematic adapted from Rastaldo et al. (2007).

1.3.4 Biphasic effect of nitric oxide

NO is involved in dilation of blood vessels. However, several studies have showed that NO exerts a biphasic effect in the heart which is dependent on concentration. Low concentration of NO induces vasoconstriction and positive inotropic effects in the heart, while high concentration promotes vasodilation and negative inotropy. A study by González et al. (2008), showed that low concentrations of the NO donor SNAP increased cardiac contractility and pressure development in isolated rat heart, and a high concentration of SNAP induced an opposite effect by increasing cGMP, leading to reduced cardiac contractility. The mechanism for positive inotropic effect of NO could be the role of eNOS and nNOS derived NO which mediates calcium handling proteins, LTCC and RyR2 during ECC and also S-nitrosylation (Campbell et al., 1996). The mechanism underlying the negative inotopic is suggested to be cGMP dependent, by reducing calcium sensitivity in the myofilaments (Cotton et al., 2002). Müller-Strahl et al. (2000) also found that reduced endogenous NO release during NOS inhibition increased myocardial contractility in the rat heart.

1.3.5 Cardioprotective effect of nitric oxide

Oxidative stress, an imbalance between reactive oxygen species and cellular antioxidant production, is the hallmark of major pathophysiological conditions in the heart. NO has antioxidant properties that prevent pathophysiological consequences of tissue damage through various mechanisms (Wink et al., 2001) and this can be achieved endogenously and exogenously. Kruzliak et al. (2014) suggested that NO acts as a radical scavenger but the mechanism is not well defined. However, NO could also prevent production of superoxide. Increase in cGMP, upregulation of ferritin production and expression of hemoxygenase has been observed as the mechanisms by which NO prevents peroxide injury in hepatocytes (Kim et al., 1995). According to Clancy et al. (1992), NO inhibits neutrophil oxygen generation and assembly of the nicotinamide adenine dinucleotide phosphate-oxidase (NADPH oxidase) complex. In rats with renal ischemia/reperfusion

injury, there was evidence that administration of NO donor, molsidomine prevented against depletion of antioxidant levels suggesting that NO production inhibits oxidative stress pathways (Chander & Chopra, 2005).

During ischemia and reperfusion (I/R), there is interruption of blood supply which can exacerbate cellular dysfunction and tissue injury/death, dependent of the duration and magnitude of ischemia (Kalogeris et al., 2012). In the human heart of patients who underwent coronary artery bypass grafting, transcardiac production of pro-inflammatory substances such as Interleukin-6 (IL-6), Tumour necrosis factor – alpha (TNF-α), activated leucocytes and platelets were reduced after SNP treatment in the first 60 minutes of reperfusion, thereby protecting against I/R injury (Massoudy et al., 2000). NO protected against hemorrhagic shock and liver injury in rats by improving hemodynamic response, scavenging reactive oxygen species, and blocking the effect of inflammatory cytokines (Anaya-Prado et al., 2003). L-arginine, a precursor of NO, protected against I/R induced hepatocyte injury in rats by preventing increase in lipid peroxidation and reducing neutrophil infiltration (Chattopadhyay et al., 2008). In a pathway independent of cGMP, NO can also protect rat cardiac cells against metabolic inhibition-induced cellular injury by preventing increase in lactate dehydrogenase levels, which is an indicator of tissue damage (Garreffa et al., 2006). Another mechanism by which NO protects the heart from I/R injury is by stimulation of cyclooxygenase-2 (COX-2) activity, which in turn leads to production of cytoprotective prostanoids (Kruzliak et al., 2014). Even though the precise mechanism of cardio-protection is complex, NO plays a role in immune response by acting as an anti-inflammatory and antioxidant agent by reducing the expression of pro-inflammatory cytokines (Rodriguez-Peña et al., 2004; Webb et al., 2004; Phillips et al., 2009; Strijdom et al., 2009).

During stress conditions that require fight or flight response, the heart requires increased blood perfusion to tissues and organs. The response of the heart to this increase in demand is a determinant of cardiac performance. NO plays a critical role in the stretch of cardiac muscle cells during increased workload in the heart. A study by Vila-Petroff et al. (1999)

showed that endogenous NO release in cardiac cells was able to influence how cardiomyocytes responded to stretch response. They suggested that the localization of eNOS, which is close to the SR T-tubule and also regulation of the RyR2 channels by S-nitrosylation during ECC, could be responsible for this effect. Therefore, NO may act as an amplifier of Ca^{2+} signaling and possibly regulate the response of cardiomyocyte to increase in preload (Prendergast et al., 1997).

NO modulates basal heart rate and induces positive chronotropic effect in cardiac myocytes. Knocking out NOS isoforms in animal models has resulted in reduced heart rate (Yang *et al.*, 1999; Rakhit *et al.*, 2001; Massion & Balligand, 2003). Mice lacking eNOS gene displayed bradycardia and mild hypertension while treatment of C57BL/6 wild-type mice with a NOS inhibitor, L-NAME also induced bradycardia (Kojda et al., 1999) suggesting that other NOS isoforms were involved in heart rate regulation. A study by Liu et al. (2002) observed that basal heart rate was lower in eNOS deficient mice compared with their control group. A contrary finding was observed by Kennedy et al. (1994) who reported that NO had no chronotropic effect in rat atrial preparation. They attributed the different observations to the difference in tissues and role of the currents contributing to pacemaker activity. Administering NO donors to isolated guinea pig atrial preparations increased spontaneous beating rate and pharmacologically blocking hyperpolarization activated inward current (I_f) prevented an increase in the beating rates with exposure to NO donors. This suggests that HR control by NO is through the cGMP pathway by modulation of I_f (Musialek et al., 1997). In summary, eNOS and nNOS are involved in regulating heart rate (Barouch et al., 2002) and could be therapeutic targets in pathophysiological conditions involving overactivation of the sympathetic nervous system.

1.3.6 Nitric oxide and regulation of intracellular calcium during ECC

Exogenous NO can modulate the opening of Ca^{2+} channels as shown in a study involving rabbit atrial cells (Wang et al., 2000). According to this study, treating cardiac cells with

GSNO (100 µM) increased basal I_{ca}. However, lowering cGMP levels by inhibiting guanylyl cyclase blocked the effect of NO on I_{ca}, suggesting that NO signaling modulates intracellular calcium levels through cGMP. Furthermore, blocking Protein Kinase A (PKA) and phosphodiesterases (PDEs) failed to inhibit the stimulatory effect of GSNO, showing that this pathway is dependent on phosphorylation of PKG and not PKA or PDEs. Therefore, NO signaling leads to PKG phosphorylation which directly mediates the opening of LTCCs involved in regulating basal I_{ca}. Another finding demonstrated at 100 µM GSNO, PKG activation prevented opening of voltage-gated calcium channels and decreased myofilament calcium sensitivity through troponin I phosphorylation, independent of cGMP (Hu et al., 1997). The disparity in findings suggest that the effect of NO on I_{ca} is both inhibitory and stimulatory, dependent on both cGMP and post translational modification signaling pathway, which further confirms its biphasic effect (Campbell et al., 1996).

1.3.7 Nitric oxide and ß-adrenergic signaling

In a previous study, it has been observed that ß-adrenergic signaling increases endogenous NO which leads to S-nitrosylation of Ca^{2+}-handling proteins (RyR2, SERCA2a, LTCC). It is also known that the isoform that plays a role in this ß-adrenergic responsiveness is NOS1 (Vielma et al., 2016) and not NOS3 (Wang et al., 2008). In the study by Vielma et al. (2016), exposing cardiomyocytes to selective NOS1 blocker led to decreased inotropic effect and results also showed that NOS1 was responsible for nitrosylation following ß-adrenergic stimulation. The mechanism of ß-adrenergic response attenuation by NO was a reduction in I_{ca} (Wang et al., 2008), which also prevents pro-arrhythmic signaling. Furthermore, acute nitrosative stress and overactivation of sympathetic stimulation can be deleterious to the heart (Gutierrez et al., 2013; Curran et al., 2014). The relationship between NO and ß-adrenergic signaling will be discussed further in Chapter 4.

1.3.8 Nitric oxide and arrhythmias

Increase in NO release is known to induce Ca^{2+} leak in cardiac myocytes and this could be a trigger for arrhythmias. In autonomically denervated dogs, NG-monomethyl-L-arginine (endogenous NO precursor) infusion reduced the incidence of ventricular arrhythmias during sympathetic stimulation (Fei et al., 1997). Kubota et al. (2000) observed that cardiomyocytes deficient of eNOS exhibited oubain-induced arrhythmias and exposure of these cells to NO donor, S-nitroso-N-acetylcysteine (SNAC), attenuated transient inward current, which is a predictor of digitalis-induced arrhythmias. These studies suggest that inhibiting NOS pathway may exacerbate proarrhythmic stimulation. Wang et al. (2008) also demonstrated that NOS3-defecient cardiomyocytes were susceptible to arrhythmias in response ß-adrenergic receptor stimulation. Therefore, blocking NOS pathway during sympathetic stimulation could aggravate arrhythmogenesis.

However, some experimental studies have contrary findings and have shown that NO is not totally cardioprotective but stimulates pro-arrhythmic signaling by mediating increase in Ca^{2+} spark frequency, a predictor of cardiac arrhythmias. Gutierrez et al. (2013) found that 150 µM GSNO (NO donor) could directly induce an increase in Ca^{2+} spark frequency independent of ß-AR stimulation and this pathway involved nitrosylation of cardiac proteins. Furthermore, they found that an inhibitor of Ca^{2+}/calmodulin dependent protein kinase II (CaMKII) attenuated the pro-arrhythmic effect of GSNO. NO donor, SNAP increased SR Ca^{2+} leak in rabbit cardiomyocytes, in the absence of ß-AR stimulation (Curran et al., 2014). The CaMKII inhibitor also prevented SR Ca^{2+} leak, suggesting that the effect of NO in cardiomyocytes was primarily through CaMKII activation.

The contradictory findings about the beneficial and deleterious effects of NO in the heart have been reported in literature, and this makes the function of NO in the heart somewhat controversial. In summary, the actions of NO are dependent on concentration, the NOS isoforms, reactive nitrogen species produced, and the role of downstream targets, which

makes the role of NO also complex. These are important when considering the role of NO in health and disease. This thesis will highlight the effects of NO and identify a CaMKII-dependent pathway through which NO could be contributing to cardiac dysfunction.

1.4 Ca^{2+}/calmodulin dependent protein kinase II

CaMKII is a multifunction protein which is expressed as a multimer comprising of 12 subunits in most commonly observed physiological conditions (Figure 1.4) (Braun & Schulman, 1995). CaMKII is a mediator of calcium linked signaling and regulates a broad range of cellular functions. Basal activity of CaMKII is responsible for calcium handling during excitation-contraction (coupling between membrane excitability and cell contraction) and excitation-transcription (coupling between cardiomyocyte activity and gene transcription) coupling in the myocardium (Mohler & Hund, 2011; Daniels et al., 2015). However, research has also shown that aberrant activation of CaMKII is the underlying cause of pro-rhythmic signaling and heart failure (Sag et al., 2009; Zhong et al., 2017).

1.4.1 Structure of CaMKII

CaMKII consists of 6-12 subunits or monomers that form a dodecameric holoenzyme. The structure of CaMKII is said to resemble a “wagon wheel” because of the way it is arranged, having each of the monomers form each spoke of the wheel around a central core (Erickson, 2014). Each monomer is comprised of three domains, an association domain, a catalytic domain and a regulatory domain. The carboxy-terminal (C-terminal) association domain directs the assembly of the dodecameric holoenzyme by associating the subunits. The amino-terminal (N-terminal) catalytic domain is responsible for the serine/threonine kinase function of CaMKII and it contains substrate binding pockets, 1 for ATP and 1 for the target protein which lies close to ATP to allow for transfer of phosphate group to a target protein thereby bind to potential substrates, while the

regulatory domain contains the binding site for Ca^{2+}/calmodulin (Ca^{2+}/CaM), the various sites of post-translational modification and also mediates the function of the catalytic domain via autoinhibition (associating with the C-terminal) in the baseline state (Hoelz et al., 2003; Erickson et al., 2015).

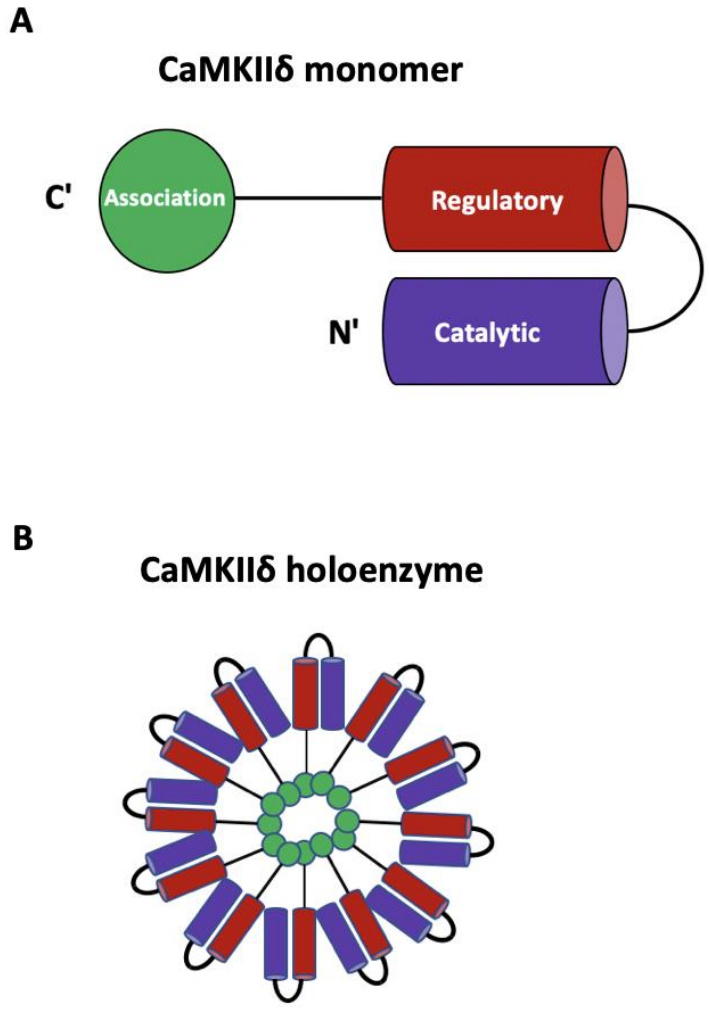

Figure 1.4 Structure of CaMKIIδ A, CaMKIIδ monomer showing the three domains; C-terminal association domain which directs the assembly of the dodecameric holoenzyme, N-terminal catalytic domain which binds to potential substrates and regulatory domain which has the binding site for Ca^{2+}/CaM. B, An assembled CaMKIIδ multimer containing 12 monomers. Original figure by Esther Asamudo.

1.4.2 Isoforms of CaMKII

CaMKII is a serine/threonine kinase widely expressed in muscle, nerve and immune tissues. It is a regulatory node in the heart and brain, and exists in four main isoforms produced by four different genes; alpha, beta, delta and gamma (α, β, δ and γ,) (Erickson et al., 2013; Hund & Mohler, 2015). The neuronal isoforms, CaMKIIα and CaMKIIβ are important for learning and memory. The predominant cardiac isoform is CaMKIIδ, with a secondary expression of CaMKIIγ and both isoforms play a role in Ca^{2+} handling (Zhang & Brown, 2004; Erickson et al., 2015). This delta isoform exists in two major splice variants in the adult heart, CaMKIIδ_B and CaMKIIδ_C. δ_B and δ_C are known to have similar sensitivity to Ca^{2+}/CaM binding and catalytic activity (Edman & Schulman, 1994; Gray & Brown, 2014), however in the variable domain of δ_B, there is insertion of an 11 amino acid sequence. The expression of the splice variant, δ_B is localised to the nucleus, as it contains a nuclear localization signaling (NLS), while the cytosolic δ_C lacks NLS and is expressed in the cytosol (Edman & Schulman, 1994). There are other splice variants ($\delta_{5\text{-}11}$) but have been found to be expressed during neonatal development (Mayer et al., 1994; Hoch et al., 1999) and CaMKIIδ_A which localises to the T-tubules and nuclear membranes is expressed in neonatal and adult models (Xu et al., 2005; Li et al., 2011).

Both δ_B and δ_C are known for their opposing roles in apoptosis, while δ_B is anti-apoptotic, δ_C promotes apoptosis (Peng *et al.*, 2010; Daniels, 2017). The difference in subcellular localisations suggests difference in Ca^{2+}-CaM sensitivity and distinct functions (Bers & Guo, 2005). δ_B signaling leads to the activation of several transcription factors that regulate gene expression and therefore over expression can induce cardiac hypertrophy (Zhang et al., 2002). Over-expression of δ_C can cause severe cardiac dysfunction, heart failure and premature death (Zhang et al., 2003). This thesis will focus on the CaMKIIδ_C variant, this will be referenced as CaMKIIδ.

1.4.3 Activation and Function of CaMKII in the Heart

Under basal conditions, the regulatory domain and the catalytic domain remain in close association preventing the binding of substrates, this ensures that the kinase is inactive or is in an autoinhibitory state (Figure 1.5) (Erickson, 2014). Influx of Ca^{2+} leads to the binding of Ca^{2+}/CaM to the regulatory domain of CaMKII, which causes a conformational change that disrupts the interaction of the regulatory domain with the ATP and protein substrate binding sites of the catalytic domain. This action exposes the catalytic domain for substrate binding and distorts the autoinhibition of the kinase. However, in pathophysiological conditions, where CaMKII is activated by prolonged Ca^{2+} cycling, the kinase is susceptible to post translational modifications, rendering the protein autonomously active.

Research has shown that CaMKII is also responsible for the mediation of the heart's fight or flight response to ß-AR stimulation (Mohler & Hund, 2011; Wu & Anderson, 2014) and there is evidence that autonomous activation or dysfunction of CaMKII activity has adverse effects in heart function. Therefore, CaMKII is also thought to play a key role in development of cardiac hypertrophy and dilated cardiomyopathy (Hoch et al., 1999; Kirchhefer et al., 1999; Zhang et al., 2003), heart failure (Zhang et al., 2003; Ai et al., 2005; Ling et al., 2009; Rajtik et al., 2017), progression of diabetes (Erickson et al., 2013; Luo et al., 2013) and arrhythmias (Wu et al., 2002; Erickson et al., 2013).

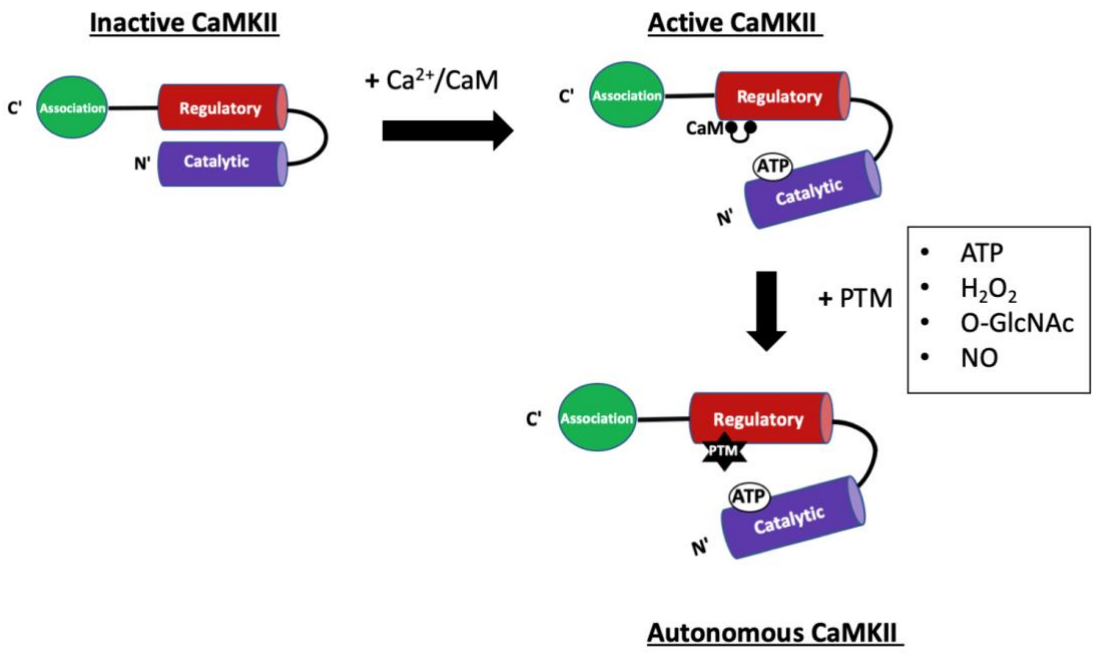

Figure 1.5 Activation of CaMKIIδ in the heart. In basal conditions, the regulatory and catalytic domains remain in close association and renders the kinase inactive. Elevation in intracellular Ca^{2+} leads to binding of Ca^{2+}/CaM to the regulatory domain which exposes the catalytic domain for substrates to bind. PTMs can occur when ATP, H2O2, O-GlcNac and/or NO residues bind to the regulatory domain. This prevents re-association of the regulatory and catalytic domain and results in prolonged activity of the kinase. Original figure by Esther Asamudo.

1.5 CaMKII and ECC

Protein kinases serve as intermediary between upstream and downstream signaling pathways and are responsible for functions like gene expression, ion transport, cell cycle activity and metabolism (Bayer & Schulman, 2001; Mollova et al., 2015). Several studies have shown that CaMKII can modulate ECC in cardiomyocytes through the phosphorylation of several important Ca^{2+} regulatory proteins like RyR2, PLN, SERCA2a (Wehrens et al., 2004; Abiria & Colbran, 2010; Grimm et al., 2015). CaMKII can phosphorylate the LTCC subunits and mediate I_{ca} to cause myocyte mishandling of Ca^{2+} and lead to contractile dysfunction, development of early after-depolarisation and arrhythmias (Bers, 2002; Zhang & Brown, 2004).

For propagation of Ca^{2+} in ECC, voltage-gated channels such as LTCCs serve as the main entry point for Ca^{2+} in cardiac cells (Bers & Grandi, 2009). CaMKII phosphorylation of LTCC subunits is important for Ca^{2+} dependent facilitation of the channel (Hudmon et al., 2005; Grueter et al., 2008). This interaction increases the opening probability of LTCCs and facilitates I_{ca} which increases cytosolic Ca^{2+} concentration and strengthens contraction (Gordan et al., 2015). Hudmon et al. (2005) showed that CaMKII can associate with the regions pore-forming alpha-1C subunit of LTCCs responsible for modulating the channel function. This phosphorylation leads to upregulation of Ca^{2+} influx during action potential, and this mechanism is called Ca^{2+}-dependent facilitation (CDF). Using a 'site specific' CaMKII inhibitor, Xiao et al. (1994) was able to determine the role of CaMKII in Ca^{2+} influx via LTCCs in cardiomyocytes, as Ca^{2+} influx was required due to the correlation between activation of the kinase and change in I_{ca}.

CaMKII also phosphorylates voltage-gated sodium channel, $Na_V1.5$ at several sites within the I-II linker loop (Ashpole et al., 2012; Marionneau et al., 2012; Grandi & Herren, 2014). The S516 site is most efficiently phosphorylated by CaMKII, and in heart failure, CaMKII phosphorylation of S571 site is increased (Wagner et al., 2006; Koval et al., 2012; Toischer et al., 2013). Phosphorylation of this channel by CaMKII is also

responsible for regulating the activation of the channel and increasing the voltage-dependent Na^+ current, leading to re-entrant arrhythmias (Herren et al., 2013), DADs (Gonano et al., 2011) and prolonged EADs as seen in ventricular cardiomyocytes of mice over expressing CaMKIIδC (Edwards et al., 2014).

During ECC, CaMKII has a direct effect on RyR2. The role of RyR2 is to facilitate/mediate Ca^{2+} release from the calcium stores in the SR and direct it into excitable cells. It is known to play a role in CICR (Wehrens et al., 2004). RyR2 phosphorylation by CaMKII occurs at Ser2809 and Ser2815 sites. This phosphorylation promotes RyR2 activity in cardiomyocytes, and inhibiting CaMKII blunts this effect (Currie et al., 2004; Grimm & Brown, 2010). In cardiomyocytes with over expression of CaMKIIδC, Maier et al. (2003) found enhanced diastolic Ca^{2+} leak and increased frequency of Ca^{2+} sparks, which indicated spontaneous Ca^{2+} release in diastole. They inferred that this process increases RyR2 phosphorylation due to CaMKII overexpression. Conversely, inhibition of CaMKII decreased Ca^{2+} spark frequency in ventricular cardiomyocytes, and the suggested mechanism was the inhibition of RyR2 phosphorylation by CaMKII (Li et al., 1997). The pathological effect of RyR2 phosphorylation by CaMKII is also seen in heart failure due to increase SR Ca^{2+} leak into the cytosol (Ai et al., 2005; Respress et al., 2012).

PLN, which is also a target of CaMKII, acts as the regulator of SERCA2a (Li et al., 1998). CaMKII phosphorylates PLN at Thr 17 to inactivate it and relieve its inhibition of SERCA2a. This action facilitates more pumping of Ca^{2+} into the SR through the SERCA2a, thereby restoring Ca^{2+} content levels in the SR (Gordan et al., 2015). CaMKII is known to decrease SR Ca^{2+} uptake as seen in heart failure, it was shown that ablation of PLN in CaMKIIδC TG mice normalised SR Ca^{2+} levels, restored Ca^{2+} transients and improved contractile function in isolated myocytes (Zhang et al., 2010).

1.6 Post-translational Modification of CaMKII

CaMKIIδ is susceptible to many forms of post-translational modifications (PTMs) (Figure 1.6), which prevent re-association of the catalytic and regulatory domains of the active kinase. PTM is a biochemical process in which amino-acid residues in a protein are covalently modified, during or after protein biosynthesis. PTM is important for several physiological and cellular processes including cellular differentiation, protein degradation, regulation of gene expression, protein-protein interactions, signaling and regulatory processes (Mollova et al., 2015; Marquez et al., 2016). PTMs have a number of roles, including stimulating or suppressing protein functions that can have an impact on downstream signaling (Mollova et al., 2015). Thus, PTMs of CaMKIIδ can induce an autonomously active form of the kinase, a process that has been associated with pathological cardiac signaling (Cutler et al., 2012; Erickson et al., 2015). While this thesis will focus on one specific PTM of CaMKIIδ, S-nitrosylation, I will briefly describe three others known to modify CaMKII activity below.

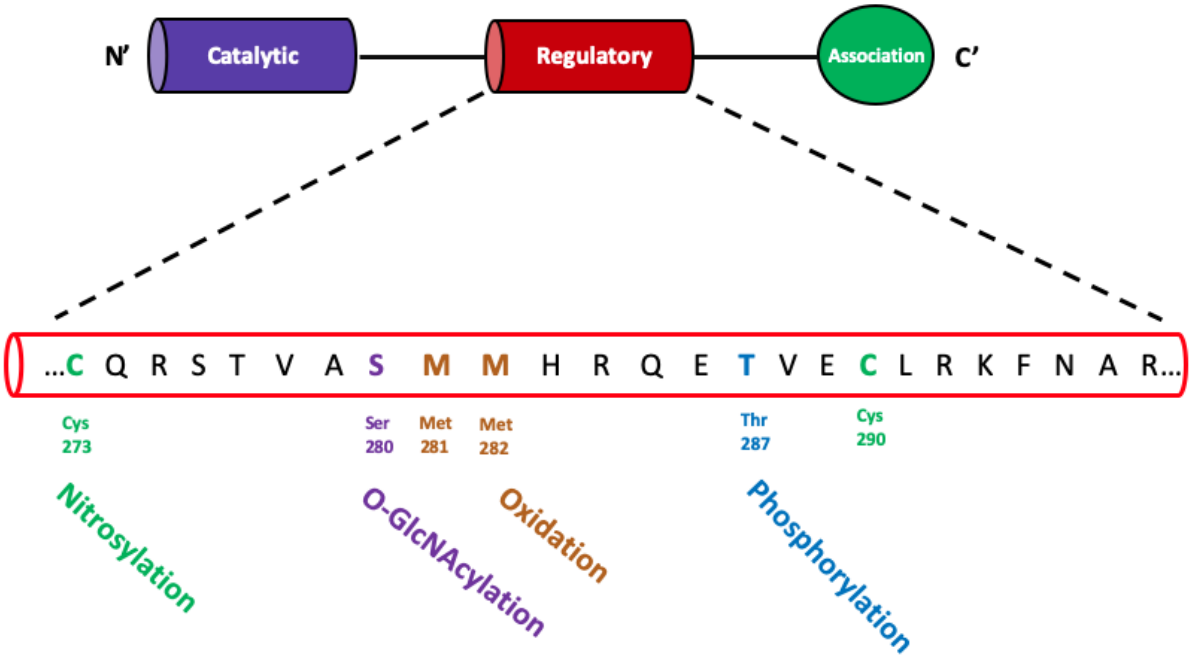

Figure 1.6 Post-translational modification sites of CaMKIIδ. CaMKII is susceptible to PTMS that can bind on the regulatory domain. Nitrosylation (Cys 273 and Cys 290 residues), O-GlcNAcylation (Ser 280 residue), Oxidation (Met 281 and Met 282 residues) and phosphorylation (Thr 287 residue). Original schematic by Esther Asamudo.

1.6.1 Auto-Phosphorylation

When CaMKIIδ activation is extended due to prolonged Ca^{2+}/CaM association, it undergoes autophosphorylation and a phosphate group is added at Thr287, resulting in autonomous activity (Erickson et al., 2008). Autophosphorylation is important because the resultant effects foster the binding affinity of CaM to the regulatory domain of CaMKII and also prohibits the autoinhibition of the kinase independent of a fall in I_{ca} and dissociation of CaM from CaMKII. Autophosphorylation of CaMKII contributes to a number of cellular processes. For example, nuclear targeting of CaMKII is mediated by autophosphorylation, which could affect both transcriptional regulation and downstream signaling of CaMKIIδ (Mollova et al., 2015). Autophosphorylation of CaMKII is known to be downstream effect of ß-adrenergic signaling which contributes to the progression of cardiac hypertrophy and dilated cardiomyopathy (Zhang et al., 2003; Erickson, 2014).

1.6.2 Oxidation

Oxidative stress is defined as an imbalance between the production of ROS and antioxidant defences which could cause injuries in the tissues (Betteridge, 2000). Ca^{2+} elevation in pro-oxidant conditions leads to facilitation of Ca^{2+}/CaM activity by ROS. Oxidation can activate CaMKII through aldosterone- and angiotensin II-dependent increase in ROS (He et al., 2011).

Elevated levels of reactive oxygen species (ROS) facilitate the development of cardiovascular diseases. Erickson et al. (2008) showed that CaMKII activity can be sustained by oxidation of paired regulatory domain methionine residues (Met281/282), and that this process could lead to myocardial apoptosis, electrical remodelling, impaired cardiac function and increased mortality after myocardial infarction (Rajtik et al., 2017). Diabetic mice which were also CaMKII oxidation-resistant were found to be protected against myocardial infarction and fibrosis compared to WT diabetic mice, suggesting that oxidation of the methionines 281/282 sites on the regulatory domain of CaMKII plays a role in myocardial infarction (Luo et al., 2013).

1.6.3 O-GlcNAcylation

This is a type of glycosylation that involves attachment of single O-linked N-acetylglucosamine (O-GlcNAc) moieties to Ser and Thr residues on the regulatory domain of CaMKII. CaMKII is autonomously activated by O-GlcNAc modification of CaMKII at Ser279 during physiological stress as seen in acute hyperglycemic conditions. This process alters protein function and contributes to cardiac mechanical function and arrhythmias in diabetes (Erickson et al., 2013; Daniels et al., 2018). Erickson et al. (2013) found that CaMKII modification by O-GlcNAc was greater in hearts of patients with heart failure and diabetes compared to patients with only heart failure but not diabetic. Spontaneous Ca^{2+} release, which is enhanced by CaMKII activation, leads to cardiac and neuronal pathophysiology in diabetes. Mesubi et al. (2020) showed that CaMKII contributed to increase susceptibility of diabetic mouse hearts to atrial fibrillation via elevated protein O-GlcNAcylation.

1.6.4 S-nitrosylation of CaMKII

One of the signaling pathways of NO involves a PTM called S-nitrosylation. S-nitrosylation is the covalent and reversible attachment of nitric oxide-related species to a thiol side chain of a cysteine residue in order to form S-nitrosothiol (Bradley & Steinert, 2016; Marquez et al., 2016). S-nitrosylation sites have been observed in the neuronal and cardiac isoforms of CaMKII. Recently, in the delta isoform of CaMKII found in the heart, two sites on the regulatory domain, C273 and C290 have been confirmed to be involved in S-nitrosylation (Erickson et al., 2015). Further details on how CaMKII S-nitrosylation may affect cardiac function will be discussed in this Section 1.7.1.

1.7 CaMKII and arrhythmias

Post-translational modification of CaMKII is known to contribute to arrhythmia in cardiac disease animal models. Calcium mishandling by Ca^{2+} handling proteins in cardiomyocytes during hyperactivation of CaMKII is the cause of proarrhythmic electrical modelling (Erickson et al., 2011). Some studies have shown links between CaMKII and arrhythmias, as seen in diabetic hyperglycaemia, ß-AR stimulation and

oxidative stress (Sag et al., 2009; Erickson et al., 2013; Lebek et al., 2018; Neef et al., 2018).

CaMKII-dependent regulation of diastolic SR Ca^{2+} release is the important cellular mechanism that enables the kinase to promote arrhythmias (Vincent et al., 2014). Intracellular Ca^{2+} release is enhanced by opening probability of the RyR2 during CaMKII phosphorylation (Wehrens et al., 2004). CaMKII phosphorylation of RyR2, increased SR Ca^{2+} leak and reduction in SERCA2a activity can result in Ca^{2+} overload in the mitochondria, potentially leading to diastolic dysfunction, arrhythmias and even cardiac death (Curran et al., 2007; Lim et al., 2017; Mohamed et al., 2018).

A study by Curran et al. (2007) showed that ß-AR activation can upregulate SR Ca^{2+} leak in rabbit cardiomyocytes via CaMKII and this was prevented by inhibiting CaMKII. Cardiac arrhythmias can be enhanced by ß-AR stimulation and inhibition of CaMKIIδ activity by knocking out CaMKIIδ prevented the induction of SR Ca^{2+} leak by isoproterenol.

Another mechanism that can lead to arrhythmia is inappropriate atrial depolarization that occurs during action potential. Development of early after depolarisations (EADs) and delayed afterdepolarisations (DADs) can be initiated by continuous CaMKII activation (Daniels, 2017). EADs occur before complete repolarisation and can be found in heart failure and arrhythmic conditions such as torsades des pointes (TdP), polymorphic ventricular tachycardia (PVT) and ventricular fibrillation (VF) (Weiss et al., 2010). DADs occur after complete repolarisation and in conditions of elevated intracellular Ca^{2+} due to SR overload (Daniels, 2017). In mice with heart failure and overexpressing CaMKIIδ, inhibition reduced the EAD arrhythmia events thereby preventing CaMKII-dependent effects on RyR2 (Sag et al., 2009).

As described earlier, oxidation is one of the several mechanisms that can prolong the activation of CaMKII. It was found that the animal model of Duchenne muscular dystrophy was more susceptible to DADs and triggered ventricular arrhythmias was observed even in isolated hearts from same mouse model. Genetic inhibition of oxidative CaMKII prevented DAD incidence and prevented ventricular arrhythmias (Wang et al., 2018). Genetically modified mice which was resistant to CaMKII oxidation were treated

with angiotensin II and found to be resistant to atrial fibrillation, a form of arrhythmia compared to wild-type mice infused with angiotensin II, suggesting that CaMKII oxidation increases AF susceptibility in response to angiotensin II in mice (Purohit et al., 2013).

In diabetic heart dysfunction, Erickson et al. (2013) reported O-GlcNAc-induced and glucose-dependent increase in Ca^{2+} sparks frequency in WT cardiomyocytes but not in CaMKIIδ-KO cardiomyocytes. This was suggested to occur through a CaMKII pathway as pharmacological inhibition using a CaMKII inhibitor reduced Ca^{2+} sparks in intact isolated cardiomyocytes. Elevated CaMKII activity has been confirmed in diabetic rat hearts, and treatment of these hearts with caffeine/dobutamine made them more susceptible to arrhythmias. This effect was blunted by an O-GlcNAc inhibitor. Taken together, these suggest arrhythmic events in diabetes are CaMKII and O-GlcNaC-dependent (Erickson et al., 2013). In pre-diabetic animal model, it was demonstrated that CaMKII-dependent phosphorylation of RyR2 promoted SR Ca^{2+} leak and led to increase in Ca^{2+} spark frequency, CaMKII inhibition in same mouse model, ablated this effect (Sommese et al., 2016). However, there has been no study that fully elucidates how NO triggers arrhythmias via CaMKIIδ signaling pathway in the whole heart.

1.7.1 CaMKII S-nitrosylation and arrhythmias

A few studies have shown that NO-mediated CaMKII signaling contributes to cardiac arrhythmias. Curran et al. (2014) showed that NO-dependent increased in SR Ca^{2+} leak led to spontaneous Ca^{2+} waves. Inhibition of NOS activity with N-omega-nitro-L-arginine methyl ester (L-NAME), a non-selective NOS inhibitor, led to reduction of SR Ca^{2+} leak when compared to myocytes stimulated with isoproterenol (ISO), a ß-AR agonist, in the absence of L-NAME. Specific inhibition of NOS1 in the presence of ISO also showed a reduction in active myocytes while inhibition of NOS3 had no effect. The NOS1 isoform also plays a role in NO-mediated CaMKII signaling as shown by Curran et al. (2014), that ß-adrenergic stimulation did not increase Ca^{2+} leak in ventricular myocytes from NOS knockout ($NOS1^{-/-}$) mice. Their study showed that ISO treatment of $NOS1^{-/-}$ mouse myocytes did not increase SR Ca^{2+} leak above control levels and inhibition of CaMKII did not facilitate the leak. However, in the presence of an NO donor, S-nitroso-N-acetyl-D,L-penicillamine (SNAP), SR Ca^{2+} leak increased in $NOS1^{-/-}$ mouse

myocytes. This showed that NOS1-dependent CaMKII activity mediates SR Ca^{2+} leak. Therefore, there is a relationship between NO-dependent activation of CaMKII and increased SR Ca^{2+} leak. ISO increased CaMKII phosphorylation in wild- type C57BL/6 mouse myocytes, but this was absent in $NOS1^{-/-}$ mouse myocytes. However, there was no difference when oxidised CaMKII was stimulated by ISO in WT and $NOS1^{-/-}$ mice. In conclusion, ISO dependent increase in SR Ca^{2+} leak was dependent on NO signaling and CaMKII activation (Curran et al., 2014).

Another study showed that CaMKII was responsible for modulation of Ca^{2+} spark frequency during ß-AR stimulation. This study involved inhibiting CaMKII activity in Guinea pig ventricular myocytes, it was observed that the CaMKII inhibitors, KN93 and Autocamtide-2-Related Inhibitory Peptide (AIP) prevented increases in Ca^{2+} spark frequency in the presence of ISO while SR Ca^{2+} content was unchanged. This finding was similar to that of Curran et al. (2014). This study demonstrated that NO donor, GSNO, reproduced increases in Ca^{2+} spark frequency induced by ß-AR stimulation. On inhibition of CaMKII with AIP, it was observed that Ca^{2+} spark frequency was not significantly elevated by GSNO. This was further confirmed by in vitro quantification of NO-dependent CaMKII activation and concluded that nitrosylation of CaMKII modulated spark frequency even in the absence of Ca^{2+} signals (Gutierrez et al., 2013).

Taken together, these results show that autonomous activation of CaMKII by NO induced an increase in frequency of spontaneous SR Ca^{2+} release (Ca^{2+} sparks) which is a predictor of arrhythmias.

1.8 CaMKII Inhibition in the heart

1.8.1 Pharmacological Inhibitors

Considering the deleterious effects of CaMKII in pathophysiological conditions, pharmacological inhibition of CaMKII has offered positive outcomes as seen in diabetic heart disease, heart failure, arrhythmias and myocardial infarction (Zhang et al., 2005; Vila-Petroff et al., 2007; Sag et al., 2009; Erickson et al., 2013; Daniels et al., 2018; Neef et al., 2018).

There are numerous CaMKII inhibitors used to elucidate the physiological effects of CaMKII in cells. However, KN93 and AIP are the widely used CaMKII inhibitors. KN93 acts by selectively and competitively binding to the Ca^{2+}/CaM thereby preventing its interaction with the binding site on the regulatory domain of CaMKII (Johnson et al., 2019; Wong et al., 2019). In a study by Sag et al. (2009), CaMKII inhibition with 20 µmol/L/kg of KN93 reduced the incidence of in vivo cardiac arrhythmias in mice overexpressing CaMKIIδ_C. However, there is also evidence that KN93 has a CaMKII-independent effect which involves its direct interaction with a variety of ion channels and potentially, other kinases (Anderson et al., 1998; Tessier et al., 1999; Wu et al., 1999; Wong et al., 2019). A drawback in the use of KN93 is its effect on delayed rectifier potassium current (I_{Kr}) which plays a role in cardiac repolarisation. KN93 can inhibit I_{Kr} through a pathway independent of CaMKII and result in cardiac arrhythmias (Hegyi *et al.*, 2015). Therefore, the use of KN93 to inhibit CaMKII may interfere with the outcomes of studies investigating CaMKII inhibition and arrhythmias.

AIP is a peptide-competitive and highly specific CaMKII inhibitor which acts by blocking the catalytic domain and is more effective in inhibiting the kinase in an autonomous state compared to KN93 (Ishida et al., 1995; Daniels et al., 2018). In a study investigating the role of CaMKII activation in cardiac function using trabeculae of rat model of type 2 diabetes, AIP fully restored developed force, and rates of contraction and relaxation compared to KN93 which partially restored the myocardial function parameters (Daniels et al., 2018).

1.8.2 CaMKII knockout mouse models

In addition to CaMKII inhibitors, transgenic mouse models with global deletion of one or more CaMKII isoforms have been developed. CaMKIIδ-deficient mice as generated by Ling et al. (2009) did not have any significant impairment in cardiac function compared to the C57BL/6 wild-type (WT) mice. CaMKIIδ deletion did not cause any increase in mortality and the mice did not exhibit any abnormality in their basal cardiac function measured via echocardiography (Backs et al., 2009; Grimm et al., 2015). According to Backs et al. (2009), CaMKIIδ-KO mice were protected against hypertrophy and fibrosis, when induced with pressure load via thoracic aortic constriction. Knocking out CaMKIIδ did not alter the response of CaMKIIδ-KO mice hearts to ß-AR stimulation

in comparison with WT mice hearts, however they were protected from fibrosis induced by chronic ß-AR stimulation (Grimm et al., 2015). In order to prevent off target effects of CaMKII inhibitors, CaMKIIδ-KO mouse model is preferred for investigating the role of CaMKIIδ in the heart.

1.9 Conclusion

Consistent with other studies, PTMs like S-nitrosylation can lead to cardiovascular diseases. Since the improvement in survival of CVDs is likely to have a great impact on the health system, it is important that the mechanism underlying this is understood. Even though previous studies have shown that NO can modulate CaMKII function via S-nitrosylation and contribute to pathological signaling, the mechanism of this process is elusive. According to Erickson et al. (2015), nitrosylation of CaMKIIδ happens at two key sites, Cys-273 and Cys-290. Depending on which of them becomes nitrosylated, CaMKII activity can either be activated or inhibited. They showed that nitrosylation at Cys-290 site increases CaM-binding and nitrosylation at Cys-273 site appears to reduce CaM-binding, therefore ablates the effect of CaMKIIδ autonomous activity. This evidence suggests that the activation state of CaMKII is important when considering the possibility of nitrosylation of the kinase.

Therefore, further understanding is required as to how S-nitrosylation affects cardiac function to cause arrhythmias, how the role of the two nitrosylation sites, Cys-273 and Cys-290 contribute to the alteration of whole heart function, and also how targeted permanent inhibition of CaMKIIδ can help attenuate the outcomes of autonomous activation of CaMKIIδ in the heart.

1.10 Overview and scope of thesis

This thesis assessed the effects of NO-mediated CaMKIIδ activity in pathological cardiac signaling. The main aim of this study was to determine the role of NO in the modulation of CaMKII and how this contributes to development of cardiac arrhythmias. Firstly, I determined the effect of acute NO treatment on contractile parameters in isolated hearts from 3 mouse models; a model with intact CaMKII, a model without CaMKIIδ, and a model lacking both cardiac isoforms CaMKIIδ and CaMKIIγ (Chapter 3). I also assessed

the effect of ß-adrenergic signaling and NO treatment on cardiac function of isolated mouse hearts with intact CaMKIIδ (Chapter 4). Finally, I investigated the effects of chronic NO treatment on cardiac function in isolated hearts from mouse models with and without CaMKIIδ (Chapter 5).

1.10.1 Aims and Hypotheses

The three key aims of this project were:

Aim 1. Effects of acute NO-mediated CaMKII activation on cardiac function.

This was to determine the acute effects of NO on the cardiac contraction and relaxation in mice lacking cardiac isoforms of CaMKII. I hypothesized that NO could alter cardiac contraction and relaxation and will prevent cardiac arrhythmias in mice lacking the cardiac isoforms of CaMKII. To test this hypothesis, I performed echocardiography to determine the baseline cardiac function of 12-week old C57BL/6 wild type mice and CaMKIIδ-KO mouse models. Subsequently, I isolated the hearts from these mouse models and treated the hearts with different concentrations of a NO donor, S-nitrosoglutathione (GSNO), using Langendorff isolated heart perfusion technique. Then I measured the contractile parameters and quantified the arrhythmias in the isolated hearts from this setup. I did gel electrophoresis and western blotting to determine expression levels of CaMKII in the stored heart tissues.

Aim 2. Effect of ß-adrenergic stimulation and NO treatment on cardiac function in WT mice.

This was to determine how NO-mediated activation of CaMKII and ß-adrenergic signaling affects cardiac function in mice with intact cardiac CaMKII. I hypothesized that treating mouse hearts with a NO donor, GSNO and a non-selective ß-AR agonist, isoproterenol (ISO) will cause S-nitrosylation of CaMKII and enhance cardiac arrhythmias. To test this hypothesis, I isolated hearts from 12-week old C57BL/6 mice and perfused them with GSNO and ISO. During the perfusion, I measured cardiac contraction and relaxation, and counted the number of arrhythmias. I alternated the order of the drug treatment, ISO before GSNO and GSNO before ISO. The aim was to

determine if the timing of NO-mediated CaMKII activation may influence ß-adrenergic induced arrhythmias in the heart. The tissues were then saved for determination of protein expression and activity levels (phosphorylated and nitrosylated proteins).

Aim 3. Cardiac alterations associated with chronic NO treatment in mouse hearts.

In this aim, I measured the chronic effects of NO on the cardiac function of wild type and CaMKIIδ-KO mice. I hypothesized that NO may alter cardiac function and mice lacking CaMKIIδ will be resistant to NO-induced cardiac arrhythmias. I administered GSNO to 13-week old mice for 5 weeks and performed echocardiography before and after the treatment. The mice hearts were isolated at the end of the treatment protocol and perfused with GSNO while the cardiac function parameters were measured. Plasma samples from the mice were obtained and analysed for NO concentration. I also determined expression levels of total, phosphorylated and nitrosylated CaMKII.

CHAPTER 2: MATERIALS AND METHODS

2.1 Animal Models

2.1.1 Wild-type C57BL/6 Mouse

The wild-type C57BL/6 mouse is an inbred laboratory genotype of mice. It is a non-pathological model that has normal expression of the δ and γ cardiac isoforms of CaMKII. It will be referred to as WT throughout this thesis.

2.1.2 CaMKIIδ-KO Mouse

I used a genetically modified genotype of mouse with the C57BL/6 background, but deficient of the predominant cardiac isoform of CaMKII, δ (Ling et al., 2009). It will be referred to as knockout (KO).

2.2 Animal Husbandry

The mice were housed and maintained in University of Otago's animal facility (Hercus Taieri Resource Unit), in a controlled environment of 12-hour light/dark cycle and temperature of 21 ± 1 ^{o}C. The mice were fed standard chow diet (Teklad Diet, Wisconsin, USA) and water was available ad libitum. All experimental protocols were carried out according to procedure guidelines approved by the University of Otago Animal Ethics Committee (Dunedin, New Zealand) (AUP – 9/15) and in accordance with New Zealand Animal Welfare Act (1999). The mice were weighed at the commencement of each experiment, and the body weights and ages were recorded. The age or weight of the animals is specified in each chapter.

2.3 Echocardiography

This is a non-invasive imaging technique used to view the anatomical structures of the the heart and assess cardiac function (Gao et al., 2000). Transthoracic echocardiography procedures in all mouse models were performed with a high-resolution ultrasound echocardiogram machine (Vivid E9, General Electric Vingmed Ultrasound, Norway).

The mouse was placed in a closed chamber and anaesthetised by continuous inhalation of 2% isoflurane gas and 0.5 L/min of 100% O_2. As soon as loss of righting reflex was observed, the mouse was taken out of the chamber and placed in a supine position, with the limbs partially taped to the board, on a warm heating pad to maintain body temperature at 37ºC. The mouse was then placed in a nose cone to ensure continuous inhalation of the isoflurane gas maintained at 1.5%. The chest hair was shaved using a hair removal cream. Ultrasound probe with the frequency of 11-MHz was coated with gel and placed on the thoracic area of the mouse to obtain images along the long and short axes of the heart (see Figure 2.1). All captures were obtained at the level of the papillary muscles. The images were analysed offline and each measurement was obtained from an average of 15 cardiac cycle measurements. To prevent bias, I was blinded by another researcher before echocardiography data analysis.

2.3.1 Left ventricle structure and systolic function

Two-dimensional (2D) echocardiographic parameters were obtained from the parasternal short-axis in M-mode (see Figure 2.2). The measurements obtained include, LV interventricular septal thicknesses at diastole and systole (IVSd, IVSs), LV internal dimension at diastole and systole (LVIDd, LVIDs), and posterior wall thicknesses at diastole and systole (LVPWd, LVPWs) and R-R Interval. End diastolic volume (EDV), end systolic volume (ESV), ejection fraction (EF), fractional shortening (%FS), stroke volume (SV), cardiac output (CO) and heart rate (HR) were calculated from the obtained measurements.

2.3.2 Left Ventricular diastolic function

Using pulse wave doppler, trans-mitral inflow doppler in the long-axis measured the peak velocities of early (E wave) and late (A wave) filling of mitral inflow, and E/A ratio. Deceleration time (DT) of early filling of mitral inflow was also obtained by measuring the peak of E wave to the baseline (Figure 2.3).

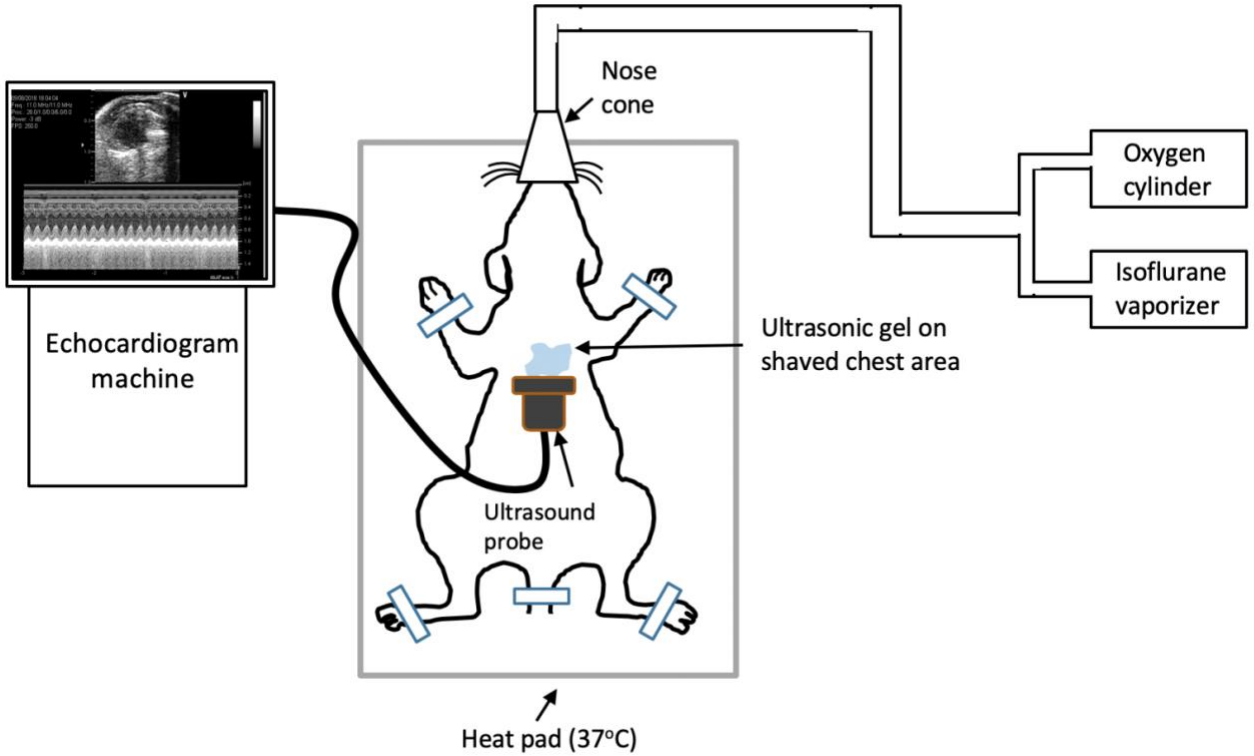

Figure 2.1 Echocardiography setup. Animal under anaesthesia placed in a supine position on a heat pad to maintain body temperature at 37 °C. Probe connected to echocardiograph machine placed on the shaved area of the chest. Anaesthesia was maintained through the nose cone with 0.5 L/min 100 % oxygen and 1.5 – 2 % isoflurane. Original Figure by Esther Asamudo.

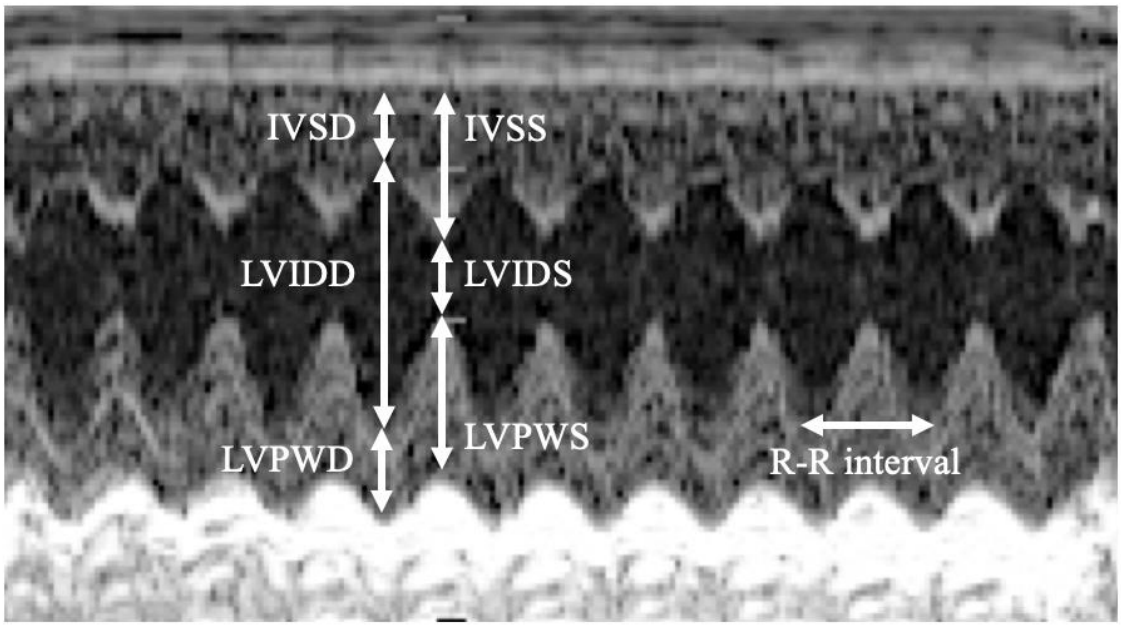

Figure 2.2 A sample M-mode image capture for assessment of left ventricular structure and systolic function. LV interventricular septal thicknesses at diastole and systole (IVSd, IVSs), LV internal dimension at diastole and systole (LVIDd, LVIDs) and Posterior wall thicknesses at diastole and systole (LVPWd, LVPWs) and R-R interval.

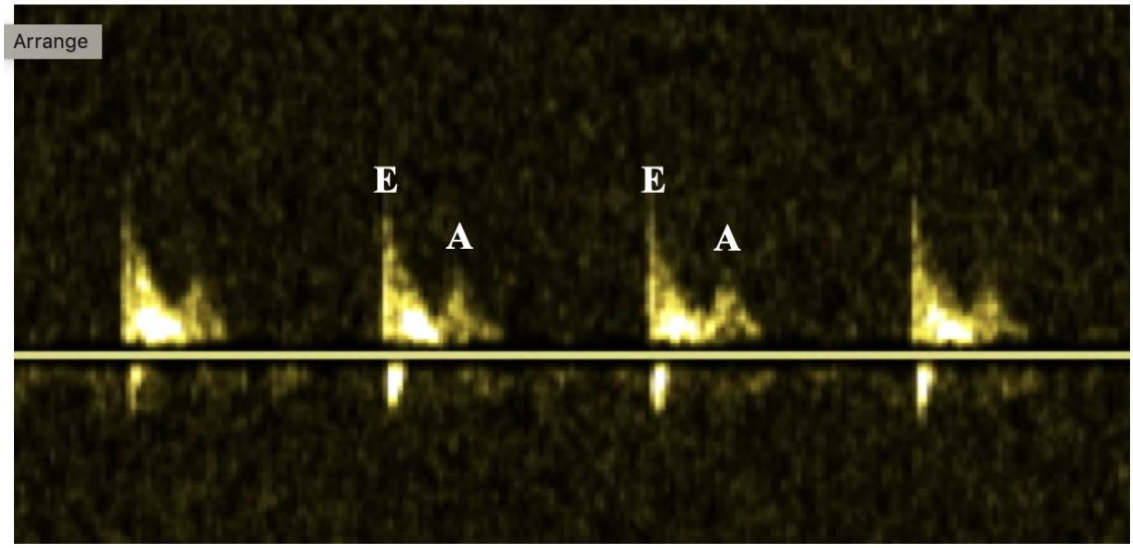

Figure 2.3 A representative pulse wave doppler image for assessment of left ventricular diastolic function. Peak velocities of early (E) and late (A) filling of mitral flow.

2.4 Langendorff isolated heart perfusion

This is a perfusion system that provides information on cardiac function, including inotropy and chronotropy without the interference of other body systems or hormones (Reichelt *et al.*, 2009; Bell *et al.*, 2011; Liao *et al.*, 2012). It is designed in a way that even though the heart is outside the body, it still receives adequate oxygenation and nutrient delivery to maintain its viability and optimal function in order to aid the experiment *ex vivo*.

The Langendorff rig setup (see Figure 2.4) consisted of a 23-guage cannula, a thermostatically controlled water bath (Lauda, Germany), peristaltic pump (Gilson, France), flow meter (Transonic systems Inc., USA) and pressure pump controllers, coronary pressure and LV pressure transducers (ADInstruments, Australia), intra ventricular (LV) balloon, bubble trap/heat chamber, compliance chamber, double-jacketed organ bath, oxygenators for carbogen, Powerlab data acquisition system and LabChart software (ADInstruments, Australia).

The heart was perfused with a modified Krebs-Henseleit Buffer (KHB) containing the following salts and concentrations: NaCl 118.5 mM, KCl 4.7 mM, $MgO_4S.7H_2O$ 1.2 mM, $KH_2PO_4.H_2O$ 1.2 mM, $NaHCO_3$ 25 mM, Glucose 11 mM, Pyruvate 2 mM, $CaCl_2.2H_2O$ 2 mM. To arrest the heart after dissection, the KHB solution was modified to KCl 18.8 mM and did not contain pyruvate and $CaCl_2.2H_2O$. The perfusion solution was stored in a cylinder and placed in the water bath heated to 37^{o}C. The solution was continuously gassed with carbogen (95% O_2 and 5% CO_2) for oxygenation and maintenance of pH at 7.4 and then delivered to the isolated heart through tubes controlled by a peristaltic perfusion pump. The compliance chamber was a 50 ml syringe filled partly with air and about 10 ml of KHB, this was to act in the way the compliant walls of the aorta would in vivo to allow for consistency in systolic and diastolic cycles and consistent perfusion. The arresting solution for the heart was in a beaker placed on ice and gassed with carbogen (95% O_2 and 5% CO_2) prior to excision of the heart.

2.4.1 Heart Excision

Under anaesthesia with isoflurane (5% at 0.5 L/min of oxygen), the mouse was injected intraperitoneally with anticoagulant, heparin (10,000 U/kg). Five minutes after the heparin injection, the fur was pulled up and cut, the peritoneum was cut to the left and right, to expose the thoracic cavity. The rib cage was cut on both sides, raised and clipped back. Once the beating heart was exposed, the aorta was identified and clipped. The heart was excised and placed in a beaker containing the gassed ice-cold high KCl KH buffer solution (arresting solution) before being transferred to the petri-dish for cannulation. The excision and cannulation was performed in less than 5 minutes to ensure viable heart function.

2.4.2 Cannulation

The aorta was identified and picked up with tweezers on the edge. Using another set of tweezers, the other edge of the aorta was clipped and pulled up like a sock on the cannula (a blunt-ended grooved 23-guage needle). Using a fine edged clip, the aorta was secured on the cannula temporarily, and then tied with a thin suture, the flow from the buffer was increased to begin perfusion and restart the heartbeat. A second suture was knotted. Excess tissues surrounding the aorta were carefully trimmed off. The cannula with the heart was hung vertically and placed in the warmed perfusate which was passed through a 0.45 μm GVS filter (GVS, USA) before entering the coronary circulation via the aorta (see Figure 2.5). The coronary pressure was maintained at an average of 75 mmHg and coronary flow rate range of 1.5 ml/min – 4.5 ml/min. The heart was allowed to stabilize for 5 minutes. Flow rate was determined by pressure pump controller to maintain constant perfusion pressure. Coronary flow was measured in real time using an in-line flow probe in the perfusion line. Hearts with coronary flow greater than 4.5 ml/min were excluded as that could be indication of a tear in the aorta and hearts with flow rate lower than 1.5 ml/min were also excluded as it indicated that there could be an air bubble in the coronary circulation therefore inadequate perfusion.

2.4.3 Pressure measurements

Coronary pressure was measured by a line connected via the sidearm of the cannula to the pressure transducer. The coronary pressure transducer was calibrated using a sphygmomanometer. LV systolic and diastolic pressures were measured using a custom-made balloon attached to a pressure transducer. The balloon was made from saran wrap and a polyethylene PE-50 tube. One end of the tube was connected to a syringe filled with ~20 µl of Milli-Q water. A small square was cut out from the saran wrap and attached to the other end of the tube, then tied loosely with a thin suture to form a balloon (see Figure 2.6). The balloon was then inflated gently with the Milli-Q water via pressure on the syringe to slowly expel air bubbles. Once it was ensured that air bubbles were expelled, the knot was then tired securely. The balloon was then inspected for leaks, and a second suture was to prevent any leaks. The LV balloon was connected to a pressure transducer. The left atrium was cut and removed to expose the atrioventricular (AV) valve. The balloon was deflated and carefully pushed into the LV and secured in place with a tape around the clamp holding the cannula.

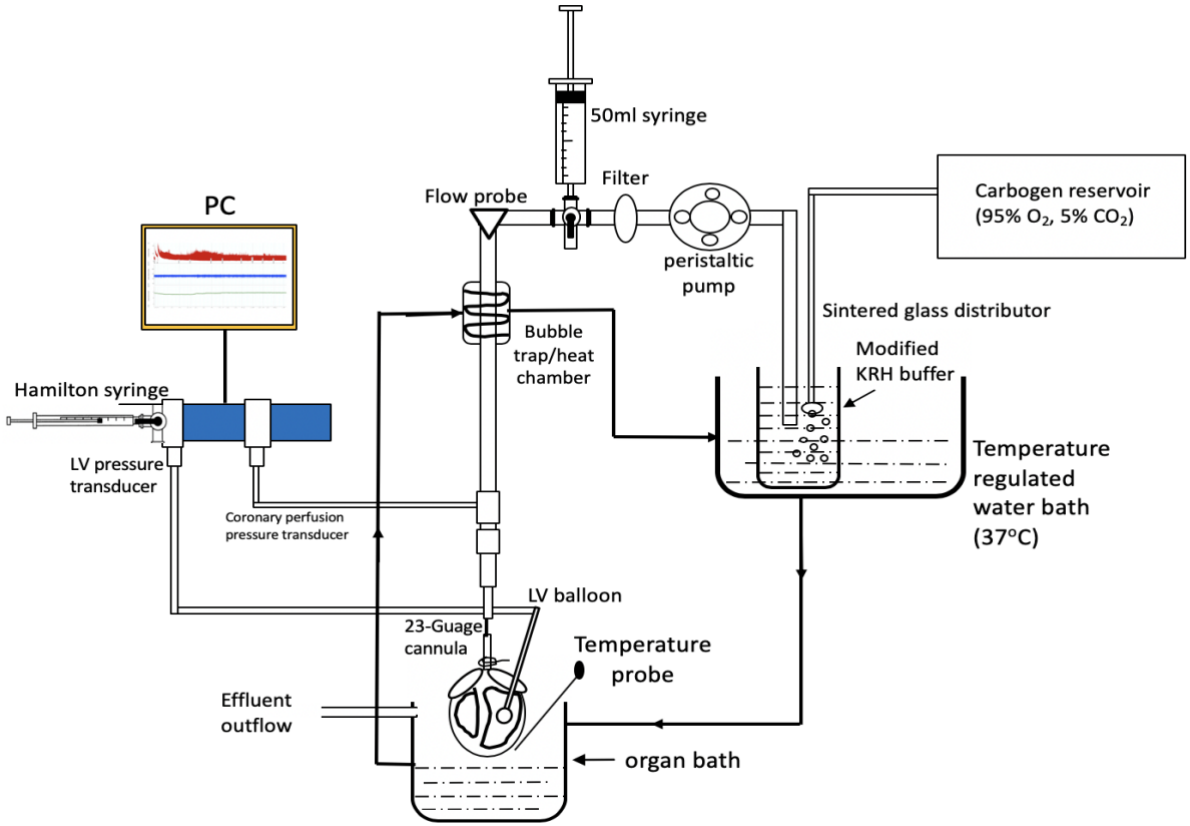

Figure 2.4 Langendorff isolated heart setup. The mouse heart cannulated and immersed in the organ bath with a temperature probe to ensure that temperature of 37°C is maintained. The gassed KHB flowed through the tubes and was pumped by the peristaltic pump into the system, it passed through the filter, compliance chamber, the in-line flow probe, the bubble trap/heat chamber and then into the isolated heart. The transducers were connected to a powerlab which generated signals that were recorded using LabChart software to determine coronary perfusion pressure and LV pressure (connected to the balloon in the left ventricle of the heart). Original figure by Esther Asamudo.

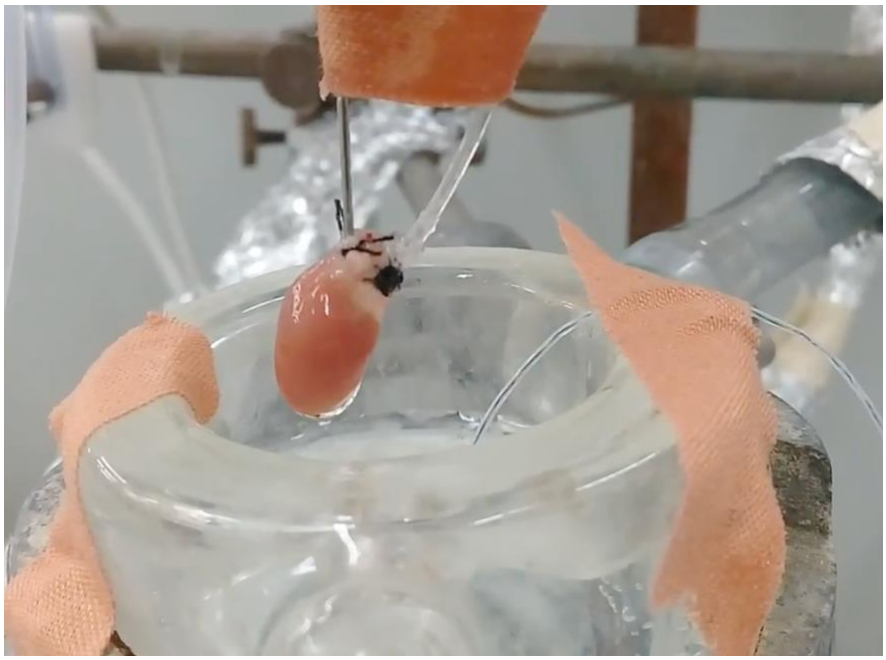

Figure 2.5 Representative image of an isolated mouse heart on a Langendorff rig. The balloon is inserted into the left ventricle of the heart via the left atrioventricular valve and secured by taping it to the top part of the cannula.

inflated **deflated**

Figure 2.6 Mouse ventricular balloon.

The balloon was custom made in the laboratory using a polyethylene tube, saran wrap and thread. Deflated before inserting into the left ventricle and inflated when it is in the left ventricle.

2.4.4 Experimental Protocol

The balloon was inflated with 5 – 15 µL of Milli-Q water in order to stretch the myocardial fibres and achieve a left ventricular end-diastolic pressure (LVEDP) of 5 – 10 mmHg. The heart was then immersed in the temperature-controlled organ bath filled with pre-warmed buffer. The LV pressure trace was monitored for consistent steady-state pressure development and normal heart rhythm before obtaining basal heart function parameters. The transducers measured coronary pressure, coronary flow rate and LV pressure. At the end of the experiment, the left and right ventricles were dissected off the cannula and snap frozen in liquid nitrogen and stored at -80^{o}C. The recorded trace (Figure 2.7) was saved for offline analysis.

2.4.5 Offline analysis

Using Labchart 7.0 software (ADInstruments, Australia), the following parameters were obtained; left ventricular developed pressure (LVDP), heart rate (HR), maximum and minimum rate of developed pressure (Max dP/dt and Min dP/dt). LVDP is the change in peak systolic pressure and diastolic pressure. Heart rate is the number of beats per 60 seconds, calculated from the systolic and diastolic cycle duration. Max dP/dt is the steepest slope during the upstroke of the LV pressure curve, indicating rate of contraction and min dP/dt is the steepest slope during the downstroke of the LV pressure curve, indicating rate of relaxation. Pressure-Time integral is the index of average pressure developed by the cardiac muscle per beat and is derived from the product of average developed pressure and systolic time. The last 3 minutes of the recorded trace (Figure 2.8) per protocol was selected and analysed to obtain the average for each parameter. The abnormal beats (arrhythmia events) were counted individually in the last 3 minutes of each protocol to obtain an average. The data from the software was exported for processing and analysis.

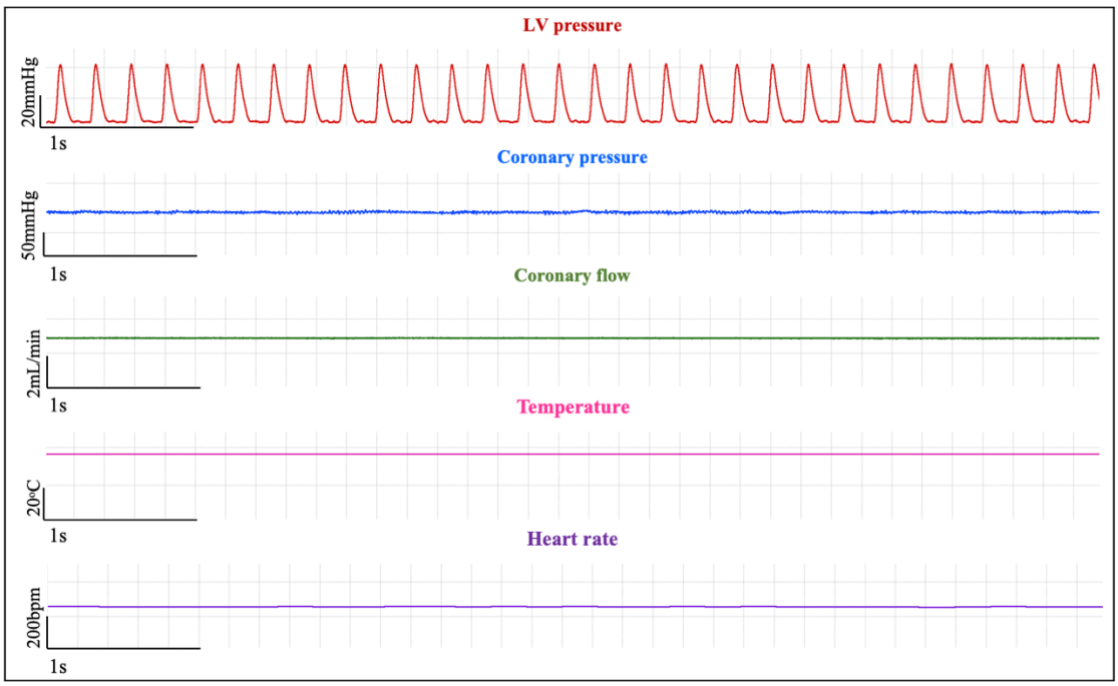

Figure 2.7 A sample trace recording from LabChart during Langendorff isolated heart Perfusion, showing the traces of a full experiment, indicating LV pressure, coronary pressure, coronary flow, temperature and heart rate of the isolated heart.

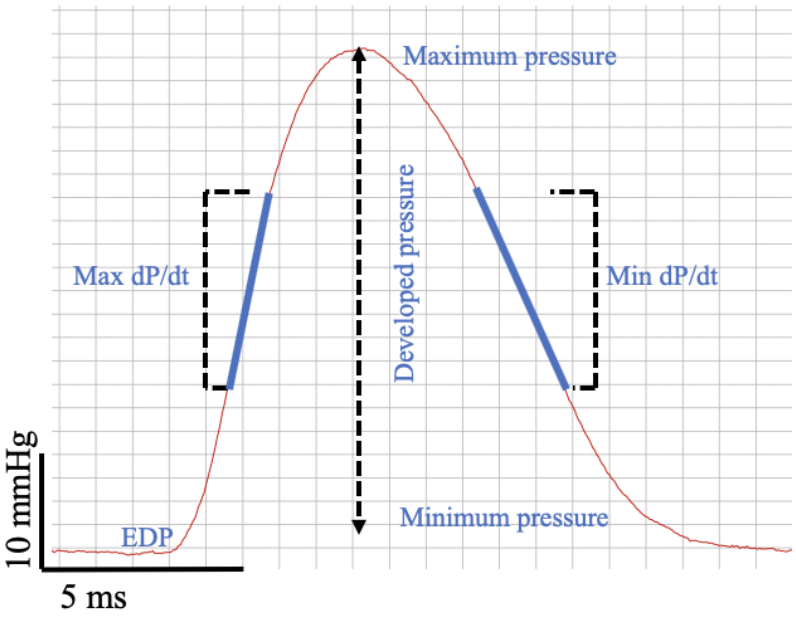

Figure 2.8 Representative image from LabChart showing analysis parameters; Developed pressure (maximum pressure – minimum pressure), Max dP/dt (Rate of contraction), Min dP/dt (Rate of relaxation) and End diastolic pressure (EDP).

2.4.6 Determination of arrhythmias

Arrhythmia count was done according to the method of Huggins et al. (2008). The different types of arrhythmias identified in the isolated mouse hearts included; ventricular premature beats (VPBs), bigeminy, trigeminy, potentiated contraction and ventricular tachycardia (VT) (Figure 2.9). VPBs were defined as an early contraction prior to relaxation and is often succeeded by a larger subsequent beat (Figure 2.9B). Bigeminy was defined as paired beats occurring in repetition (Figure 2.9C). Trigeminy was defined as a triplet beat occurring in repetition with every third beat as a premature beat (Figure 2.9D). Potentiated contraction was referred to as normal sinus rhythm then a slight delay before an increased single contraction and followed by resumption of sinus rhythm (Figure 2.9E). Ventricular tachycardia was defined as a run of four or more ventricular premature beats in quick succession (Figure 2.9F).

To determine severity, each heart was also evaluated by a 5-point arrhythmia score adopted from Curtis and Walker (1988). Score E from this previous study, was modified to include the following characteristics;

Table 2.1 Arrhythmia score classification

Arrhythmia Score	Characteristics
0	0 – 5 VPBs (no arrhythmias or isolated VPBs)
1	6 – 20 VPBs (very occasional bigeminy and trigeminy)
2	21 – 100 VPBs (frequent bigeminy, trigeminy and PCs)
3	> 100 VPBs or 1 – 2 episodes of VT
4	≥ 3 VT
5	VF or death

VPB, ventricular premature beats; PC, potentiated contraction; VT, ventricular tachycardia

The arrhythmias were counted from the start to the end of each protocol, characterized according to the arrhythmia scores and then recorded against the time (8, 16, 24, 32 minutes) and different doses depending on the group.

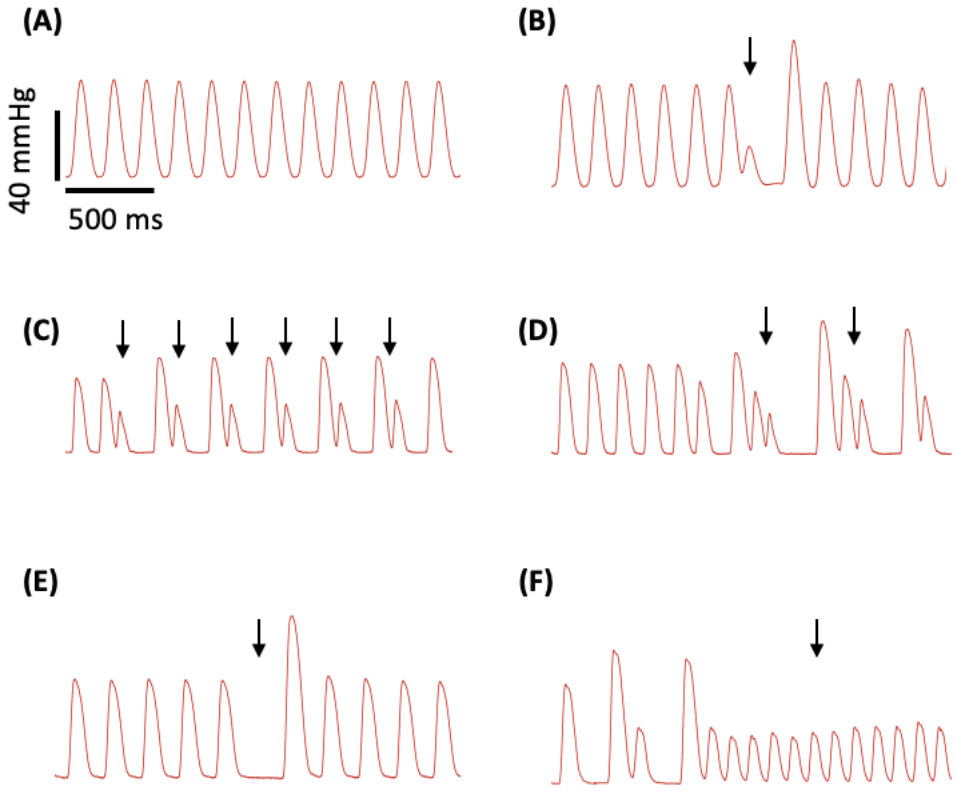

Figure 2.9 Sinus rhythm and arrhythmia events identified in isolated hearts. Representative traces showing (a) sinus rhythm (b) ventricular premature beats (c) bigeminy (d) trigeminy (e) potentiated contraction, and (f) ventricular tachycardia.

2.5 Sodium Dodecyl Sulphate – Polyacrylamide Gel Electrophoresis (SDS-PAGE) and Western Blotting

2.5.1 SDS-PAGE

To determine protein expression in mice heart tissues, acrylamide gels of 6% or 10% were made in gel casting plates with 1.5 mm spacers (BioRad) depending on the protein of interest. A resolving gel (see Table 2.2) was cast and topped up with Milli-Q water to prevent an uneven layer and achieve a flat-topped gel solution. The resolving gel was left to polymerise for 1 hour. This process was followed by discarding the Milli-Q water overlaying the resolving gel and loading of the stacking gel (see Table 2.2). This was immediately followed by inserting a 15-well comb to create wells for loading samples. The stacking gel was allowed to polymerise for 1 hour.

2.5.2 Homogenisation of cardiac tissue

Ventricular heart samples were obtained from perfused isolated hearts tissues and used for Western blotting . The frozen tissues were thawed and placed in 2 ml micro centrifuge tubes. Magnetic beads (Advance Inc., USA) were added to the centrifuge tubes with Radio Immunoprecipitation Assay (RIPA) buffer including phosphatase and protease inhibitors (see Table 2.3). The tubes were placed carefully in a bullet blender and the tissues were blended for 4 minutes at speed 8 after which samples were taken out and visually inspected for complete homogenization. The samples were left to cool on ice for 15 minutes, then centrifuged at a speed of 15,000 rcf at 4^{o}C for 15 minutes. The supernatant was taken and stored in 1.5 ml tubes. The total protein concentrations of the homogenates were measured using the protein A280 method (Simonian & Smith, 2006), RIPA buffer was used as blank. The homogenates were aliquoted, snap-frozen in liquid nitrogen and stored in -80^{o}C for future analysis.

Table 2.2 Constituents of resolving and stacking acrylamide for 10% gel

Chemicals	Resolving (µl)	Stacking (µl)	Supplier
Milli-Q water	3832	2516	Merck Millipore
1.5 M Resolving buffer (375 mM Tris)	2000	-	Biofroxx
0.5 M Stacking buffer (375 mM Tris)	-	1000	Biofroxx
40 % Acrylamide	2000	400	Merck
10 % SDS	80	40	Merck
10 % Ammonium Persulfate (APS)	80	40	Sigma
Tetramethylethylenediamine (TEMED)	8	4	Merck

Table 2.3 Constituents of RIPA Buffer

Chemical	Concentration	Supplier
Triton X-100	1 % (w/vol.)	Applichem
SDS	0.1 %	Merck
Tris-HCL (pH 7.4)	50 mM	Biofroxx
NaCl	150 mM	Applichem
EDTA	1 mM	Applichem
Phosphatase and Protease Inhibitors		
PMSF (Phenylmethane sulfonyl fluoride)	1 mM	Sigma
PhosSTOP	1X	Roche
cOmpleteTM	1X	Roche

2.5.3 Gel Electrophoresis

For gel electrophoresis, Milli-Q water was added to sample tubes, followed by 20 µg of protein homogenates and sample buffer (Tris 0.31 M pH 6.8, Glycerol 50 %, SDS 10 %, Dithiothreitol 0.5 M, Bromophenol blue 0.05 %). The diluted samples were then incubated on the heat block for protein denaturation. The temperature of the heat block and length of time was dependent on the protein of interest (Table 2.4). After protein denaturation, the sample combination was centrifuged at 13,500 rpm for 30 seconds at room temperature. When samples were ready to be loaded into the wells, the gel was placed in a vertical electrophoresis tank (BioRad) filled with running buffer (Glycine 1.92 M, Tris 0.25 M, SDS 1 %). Precision protein plus dual colour standard (4 µl; BioRad) was added to the first well to serve as molecular weight marker. The aim was to monitor the protein migration and also to help determine the size of protein of interest on the membrane. The subsequent wells were loaded with 5 µl of the prepared protein samples. Electrophoresis was then performed using the voltage and running times specified in Table 2.4.

2.5.4 Western blotting

A wet tank transfer of the proteins from the acrylamide gel to a polyvinyl difluoride (PVDF) membrane with porosity of 0.22 – 0.45 µm (BioRad) was used. To begin, the PVDF membrane was activated in 2 ml of 20% methanol (Merck Millipore). The sponge, filter paper, PVDF membrane, gel, filter paper and sponge were soaked in transfer buffer (Glycine 1.92 M, Tris 0.25 M, SDS 10 %, methanol 20 %) and placed in the cassette in the same order. Attention was placed on the orientation of the membrane and the gel; the former was placed towards the anode and the latter towards the cathode. The sandwich was made in a cassette, rolled after each layer to prevent air bubbles existing between the gel and the membrane, thereafter, sealed tightly and placed in a tank filled with transfer buffer (Transfer time specified in Table 2.4).

At completion of the transfer process, the membrane was removed from the cassette and blocked by incubating with 5% skimmed milk in Tris-buffered saline (Tris 0.5 M, NaCl 1.5 M) containing 0.5 % Tween-20 (TBS-T) for 2 hours. After this, the membrane was washed twice in quick succession and allowed to sit in TBS-T for 1 minute at room

temperature. Subsequently, depending on the protein of interest, the membranes were incubated with their corresponding primary antibodies (see Table 2.5). The antibody concentrations for Western blotting were based on optimization from pre-established laboratory protocols. Thereafter, the membranes were washed four times in TBS-T (5 minutes between each wash). The membranes were further incubated with secondary antibodies (see Table 2.5) for 1 – 2 hours at room temperature. This was followed by washing with TBS-T four times after every 10 minutes.

2.5.5 Blot analysis

The membranes were incubated in freshly prepared Clarity Western ECL substrate (Bio-Rad) for 5 minutes at room temperature. Each membrane was placed between two transparent plastic sheets and placed in the SynGene Imager Pxi 4 (Cambridge, UK) for visualization and detection of chemiluminescent signal via the GeneSys image acquisition software. To test for total and phosphorylated proteins on the same blot, the membrane was stripped of antibodies and re-probed. The membrane was incubated in low pH (2.0) stripping buffer (Glycine 25 mM, SDS 1 %, distilled water 400 ml) for 10 minutes at room temperature and washed in TBS-T 3 times for 10 minutes each time and finally once in TBS for 5 minutes. The membrane was imaged to confirm completion of stripping. To re-probe with different antibody, the membrane was blocked in 5% milk in TBS-T and incubated in primary and secondary antibodies.

The blot images were analysed with Genetools 1.0, a SynGene image analysis software. The densitometry values of total protein were normalized to that of GAPDH (housekeeping protein). The ratio of phosphorylated to total proteins was then calculated.

Table 2.4 Specific SDS-PAGE and Western blotting protocols for each protein

	Protein of interest		
	CaMKII	**CaMKII Thr 287**	**GAPDH**
Molecular weight (kDa)	50	50	37
% Gel	10	10	10
Heat block temperature (oC)	95	95	95
Heat block duration (minutes)	5	5	5
Protein loading (µg)	20	20	20
Gel running duration (minutes)	100	100	100
Running voltage (V)	120	120	120
Membrane type	PVDF	PVDF	PVDF
Transfer duration (minutes)	180	180	180
Transfer voltage (V)	100	100	100
Primary antibody incubation duration (minutes)	overnight	overnight	60
Secondary antibody incubation duration (minutes)	60	120	60

Table 2.5 Western Blotting Antibodies

Protein	**Primary antibody**			**Secondary antibody**		
	Concentration	**Species**	**Supplier**	**Concentration**	**Species**	**Supplier**
CaMKII	1:30,000	Rabbit	Thermo-Fisher	1:30,000	Anti-rabbit HRP	Abcam
CaMKII Thr 287	1:5,000	Rabbit	Abcam	1:30,000	Anti-rabbit HRP	Abcam
GAPDH	1:30,000	Mouse	Genetex	1:30,000	Anti-mouse HRP	Abcam

All antibodies were diluted in Tris-buffered saline containing Tween-20.

2.6 Statistical analyses

All numerical data were exported to Microsoft Excel 2016 and statistical analysis was done with GraphPad Prism (version 8.4.0). All data are presented as mean ± standard error of the mean (S.E.M). Shapiro-Wilk normality test was carried out to determine statistical distribution of data. Mean comparison of normally distributed data was performed using parametric test. Unpaired t-test was used to compare two population means that did not belong to the same sample group. One-way analysis of variance (ANOVA) was used to compare variance between group means of three or more categorical groups with one independent factor and two-way ANOVA was used to compare between group means with two independent factors. Three-way ANOVA was used to compare three independent variables and one dependent variable. Repeated measures ANOVA was used in analysis of data that involved repeated measurements, for example, drug concentration. ANOVA analyses were followed by multiple comparisons using uncorrected Fisher's LSD test. Data that did not pass normality test were subjected to non-parametric Mann-Whitney test (for unpaired t-test) or Kruskal Wallis test (for ANOVA). Correlation between two variables was determined by correlation. Pearson correlation coefficient was used for normally distributed and Spearman correlation was used to data that did not pass the normality test. Statistical significance was indicated as $p < 0.05$.

CHAPTER 3: EFFECTS OF ACUTE GSNO TREATMENT AND LOSS OF CAMKII ON CARDIAC FUNCTION

3.1 Introduction

NO plays a role in pro-arrhythmic signaling in cardiac cells, and the pathway for this action is mediated by CaMKII (Gutierrez et al., 2013). Currently, how CaMKII contributes to arrhythmias in the whole heart is not fully understood. This chapter is focused on assessing the acute effects of GSNO on cardiac function in the presence and absence of CaMKIIδ, using C57BL/6 wild-type (WT) and CaMKIIδ-KO mice.

It is well known that ECC involves the propagation of electrical signaling in cardiomyocytes, which leads to Ca^{2+} release from the SR into the cytoplasm via a CICR mechanism. Ca^{2+} binds to myofilaments to initiate contraction and dissociation of Ca^{2+} from troponin C which is facilitated by Ca^{2+}. Reuptake via Ca^{2+} transporters leads to relaxation (Bassani et al., 1994). The amount of Ca^{2+} flux through the cardiomyocyte during ECC determines the inotropic and lusitropic response (the contractile force and the rate of relaxation) (Dibb et al., 2007; Landstrom et al., 2017). Since Ca^{2+} is the critical ion that mediates this process, it is important to have a balance between SR Ca^{2+} release and uptake. A disruption in intracellular Ca^{2+} handling can result in cardiac dysfunction. Research has shown that reactive nitrogen species including NO can play a role in dysregulation of ECC, leading to calcium mishandling and arrhythmogenesis (Gutierrez et al., 2013; Curran et al., 2014).

NO is widely known for its protective role in the cardiovascular system by preventing hypertension and arrhythmias (Rees *et al.*, 1996; Shesely *et al.*, 1996; Kubota *et al.*, 2000; Rakhit *et al.*, 2001; Gonzalez *et al.*, 2007). However, novel evidence has emerged showing that NO can induce spontaneous Ca^{2+} release events (known as Ca^{2+} sparks) from the SR via RyR2 channels during diastole in cardiomyocytes. Increased Ca^{2+} spark frequency is an indicator of SR Ca^{2+} leak (Bers, 2014) due to RyR2 phosphorylation (Wehrens et al., 2004; Zima et al., 2010). When these Ca^{2+} sparks build up with synchronisation in space and time, they evolve into Ca^{2+} waves (Shiferaw et al., 2012). The Ca^{2+} waves release Ca^{2+} ions, which activate Ca^{2+} sensitive currents and result in

afterdepolarisations, the underlying mechanism of triggered arrhythmias (Shiferaw et al., 2012). Using isolated NOS1 knockout hearts, Wang et al. (2010) demonstrated a decrease in Ca^{2+} spark frequency associated with decreased opening rate of RyR2 channels, and this effect was reversed with exposure to a NO donor. These results suggested that increased SR Ca^{2+} leak associated with NO signaling does not occur via direct action on RyR2 rather through CaMKII phosphorylation of RyR2. Gutierrez et al. (2013) found that NO caused an increase in Ca^{2+} spark frequency in cardiomyocytes and confirmed that this was primarily due to CaMKII activity.

NO-induced spontaneous Ca^{2+} waves in cardiomyocytes result in part from nitrosylation of CaMKII leading to its aberrant activation, which can cause deleterious effects including arrhythmias (Gutierrez et al., 2013). There is limited knowledge from previous studies about how NO modulates CaMKII activity to affect whole heart function as all studies investigating the relationship between NO, CaMKII and arrhythmias have been carried out using cardiomyocytes. In cardiomyocytes, according to Curran et al. (2014), NO exposure induced Ca^{2+} leak, and this effect was ablated with a CaMKII inhibitor. This suggests that CaMKII activation was required to facilitate SR Ca^{2+} leak during NO signaling. At the cellular level, there is evidence that NO activates CaMKII inducing spontaneous Ca^{2+} leak and this could result in cardiac arrhythmias. Erickson et al. (2015) reported that NO could directly regulate the activity of the primary cardiac isoform of CaMKII (CaMKIIδ). They demonstrated that activation of CaMKIIδ with Ca^{2+}/CaM followed by addition of a NO donor (GSNO) induced Ca^{2+} sparks in mouse ventricular myocytes.

These studies show that CaMKII plays a role in mediating NO-induced arrhythmogenesis in cardiac cells, and that CaMKII inhibition protects against spontaneous Ca^{2+} release. Taken together, it suggests this protein is a potential therapeutic target in preventing arrhythmias associated with NO signaling. As described in Chapter 1, pharmacological inhibitors of CaMKII have shown promising results in preventing cardiac arrhythmias; however, they also have off target effects when compared to the knockout models of CaMKIIδ where there is loss / reduction of protein expression. The use of the CaMKIIδ knockout model could provide a clearer understanding about how NO alters CaMKII signaling pathway and the downstream effects on cardiac function.

3.1.1 Objectives and hypotheses

The aim of the study described in this chapter was to determine the influence of NO on CaMKII signaling in isolated perfused hearts and how this contributes to cardiac dysfunction. The following objectives were outlined to determine the effect of GSNO on CaMKII activity and how this affects cardiac function:

1) To determine total CaMKII expression levels in WT and CaMKIIδ-KO mouse models using Western blotting. I hypothesised that WT mouse hearts would have a relatively higher expression of total CaMKII compared to KO mouse hearts.

2) To measure the in vivo basal cardiac function of WT and CaMKIIδ-KO mouse models via echocardiography. Based on the knowledge of basal CaMKII activity, I hypothesised that loss of CaMKIIδ would not alter cardiac function at baseline.

3) To determine the effect of GSNO treatment on cardiac function using Langendorff isolated heart perfusion technique. I hypothesised that treating the isolated hearts with a NO donor would alter heart rate and contractility in WT and CaMKIIδ-KO mouse hearts.

4) To investigate how loss of CaMKIIδ affects arrhythmias with GSNO treatment. I hypothesised that GSNO would trigger arrhythmias in WT mouse hearts but not in the CaMKIIδ-KO mouse models.

3.2 Experimental Design

To test the first hypothesis, I determined CaMKIIδ expression levels in the WT and KO mice using Western blotting in frozen cardiac tissues.

I performed echocardiography (protocol described in chapter 2, section 2.3) to determine the in vivo baseline cardiac function of 12-week-old WT and CaMKIIδ-KO mice. After echocardiography, I randomly assigned the animals into 4 groups and subsequently used Langendorff isolated heart perfusion technique to isolate the hearts and treat with a NO donor, GSNO. The WT and KO animal models had treatment and control groups. The control groups served as time control to account for variations in the isolated hearts during

the experiment (Appendix 1). The treatment groups received different concentrations of GSNO (100 µM, 600 µM, 1600 µM).

The hearts were isolated from the mice (described in Chapter 2, section 2.4). After initial stabilisation and achieving LVEDP of 5 – 10 mmHg (see Figure 3.1), each heart was allowed to stabilise for another 20 minutes, a total of 30 minutes. The first 8 minutes after that was considered baseline, then depending on the group (control or treatment), the heart was perfused with vehicle for 24 minutes or increasing concentrations of GSNO (100 µM, 600 µM and 1600 µM) were added every 8 minutes.

The arrhythmias were counted individually from the start to the end of each protocol and then recorded against the duration (8, 16, 24, 32 minutes) or different GSNO concentrations, depending on the group.

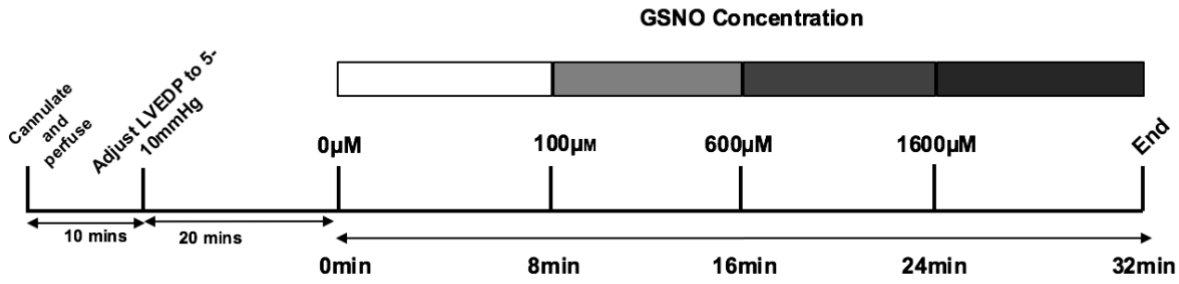

Figure 3.1 A time course protocol for Langendorff isolated heart perfusion experiment

3.2.1 Statistical Analyses

Data was represented as mean ± standard error of mean (SEM). Normality of the data was determined with Shapiro-Wilk normality test. Unpaired t-test was used to compare baseline WT and KO contractile parameters. To determine the difference in GSNO effect and animal genotype effect, two-way ANOVA with repeated measures, followed by uncorrected Fisher's LSD test was used. All data from the isolated heart protocols was imported from Lab chart 8 and analysed on GraphPad Prism (version 8). Data was accepted as statistically significant if $p<0.05$.

3.3 Results

3.3.1 Animal Characteristics

Table 3.1 shows the body weight of 12-week-old male and female WT and KO mice used for Langendorff isolated heart perfusion experiments. Overall, the KO mice had similar body weight with WT mice at the same age (p = 0.15).

Table 3.1 Animal characteristics of the WT and KO mice

Parameter	**Animal Genotype**		**P value**
	WT	**KO**	
Body Weight (g)	26.81 ± 1.11	30.06 ± 1.92	0.15
Ratio M:F	9:3	3:8	

WT = Wild Type; KO = CaMKIIδ-knockout; M = Male; F = Female. Data are expressed as mean ± SEM. Independent t-test was used to compare between WT (n = 12) and KO (n = 11) values.

3.3.2 CaMKIIδ expression

Ventricular cardiac tissues from WT and KO mice was used to determine total CaMKII expression (Figure 3.2). As expected, the KO mice had significantly lower CaMKII expression compared to the WT mice (5.25 ± 0.94 vs 1.82 ± 1.12).

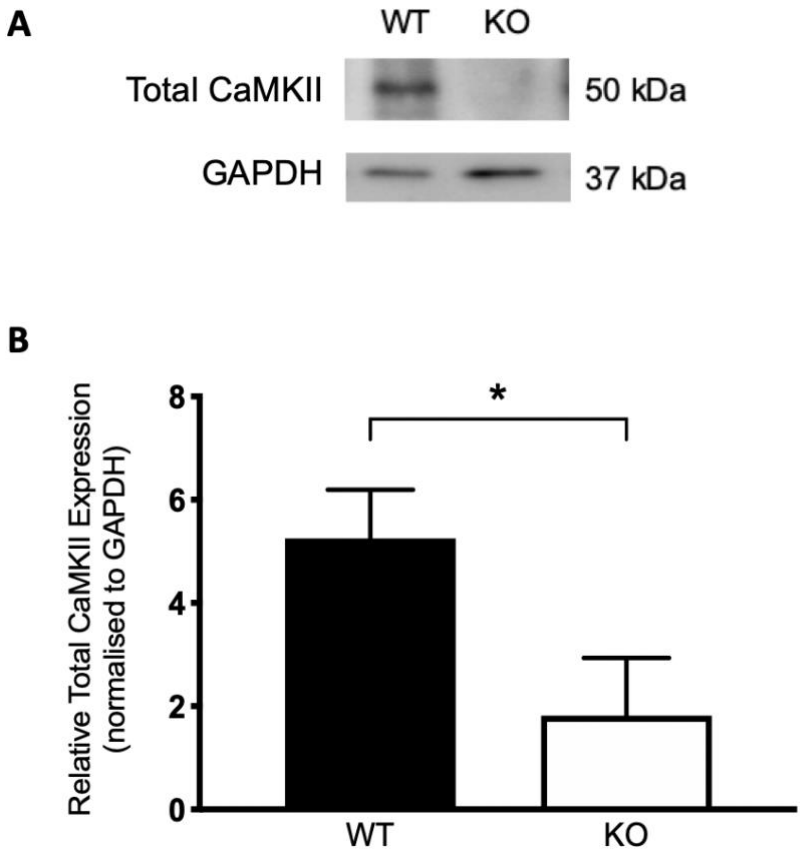

Figure 3.2 Western blot for total CaMKII expression. A, Representative immunoblot of total CaMKII expression in WT and KO heart tissues and GAPDH as loading control. B, Quantification of total CaMKII levels in WT (n = 8) and KO (n = 8). Data represented as mean ± SEM. Unpaired t-test was used to compare WT and KO, p = <0.05

3.3.3 Echocardiographic measurements

There was no significant difference in IVSd, IVSs, LVIDd, LVIDs, LVPWd, LVPWs, LVESV, FS, EF, CO, HR, R-R interval for the WT and KO (Table 3.2). There was a significantly lower SV in the KO compared to the WT (p = 0.04). There was also a trend towards reduced LVEDV in the KO (p = 0.05) but this was not significant. Altogether, these results reflect that the KO had very mild systolic dysfunction, which is seen in the reduced SV. However, the KO mice have a comparable systolic function to the WT mice and there was no evidence of severe cardiac dysfunction in the healthy KO mice at baseline.

Table 3.2 Echocardiography parameters in WT and KO mice at 12 weeks

Parameter	WT	KO	Genotype effect (P value)
IVSd (mm)	1.07 ± 0.07	0.90 ± 0.04	0.06
IVSs (mm)	1.32 ± 0.08	1.12 ± 0.06	0.07
LVIDd (mm)	3.03 ± 0.09	2.82 ± 0.06	0.07
LVIDs (mm)	1.65 ± 0.07	1.58 ± 0.06	0.50
LVPWd (mm)	1.00 ± 0.04	0.96 ± 0.02	0.40
LVPWs (mm)	1.37 ± 0.05	1.25± 0.04	0.08
LVEDV (ml)	0.07 ± 0.01	0.06 ± 0.00	0.05
LVESV (ml)	0.01 ± 0.00	0.01 ± 0.00	0.45
FS (%)	45.77 ± 1.29	43.79 ± 1.81	0.38
EF (%)	82.50 ± 1.25	80.19 ± 1.67	0.27
SV (ml)	0.06 ± 0.00	0.05 ± 0.00	0.04*
CO (ml/min)	26.31 ± 0.00	20.75 ± 0.00	0.10
HR (beats/min)	429.30 ± 18.09	421.60 ± 14.75	0.75
R-R Interval (ms)	143.20 ± 6.36	144.2 ± 5.12	0.90

HR, heart rate; FS, Fractional shortening; EF, Ejection Fraction; IVSD, interventricular septum diastolic thickness; IVSS, interventricular septum systolic thickness; LVIDD, left ventricular internal dimension at diastole, LVIDS, left ventricular internal dimension at systole; LVPWD, left ventricular posterior wall thickness at diastole; LVPWS, left ventricular posterior wall thickness at systole. Data are expressed as mean ± SEM. Independent t-test was used to compare between WT (n = 12) and KO (n = 11) values, * = P< 0.05 WT vs KO

3.3.4 Cardiac contraction and relaxation parameters in isolated WT and KO mouse hearts at baseline.

I analysed the cardiac function in both mouse models at baseline after Langendorff isolation prior to drug treatment. Figure 3.3 shows the average baseline contractile parameters; LVDP, HR, max dP/dt and min dP/dt in in isolated WT and KO hearts. As seen in Figure 3.3A-D, there was no significant difference in LVDP ($p = 0.07$), HR ($p = 0.12$), max dP/dt ($p = 0.63$) and min dP/dt ($p = 0.44$). Arrhythmias (Figure 3.3E-F) were grouped according to the number of events and severity. Arrhythmic events were also expected; however, there was no difference in the number of arrhythmias ($p = 0.68$) or severity ($p = 0.91$) between the WT and KO hearts.

The isolated hearts were perfused with buffer containing 2 mM Ca^{2+}, which is higher than physiological Ca^{2+} concentration of 1.35 mM (Reichelt et al., 2009) to mimic a high intracellular Ca^{2+} concentration condition. The isolated WT and KO hearts had similar baseline cardiac function. These data suggest that ex vivo cardiac function was not severely impacted in the KO mouse hearts, highlighting once again that removal of CaMKIIδ did not affect baseline cardiac function.

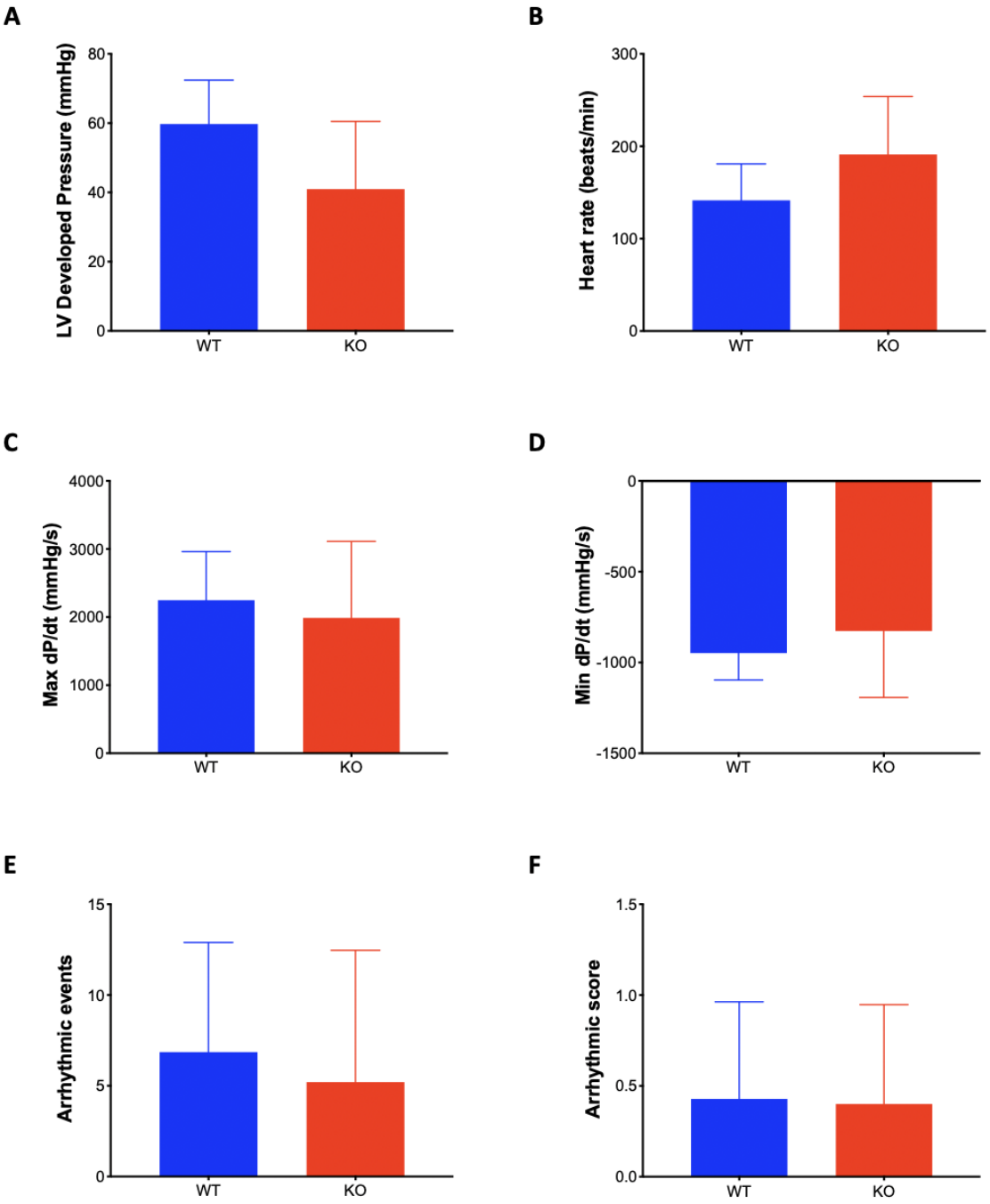

Figure 3.3 Basal contraction and relaxation parameters and quantification of arrhythmias in WT and KO mouse hearts. A, LV Developed Pressure. B, Heart rate. C, Maximum rate of contraction (Max dP/dt). D, Minimum rate of relaxation (Min dP/dt). E, Arrhythmic events F, Arrhythmia scores. Data are means ± SEM. WT, blue bar, n = 7 hearts; KO, red bar, n = 5 hearts. Unpaired t-test was used to compare between animal models.

3.3.5 Effect of GSNO treatment on cardiac contraction and relaxation in isolated WT and KO mouse hearts

Previous studies showed that NO has a dual role of increasing or reducing contractility depending on concentration (Vila-Petroff et al., 1999; González et al., 2008). I hypothesised that low concentration of GSNO would increase force of contraction, and there would be reduced contractility with increased GSNO concentration. To test this hypothesis, I examined the response of isolated WT and KO hearts to increasing GSNO concentrations (100 µM, 600 µM and 1600 µM) in the presence of 2 mM Ca^{2+}.

GSNO treatment did not significantly affect LV pressure development when WT and KO hearts were compared ($p = 0.39$) (Figure 3.4A). There was no difference in the slope of LV pressure in WT hearts compared to KO hearts ($p = 0.07$). However, there was a significant difference between LVDP at 100 µM and 1600 µM ($p = 0.03$) in WT hearts. There was no change in LVDP in the KO hearts with increased GSNO concentration. Interestingly, GSNO treatment significantly sped up the heart rate (Figure 3.4B) in WT hearts at 1600 µM GSNO compared to KO hearts at same concentration ($p = 0.002$). The slope of the line for heart rate in the WT hearts was significantly different than zero ($p = 0.01$), suggesting that heart rate changed in response to GSNO concentration but this effect was not observed in the KO hearts ($p = 0.11$). Overall, GSNO induced a significantly faster heart rate in WT hearts compared to KO hearts ($p < 0.05$). For all concentrations of GSNO tested, there was no significant difference in rate of contraction (max dP/dt) (Figure 3.5A) between the WT and KO hearts ($p = 0.4$). There was a trend towards reduced max dP/dt in the WT hearts in comparing 100 µM and 1600 µM GSNO concentrations but this was not statistically significant ($p = 0.06$). In the KO hearts, the slope of the line ($p = 0.54$) showed that there was no GSNO-dependent change in max dP/dt. There was no GSNO-dependent significant change in rate of relaxation (min dP/dt) (Figure 3.5B) in WT and KO hearts ($p = 0.22$).

In summary, GSNO treatment did not induce significant alteration in contractile function in WT and KO mouse hearts but increased chronotropy in WT hearts. The data in this section were presented as fold change to account for the variation in baseline developed pressure. Absolute values for all parameters can be found in Appendix 1.

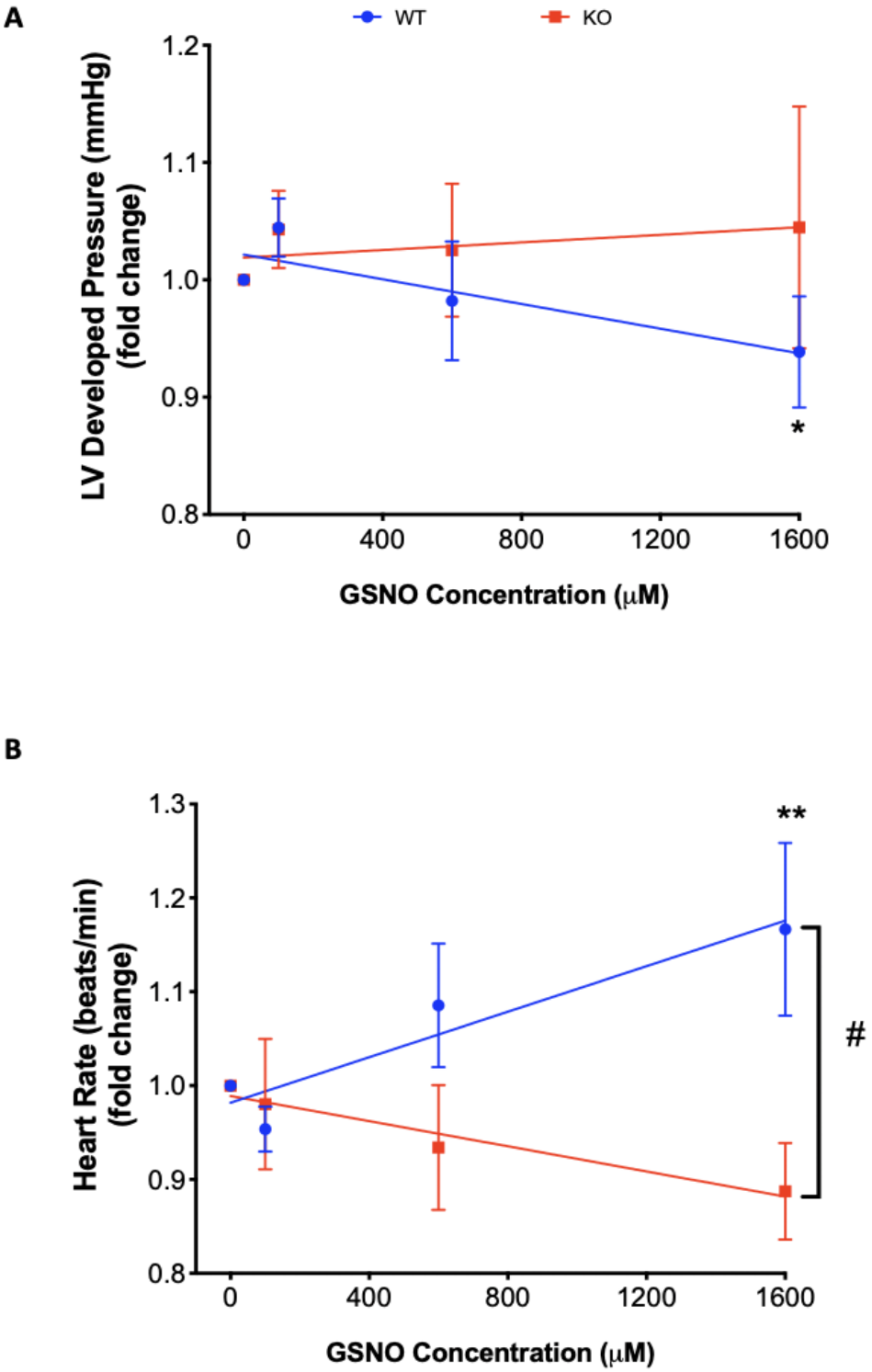

Figure 3.4 LV pressure and heart rate in WT and KO mouse hearts with GSNO treatment (100 µM, 600 µM and 1600 µM). A, LV developed pressure B, Heart rate. Data are means ± SEM. WT, blue line, n = 7 hearts; KO, red line, n = 5 hearts. Two-way ANOVA (uncorrected Fisher's LSD test) was used to compare between groups. * = P < 0.05, ** = P < 0.01 treatment effect (100 µM vs 1600 µM), # = P <0.05 genotype effect (WT vs KO).

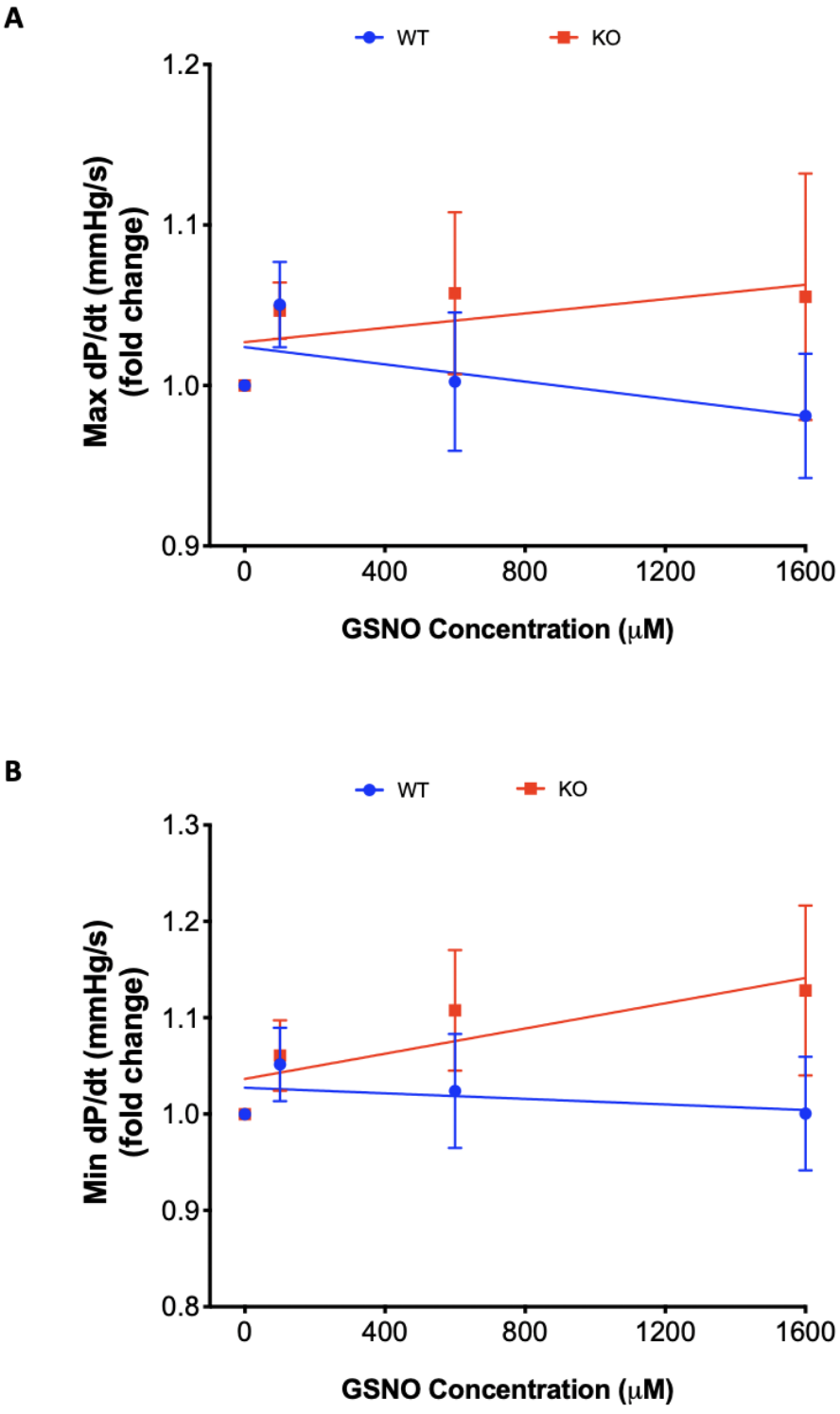

Figure 3.5 Rates of contraction and relaxation in WT and KO mouse hearts with GSNO treatment (100 µM, 600 µM and 1600 µM). A, Rate of Contraction (Max dP/dt) B, Rate of Relaxation (Min dP/dt). Data are means ± SEM. WT, blue line, n = 7 hearts; KO, red line, n = 5 hearts. Two-way ANOVA (uncorrected Fisher's LSD test) was used to compare between groups.

3.3.6 Effect of GSNO on coronary flow and pressure-time integral in isolated WT and KO mouse hearts

The effect of GSNO on vascular flow was not evident in this Chapter. Overall, there was no significant difference in coronary flow during GSNO treatment between WT and KO hearts ($p = 0.90$) (Figure 3.6a). In the KO hearts, 100 µM GSNO significantly elevated coronary flow compared to baseline ($p = 0.008$). The effect of heart rate on pressure development was measured through pressure-time integral. Pressure-time integral was unaffected by GSNO treatment in WT and KO hearts (Figure 3.6b).

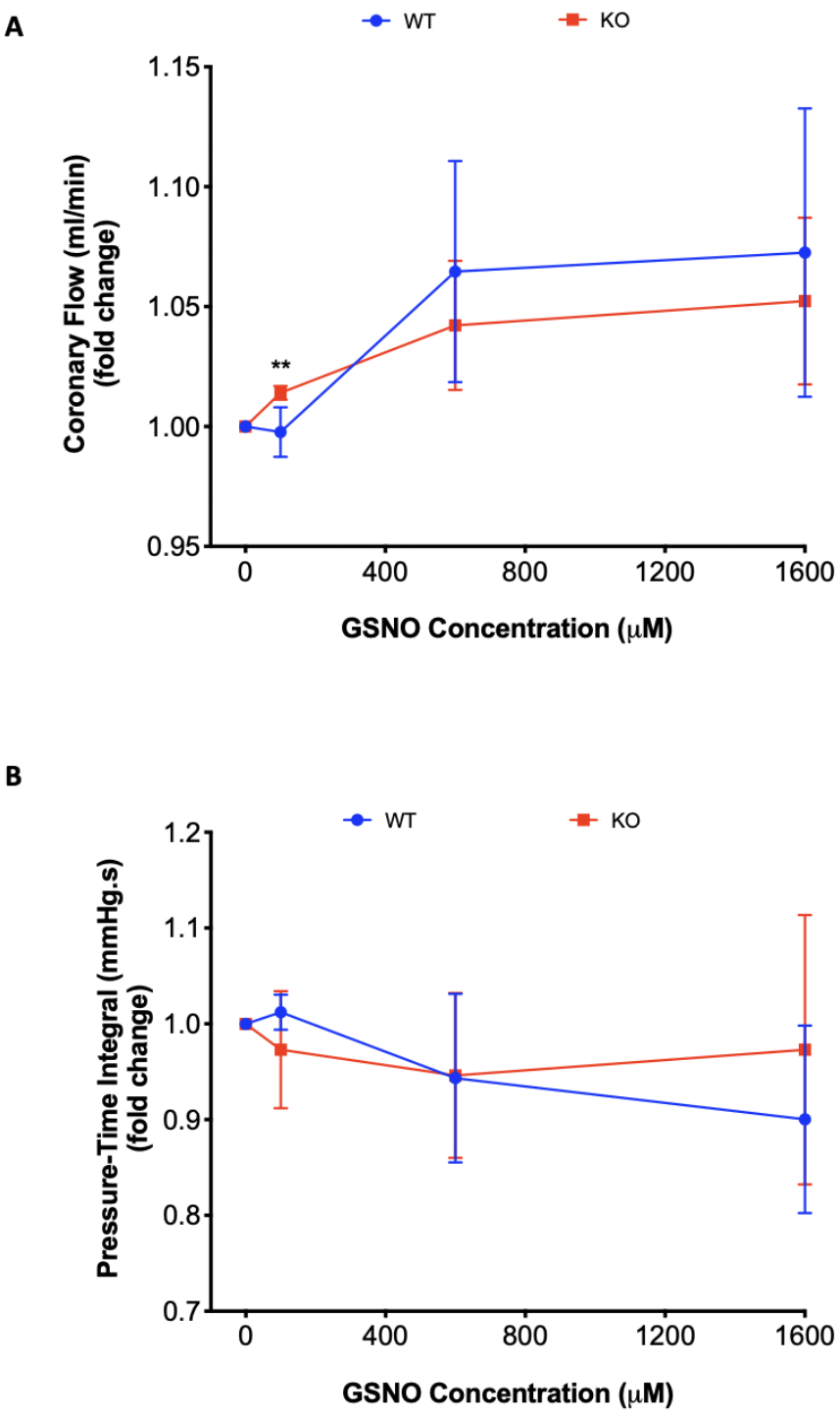

Figure 3.6 Cardiac response to GSNO treatment (100 µM, 600 µM and 1600 µM) in WT and KO mouse hearts. A, Coronary flow (ml/min) B, Pressure-time integral (mmHg.s). Data are means ± SEM. WT, blue line, n = 7 hearts; KO, red line, n = 5 hearts. Two-way ANOVA (uncorrected Fisher's LSD test) was used to compare between groups. ** $p < 0.01$ vs baseline

3.3.7 CaMKIIδ knockout prevents cardiac arrhythmias in isolated hearts from WT and KO mice treated with GSNO

I hypothesised that GSNO would increase arrhythmias, but would be reduced in the absence of CaMKIIδ. To test this hypothesis, I quantified arrhythmic events and grouped them according to frequency and severity.

Figure 3.6A shows the number of arrhythmic events in WT and KO hearts at different concentrations of GSNO. GSNO did induce arrhythmic events in the WT hearts. The slope of the regression line for WT hearts was significantly different from zero ($p = 0.02$) meaning that an increase in GSNO concentration corresponded with increase in arrhythmic events. There was a significant difference in the number of arrhythmic events at 100 µM GSNO compared to 1600 µM GSNO in the WT hearts. In the KO hearts, there was no significant change in arrhythmia count with increase in GSNO concentration ($p = 0.23$). There was also no significant difference in arrhythmic events between the WT and KO hearts ($p = 0.68$).

There was a trend towards higher severity of arrhythmias as measured by arrhythmia score in WT at the highest concentration of GSNO compared to the lowest concentration (Figure 3.6B). However, this was not statistically significant ($p = 0.06$). In the KO hearts, there was no significant effect of GSNO on arrhythmia scores ($p = 0.16$). At 1600 µM GSNO, there was no significant difference in arrhythmic severity between the WT and KO hearts ($p = 0.16$). GSNO treatment did not induce any overall significant difference in arrhythmic scores between the WT and KO ($p = 0.71$).

There was no relationship between heart rate and arrhythmia score in WT hearts ($r = -0.09$, $p = 0.67$) and KO hearts ($r = -0.53$, $p = 0.06$) (Figure 3.8).

Taken together, GSNO induced arrhythmias in the WT hearts, and this effect was dependent on the concentration. The GSNO concentration-effect suggested that increase in GSNO in the presence of CaMKIIδ contributed to a significant increase in arrhythmic events in WT and this was no observed in the KO hearts. This finding is similar to the observation in cardiomyocytes and is consistent with the hypothesis that loss of CaMKIIδ can prevent GSNO-induced cardiac arrhythmias (Gutierrez *et al.*, 2013).

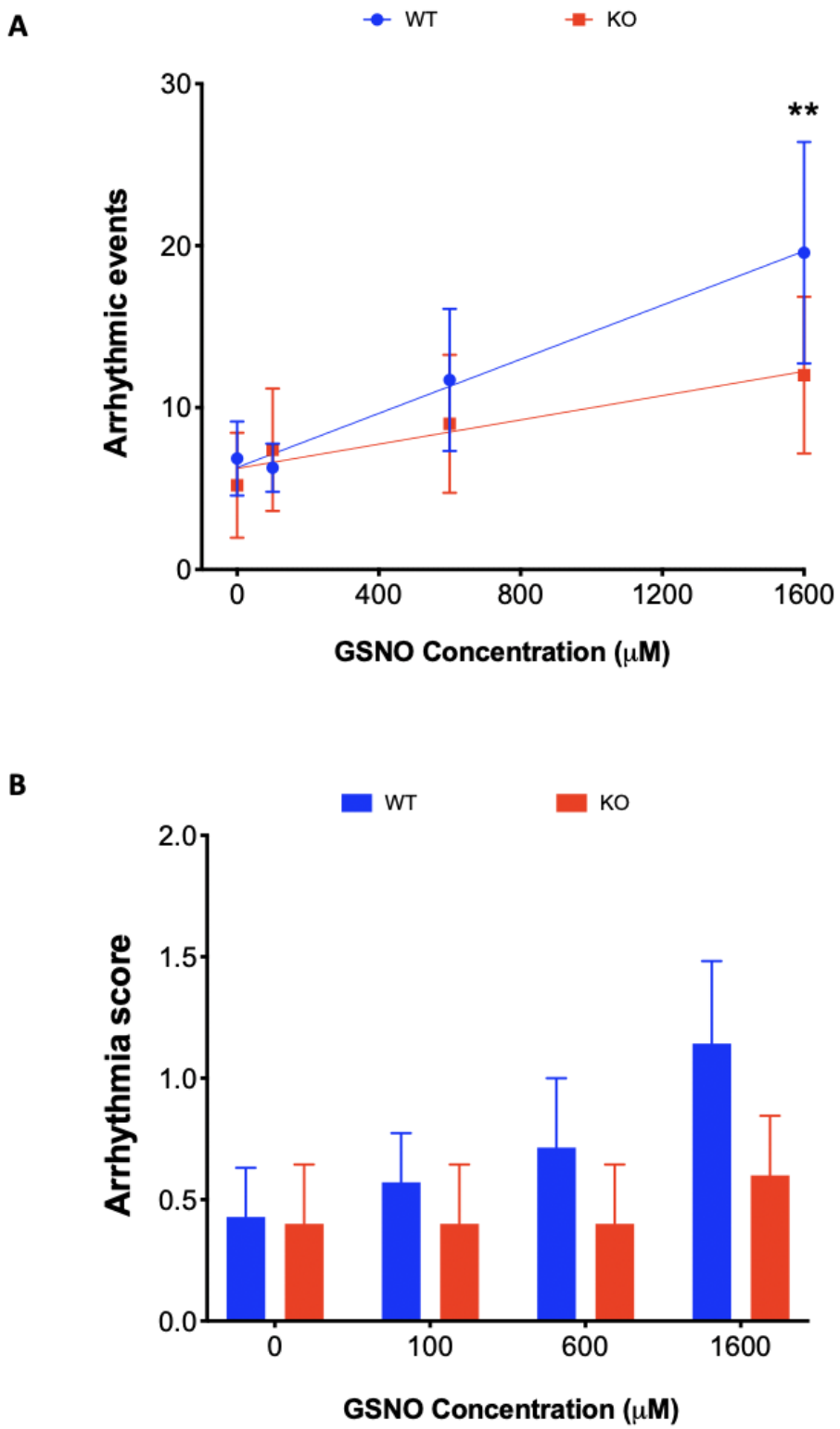

Figure 3.7 Arrhythmias during GSNO treatment (100 µM, 600 µM and 1600 µM) in WT and KO mouse hearts A, Arrhythmic events B, Arrhythmia scores. Data are means ± SEM. WT, blue line, blue bar, n = 7 hearts; KO, red line, red bar, n = 5 hearts. Two-way ANOVA (uncorrected Fisher's LSD test) was used to compare between groups. ** = $P < 0.01$ treatment effect (100 µM vs 1600 µM).

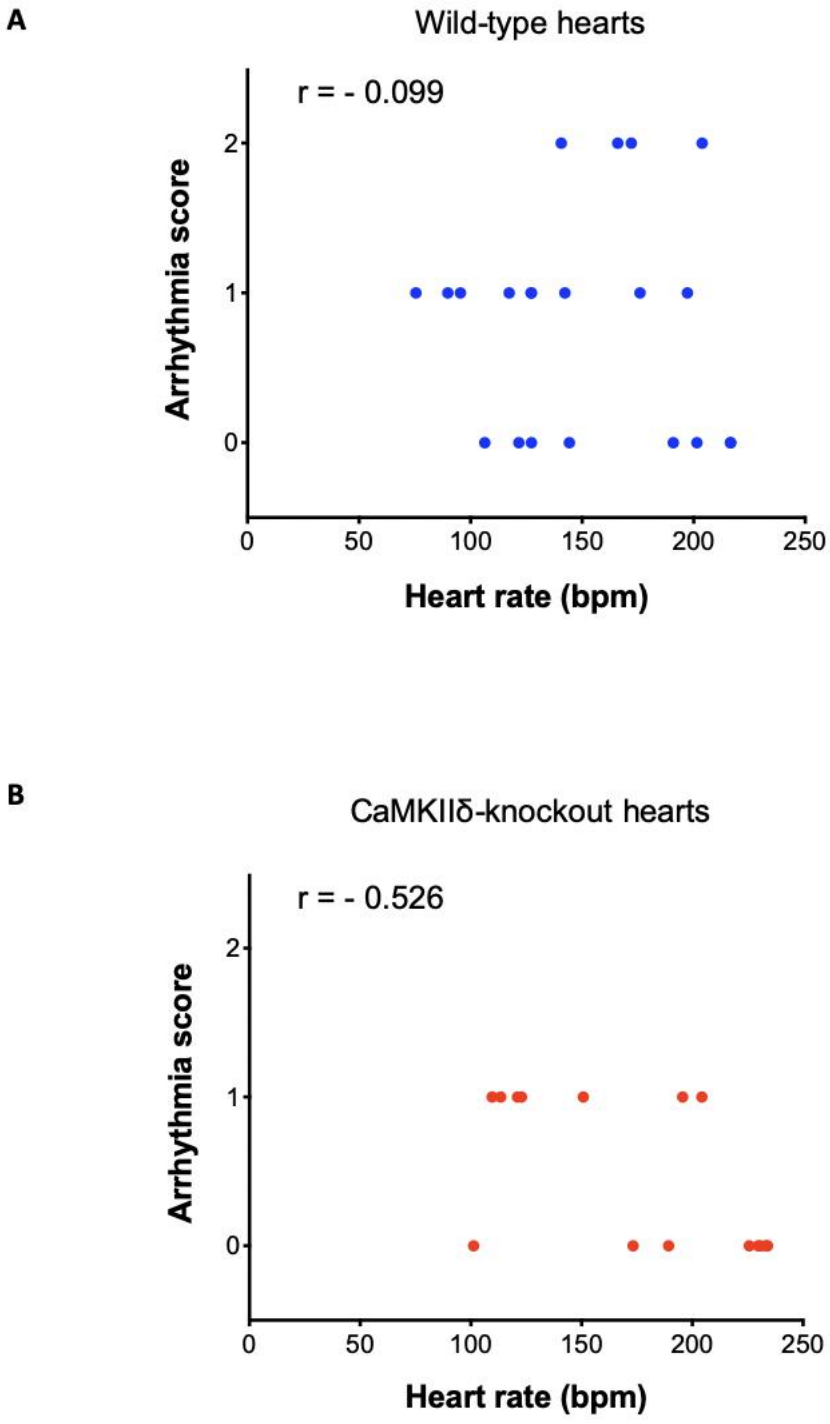

Figure 3.8 Effect of heart rate on arrhythmia severity during GSNO treatment in WT and KO mouse hearts A, Wild-type hearts B, CaMKIIδ hearts. Data are means ± SEM. WT, n = 7 hearts; KO, n = 5 hearts.

3.4 Discussion

The main aim of this chapter was to investigate the effects of NO and CaMKIIδ on cardiac function. To accomplish this, I determined basal cardiac function in WT and CaMKIIδ-KO mice. The hearts were then isolated and treated with NO donor GSNO. I examined the effect of GSNO on cardiac contraction, relaxation and arrhythmias. The main findings were: (a) WT and KO mice had similar basal cardiac function (b) GSNO treatment did not alter pressure development in the isolated hearts. (c) high concentration of GSNO treatment increased chronotropy in WT mouse hearts but not in KO hearts. (d) GSNO treatment induced cardiac arrhythmias in the isolated WT hearts and CaMKIIδ loss prevented arrhythmias.

3.4.1 Basal cardiac function is not severely altered with CaMKIIδ loss

Studies have reported that even though presence of CaMKII is of physiological importance, the loss of CaMKIIδ does not impact basal cardiac function (Backs et al., 2009; Ling et al., 2009; Grimm et al., 2015; Mohamed et al., 2018). Data from Western blotting in my study confirmed a reduction in CaMKII expression in KO mouse hearts due to knocking out CaMKIIδ. There is still some level of CaMKII expression in KO mouse hearts which is attributed to the presence of the secondary cardiac isoform, CaMKIIγ. Consistent with previous studies (Ling et al., 2009; Grimm et al., 2015), echocardiography data of WT and KO mice from my study showed comparable cardiac structure and function of both animal models at 12 weeks (Table 3.2). I also examined baseline function prior to GSNO treatment and observed that isolated and perfused WT and KO hearts showed no difference in contractile function (Figure 3.3), which is similar to a finding by Grimm et al. (2015) where they measured baseline isovolumetric cardiac performance in isolated WT and KO hearts prior to isoproterenol treatment. CaMKII is activated by stress conditions and at basal conditions in healthy unconscious WT mice, it was expected that CaMKII is mostly inactive. This would be comparable to the KO mice which have about 80% reduction in CaMKII expression and therefore less activity. Thus, there would be the possibility that basal cardiac parameters are not severely impacted in vivo and ex vivo with CaMKIIδ loss.

3.4.2 Impact of GSNO on contractile performance of the heart

It was surprising to find that overall, GSNO had no effect on LV pressure development in isolated WT and KO hearts (Figure 3.4A). Previous studies have tested the effect of NO donors on contractility in different animal models (Wyeth et al., 1996; Chesnais et al., 1999; Vila-Petroff et al., 1999; Paolocci et al., 2000). González et al. (2008) reported that SNAP concentrations of 0.1 – 10 µM increased cardiac inotropy in isolated rat hearts while 100 µM led to reduced contractility, which indicated that the dual effect of NO in the heart was concentration-dependent. This is due to the ability of NO to activate two signaling pathways. High NO concentration activates the cGMP pathway and low NO concentration activates the S-nitrosylation pathway. According to my findings, GSNO did not improve cardiac contractility in isolated WT or KO mouse hearts regardless of the concentration, even when both were compared. This was not consistent with my hypothesis that NO would significantly alter cardiac contraction and relaxation. In the WT hearts, there was a significant negative inotropic effect at the highest concentration of 1600 µM compared to lowest concentration of 100 µM. With a different NO donor, it was found that 100 µM of SNAP depressed contractile amplitude in rat cardiomyocytes (Kojda et al., 1996; Vila-Petroff et al., 1999). It appears that NO donor concentrations less than 100 µM cause increase in inotropic effect or no change in contractility while concentrations greater than 100 µM produce negative inotropic effect in the heart (Sarkar et al., 2000). González et al. (2008) suggested that reduction in contractility induced by NO donors at high concentration was due to activation of guanylyl cyclase and cGMP-PKG pathway due to increased cardiac cGMP production.

Müller-Strahl et al. (2000) showed that low concentrations (< 100 µM) of exogenous NO can increase chronotropy induced in isolated rat hearts. A similar finding was observed by Musialek et al. (1997) in spontaneously beating sinoatrial node/atrial preparations of isolated guinea pig hearts. The findings from this chapter showed a significant difference in HR in KO hearts during GSNO treatment compared to WT hearts (Figure 3.4B). Increased concentration of GSNO (1600 µM) elicited a positive chronotropic response in WT hearts, however this effect was not observed in KO hearts. According to Müller-Strahl et al. (2000), chronotropic effect induced by a NO donor, was suggested to be due to stimulation of hyperpolarisation-activated inward current (I_f) via the cGMP pathway activated by NO, however this was at a NO donor concentration lower than in my

protocol. In contrast to the increased chronotropic effect associated with high GSNO concentration that I observed. Kennedy et al. (1994) found that 300 µM of NO donor (SIN-1) induced negative chronotropic effect in right atria from isolated rat heart and an increase in concentration of SIN-1 to 3000 µM led to a further 27% decline in spontaneous beating rate. The observation was that chronotropic effect of SIN-1 was not induced by NO-cGMP pathway but could possibly be mediated by other compounds including reactive oxygen species (Kennedy et al., 1994). As observed in the isolated WT and KO hearts, it is possible that the presence of CaMKII contributed to the cardiac excitation and increase in HR, and the absence of CaMKIIδ in the KO hearts prevented that positive chronotropic effect. The specific mechanism underlying this effect is unknown. With literature suggesting that NO donors can mediate either increase or decrease chronotropic effect depending on the concentration and signaling pathway (Hogan et al., 1999), the effect of GSNO on heart rate could either be mediated by S-nitrosylation, cGMP activation targetting I_f. The release of NO from GSNO is spontaneous and literature has shown that GSNO can induce S-nitrosylation of CaMKII (Curran et al., 2014; Erickson et al., 2015). Therefore, S-nitrosylation of CaMKII could also be playing a role in the effect of NO observed in the WT hearts. In this chapter, I was unable to measure S-nitrosylation levels and cGMP levels in the preserved hearts, and this was a limitation to the aim because there is not enough evidence to prove that the observed effects are primarily due to CaMKII S-nitrosylation and not via another NO-dependent mechanism, such as activation of guanylyl cyclase.

No significant change in speed of contraction and relaxation with GSNO treatment was observed in the WT and KO hearts (Figure 3.5 A-B). Inotropic effects of NO donor concentrations higher than 100 µM is yet to be studied in isolated hearts. However, published literature has shown that NO can alter cardiac contractility by facilitating myocardial contraction and relaxation in isolated working rat hearts (Müller-Strahl et al., 2000). 10 µM SIN-1 (NO donor) was seen to induce positive lusitropic effects in isolated crystalloid perfused hearts and attributed this effect to S-nitrosylation (Paolocci et al., 2000). The absence of changes in rates of contraction and relaxation in WT and KO hearts in this study could be attributed to a difference in concentration and type of NO donor, and not CaMKIIδ.

NO is widely established as a vasodilator therefore NO donors would ideally increase coronary flow rate in isolated hearts. However, the change in coronary flow rate during GSNO treatment was not pronounced in the isolated hearts in my study (Figure 3.6A). Since coronary flow remained largely unchanged, any change in the number of arrhythmic events was unlikely to be as a result of GSNO on the coronary circulation. There was also no change in PTI in WT and KO hearts during GSNO exposure (Figure 3.6B). This suggests that GSNO had no effect on the average work of contraction in the heart.

3.4.3 CaMKIIδ loss attenuates arrhythmogenic effect of nitric oxide-induced cardiac arrhythmias

I analysed arrhythmic events and severity in WT and KO isolated hearts treated with GSNO. These data shows for the first time that high concentration of NO contributes to a higher number of cardiac arrhythmias in WT mice compared to KO mice (Figure 3.7A), suggesting that CaMKIIδ could be responsible for this deleterious effect of NO. Results from this study also showed no difference in arrhythmia severity between WT and KO mice (Figure 3.7B) and arrhythmia was unrelated to change in heart rate (Figure 3.8). This was a striking observation, considering that NO is a vasodilator known for its cardioprotective function in the cardiovascular system, as studied in animals (Shesely et al., 1996; Preckel et al., 1997) and humans (Haynes et al., 1993; Sander et al., 1999). This data now unveils a more complex role for NO involving arrhythmias. Previous work on NO and arrhythmias has been performed in cardiomyocytes where it was found that in the absence of β-AR stimulation, 150 µM GSNO caused an increase Ca^{2+} spark frequency due to SR Ca^{2+} leak via RyR2 (Gutierrez et al., 2013). In the same study, acute CaMKII inhibition using AIP prevented the GSNO-induced Ca^{2+} sparks. This finding suggested that NO may directly modulate the activity of CaMKII through nitrosylation. This was confirmed in a different study which involved treating rabbit cardiomyocytes with 100 µM SNAP, and it was found that SNAP independently induced higher SR Ca^{2+} leak (Curran et al., 2014). This was compared to treatment with SNAP and the CaMKII inhibitors AIP and KN93. Taken together, this provides a compelling evidence that CaMKII inhibition could be a potent way to prevent arrhythmias during increased NO production in the heart. It is also critical to understand the mechanism underlying arrhythmogenesis associated with exogenous NO treatment. In this chapter, CaMKII

nitrosylation levels were not measured; however, the KO mouse model provides a clue that loss of CaMKII can prevent NO-mediated CaMKII arrhythmias.

3.4.4 Limitations

These experiments were performed in isolated hearts, which can spontaneously beat for several hours while perfused with buffer at optimal temperature. However, there is a tendency for the contractility of the isolated heart to deteriorate with time, about 5-10% per hour depending on several factors (Sutherland & Hearse, 2000). To account for this, there was a time control group for each animal model, and no significant change was observed compared to the GSNO treatment groups. The drug in the buffer was delivered through long perfusate lines to the heart, and this may have affected the time of drug delivery and effect. To account for this, the time of delivery was pre-established through pilot experiments to be 2 – 3 minutes, while each protocol ran for 8 minutes. Future studies could employ the use of a drug infusion pump closer to the isolated heart. The isolated hearts were unpaced in order not to mask the incidence of arrhythmias, and therefore HR was below physiological range of 400 – 600 beats/minute in mice. Also, there was individual-to-individual variability in LV developed pressure due to variability in HR and the need to use different balloons which could have affected the contractility. However, all cardiac parameters in the isolated hearts were normalised to the baseline established for that heart before analysis.

3.4.5 Conclusion

The observations from this chapter support the hypothesis that CaMKIIδ could be responsible for pro-arrhythmic signaling associated with NO exposure. The results from this chapter highlight a possible mechanism involving NO and CaMKII regarding impaired cardiac function. This provides some information towards CaMKIIδ being a potential candidate, as a therapeutic target for cardiac arrhythmias. Since NO production is increased with β-AR signaling, there is a possibility that adrenergic stress could exacerbate cardiac arrhythmias mediated by NO and CaMKII. Future studies will assess the effect of adrenergic stress and NO treatment on cardiac function in animal models with intact CaMKIIδ. Based on the findings in this chapter, arrhythmias will be analysed and nitrosylation levels will also be assessed.

CHAPTER 4: CARDIAC RESPONSE TO CHRONIC NITRIC OXIDE TREATMENT

4.1 Introduction

CaMKII is a critical calcium-handling protein that is important for enhancing Ca^{2+} flux through the cardiomyocyte during contraction and relaxation (Komukai et al., 2010). Aberrant activation of CaMKIIδ due to post translational modifications in pathological conditions has contributed to deleterious effects in the heart (Erickson et al., 2013; Gutierrez et al., 2013; Federico et al., 2017; Daniels et al., 2018). In Chapter 3, data showed that acute exogenous nitric oxide (NO) exposure increased arrhythmias in wild-type (WT) mouse hearts with intact CaMKIIδ, while CaMKIIδ-knockout (KO) mouse hearts were protected against arrhythmias. NO treatment did not alter cardiac contraction or relaxation in WT and KO hearts, and enhanced cardiac chronotropy in WT hearts but not in KO hearts. These results suggested that loss of CaMKIIδ in the presence of upregulated NO signaling prevents arrhythmogenesis. This chapter explores the long-term effects of NO treatment on cardiac function of WT and KO mice.

4.1.1 Nitric oxide and the cardiovascular system

NO plays a vital role in the cardiovascular system by enhancing vasodilation. The action of nitric oxide synthase (NOS) is responsible for platelet aggregation and leukocyte activation in the cardiovascular system (Lefer et al., 1999). In the heart, NO is essential for regulating blood pressure, maintaining vascular tone and mediating cardiac contractility (Dietz et al., 1994; Mohan et al., 1996; Prendergast et al., 1997; Müller-Strahl et al., 2000). Disruption in NO signaling, which leads to an imbalance in NO levels, is a marker of cardiac dysregulation. For example, inhibition of NOS resulted in a reduction in basal endogenous NO release in patients with congestive heart failure (Mohri et al., 1997). The onset of myocardial infarction in spontaneously hypertensive rats was marked by decreased NO availability (Wiemer et al., 2001). Reports have confirmed that reduced NO release due to NOS1 inhibition in the presence of increased intracellular Ca^{2+} can promote ventricular arrhythmias, suggesting that increased NO levels can prevent arrhythmias (Cutler et al., 2012). Enhanced NO bioavailability has been found to prevent

stroke, myocardial infarction and congestive heart failure (Ruschitzka et al., 2000; Jones et al., 2003). In contrast to the known protective role of NO, studies have also revealed that NO can promote arrhythmias in cardiomyocytes (Curran et al., 2014; Erickson et al., 2015). Currently, there is a debate surrounding the role of NO in the heart and the pathway by which it could be mediating cardiac arrhythmias. One suggested mechanism is through CaMKII S-nitrosylation (Gutierrez et al., 2013).

4.1.2 Regulation of CaMKII activity by NO

NO signaling can activate Ca^{2+}-handling proteins by modifying them via addition of NO molecules to their cysteine residues. This process, called S-nitrosylation, enhances Ca^{2+} cycling and thereby contraction and relaxation. S-nitrosylation is important for regulation of many biological processes. For example, increased S-nitrosylation of RyR2 can impair Ca^{2+} handling (Gonzalez et al., 2009). Gonzalez and colleagues (2007) showed in NOS1 deficient mouse cardiomyocytes that deficient S-nitrosylation of RyR2 promotes SR Ca^{2+} leak and pro-arrhythmic spontaneous Ca^{2+} waves. This suggested that S-nitrosylation of RyR2 can prevent Ca^{2+} mishandling in cardiomyocytes and, potentially, cardiac arrhythmias. This finding was in contrast to what has been observed in CaMKII nitrosylation. Experimental evidence has shown that increased CaMKII S-nitrosylation can be detrimental to cardiomyocytes due to its tendency to increase SR Ca^{2+} leak. Previous studies also support the concept that CaMKII could be responsible for arrhythmogenesis as a result of increase NO bioavailability by exogenous NO donors (Gutierrez *et al.*, 2013; Curran *et al.*, 2014; Erickson *et al.*, 2015).

Low bioavailability of NO has been associated with impaired cardiac function (Shesely et al., 1996; Jones et al., 2003). In clinical settings, NO donors are administered to control blood pressure in hypertensive patients (Houston & Hays, 2014), and also in pathological conditions associated with increased CaMKII expression, such as heart failure (Chirinos et al., 2016). Given what is known about GSNO and proarrhythmic signaling, there could be a possibility that increased NO levels and overexpression of CaMKII can jointly promote cardiac arrhythmias. Long-term GSNO treatment is known to improve insulin signaling and also play a role in neuroprotection (Rauhala *et al.*, 2005; Giri *et al.*, 2014; Jiang *et al.*, 2014; Aggarwal *et al.*, 2018; Khan *et al.*, 2019; Khan & Singh, 2019). However, the effect of chronic GSNO exposure on cardiac arrhythmias is unknown.

In Chapter 3, I found that acute GSNO treatment can induce cardiac arrhythmias. This raised a question as to whether constant elevation of NO levels in the blood would alter cardiac function and promote arrhythmogenesis in mouse hearts. Based on this, it was important to determine how chronic NO exposure would affect cardiac function and the potential role of CaMKIIδ. The aim of this Chapter was to investigate the role of CaMKIIδ signaling during chronic NO treatment in isolated WT and KO hearts.

4.1.3 Aims and hypotheses

This chapter addressed the effect of chronic GSNO treatment on cardiac function in WT and KO mice. The aims were as follows:

1) Measured nitrosylated CaMKII expression levels in mice after GSNO treatment. I hypothesised that there will be an increase in protein nitrosylation after chronic GSNO treatment.

2) Investigated the effect of GSNO on cardiac function in vivo and ex vivo after chronic treatment. I hypothesised that GSNO would alter cardiac structure and function in mice.

3) Determined the effect of GSNO on cardiac arrhythmias in WT and CaMKIIδ-KO mice chronically treated with GSNO. I hypothesised that KO mice would be protected against cardiac arrhythmias induced by chronic GSNO treatment.

4.2 Experimental methods

4.2.1 Administration of GSNO in drinking water

12-week old WT and KO mice were randomly assigned into 4 experimental groups: WT and KO control groups, and WT and KO treatment groups. The treatment groups received 50 mg/L of the NO donor (GSNO) in drinking water, refreshed every other day for 5 weeks (Figure 4.1). This method of administration was adopted from previous studies that showed that long-term oral NO therapy using NO donors can increase NO production in the body. Chronic oral administration of 50 mg/L sodium nitrite in drinking water was found to increase plasma nitrite levels in healthy and hypertensive rats (Ling *et al.*, 2018).

100 mg/L nitrite in drinking water restored depleted NO levels in diabetic rats to normal (Khalifi *et al.*, 2015). Sindler *et al.* (2015) showed that there was increase in plasma nitrite concentration in mice after a 5-week treatment of sodium nitrite in drinking water. Together, these studies confirm to an extent, the effectiveness of NO donor delivery in animals.

The experimental animals were housed in their usual cages (two mice per cage) and allowed to acclimatise for 7 days. Their water bottles were filled with 250 ml of water and weighed using digital scale to 0.1 g accuracy. To determine the average 24-hour water consumption per cage prior to the start of the experiments, the water bottles were weighed every day at the same time of the day for one week.

During GSNO treatment experiment, Fluid intake was documented daily throughout the treatment. After 5 weeks, the hearts were isolated from the mice and treated again ex vivo with different concentrations of GSNO (100 µM, 600 µM, 1600 µM), while cardiac function was measured (Chapter 3, Section 3.1.2). Cardiac tissue was saved for Western blotting to determine protein expression levels.

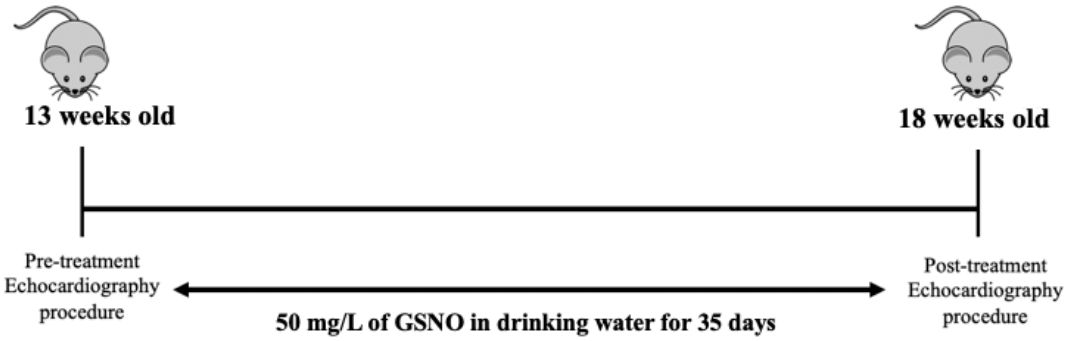

Figure 4.1 Timeline for GSNO treatment protocol in mice.

4.2.2 Biotin switch assay

A biotin switch assay is used to measure the level of S-nitrosylated proteins in cells or tissues. The process involves blocking free thiol sites on protein of interest with methyl methanethiosulfonate (MMTS), followed by reducing the S-nitrosylated sites with ascorbate. The S-nitrsoyalted sites on the protein are then labelled with biotin. Gel electrophoresis followed by Western blotting can be performed to measure the S-nitrosylation levels.

In this Chapter, biotin switch assay was carried out using an S-nitrosylated protein detection kit (Cayman Chemical). Left ventricular cardiac tissues were homogenized in 0.1 g/ml lysis buffer (50 mM Tris-HCl – pH 7.5; 3% SDS) using a bullet blender homogeniser and left on ice for 10 minutes. The sample was subjected to centrifugation and supernatant was aliquoted and stored in -80^{o}C.

The following steps were performed in the dark. 100 µl DMF and add 900 µl of buffer A was added to 1 vial of blocking reagent to form Buffer A reconstituted blocking reagent. Buffer A reconstituted blocking solution was added to samples as 1:9 (1µl per 9µl) to sample. Samples were placed on a shaker/rocker at a lowest speed for 30 min at 4^{o}C. Lysate was clarified by centrifugation for 10 min at 4^{o}C in table top microcentrifuge. Supernatants were transferred into separate cold pre-labelled 15 ml conical polypropylene tubes and 4 volumes of ice-cold acetone were added to each sample. Initial volume plus buffer A volume. The samples were mixed by inversion and incubated at -20^{o}C for 1 hr. Samples were removed from -20^{o}C and centrifugation was done at 3,000 x g for 10 min at 4^{o}C. During centrifugation, 1 vial of S-NO reducing agent was reconstituted with 1 ml buffer B. 1 vial of S-NO labelling reagent was dissolved with 100 µl DMF followed by 900 µl Buffer B. When each reagent is fully dissolved, 0.5 ml of Reducing Agent and 0.5 ml of Labelling Reagent were mixed in a graduated cylinder and the dissolved S-NO labelling agent was added alongside 4 ml of Buffer B. This mixture was labelled Buffer B containing reducing and labelling reagents. Samples were removed from centrifuge and supernatants (mostly acetone) were carefully decanted without disturbing the protein pellets. Protein pellet tubes were placed on ice. Excess residue of acetone was removed with pipette. Each pellet was resuspended with 0.5 ml Buffer B containing reducing and labelling reagents. For control, cell pellet was resuspended in Buffer B alone.

The subsequent steps were performed outside the dark room. The mixture of protein pellet and Buffer B containing reducing and labelling reagents and incubated for 1 hr at RT. Afterwards, 4 volumes of ice-cold acetone was added to each sample, mixed by inversion and incubated for 1 hr at -20^{o}C. Samples were removed from -20^{o}C and spun in a centrifuge at 3,000 x g for 10 min at 4^{o}C. Supernatant containing acetone was decanted and tubes containing the pellets were placed on ice. Pellets were resuspended in a minimal volume (100 µl) of cold wash buffer. 10 µl was used for protein estimation using the A280 method. The samples were aliquoted and stored at -20^{o}C for Western blotting.

For Western blotting (Chapter 2, section 2.5.3), sample was added to sample buffer and Milli-Q water. 20 µg of each sample were loaded on a fast cast 4-15% gel (Bio-Rad), and the gel was run for 45 minutes at 200 V. Gel was visualised on ChemiDoc MP Imaging System (Bio-Rad) to confirm protein load. The proteins were transferred onto a PVDF membrane at 30V overnight. Membrane was blocked in 2% BSA in PBS. The membrane was incubated in 1:100 dilution of Detection Reagent 1 (HRP) in Milli-Q water for 1 hour at RT, followed by a 10-minute wash, four times in TBS. The membrane was incubated in freshly prepared Clarity Western ECL substrate (Bio-Rad) and developed on ChemiDoc MP Imaging System (Bio-Rad) and analysed on ImageLab software (Bio-Rad).

4.3 Results

This section describes data from echocardiography in WT and KO mice prior to GSNO treatment at 13 weeks and at 18 weeks post treatment with GSNO. Functional parameters in the isolated hearts with and without GSNO treatment in all groups are also reported here.

4.3.1 Animal Characteristics

Body weight and sex ratio from WT and KO mice at 18 weeks of age post treatment with GSNO are shown in Table 4.1. In the control group that did not receive GSNO, KO mice had a significantly higher average body weight compared to WT mice at 13 and 18 weeks ($p < 0.05$). In the GSNO treatment groups, WT and KO mice had similar body weights ($p > 0.05$). There was no difference between WT control and GSNO treatment groups at 13 weeks ($p = 0.98$) or 18 weeks ($p = 0.96$). A similar observation was seen in the KO control and GSNO treatment groups at 13 ($p = 0.54$) and 18 weeks ($p = 0.56$). The average daily water intake per mouse in WT and KO mice is shown in Table 4.1. WT and KO mice control groups had similar initial and final daily water intake ($p = 0.81$; $p = 0.44$). There was also no significant difference in the average daily water consumption in the GSNO treatment groups of the WT mice compared to KO mice before commencement of experiment ($p = 0.82$) and after GSNO supplementation in drinking water ($p = 0.84$).

Table 4.1 Animal characteristics of WT and KO mice at 13 and 18 weeks

Parameter	**Control**		**Treatment**	
	WT (n=8)	**KO (n=8)**	**WT (n=6)**	**KO (n=6)**
Body weight (g) at 13 weeks	24.41 ± 1.37	27.40 ± 1.56*	24.30 ± 1.51	26.03 ± 1.70
Body weight (g) at 18 weeks	26.45 ± 1.39	32.05 ± 1.75*	26.38 ± 1.59	30.06 ± 1.81
Initial average daily water intake per mouse (ml)	5.26 ± 0.32	5.35 ± 0.19	4.65 ± 0.33	4.75 ± 0.19
Final average daily water intake per mouse (ml)	5.64 ± 0.58	6.26 ± 0.26	6.04 ± 0.70	5.85 ± 0.91
Ratio (M:F)	4:4	4:4	3:3	3:3

WT = Wild Type; KO = CaMKIIδ-knockout. Data are expressed as mean ± SEM. Two way-ANOVA was used to compare between animal genotypes and GSNO treatment effect between groups * = P< 0.05 vs WT

4.3.2 Total protein nitrosylation

Using biotin switch assay, protein nitrosylation was measured in the control and GSNO treatment groups of WT and KO hearts. All bands were normalised to loading control (stain free gel).

Global protein nitrosylation was observed across all groups, a representative blot is shown in Figure 4.2. Results from Western blotting showed that there was no significant difference in nitrosylated proteins in the KO GSNO treatment group compared to KO control ($p = 0.40$). There was also no significant difference in nitrosylation levels between WT and KO hearts in the control and GSNO treatment groups ($p = 0.27$). However, there was increased nitrosylation in the WT GSNO treatment group compared to WT control group ($p = 0.03$). These data suggest GSNO induced higher protein nitrosylation levels in WT compared to KO hearts.

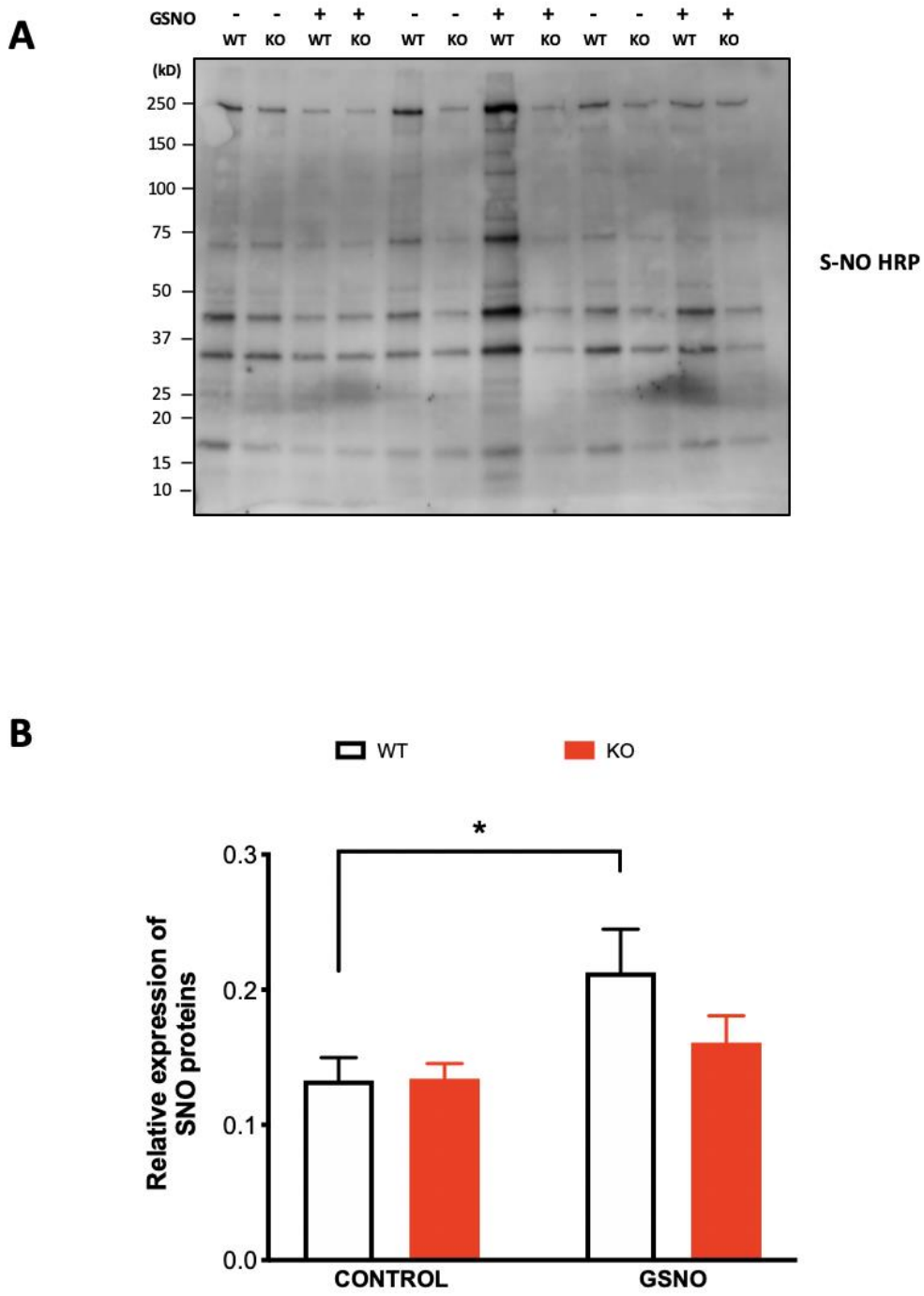

Figure 4.2 Quantification of S-nitrosylation in WT and KO mouse hearts chronically treated with GSNO A, Representative blot showing global protein nitrosylation in WT and KO mouse hearts. B, Total protein nitrosylation levels. Data are expressed as mean ± SEM. WT Control, n = 3, KO Control, n = 3 WT GSNO, n = 3, KO GSNO, n = 3. Two-way ANOVA (uncorrected Fisher's LSD test) was used to compare between treatment groups and animal models. * = $p < 0.05$. S-nitrosylation horseradish peroxidase (S-NO HRP)

4.3.3 Echocardiography parameters for WT and KO mice before and after GSNO treatment

Echocardiography data was obtained from WT and KO mice at 13 and 18 weeks, pre- and post-treatment with GSNO respectively (Table 4.2). There were four groups of mice, WT and KO treatment and control groups. The treatment groups were given GSNO in drinking water for 5 weeks. I hypothesized that WT and KO mice would share similar baseline cardiac structure and function before GSNO treatment, since healthy animals were used, no significant effect of GSNO on cardiac function at 18 weeks post-treatment was expected. Data from echocardiography revealed no overall measurable difference between the WT and KO mice in LVIDd, LVPWd, EDV, ESV, SV, CO both at 13 weeks and 18 weeks. However, echocardiography analysis showed significant differences in LVIDs, IVSs, FS% and EF in WT and KO mice at 13 weeks. At 18 weeks, there was a significant change in IVSd, LVIDs, FS%, EF and heart rate. In the control group, KO mice had significantly lower fractional shortening compared to WT mice at 13 weeks ($p = 0.02$) and 18 weeks ($p = 0.007$). The KO GSNO treatment groups also had significantly reduced fractional shortening at 13 weeks ($p = 0.0005$) and 18 weeks ($p = 0.004$). Ejection fraction of KO mice in the control group was significantly lower at 13 weeks ($p = 0.01$) and at 18 weeks (0.007) compared to WT. This was similar to that of the treated KO mice compared to WT mice at 13 weeks ($p = 0.0004$) and 18 weeks ($p = 0.007$). At 18 weeks, heart rate in the treated KO mice was significantly reduced compared to WT ($p = 0.004$). LVPWs at 13 weeks reduced in the KO control mice compared to WT ($p = 0.005$). At 13 weeks, LVIDs in the GSNO treatment group showed a significant reduction in KO mice compared to WT mice ($p = 0.008$). A significant reduction in IVSs was observed in KO mice compared to WT mice at 13 weeks. IVSd was also significantly reduced in the KO mice control group at 18 weeks ($p = 0.0004$). Results also showed that GSNO had no significant effect on any of the echocardiographic parameters after 5 weeks of treatment in the WT and KO groups.

The main aim of this experiment was to measure the difference in cardiac function due to impact of chronic GSNO administration. Overall, there was no effect of GSNO on the treated WT and KO mice. The echocardiographic data showed reduced systolic function in the KO mice at 13 and 18 weeks of age independent of GSNO treatment. These results suggest that chronic GSNO treatment does not alter cardiac structure and function in

healthy mice and deletion of CaMKIIδ reduces the functional output of the heart, including heart rate. These results are consistent with a known role for cardiac CaMKII in enhancing the chronotropic and inotropic properties of the heart.

Table 4.2 Echocardiographic parameters of left ventricle structure & function in WT and KO mice at 13 and 18 weeks of age

Parameter	Week	Control		GSNO Treatment	
		WT (n = 8)	KO (n = 8)	WT (n = 6)	KO (n = 6)
IVSd (mm)	13	0.91 ± 0.04	0.86 ± 0.02	0.90 ± 0.03	0.84 ± 0.03
	18	0.99 ± 0.02	0.87 ± 0.02***	0.92 ± 0.03	0.92 ± 0.01
IVSs (mm)	13	1.12 ± 0.04	1.05 ± 0.02 *	1.19 ± 0.07	1.05 ± 0.05*
	18	1.23 ± 0.03	1.14 ± 0.02	1.16 ± 0.07	1.15 ± 0.03
LVIDd (mm)	13	2.74 ± 0.07	2.64 ± 0.07	2.72 ± 0.09	2.69 ± 0.06
	18	3.06 ± 0.16	3.08 ± 0.14	3.02 ± 0.20	3.00 ± 0.10
LVIDs (mm)	13	1.62 ± 0.09	1.74 ± 0.10	1.46 ± 0.08	1.78 ± 0.10**
	18	1.88 ± 0.18	2.11 ± 0.13	1.63 ± 0.13	2.04 ± 0.09
LVPWd (mm)	13	0.91 ± 0.02	0.89 ± 0.02	0.94 ± 0.03	0.95 ± 0.06
	18	0.91 ± 0.02	0.89 ± 0.05	0.90 ± 0.03	0.92 ± 0.04
LVPWs (mm)	13	1.13 ± 0.04	0.98 ± 0.02**	1.13 ± 0.05	1.01 ± 0.05
	18	1.07 ± 0.04	1.02 ± 0.04	1.05 ± 0.02	1.03 ± 0.02
EDV (ml)	13	0.06 ± 0.00	0.05 ± 0.00	0.05± 0.01	0.05 ± 0.01
	18	0.08 ± 0.01	0.08 ± 0.01	0.06 ± 0.01	0.07 ± 0.01
ESV (ml)	13	0.01 ± 0.00	0.02 ± 0.00	0.01 ± 0.00	0.01 ± 0.00
	18	0.02 ± 0.01	0.03 ± 0.00	0.02 ± 0.00	0.02 ± 0.00
FS %	13	40.79 ± 2.20	34.08 ± 1.13*	46.30 ± 2.74	33.87 ± 2.05***
	18	39.18 ± 2.73	31.59 ± 1.41**	42.03 ± 1.86	32.56 ± 0.47**
EF	13	77.17 ± 2.18	69.36 ± 1.46*	82.58 ± 2.56	68.93 ± 2.65***
	18	74.85 ± 3.06	66.03 ± 2.06**	77.97 ± 1.80	67.81 ± 0.62**
SV (ml)	13	0.04 ± 0.00	0.04 ± 0.00	0.04 ± 0.01	0.04 ± 0.00
	18	0.06 ± 0.01	0.05 ± 0.01	0.05 ± 0.01	0.05 ± 0.01
CO (ml/min)	13	24.33 ± 1.91	16.99 ± 1.46	23.21 ± 2.57	16.10 ± 2.91
	18	26.43 ± 4.07	22.40 ± 1.64	21.72 ± 5.27	19.84 ± 2.84
HR (bpm)	13	483.00 ± 11.36	517.92 ± 17.70	490.50 ± 9.76	473.41 ± 30.82
	18	421.14 ± 7.32	410.04 ± 12.05	438.00 ± 8.89	379.24 ± 19.42**

WT= wild type; KO = knockout mice; IVSd= inter ventricular wall thickness diastole; IVSs= inter ventricular wall thickness systole; LVIDd= left ventricular internal diameter diastole; LVIDs= left ventricular internal diameter systole; LVPWs= left ventricle posterior wall thickness systole; LVPWd= left ventricle posterior wall thickness diastole; EDV= end diastolic volume; ESV= end systolic volume; FS= fractional shortening; EF= ejection fraction; SV= stroke volume; CO= cardiac output; HR= heart rate. Data are mean ± SEM. Two-way ANOVA (uncorrected Fisher's LSD test) was used for comparison of WT and KO genotypes and the effect of GSNO treatment between groups, * = P <0.05, ** = P <0.01, *** = P <0.001 versus WT.

4.3.4 Cardiac contraction and relaxation parameters in isolated WT and KO mouse hearts after GSNO supplementation.

I next determined cardiac function in isolated hearts of both animal models post treatment with GSNO. The hearts were isolated from WT and KO mice at 18 weeks of age, and perfused with Krebs-Henseleit buffer for 38 minutes before cardiac contractile parameters were measured.

The contractile parameters in WT and KO mice at 18 weeks have been outlined in Table 4.3. I observed no significant difference in LVDP in the KO compared to the WT hearts ($p = 0.13$). There was a significant difference in the heart rate between the WT and KO hearts ($p < 0.05$). However, the heart rate of the WT vs KO control and WT vs KO treatment groups were comparable ($p = 0.26$; $p = 0.69$). The difference in max dP/dt ($p = 0.30$) and min dP/dt ($p = 0.13$) remained insignificant in KO mice compared to WT mice. This observation in contractile parameters in the isolated hearts did not correspond with my data from echocardiography, in vivo. Both WT and KO exhibited arrhythmias at baseline, but there was no significant difference in the number of arrhythmic events ($p = 0.83$) or in arrhythmia scores ($p = 0.78$) between WT and KO hearts. Additionally, there was also no effect of GSNO supplementation on any of the contractile parameters or arrhythmias across all treatment groups (Table 4.3). Having shown that WT and KO mouse hearts had similar isolated heart function after 5 weeks of GSNO supplementation, the next experiment involved subjecting the isolated hearts to another GSNO treatment

Table 4.3 Baseline contractile parameters and quantification of arrhythmias in isolated WT and KO mouse hearts at 18 weeks after GSNO supplementation

Parameter	WT		KO		Genotype effect (P value)	GSNO Treatment effect (P value)
	Control (n=8)	Treatment (n=6)	Control (n=8)	Treatment (n=6)		
LVDP (mmHg)	62.47 ± 10.29	54.56 ± 4.31	78.62 ± 13.45	73.30 ± 11.64	0.13	0.55
HR (beats/min)	245.68 ± 19.95	275.91 ± 11.86	196.31 ± 28.63	221.40 ± 24.37	0.04*	0.24
Max dP/dt (mmHg/s)	2311.02 ± 353.58	2711.09 ± 166.48	3007.53 ± 601.96	2968.40 ± 450.17	0.30	0.69
Min dP/dt (mmHg/s)	-1215.83 ± 169.59	-1147.44 ± 66.74	-1517.67 ± 251.36	-1449.72 ± 186.93	0.13	0.72
Arrhythmic events	13.67 ± 3.88	8.40 ± 5.47	8.67 ± 3.46	15.20 ± 4.02	0.83	0.88
Arrhythmia score	0.67 ± 0.21	1.0 ± 0.32	0.83 ± 0.31	1.0 ± 0.32	0.78	0.40

WT = Wild Type; KO = CaMKIIδ-knockout; LVDP = Left ventricular developed pressure; HR = heart rate. Data are expressed as mean ± SEM. Two-way ANOVA (uncorrected Fisher's LSD test) was used to compare between WT and KO genotypes and GSNO treatment effect between groups. *P = <0.05

4.3.5 Effect of GSNO treatment on cardiac parameters in isolated WT and KO mouse hearts after in vivo GSNO supplementation

To investigate the potential role of CaMKII during chronic NO signaling, WT and KO hearts were treated again with GSNO at different concentrations (100 µM, 600 µM and 1600 µM), similar to the method in Chapter 3. I hypothesised that surplus GSNO treatment would alter cardiac contractility in WT and KO mouse hearts.

Results showed that GSNO reduced LV developed pressure in the WT and KO mice (Figure 4.3A). There was no difference in the LVDP between WT and KO hearts ($p = 0.18$). At the highest concentration of GSNO (1600 µM), there was a 16% reduction of LVDP in KO hearts compared to baseline, and this difference was significant ($p = 0.001$). GSNO at 600 µM also significantly depressed LVDP in the KO hearts compared to baseline ($p = 0.03$). The WT hearts exhibited a significant decrease (24.3%) in LVDP at the highest concentration of GSNO ($p = 0.01$).

The different concentrations of GSNO had no significant effect on heart rate in WT and KO hearts ($p = 0.26$) (Figure 4.3B). In addition, there was also no overall change in heart rate between the WT and KO mouse hearts ($p = 0.27$). WT hearts subjected to 1600 µM GSNO resulted in a 22.9% decrease in max dP/dt, compared to baseline and this change was significant ($p = 0.03$) (Figure 4.4A). In the KO hearts, 1600 µM GSNO caused a significant reduction (14.3%) in max dP/dt compared to baseline ($p = 0.003$). There was no overall significant difference in min dP/dt between WT and KO hearts ($p = 0.07$). There was a trend towards lower max dP/dt in the WT compared to the KO at the highest concentration of GSNO but this difference was not significant ($p = 0.07$). The highest concentration of GSNO resulted in a significant decrease in min dP/dt in WT hearts compared to baseline ($p = 0.04$). The highest concentration of GSNO had no effect on min dP/dt in KO hearts compared to baseline ($p = 0.48$) (Figure 4.4B).

In summary, high concentrations of GSNO depressed LV developed pressure and rates of contraction and relaxation in WT and KO hearts. However, there was no effect of GSNO on cardiac chronotropy.

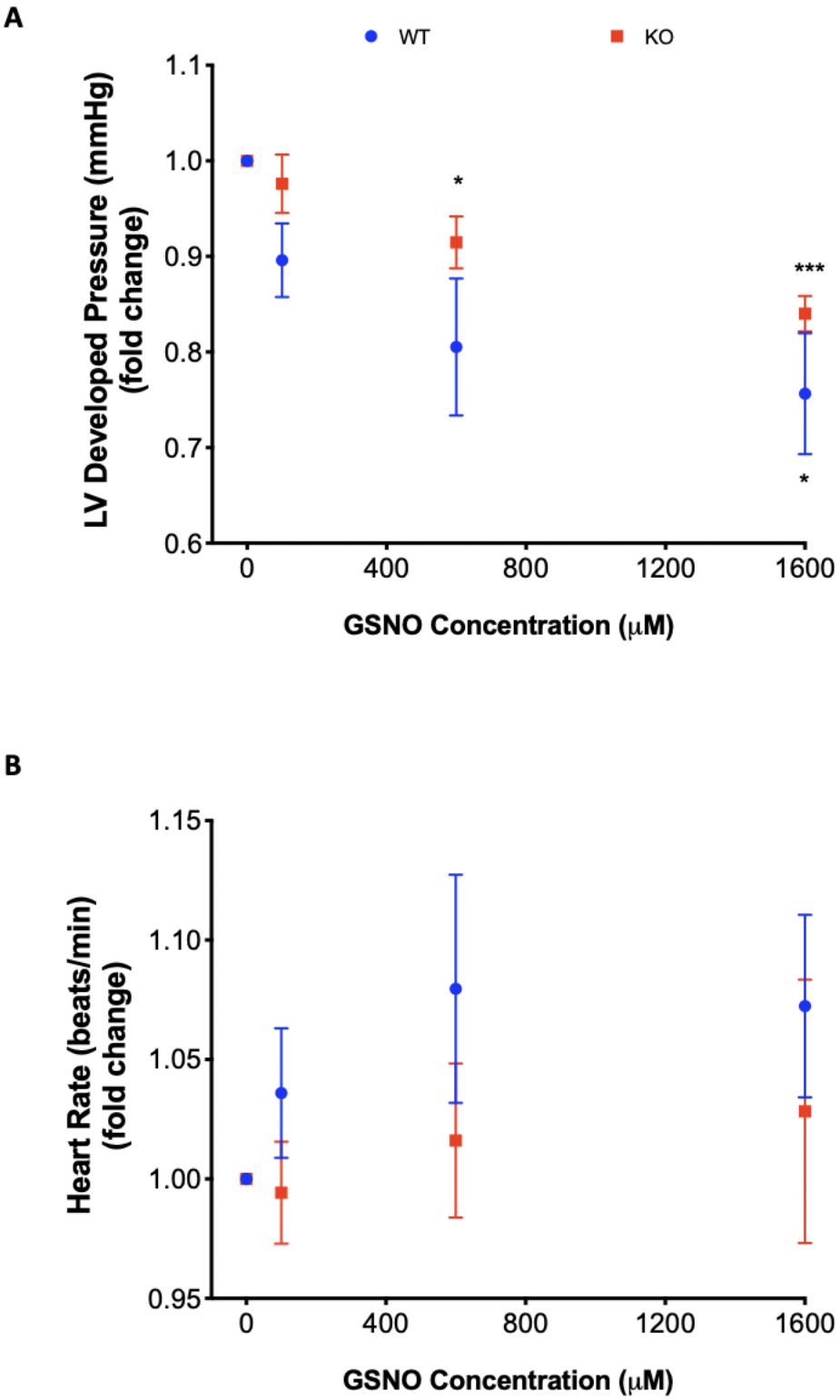

Figure 4.3 LV pressure and heart rate in WT and KO mouse hearts with GSNO treatment (100 µM, 600 µM and 1600 µM) A, LV developed pressure B, Heart rate. Data are means ± SEM. WT, blue line, n = 5 hearts; KO, red line, n = 5 hearts. Two-way ANOVA (uncorrected Fisher's LSD test) was used to compare between groups. * = P<0.05, *** = P<0.001, GSNO treatment effect (vs baseline).

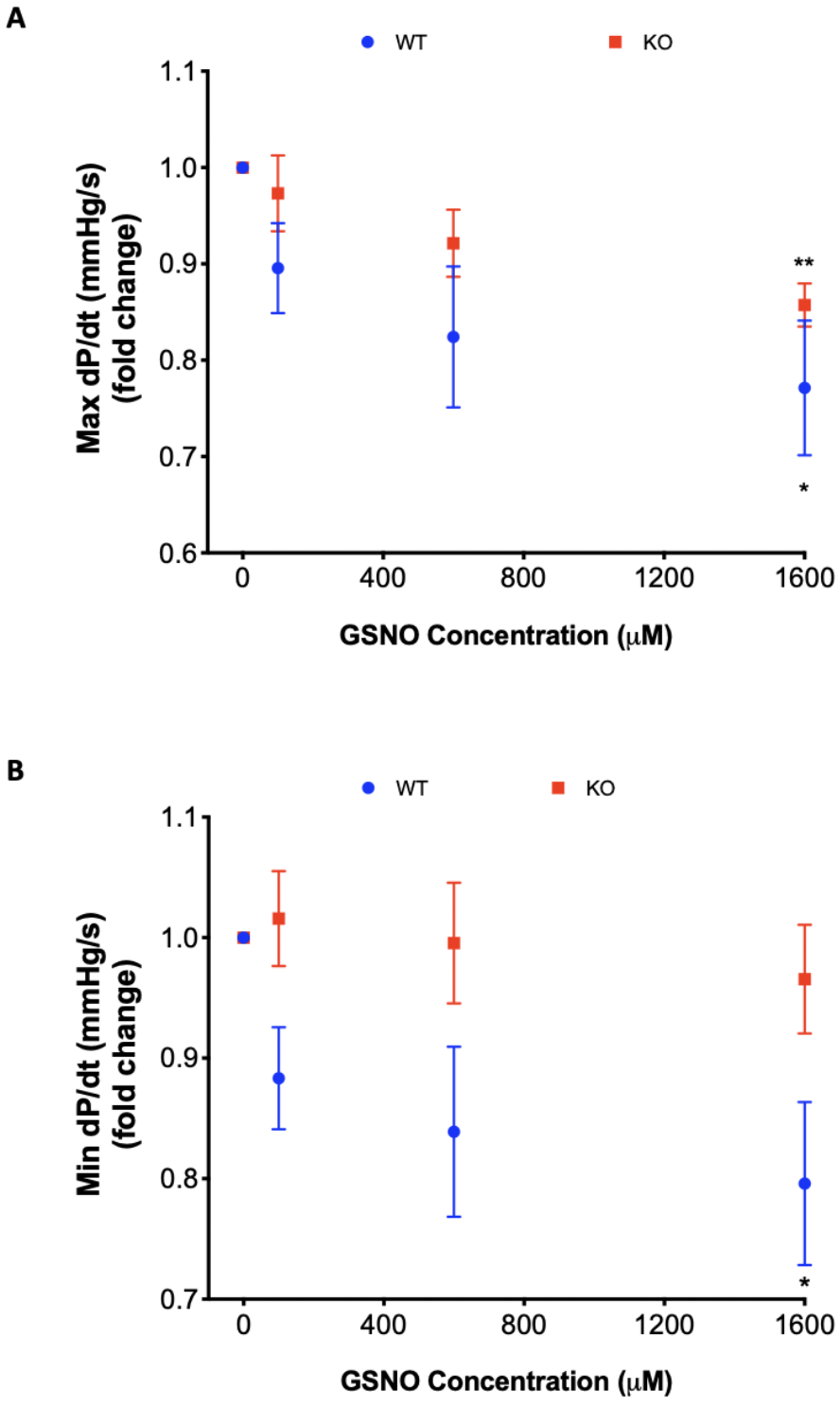

Figure 4.4 Rates of contraction and relaxation in WT and KO mouse hearts with GSNO treatment (100 µM, 600 µM and 1600 µM) A, Rate of Contraction (Max dP/dt) B, Rate of Relaxation (Min dP/dt). Data are means ± SEM. WT, blue line, n = 5 hearts; KO, red line, n = 5 hearts. Two-way ANOVA (uncorrected Fisher's LSD test) was used to compare between groups. * = P<0.05, ** = P<0.01, GSNO treatment effect (vs baseline).

4.3.6 Effect of GSNO on coronary flow and pressure-time integral in isolated WT and KO mouse hearts

No effect of GSNO on coronary function of isolated WT and KO hearts was observed after chronic treatment and subsequent perfusion with GSNO. There was no significant difference in coronary flow between WT and KO hearts ($p = 0.65$) (Figure 4.5A).

The tension in the myocardium per beat measured as pressure-time integral (PTI) was altered in WT and KO hearts during GSNO treatment (Figure 4.5B). WT hearts showed significant decline in PTI after 600 µM and 1600 µM GSNO treatment compared to baseline ($p = 0.03$; $p = 0.005$). This effect was not pronounced in KO hearts as PTI declined only after 100 µM compared to baseline ($p = 0.01$), and remained stable with further increase in GSNO. There was no overall significant difference in pressure-time integral between WT and KO hearts ($p = 0.10$).

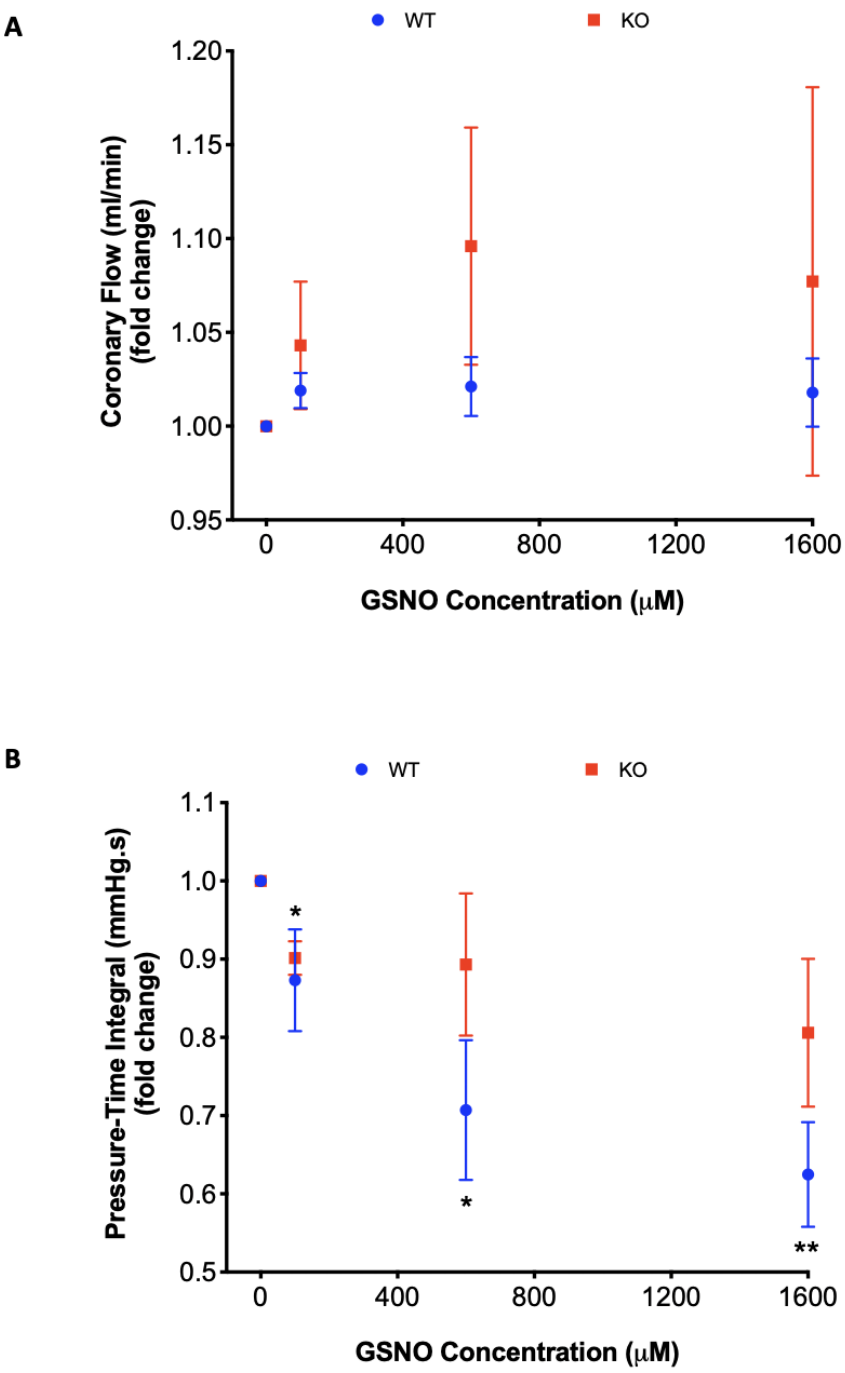

Figure 4.5 Cardiac response to GSNO treatment (100 µM, 600 µM and 1600 µM) in WT and KO mouse hearts. A, Coronary flow (ml/min) B, Pressure-time integral (mmHg.s). Data are means ± SEM. WT, blue line, n = 7 hearts; KO, red line, n = 5 hearts. Two-way ANOVA (uncorrected Fisher's LSD test) was used to compare between groups. * = P<0.05, ** = P<0.01, GSNO treatment effect (vs baseline).

4.3.7 Effect of GSNO on cardiac arrhythmias post GSNO supplementation

To further investigate the effect of GSNO on arrhythmias, I quantified the number of arrhythmic events and arrhythmia scores in WT and KO mouse hearts (Figure 4.6). WT and KO mouse hearts exhibited arrhythmias at baseline; however, no significant difference was observed in the number of arrhythmic events ($p = 0.70$) (Figure 4.6A). There was a trend towards increase in arrhythmias in both animal models with GSNO treatment but this did not attain a level of significance ($p = 0.06$). The WT and KO mouse hearts exhibited similar arrhythmia scores ($p = 0.91$). GSNO treatment did not affect the severity of arrhythmias in the WT and KO hearts ($p = 0.40$) (Figure 4.6B). There was no relationship between heart rate and arrhythmia score in WT hearts ($r = 0.07$, $p = 0.79$) and KO hearts ($r = - 0.32$, $p = 0.24$) (Figure 4.7).

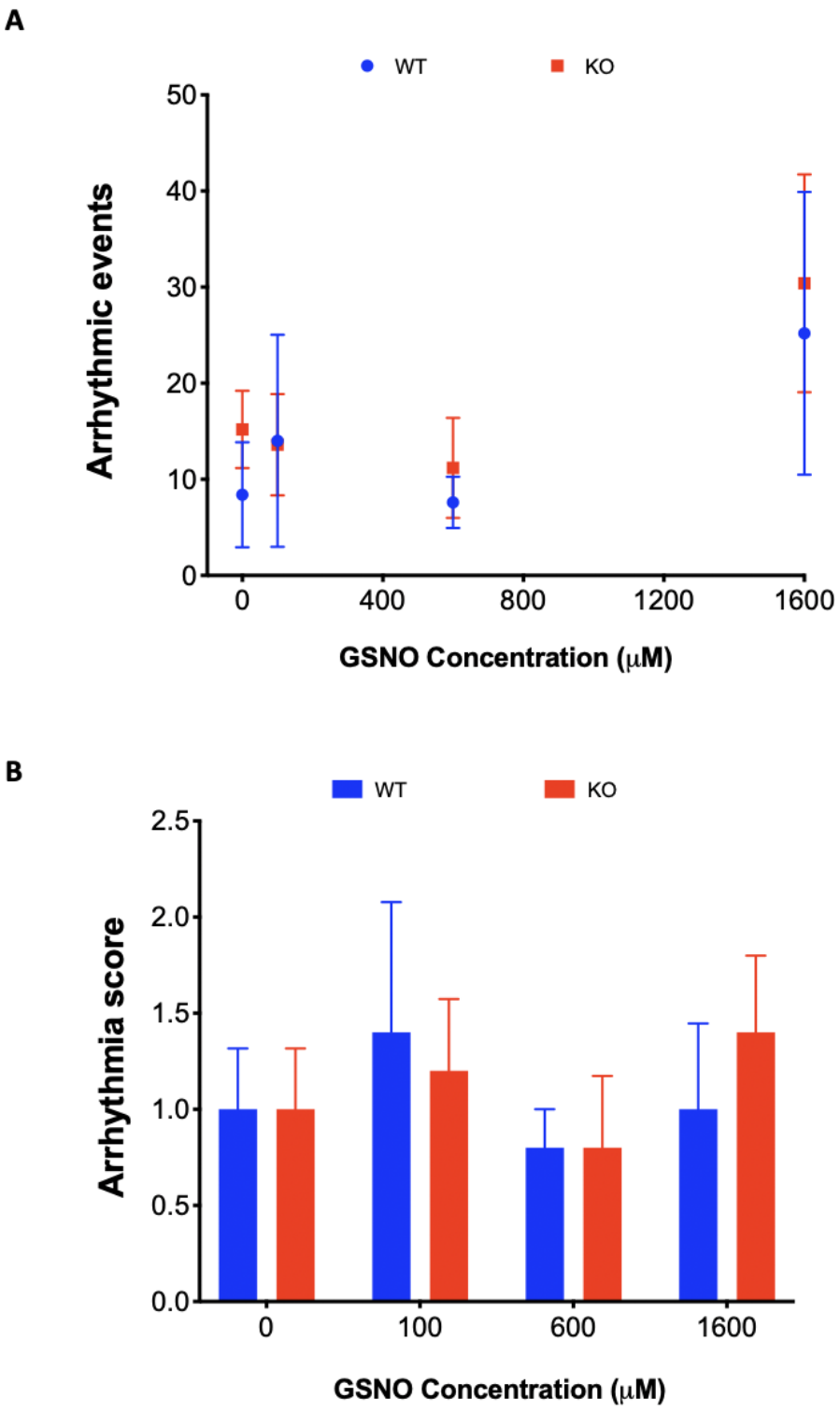

Figure 4.6 Arrhythmias during GSNO treatment (100 µM, 600 µM and 1600 µM) in WT and KO mouse hearts A, Arrhythmic events B, Arrhythmia scores. Data are means ± SEM. WT, blue line, blue bar, n = 5 hearts; KO, red line, red bar, n = 5 hearts. Two-way ANOVA (uncorrected Fisher's LSD test) was used to compare between groups.

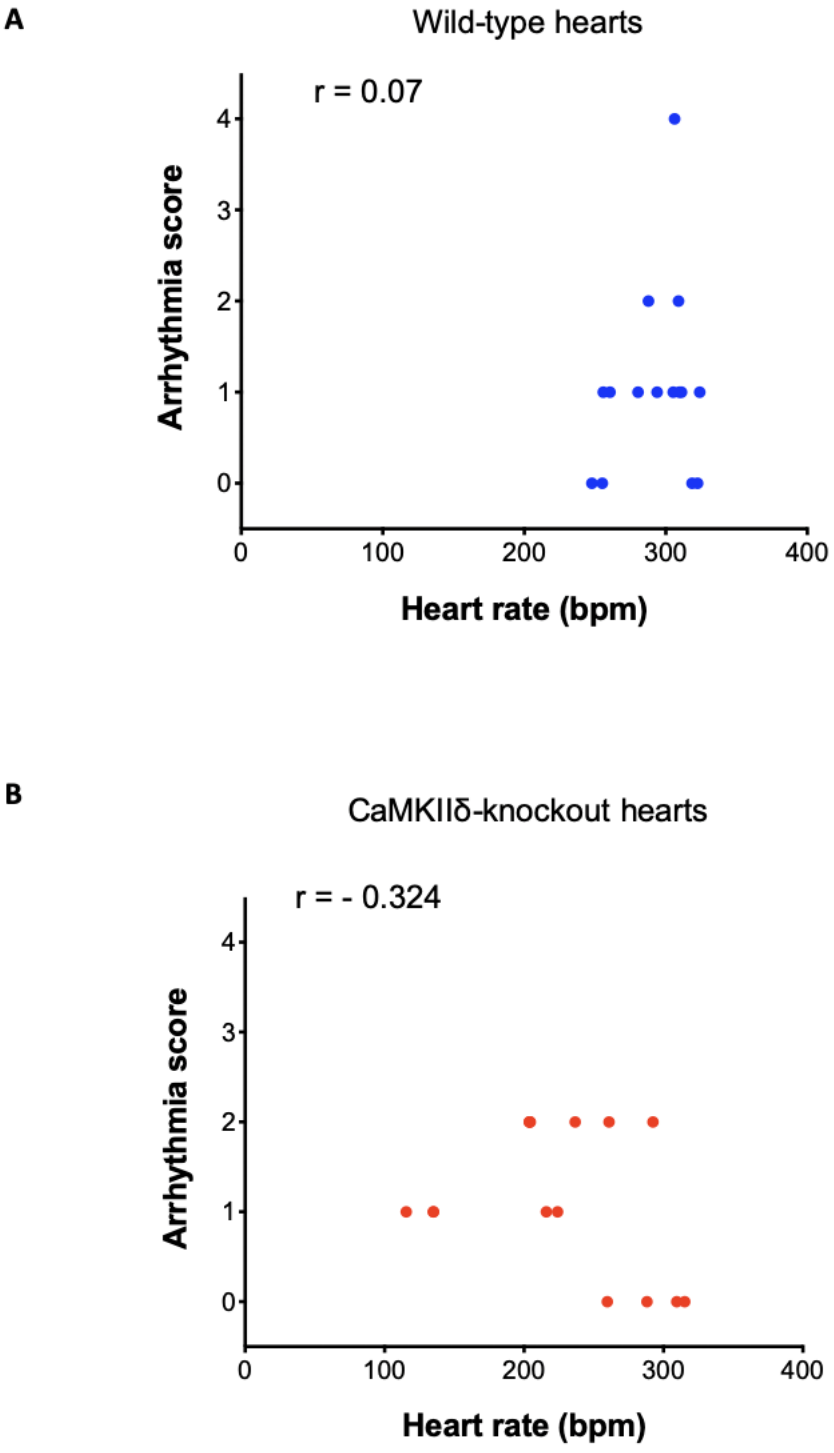

Figure 4.7 Effect of heart rate on arrhythmia severity during GSNO treatment in WT and KO mouse hearts A, Wild-type hearts B, CaMKIIδ hearts. Data are means ± SEM. WT, n = 5 hearts; KO, n = 5 hearts.

4.3.8 Effect of acute and chronic GSNO treatment on arrhythmias in WT and KO mouse hearts

To analyse the effect of duration of GSNO treatment on isolated WT and KO hearts, I compared the arrhythmic events between the baseline and highest concentration of GSNO used in this study during acute and chronic treatment.

In chapter 3 (section 3.2.6), data showed that WT mice exhibited significant elevation in arrhythmic events in the acute GSNO treatment at the highest concentration of GSNO relative to baseline whereas there was no significant effect of acute GSNO treatment on arrhythmic events in the KO hearts at any concentration. In this chapter, there was a trend effect of GSNO showing an increase in arrhythmias in WT and KO in the chronic phase; however, this difference was not statistically significant ($p = 0.06$) (Figure 4.6A).

There was an overall trend towards a difference in the amount of arrhythmias between the WT and KO hearts ($p = 0.09$) (Figure 4.8). There was a significant effect of GSNO treatment on number of arrhythmic events in WT and KO isolated hearts, irrespective of the treatment duration ($p = 0.02$). Post-hoc test revealed that there was a trend towards higher number of arrhythmias during GSNO treatment in the WT hearts during chronic treatment compared to acute treatment phase but level of significance was not achieved ($p = 0.07$). There was also a trend towards an increase in number of arrhythmic events in the KO hearts in the chronic GSNO treatment phase compared to acute GSNO treatment phase ($p = 0.09$).

Overall, I cannot conclude that GSNO treatment influenced the number of arrhythmias in WT and KO hearts when duration of treatment was considered. However, though statistically insignificant, there was a trend indicating that chronic treatment with GSNO may have led to an increase in arrhythmias for the KO animals.

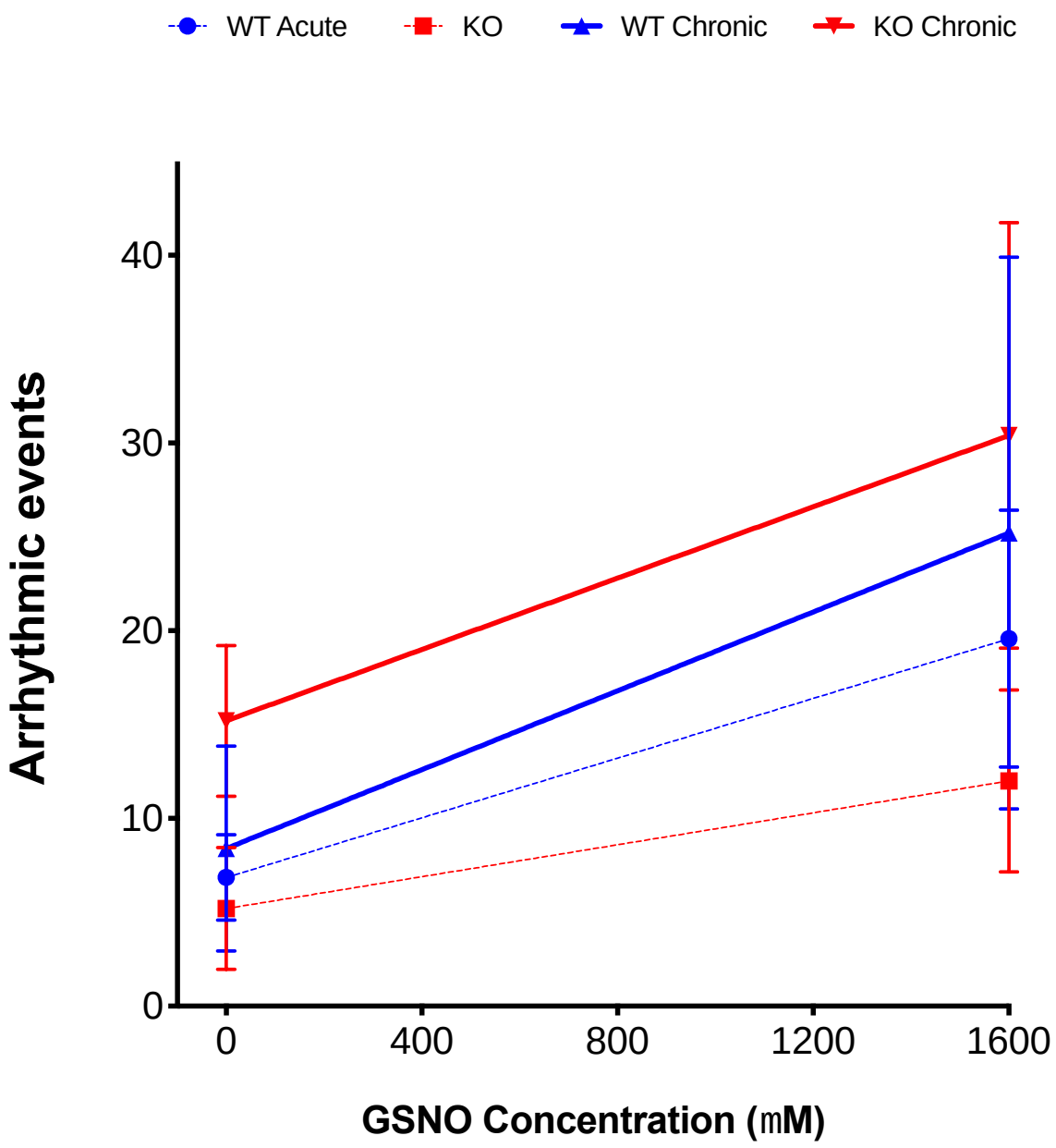

Figure 4.8 Arrhythmias during acute and chronic phases of GSNO treatment in WT and KO mouse hearts Data are means ± SEM. WT acute phase, broken blue line, n = 7 hearts, KO acute phase, red broken line, n = 5 hearts, WT chronic phase, n = 5 hearts, KO chronic phase, n = 5 hearts. Three-way ANOVA (uncorrected Fisher's LSD test) was used to compare between across groups.

4.4 Discussion

The aim of this Chapter was to investigate the role of chronic GSNO treatment on cardiac function in WT and CaMKIIδ-KO mice. GSNO was administered to mice for 5 weeks, from 13 to 18 weeks of age. Echocardiography to assess LV structure and function was performed at week 13 and week 18. The hearts were then isolated and treated again with GSNO at different concentrations while cardiac contractility was measured. Protein nitrosylation level was quantified via Western blotting. The main findings of this study are as follows: (a) GSNO treatment induced protein nitrosylation, but KO mice appeared to be more resistant to these effects, (b) Long term GSNO treatment has no effect on in vivo cardiac function (c) isolated WT and KO mouse hearts that received chronic GSNO treatment exhibit reduced contractility and reduced rates of contraction and relaxation with increasing concentrations of GSNO treatment, (d) chronic GSNO treatment phase does not significantly enhance the number of arrhythmic events in WT and KO hearts.

4.4.1 GSNO induces S-nitrosylation in the heart

Cardiac tissues from WT and KO mice exposed to different concentrations of GSNO and further treated with GSNO after heart isolation were subjected to biotin switch assay to analyse levels of cardiac SNO proteins (Figure 4.2). Studies have shown that NO signaling can be regulated through the S-nitrosylation which involves covalent attachment of NO-related species to cysteine residues (Gonzalez et al., 2007; González et al., 2008; Cutler et al., 2012; Irie et al., 2015). Previous studies show that GSNO mediates its effects through S-nitrosylation (Sun et al., 2007; Erickson et al., 2015). In this study, effect of GSNO was evaluated in the heart and there was upregulated S-nitrosylation in WT hearts compared to KO hearts. It is unclear whether the lack of change in S-nitrosylation levels in the KO mice is due to loss of CaMKIIδ. There was no significant difference in GSNO water consumption between the WT and KO animals, and thus any differences in S-nitrosylation should not be a product of unequal exposure to GSNO. The level of CaMKII S-nitrosylation in the WT animals could not be directly measured due to difficulty in optimising this aspect of the biotin switch assay. One possibility to consider is that CaMKII, once activated, may interact with the nitric oxide synthase family of proteins to induce enhanced NO production, further increasing S-nitrosylation of many protein targets. This feedback loop would not occur in the CaMKIIδ KO animals,

which could account for why less overall S-nitrosylation was observed. Overall, my results suggest that the effect of GSNO observed in the isolated hearts may be mediated through S-nitrosylation.

4.4.2 Effect of GSNO and deletion of CaMKIIδ on cardiac function

Aberrant CaMKII activity has been associated with altered Ca^{2+} homeostasis and proarrhythmic remodelling (Wu et al., 2002; Erickson et al., 2013; Erickson et al., 2015; Grimm et al., 2015; Feng et al., 2017; Lebek et al., 2018). A previous study by Grimm et al. (2015) has demonstrated that genetic deletion of CaMKIIδ is protective against pathological signaling in the heart. The results from my study showed that KO mice had altered cardiac function at baseline compared to WT mice (Table 4.2). Comparing the WT and KO treatment groups in this Chapter, I showed that the structural and functional differences observed at baseline still persisted after 5 weeks. I hypothesised that deletion of CaMKIIδ would not affect basal cardiac structure and function. The findings from this Chapter reject my hypothesis. It is also contrary to other studies that have characterised this CaMKIIδ KO model and found no altered basal cardiac function in KO mice compared to the WT mice (Backs et al., 2009; Ling et al., 2009). Ling et al. (2009) developed the KO mouse model, measured cardiac function using echocardiography at 2 and 10 months and found no difference in LV chamber or wall thickness. The differences observed in echocardiography parameters in the WT and KO mice used in this chapter suggest that deletion of CaMKIIδ is detrimental to mouse hearts. Despite the systolic dysfunction observed in the KO mice, they had no obvious alterations in phenotype except for significant weight gain in the control group at 13 and 18 weeks compared to WT mice (Table 4.1). After in vivo cardiac function assessment, the WT and KO hearts were isolated and cardiac contractile parameters were measured. I observed no significant change in cardiac function between WT and KO hearts after the 5-week GSNO administration. Grimm et al. (2015) found no significant differences in cardiac parameters of WT and KO mice using echocardiography and this result remained the same after isolated heart perfusion. This raises the question as to what could be happening in vivo that resulted in altered cardiac function while WT and KO hearts shared similar basal cardiac function ex vivo. The disparity in findings could be due to a factor such as level of anaesthesia (Gao et al., 2011).

Following GSNO treatment for 5 weeks, there was no difference in echocardiography parameters between treatment groups of each animal model (Table 4.2). My hypothesis was that long term GSNO treatment would upregulate NO levels and alter cardiac function. My data suggest that GSNO had no significant effect on cardiac structure and function which is not consistent with my hypothesis. To my knowledge, no study has measured cardiac function with chronic GSNO treatment. Other groups have reported that 50 mg/L of a NO donor, sodium nitrite, was sufficient to improve insulin signaling and vascular function in mice (Jiang et al., 2014; Sindler et al., 2015). It is possible that the duration of GSNO treatment was not sufficient to induce significant changes in the WT and KO mouse hearts, and a longer duration of treatment could be required.

4.4.3 GSNO treatment alters cardiac contractility in isolated WT and KO hearts after GSNO supplementation

Another aim of this study was to investigate the effect of GSNO on the contractile parameters of isolated WT and KO hearts after chronic treatment with a NO donor. GSNO can induce S-nitrosylation which in turn modulates the activity of cardiac Ca^{2+}-handling proteins (Gonzalez et al., 2007; Sun et al., 2008; Cutler et al., 2012). GSNO therapy has been found to have cardioprotective effects in animals and humans (Konorev et al., 1995; Rassaf et al., 2006; Sun et al., 2007). For example, GSNO protects cardiomyocytes from hypoxic damage and accelerated cardiac contractility after ischaemia/reperfusion in isolated rat hearts (Poluektov et al., 2019). On the other hand, GSNO exposure in cardiomyocytes has been found to result in pro-arrhythmic remodelling by inducing increased Ca^{2+} spark frequency in the presence of CaMKII activity (Gutierrez et al., 2013; Curran et al., 2014). In cardiomyocytes, SR Ca^{2+} leak leads to an increase in Ca^{2+} spark frequency which generates into spontaneous Ca^{2+} waves and suggests susceptibility of the heart to arrhythmias (Landstrom et al., 2017).

First, I determined the impact of GSNO on inotropy in isolated hearts. I hypothesised that GSNO would increase or reduce LVDP depending on the concentration. The results showed reduced LVDP in WT and KO mice at high GSNO concentration (Figure 4.3A). Developed pressure in WT and KO mouse hearts had a similar response to GSNO which suggests that this observation may not be dependent on CaMKIIδ activity. These results add to the body of work from previous studies showing that high concentrations of NO

result in negative inotropy (Mohan et al., 1996; Vila-Petroff et al., 1999; Brunner et al., 2001; González et al., 2008). To my knowledge, research has focused on the effect of GSNO on contractility in cardiomyocytes and there is no documented literature on the effect of GSNO on cardiac function in isolated mouse hearts. However, the biphasic effect of NO donors has been established. A previous study by González et al. (2008) has revealed that low concentrations of the NO donor SNAP enhanced contractility in isolated rat hearts and high concentrations had the opposite effect. This was due to activation of the cAMP and cGMP pathways, depending on the concentration. Therefore, as observed in my study, reduced LVDP due to high GSNO concentrations suggests an activation of the cGMP-dependent PKG pathway which results in negative inotropy (Vila-Petroff et al., 1999).

Secondly, I observed no effect of GSNO on heart rate in the WT and KO mice (Figure 4.3B). Previous work has shown that isolated rat hearts exhibited increased heart rate with low concentrations of exogenous NO donors (Müller-Strahl et al., 2000). Pabla and Curtis (1995) found that in isolated rat hearts, 10 mM L-arginine, a precursor of NO, had no effect on heart rate while 10 µM of the NO donor SNP increased heart rate prior to ischaemia and during reperfusion. This suggests that low concentrations of exogenous NO, and not endogenous NO, can enhance heart rate. In another study, high concentrations of NO (> 300 µM) resulted in a reduction of heart rate in isolated rat atria (Kennedy et al., 1994). My findings show no change in heart rate at low or high concentration of GSNO. It is unclear whether the treatment with GSNO before subsequent application of GSNO to the isolated hearts has contributed to this observation. The mechanism responsible for no change in heart rate, despite altered inotropy and lusitropy could not be identified in this study.

GSNO treatment also decreased max dP/dt and min dP/dt at a high concentration of GSNO (1600 µM) (Figure 4.4). It was surprising that KO hearts did not exhibit any change in rate of relaxation with increasing GSNO concentration (Figure 4.4B). The effect of NO on rates of contraction and relaxation has been well documented. Kojda et al. (1997) showed that low concentration (< 1 µM) of a NO donor, DEA/NO, induced an increase in max dP/dt and min dP/dt in healthy isolated rat hearts. This was similar to what this group previously observed when investigating low concentrations of NO on cardiac contractility in rat cardiomyocytes (Kojda et al., 1996). The negative inotropy and

lusitropy due to high concentrations of GSNO as observed in the WT and KO hearts could be attributed to the concentration-dependent biphasic effect of NO (Mohan et al., 1996; Musialek et al., 1997; Preckel et al., 1997; Müller-Strahl et al., 2000; González et al., 2008). Therefore, the reduced max dP/dt and min dP/dt in the WT and KO hearts is mediated by the cGMP dependent pathway due to high levels of cGMP produced by high concentrations of NO donors and subsequent activation of protein kinase G, as observed in previous studies (Sandirasegarane & Diamond, 1999; Layland et al., 2002).

Coronary function was unchanged during GSNO treatment in WT and KO hearts (Figure 4.5A). Previous study showed that inhibition of NOS can modify coronary flow in isolated hearts and this is related to a change in developed pressure (Bouma et al., 1992). My data shows GSNO induced a reduction in contractile function and this did not result in a change in coronary flow. It was also unclear if the lack of GSNO effect on coronary flow was related to arrhythmic events. There was a reduction in the average developed pressure per beat (PTI) with increase in GSNO concentration in WT hearts, however, this effect was not so pronounced in the KO hearts (Figure 4.5B). This suggests that the amount of energy used for contraction was lower in presence of CaMKIIδ during GSNO treatment, and this corresponded with the LV developed pressure.

To summarise my findings, the resultant effect of GSNO on cardiac function in this chapter indicates that high concentrations of NO can negatively affect cardiac contractility in mice even in the absence of CaMKIIδ.

4.4.4 GSNO treatment has no effect on cardiac arrhythmias in isolated WT and KO hearts after GSNO supplementation

Chapter 3 of this thesis investigated the acute effects of GSNO exposure and found enhanced cardiac arrhythmias with increasing GSNO concentrations in the WT mouse hearts while the KO hearts were protected from GSNO-induced arrhythmias. In this Chapter, the result is contrary and shows that after chronic GSNO treatment, increasing concentrations of GSNO had no effect on arrhythmias in isolated WT and KO hearts (Figure 4.6). Thus, my findings reject the hypothesis that GSNO would induce cardiac arrhythmias in WT hearts. In addition, there absence of relationship between heart rate

and arrhythmia scores showed that there was change in heart rate did not influence the severity of arrhythmias (Figure 4.7).

The anti-arrhythmic property of NO has been documented in literature. Inhibition of NOS using knockout models has been used to investigate the role of NO in cardiac arrhythmias (Kubota *et al.*, 2000; Rakhit *et al.*, 2001; Burger *et al.*, 2009). Ventricular myocytes from mice lacking eNOS were found to be more susceptible to arrhythmias (Kubota et al., 2000). Previous literature has also documented a contrary report concerning NO and arrhythmias. Gutierrez et al. (2013) showed that CaMKII activity in guinea pig cardiomyocytes enhanced Ca^{2+} spark frequency after GSNO exposure suggesting that NO contributed to the susceptibility of the heart to arrhythmias during CaMKII activation. A similar study by Erickson et al. (2015) also implicated the activation of CaMKIIδ to be responsible for increased Ca^{2+} spark frequency in WT ventricular cardiomyocytes. CaMKIIδ is known to be an arrhythmogenic molecule and its inhibition has been a target towards protecting against proarrhythmic signaling (Sag et al., 2009; Erickson et al., 2013; Sommese et al., 2016; Feng et al., 2017). In this Chapter, the expectation was that deletion of CaMKIIδ would protect the KO mouse hearts against arrhythmias, after exposure to GSNO. The isolated hearts from both animal models used in this chapter developed arrhythmias and KO hearts were not protected against ventricular arrhythmias regardless of GSNO concentration, suggesting that NO and CaMKIIδ may not be playing a role in the arrhythmogenesis. Measurement of CaMKIIδ S-nitrosylation and NOS activity in future studies could provide more insight into the possible underlying mechanism for this finding.

In summary, GSNO may not be responsible for cardiac arrhythmias even at low concentrations even in the presence of CaMKIIδ. This does not correspond with data reported in Chapter 3 and previous reports (Gutierrez et al., 2013; Curran et al., 2014).

4.4.5 Duration of GSNO treatment does not affect arrhythmias in WT and KO hearts

Data from my study demonstrated that the duration of treatment did not significantly affect the response of WT hearts and KO hearts to GSNO-induced arrhythmic events (Figure 4.8). In acute treatment, GSNO increased arrhythmias in WT hearts and

chronically, there was no significant increase in arrhythmias in response to GSNO. When GSNO was administered to KO isolated hearts acutely, the KO hearts were protected from arrhythmias (Chapter 3), whereas in the chronic treatment phase, the KO hearts started to exhibit a trend towards increased arrhythmias with GSNO. This suggests that acutely, knocking out CaMKIIδ can protect the heart from GSNO-induced proarrhythmic remodelling. This is similar to the finding that CaMKII inhibition can prevent increase in Ca^{2+} spark frequency after GSNO treatment in cardiomyocytes (Gutierrez et al., 2013; Curran et al., 2014; Erickson et al., 2015). There is no published study that examines chronic GSNO treatment related to CaMKII inhibition. Comparing data from Chapter 3 and Chapter 4, the presence of CaMKII during GSNO treatment induces arrhythmias as seen in WT hearts, whereas in long term GSNO administration, the presence or absence of CaMKII does not contribute to cardiac arrhythmias. The chronic administration of GSNO prior to heart isolation and second phase of treatment may have rendered the KO mice more sensitive to NO. The mechanism underlying this effect is not completely understood. Combined, these data provide the first evidence that chronic GSNO treatment does not induce arrhythmias in WT hearts and KO hearts.

4.4.6 Conclusion

In summary, this study shows the first evidence of the effect of chronic GSNO exposure on cardiac function. Data presented in this chapter show that KO mice exhibited systolic dysfunction at baseline and prolonged GSNO treatment can result in negative inotropy, however, it does not contribute to increased cardiac arrhythmias in WT and KO hearts. Results from this chapter also indicate that the CaMKIIδ deletion results in systolic dysfunction in vivo, and chronic GSNO exposure in mice is not deleterious to cardiac function except at a high concentration.

CHAPTER 5: THE ROLE OF NITRIC OXIDE AND β – ADRENERGIC RECEPTOR STIMULATION IN CARDIAC FUNCTION

5.1 Introduction

β-adrenergic receptor (β-AR) stimulation induces the "fight or flight" response of the heart to cope with stress by increasing cardiac output. β-AR signaling is an essential regulator of cardiac Ca^{2+} homeostasis and cardiac function as a whole (Yoo et al., 2009). β-ARs are G-protein-coupled receptors involved in regulating the heart's response to catecholamines (Chruscinski et al., 1999; Ferrero et al., 2007; Calvert & Lefer, 2013). When β-ARs are stimulated, adenylyl cyclase is activated, increasing cAMP production and activating PKA and other downstream mediators, including Ca^{2+} handling proteins. The heart's response to this stimulation is enhanced force and frequency of myocardial contraction and accelerated relaxation (Grimm & Brown, 2010). Excessive sympathetic stimulation has been implicated in various cardiac pathologies, such as heart failure and arrhythmia (Shizukuda et al., 1998; Iwai-Kanai et al., 1999; Floras, 2009; Bovo et al., 2012; Joca et al., 2020).

ß-AR stimulation has been shown to be an activator of CaMKII in the heart, as seen in Langendorff perfused mouse hearts (Grimm et al., 2015). Alongside β-AR stimulation, the effect of overexpression of the cardiac protein kinase CaMKII has also been observed in pathological cardiac conditions (Ai et al., 2005; Khoo et al., 2006; Kohlhaas et al., 2006; Said et al., 2008). Studies have suggested that even though these two pathways can be independent, the β-adrenergic pathway can also modulate CaMKII activity (Wu et al., 2002; Wang et al., 2004; Sag et al., 2009; Grimm & Brown, 2010). For example, the β-AR agonist isoproterenol (ISO) induces spontaneous SR Ca^{2+} leak in cardiomyocytes and arrhythmias in the heart (Wu et al., 2002; Curran et al., 2007; Grimm et al., 2015). Since CaMKII is a downstream mediator of deleterious ß-adrenergic signaling as in heart failure, inhibition of CaMKII could be an effective therapeutic strategy in addressing heart failure (Mollova et al., 2015; Dewenter et al., 2017) and protecting the heart against cardiac dysfunction. Sag et al. (2009) tested the influence of CaMKII on ISO-dependent arrhythmias and observed that inhibition of CaMKII reduced the incidence of cardiac

arrhythmias in mice overexpressing CaMKIIδ. Increased Ca^{2+} spark frequency in cardiomyocytes, which is a predictor of cardiac arrhythmias, is attenuated in CaMKIIδ-KO mouse cardiomyocytes exposed to ISO (Grimm et al., 2015). Findings from Curran et al. (2007) indicate that ISO-induced SR Ca^{2+} leak in intact rabbit ventricular cardiac cells was prevented by CaMKII inhibition, and this effect was not dependent on PKA. Taken together, these suggest that CaMKII activity contributes to cardiac pathological signaling during β-AR stress via a complex pathway that is not well understood.

Interestingly, there is a link between β-adrenergic response in the heart and NO signaling. During basal cardiac contractility, NOS activity can induce S-nitrosylation of RyR2, LTCC and SERCA2 which is enhanced by β-AR stimulation (Vielma et al., 2016). Increased β-AR stimulation activates eNOS to increase NO bioavailability, though the exact mechanism is yet to be elucidated (Calvert & Lefer, 2013). NO bioavailability can improve vascular compliance and regulate blood pressure in hypertension (Rees et al., 1996; Houston & Hays, 2014). NO can also modify RyR2 and protect against SR Ca^{2+} leak in cardiomyocytes (Gonzalez et al., 2007), and even prevent arrhythmias under elevated intracellular Ca^{2+} conditions in the heart (Cutler et al., 2012).

Despite the well-established cardioprotective role of NO (Phillips et al., 2009; Houston & Hays, 2014; Grievink et al., 2016), evidence has emerged that shows the role of NO in the heart could be more complicated than described in previous studies. Recent studies have now identified a unique cardiac arrhythmogenesis pathway involving β-AR stimulation, NO and CaMKII, which induce SR Ca^{2+} leak in cardiomyocytes (Gutierrez et al., 2013). According to data reported in chapter 3, NO could potentially have an arrhythmogenic effect in a heart with intact CaMKIIδ. Some studies have revealed that even though NO can directly activate CaMKII (Erickson et al., 2015), β-AR stimulation can also influence CaMKII activation by NO (Gutierrez et al., 2013; Curran et al., 2014).

Gutierrez et al. (2013) observed that CaMKII could be activated by direct NO signaling. In guinea-pig ventricular myocytes exposed to a NO donor, GSNO, they observed an increase in Ca^{2+} spark frequency, which mimicked the similar effect of ISO application. They confirmed the involvement of CaMKII using the inhibitors KN93 and AIP. Similarly, in rabbit ventricular myocytes, inhibition of NOS in the presence of ISO

ablated arrhythmogenic spontaneous Ca^{2+} waves and inhibition of CaMKII in the presence of a NO donor, SNAP, prevented increase in SR Ca^{2+} leak (Curran et al., 2014).

To summarise, CaMKII plays a unique role in arrhythmogenesis in the presence of NO in cardiomyocytes. CaMKII activation by β-AR stimulation and NO is the pathway that promotes SR Ca^{2+} leak in cardiac cells and could be responsible for arrhythmias in the heart. The influence of β-AR stimulation on the NO-CaMKII pathway has only been tested in cardiomyocytes, and there is limited evidence to determine if the same pathway could be involved in cardiac arrhythmias.

The results detailed in Chapter 3 showed that knocking out CaMKIIδ prevented cardiac arrhythmias associated with NO signaling. The next step was to determine the relationship between CaMKIIδ and NO during increased β-adrenergic stimulation. The experiments in this chapter focused on the effects of β-adrenergic stress and NO signaling in cardiac function in WT mice with intact CaMKII.

5.1.1 Aims and hypothesis

The aims of this chapter were;

1) To determine if NO will also modify CaMKII via nitrosylation. I hypothesised that the NO donor GSNO will induce S-nitrosylation of CaMKII in WT hearts.

2) To assess cardiac response of KO hearts to β-adrenergic stimulation and to further measure the effect of β adrenergic stimulation on arrhythmias. I hypothesised the β-adrenergic stimulation would alter cardiac contraction in KO mouse hearts and have no effect on arrhythmias.

3) To determine if NO exposure and CaMKII activation via β-adrenergic stimulation would alter cardiac function in WT mice. I hypothesised that β-adrenergic signaling would activate CaMKII and increase cardiac inotropy and chronotropy.

4) To measure cardiac contraction and relaxation of WT hearts treated with the NO donor, GSNO, and β-adrenergic agonist, ISO. I hypothesised that ISO and GSNO would alter cardiac contractility and relaxation in WT hearts.

5) To investigate the effect of NO and β-adrenergic stimulation on cardiac arrhythmias in isolated WT mouse hearts. I hypothesised that WT hearts will be susceptible to cardiac arrhythmias induced by NO and β-adrenergic stress.

5.2 Methods

5.2.1 Experimental protocol

To measure cardiac function in WT mice, I used echocardiography (Chapter 2, section 2.3). To determine if NO and β-adrenergic stimulation mediated CaMKII activity, I performed Western blotting (as described in Chapter 2, section 2.5) to measure expression levels of total and phosphorylated CaMKII. To determine the effect of NO and β-adrenergic stimulation on cardiac contractility, I isolated the hearts from healthy 12-week old WT mice and perfused the hearts while measuring cardiac function (described in Chapter 2). I perfused the isolated hearts with a single dose (100 nM) of Isoproterenol (ISO) and a single dose (150 µM) of GSNO for 10 minutes.

I randomly divided the isolated hearts into different groups in the following order;

ISO-WASH group: ISO treatment before wash with KRH buffer.
ISO-GSNO group: ISO treatment before GSNO treatment.
GSNO-ISO group: GSNO treatment before ISO treatment.

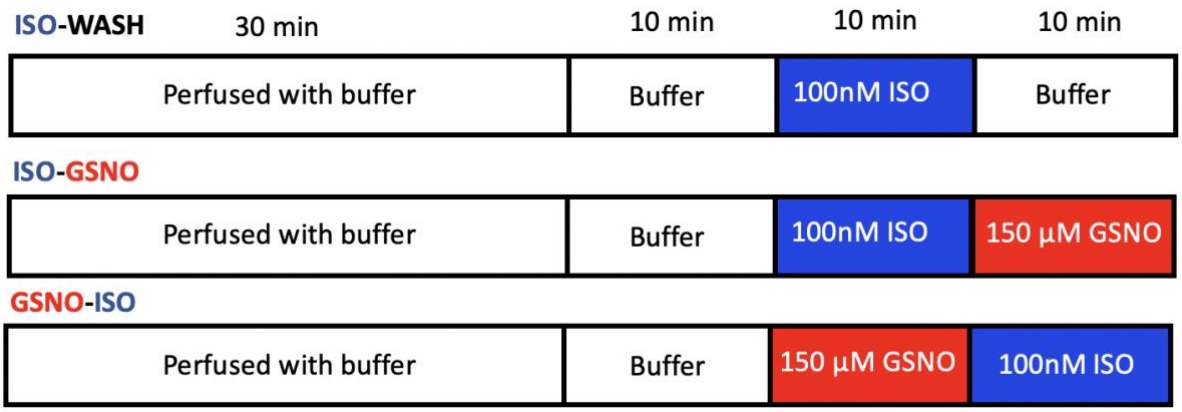

Figure 5.1 A time course protocol for the Langendorff perfusion experiment showing groups for ISO (100 nM) and GSNO (150 µM) treatment conditions. Groups are ISO-WASH, ISO-GSNO, GSNO-ISO.

5.2.2 Modified biotin switch assay

Modified biotin switch assay is a modified method of the biotin switch assay where the labelling of S-nitrosylated proteins is done with a fluorophore instead of biotin. This experiment was performed by Dr Oby Ebenebe in Kohr Laboratory of Cardiovascular Redox Signaling, Johns Hopkins University, Baltimore, MD, USA. All animal handling and sample preparations were carried out by me in University of Otago, New Zealand prior to shipping to USA.

Steps for sample preparation for S-NO detection were carried out in the dark and where not possible, samples were protected from direct light. Whole heart samples were homogenized in 1 mL cold homogenization buffer (Table 5.1) in brown tubes.

Table 5.1 Homogenisation Buffer

Homogenization Buffer (pH 7.7/7.8): for 10 mL	**FINAL CONCENTRATIONS**
1.0269 g Sucrose (Fw342.3)	0.3 M
2.5 mL of 1M HEPES-NaOH (pH7.7)	250 mM
20 µL of 500 mM EDTA	1 mM
125 µL of 2 M NEM	25 mM
250 µL Triton-X 100	0.5 %
pH was adjusted to 7.7-7.8 with NaOH and solution was made up to 10 mL with distilled water. NEM was made fresh by weighing out in the dark in a brown tube with 65 mg in 250 µL methanol. One tablet of EDTA-free protease-inhibitor was added to 5 µL of 0.2 M Neocuproine per 10 mL.	

Samples were homogenized and left on ice for 15 – 20 mins, followed by centrifugation at 14000 x g for 10 mins at 4°C. Supernatant was taken and placed in pre-labelled brown tube. Pellets were discarded or stored at -80°C if needed. ~10 µL of supernatant was aliquoted to determine protein concentration using Bradford assay (He, 2011). Remaining supernatants were aliquoted into brown tubes 2x 100 µL aliquots, snap frozen in liquid nitrogen and stored in -80^{o}C.

HEN buffer was prepared (Table 5.2). Volume of sample required for 100 µg protein and final volume of 200 µL was prepared (Table 5.3). Samples were incubated in thermo-shaker at 50°C for 40 mins (80 rpm)

While samples were incubating, DyLight Malemide 800 (stock 4 mM, Thermo Fisher Scientific) was thawed on ice (and dissolved in 233 µL DMF, if still lyophilized) and 1% SDS was added to HEN buffer. After incubation, 1.2 mL of acetone was added to each sample and mixed with vortex mixer at lowest speed. This mixture was incubated for 20 mins at -20°C and afterwards placed in a centrifuge to spin at 10,000 x g for 10 mins at 4°C. Supernatant was decanted and discarded without disturbing pellet. Pellet was air dried using compressed air to get rid of acetone, with extra care to prevent loss of pellet and to prevent precipitation in subsequent steps. Pellet was resuspended in 50 µL HEN buffer + 1% SDS solution and a quick spin was done to get rid of bubbles.

Table 5.2 HEN buffer

HEN Buffer for 10 mL	
2.5 mL of 1M HEPES-NaOH (pH7.7)	250 mM
20 µL of 500 mM EDTA	1 mM
5 µL of 0.2 M Neocuproine	

Table 5.3 Recipe for sample mixture

Reagent	**Volume (µL)**	**Final concentration**
25%SDS	16 µL	2%
2 M- NEM	2 µL	20mM
HEN	182 – Protein sample	-
Protein sample	$\frac{100\ \mu g}{protein\ concentration\ (\mu g/\mu L)}$	-

For DyLight switch, 2 µL of 4mM DyLight Malemide 800 was added to sample. 1 µL of freshly dissolved Ascorbate (1 M, 1:50 v/v, Ascorbate = 0.198g in 1 mL Milli-Q water). This solution was incubated in the dark for 1hr at RT. 1.2 mL ice-cold acetone was added to each sample, and mixed using a vortex mixer gently at lowest speed. The mixture was incubated for 20mins at -20°C followed by centrifugation at 10,000xg for 10mins at 4°C.

Supernatant was decanted and discarded, while ensuring that pellet was not disturbed. Pellet was air dried using compressed air to get rid of acetone to prevent precipitation in subsequent steps.

The pellet was resuspended in 50 µL of 1X sample buffer containing thiol reducing agent, 5% beta-mercaptoethnol (BME). The mixture was boiled at 95°C for 5mins and subsequently 5 µL of this per sample was loaded onto a 4 – 12% SDS PAGE gel. The gel was run at 75 volts for 20 mins and 150 volts for 80 mins, and was then rinsed in Milli-Q water and visualised in iBright imaging system under fluorescence channel 800 nm wavelength (ThermoFisher Scientific, USA). Proteins on the gel were transferred onto a PVDF membrane, probed for CaMKII expression and imaged on iBright imaging system.

5.3 Results

5.3.1 Animal Characteristics

WT male mice shown in Table 5.4 were used for measuring effect of GSNO and ISO on cardiac function. There was no significant difference in body weight among the mice comprising each group. Measurement of CaMKII nitrosylation required another set of WT mouse hearts (Table 5.5). The weight of the animals in these ISO and GSNO treatment groups were not statistically significant compared to control ($p > 0.05$). KO mice were used to measure effect of ISO on cardiac function in the absence of CaMKIIδ (Table 5.6).

Table 5.4 Animal Characteristics for 12-week old WT male mice

Parameter	**Experimental Groups**		
	ISO-WASH	**ISO-GSNO**	**GSNO-ISO**
Body Weight (g)	27.57 ± 0.30	27.90 ± 0.43	27.46 ± 1.10
Number (n)	6	5	5

Data are expressed as mean ± SEM

Table 5.5 Animal Characteristics for 12-week old WT male mice for measurement of S-nitrosylation levels

Parameter	**Experimental Groups**			
	CONTROL	**ISO-WASH**	**ISO-GSNO**	**GSNO-ISO**
Body Weight (g)	29.27 ± 0.48	27.80 ± 0.23	28.15 ± 0.09	29.70 ± 0.54
Number (n)	3	4	4	4

Data are expressed as mean ± SEM and were statistically analysed using one-way ANOVA.

Table 5.6 Animal Characteristics for 12-week old KO male mice

Parameter	**ISO-WASH**
Body Weight (g)	34.55 ± 1.75
Number (n)	4

Data are expressed as mean ± SEM

5.3.2 Echocardiography measurements for 12-week old WT male mice

Table 5.7 shows the echocardiography data for WT mice of the three experimental groups at 12 weeks old prior to heart isolation and drug treatment. There was no significant difference in systolic or diastolic function parameters. Therefore, all animals used in this chapter had similar baseline cardiac function.

Table 5.7 Echocardiography parameters of 12-week old WT male mice

Parameter	ISO - WASH	ISO - GSNO	GSNO - ISO	P value
IVSd (mm)	1.03 ± 0.05	0.98 ± 0.04	1.01 ± 0.04	0.69
IVSs (mm)	1.36 ± 0.07	1.24 ± 0.05	1.32 ± 0.07	0.46
LVIDd (mm)	2.85 ± 0.07	2.82 ± 0.06	3.09 ± 0.12	0.11
LVIDs (mm)	1.63 ± 0.15	1.29 ± 0.12	1.41 ± 0.27	0.35
LVPWd (mm)	1.00 ± 0.08	1.41 ± 0.16	1.30 ± 0.19	0.12
LVPWs (mm)	1.31 ± 0.03	1.28 ± 0.04	1.32 ± 0.04	0.81
LVEDV (ml)	0.06 ± 0.00	0.06 ± 0.00	0.07 ± 0.00	0.15
LVESV (ml)	0.01 ± 0.00	0.01 ± 0.00	0.01 ± 0.00	0.98
FS (%)	42.88 ± 0.92	42.49 ± 1.80	42.68 ± 3.45	0.99
EF (%)	79.56 ± 0.89	79.02 ± 1.76	82.65 ± 4.16	0.57
SV (ml)	0.05 ± 0.00	0.05 ± 0.00	0.06 ± 0.01	0.08
CO (ml/min)	21.49 ± 0.00	24.19 ± 0.00	27.90 ± 0.00	0.21
HR (beats/min)	412.4 ± 13.65	433.7 ± 9.63	409.2 ± 17.12	0.44
R-R Interval (ms)	147.1 ± 4.69	138.9 ± 2.98	148.3 ± 6.17	0.37
E:A ratio	2.24 ± 0.06	2.44 ± 0.17	2.33 ± 0.18	0.59
E velocity (cm/s)	42.4 ± 1.82	49.23 ± 3.64	45.91 ± 2.79	0.24
A velocity (cm/s)	19.20 ± 1.08	20.25 ± 0.29	20.19 ± 1.38	0.72

HR, heart rate; FS, Fractional shortening; EF, Ejection Fraction; IVSD, interventricular septum diastolic thickness; IVSS, interventricular septum systolic thickness; LVIDD, left ventricular internal dimension at diastole, LVIDS, left ventricular internal dimension at systole; LVPWD, left ventricular posterior wall thickness at diastole; LVPWS, left ventricular posterior wall thickness at systole. Data are expressed as mean ± SEM. One-way ANOVA was used to compare between ISO-WASH (n = 6), ISO-GSNO (n=5) and GSNO-ISO (n=5) groups.

5.3.3 CaMKIIδ expression and activation in WT hearts

After heart isolation and treatment with GSNO and ISO, CaMKII expression and activation levels in WT mouse hearts were measured in preserved cardiac tissues using the Western blotting method described in Chapter 2. CaMKII activation in LV tissue was similar across all groups ($p = 0.18$). CaMKII phosphorylation, which is often used as a proxy for CaMKII activity, was also measured in all groups (Figure 5.2). This result confirmed CaMKII expression and activation in WT isolated hearts.

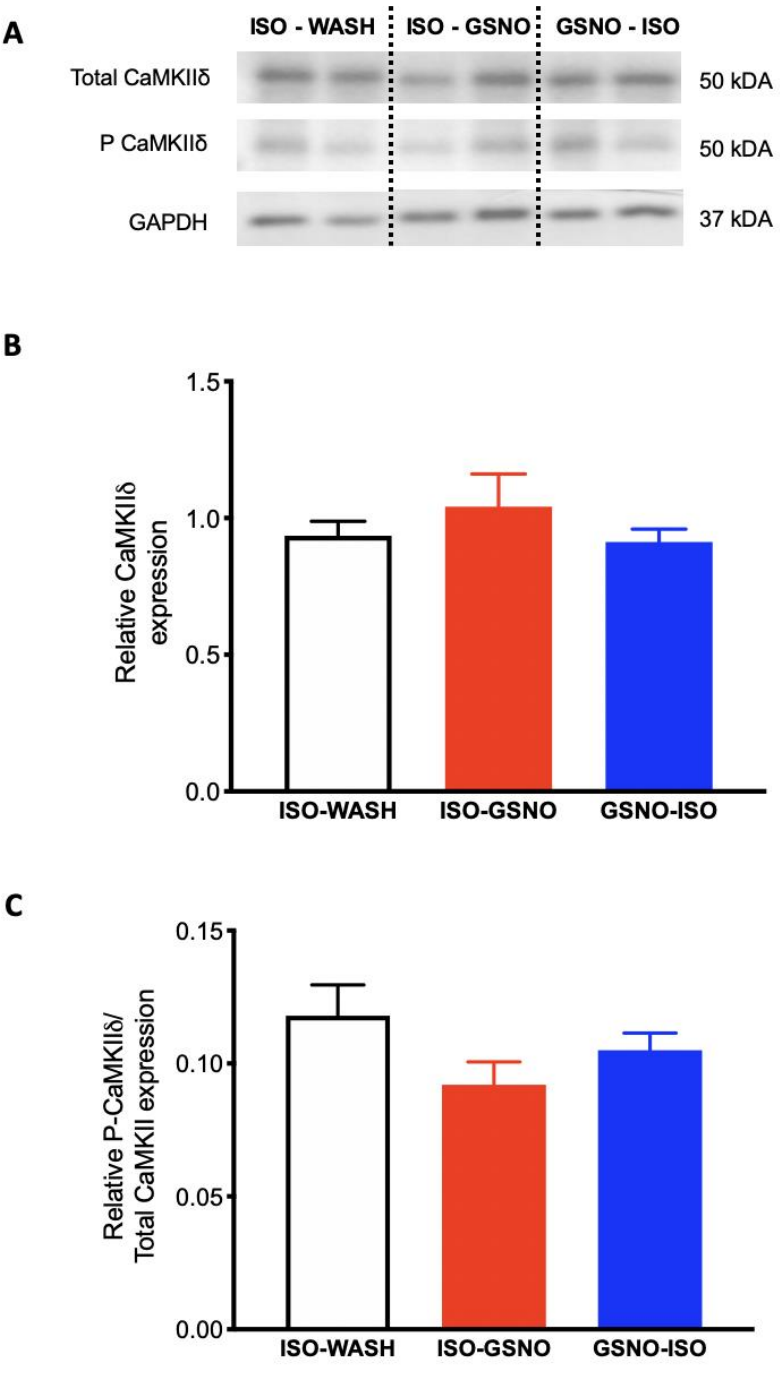

Figure 5.2 Western blot for total and phosphorylated CaMKIIδ at Thr287 A, Representative immunoblot of total CaMKIIδ, phosphorylated CaMKIIδ at Thr287 in WT LV tissue and GAPDH as loading control. B, Quantification of total CaMKII levels in ISO-WASH (n = 5), ISO-GSNO (n = 5) and GSNO-ISO (n = 4). C, Quantification of P-CaMKIIδ levels in ISO-WASH (n = 5), ISO-GSNO (n = 5) and GSNO-ISO (n = 4). Data represented as mean ± SEM. One-way ANOVA (uncorrected Fisher's LSD test) was used to compare all groups.

5.3.4 Quantification of S-nitrosylation levels in WT mice treated with ISO and GSNO

To assess the level of CaMKII S-nitrosylation, hearts were isolated from WT animals (Table 5.3) and subjected to different treatment protocols, as earlier defined in this Chapter. The hearts were treated with single doses of 100 nM ISO and 150 µM GSNO for 10 minutes each. The control group received no treatment, the ISO-WASH group, received ISO for 10 minutes followed by a wash phase, ISO-GSNO received ISO followed by GSNO and the GSNO-ISO group received GSNO followed by ISO.

To confirm if GSNO and ISO promoted S-nitrosylation in the WT hearts, a modified biotin switch method using sulfhydryl-reactive DyLight-maleimide fluorescent dye (Figure 5.3A) was performed. The results showed that was no significant difference in global protein nitrosylation between ISO-WASH group and control ($p = 0.77$), this result was similar to GSNO-ISO compared to control ($p = 0.12$). However, global protein nitrosylation was upregulated in the ISO-GSNO group compared to control, and this was significant ($p < 0.01$) (Figure 5.3B). DyLight fluorescence was measured relative to CaMKII expression to probe for CaMKII S-nitrosylation (SNO) (Figure 5.3C). The ISO-WASH and GSNO-ISO groups had similar CaMKII SNO levels compared to control ($p = 0.56$; $p = 0.78$). Strikingly, there was a trend towards increased CaMKII S-nitrosylation in the ISO-GSNO group compared to control ($p = 0.06$). These data suggest that there was CaMKII S-nitrosylation and global protein nitrosylation under the ISO and GSNO conditions.

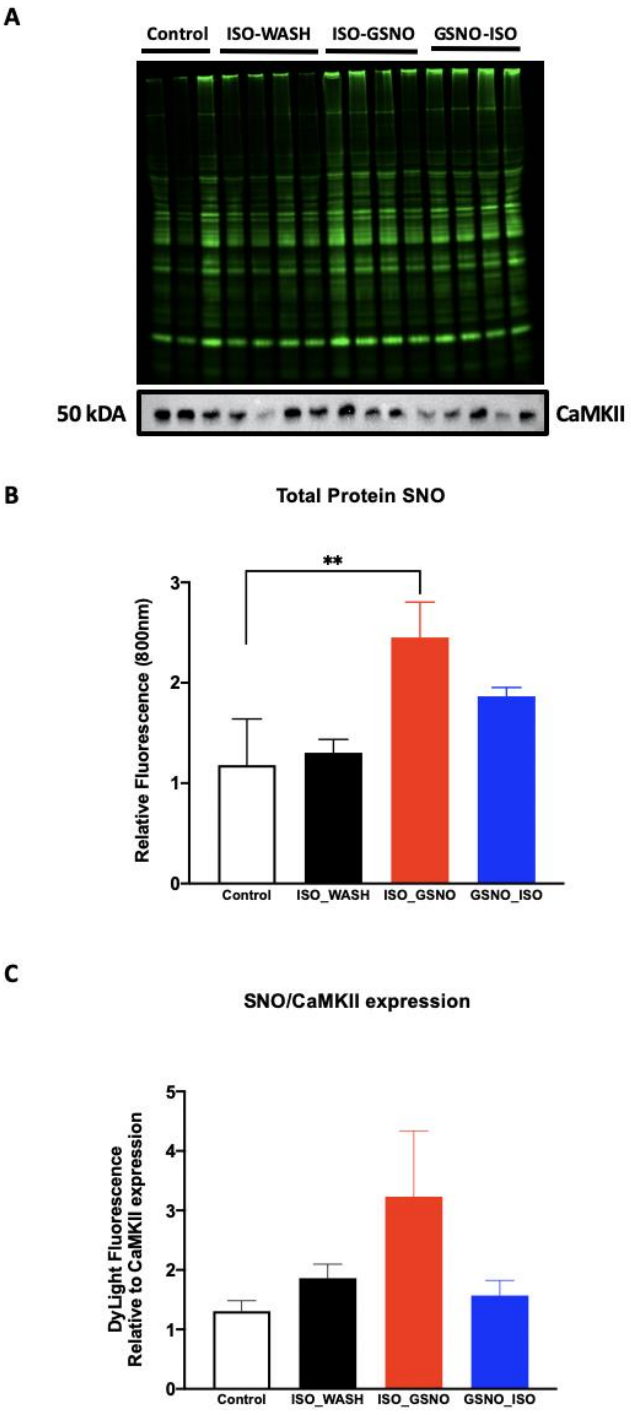

Figure 5.3 Quantification of CaMKII S-nitrosylation in WT mouse hearts treated with GSNO and ISO A, Representative images of DyLight Maleimide gel showing global protein nitrosylation in different groups of drug treatment and a Western blot of CaMKII expression in WT mouse hearts. B, Total protein nitrosylation levels. C, CaMKII nitrosylation levels expressed relative to the DyLight fluorescence. Data are expressed as mean ± SEM. Control, white bar, n = 3, ISO-WASH, black bar, n = 4, ISO-GSNO, red bar, n = 4, GSNO-ISO, blue bar, n = 4. One-way ANOVA (uncorrected Fisher's LSD test) was used to compare groups to control: * = $p < 0.05$.

5.3.5 Effect of ß-adrenergic stimulation on contractile parameters of isolated WT hearts

Studies have shown that ß-adrenergic receptor stimulation promotes inotropic and chronotropic effects in isolated hearts and this response could be associated with activation of CaMKII, one of the downstream proteins of sympathetic stimulation (Xu et al., 2010; Grimm et al., 2015). Data from Chapter 3 and the previous section in this Chapter showed that KO hearts are protected from stress-induced arrhythmias, therefore the aim of this section was to investigate the response of isolated WT hearts to ß-adrenergic stress. I measured LV developed pressure, heart rate, rates of contraction and relaxation, arrhythmia events and severity.

There was no significant difference in pressure development as ISO treatment failed to increase LVDP ($p = 0.58$). The wash phase that followed ISO exposure also did not alter LVDP compared to ISO ($p = 0.39$) and baseline ($p = 0.76$) (Figure 5.4A). As displayed in figure 5.4B, ISO did not significantly increase heart rate compared to baseline heart rate ($p = 0.22$). Interestingly, in the wash phase after ISO treatment, there was a significantly higher heart rate compared to baseline ($p = 0.02$), but no significant difference with ISO treatment ($p = 0.24$). There was an increase in rate of contraction, Max dP/dt, with ISO exposure compared to baseline ($p = 0.12$) although it was not significant and the wash phase did not cause any change compared to baseline ($p = 0.46$) and ISO treatment (0.40) (Figure 5.5A). Unlike the Max dP/dt, there was a significantly faster rate of relaxation, Min dP/dt, during ISO treatment ($p = 0.04$) and no difference in the wash phase ($p = 0.21$) (Figure 5.5B). ISO perfusion had no effect on PTI in WT hearts. However, there was significant decrease in PTI during the wash phase compared to baseline ($p = 0.03$) (Figure 5.6).

Combined, the results show that ISO did induce a mild inotropic and chronotropic response in WT hearts.

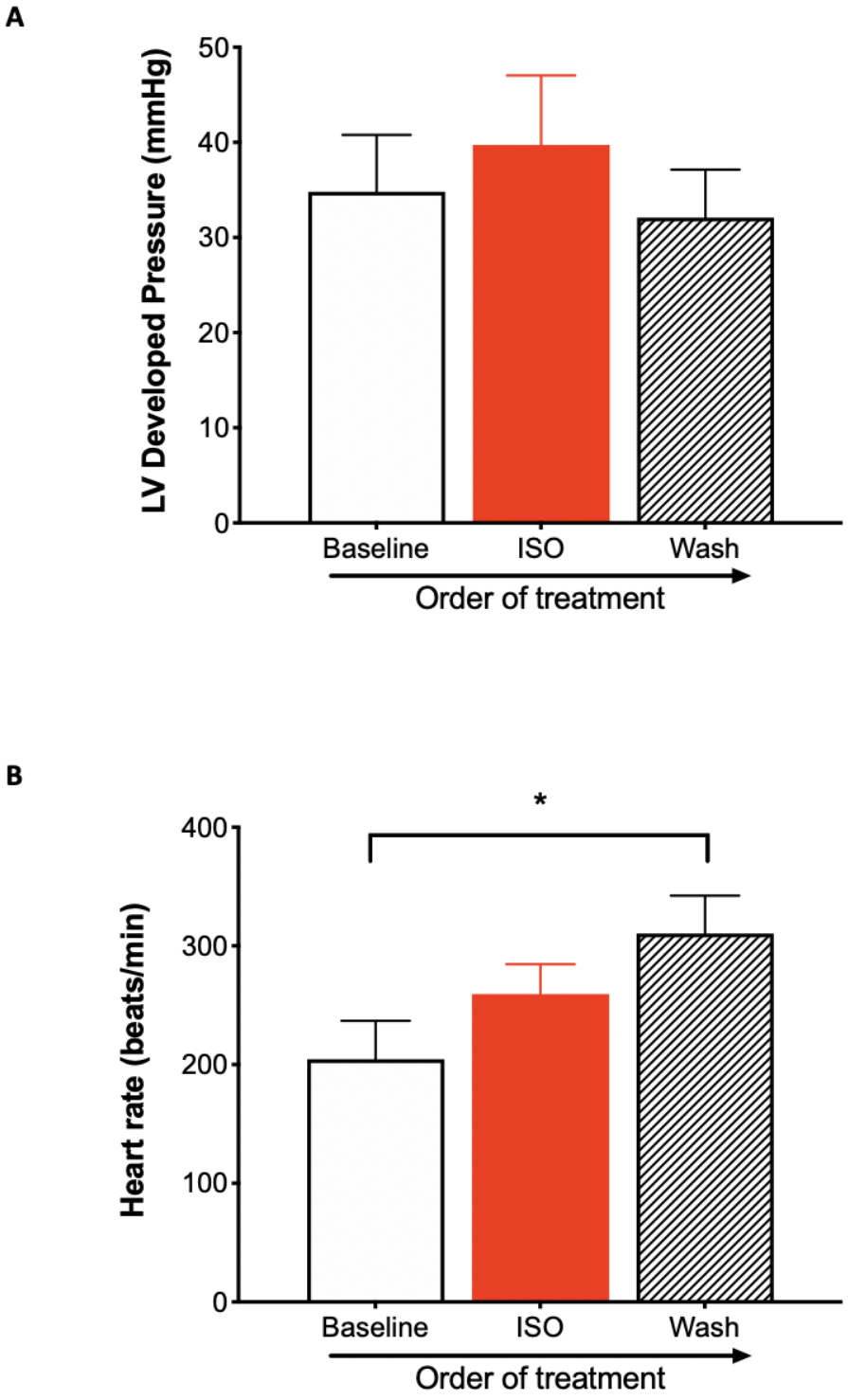

Figure 5.4 LV developed pressure and heart rate in WT hearts with ISO (100 nM) treatment A, LV developed pressure B, Heart rate. Data are means ± SEM. Order of treatment; baseline, ISO, wash, n = 6 hearts. One-way ANOVA (uncorrected Fisher's LSD test) was used to compare across conditions * = $P < 0.05$ vs baseline.

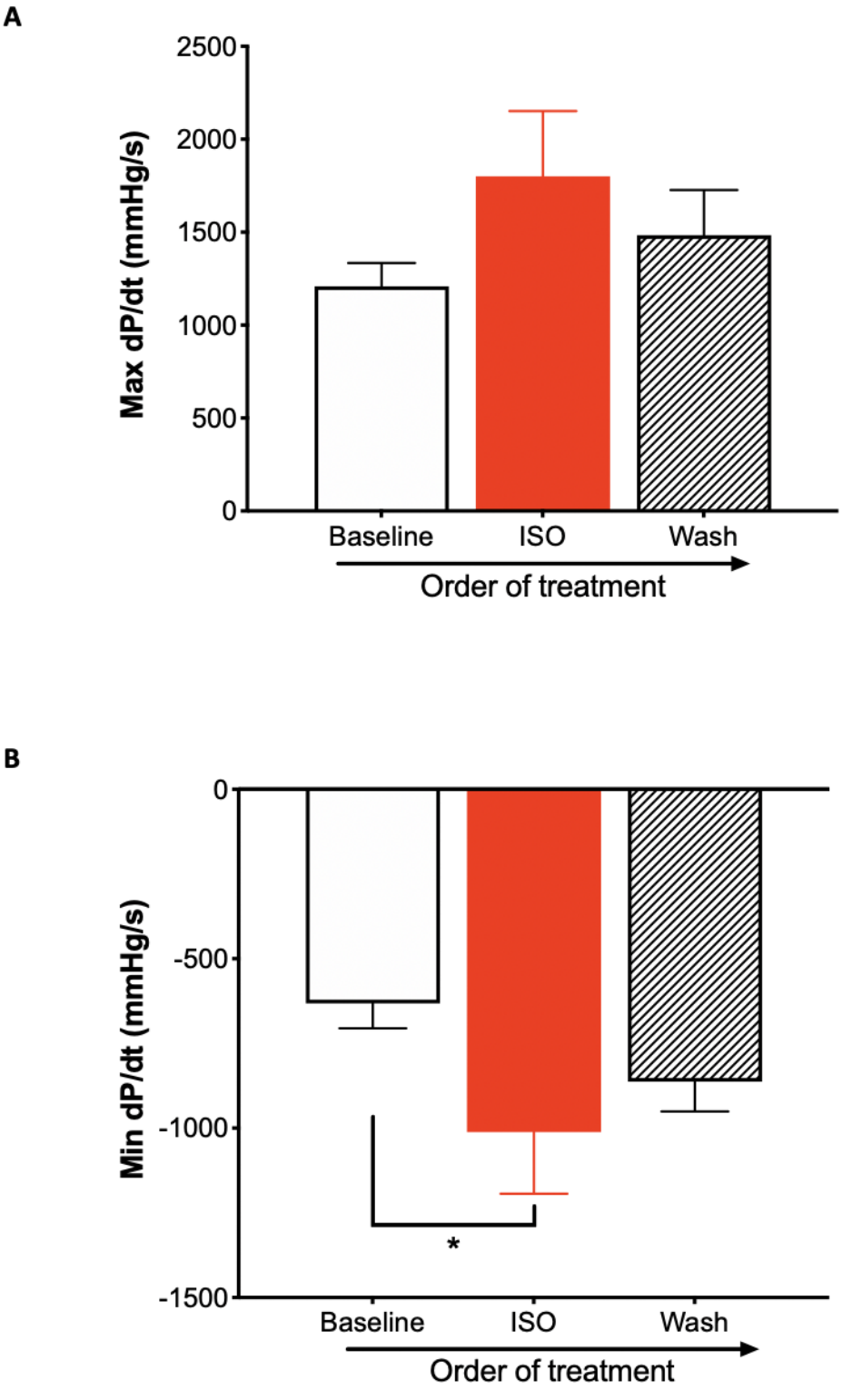

Figure 5.5 Rates of contraction and relaxation in WT hearts with ISO (100 nM) treatment. A, Max dP/dt B, Min dP/dt. Data are means ± SEM. Order of treatment; baseline, ISO, wash, n = 6 hearts. One-way ANOVA (uncorrected Fisher's LSD test) was used to compare across conditions * = $P < 0.05$ vs baseline.

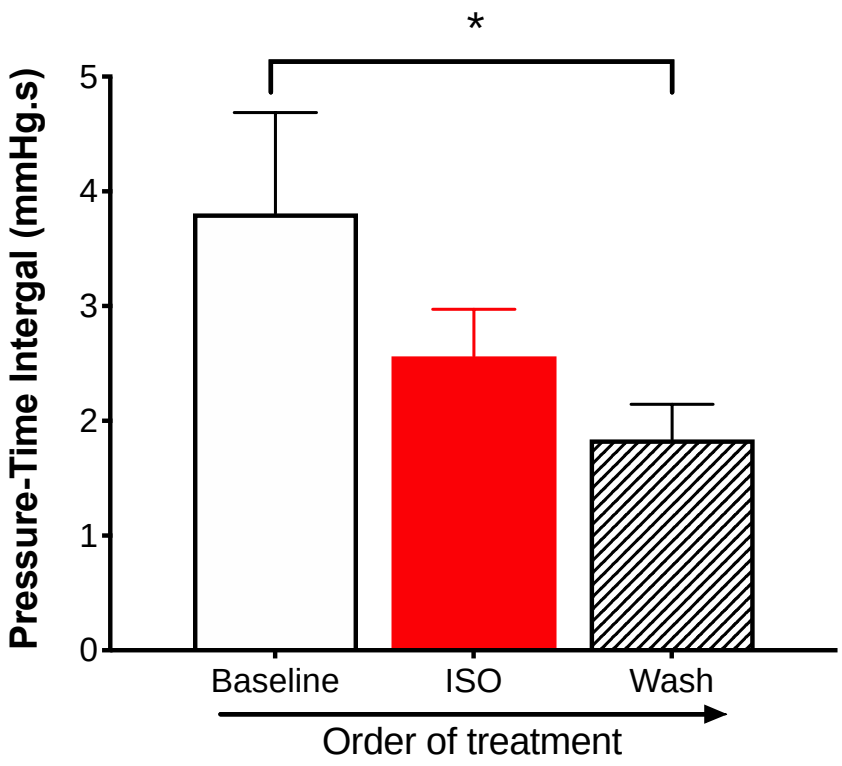

Figure 5.6 Pressure-Time Integral in WT hearts with ISO (100 nM) treatment. Data are means ± SEM. Order of treatment; baseline, ISO, wash, n = 6 hearts. One-way ANOVA (uncorrected Fisher's LSD test) was used to compare across conditions * = $p < 0.05$ vs baseline.

5.3.6 Effect of ß-adrenergic stimulation on arrhythmias in isolated WT hearts

To test the hypothesis that ß-AR stimulation induces cardiac arrhythmias, I quantified arrhythmias observed in the isolated hearts. Figure 5.7A shows a representative trace of the parameters recorded under baseline conditions, followed by the ISO (150 μM) treatment phase and a wash phase.

Figure 5.7B shows that ISO induced a significantly higher number of arrhythmic events in the isolated hearts compared to baseline ($p < 0.0001$), while the wash phase significantly ablated the number of arrhythmic events compared to that of ISO treatment ($p < 0.01$). There was a trend towards a higher number of arrhythmic events in the wash phase compared to baseline, however this was not significant ($p = 0.06$). These data show that wash phase reduced the number of arrhythmic events but not completely. I quantified the arrhythmia score (criteria described in Chapter 2) to determine the severity of arrhythmias. ISO treatment increased severity of arrhythmic events ($p < 0.0001$) and the wash phase after ISO significantly depleted the number of arrhythmic events compared to ISO ($p = 0.0001$) but remained significantly elevated compared to baseline ($p < 0.001$) (Figure 5.7C).

In summary, these results show that ISO contributed to a significant increase in the number and severity of arrhythmic events.

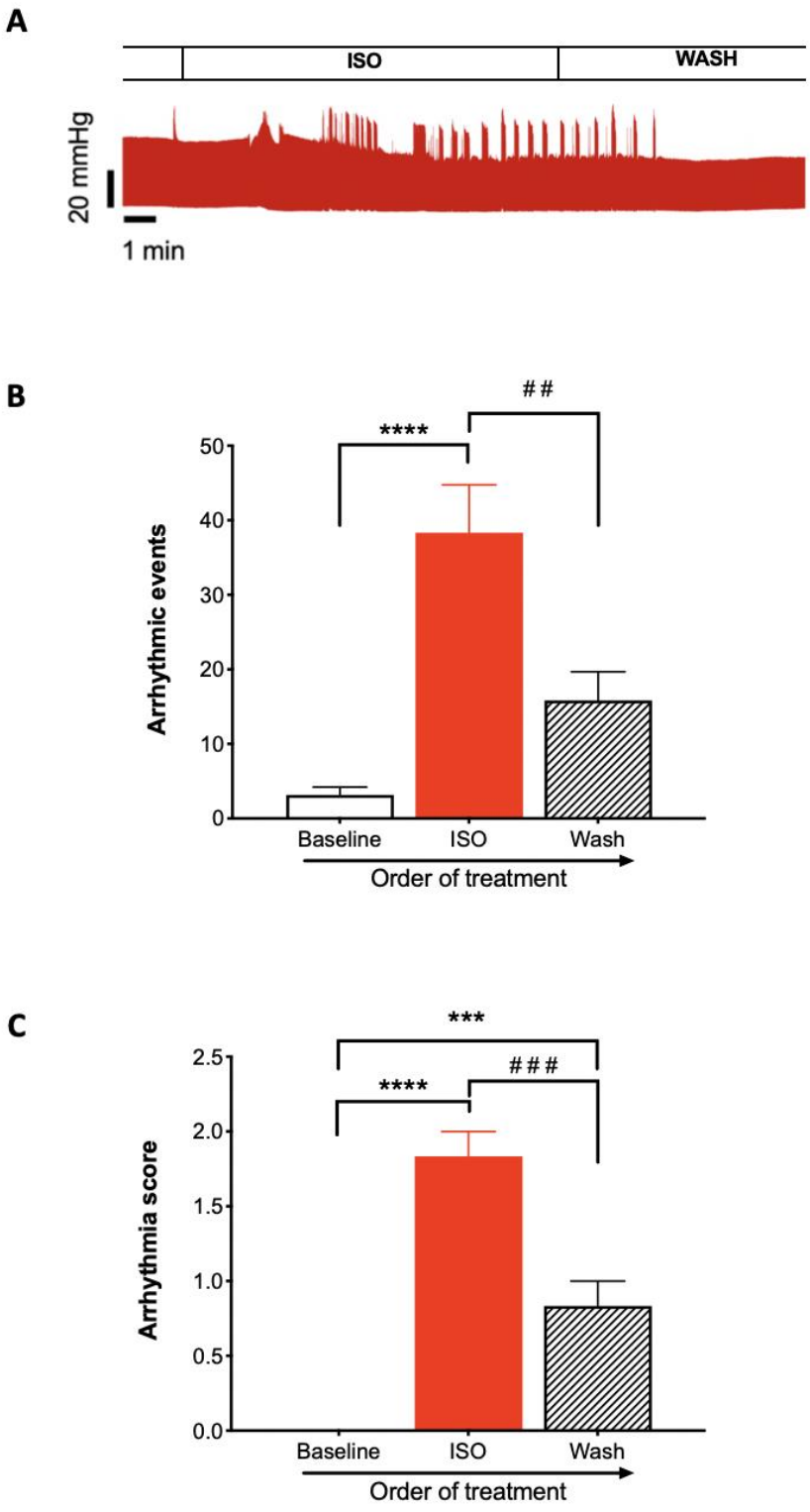

Figure 5.7 Quantification of arrhythmias in WT hearts with ISO (100 nM) treatment A, Arrhythmic events B, Arrhythmia score. Data are means ± SEM. Order of treatment; baseline, ISO, wash, n = 6 hearts. One-way ANOVA (uncorrected Fisher's LSD test) was used to compare across conditions *** = $P < 0.001$, **** = $P < 0.0001$ vs baseline, ### = $P < 0.001$ vs ISO.

5.3.7 Effect of β-AR stimulation on isolated KO mouse hearts

To determine the effect of CaMKIIδ loss on cardiac function during β-AR stimulation, I used CaMKII KO hearts (Table 5.3). I perfused these hearts with 100 nM ISO followed with a wash phase and measured cardiac function and arrhythmias. Results in Chapter 3 showed that loss of CaMKIIδ in isolated KO mouse hearts prevented stress-induced arrhythmias. I hypothesised that KO hearts would respond to β-AR stimulation but would also be protected from arrhythmias induced by ISO treatment.

LV pressure development trended towards an increase after ISO treatment compared to baseline but remained statistically insignificant ($p = 0.08$) (Figure. 5.8A). After a wash, LV developed pressure reduced significantly compared to ISO treatment ($p = 0.006$) and became similar to baseline ($p = 0.15$). Heart rate remained unchanged in KO hearts overall, during ISO treatment and in the wash phase ($p = 0.78$) (Figure 5.8B). ISO treatment significantly elevated rate of contraction (max dP/dt) compared to baseline ($p = 0.001$) (Figure 5.9A). Max dP/dt declined in the wash phase to baseline levels ($p = 0.15$), a significant difference compared to ISO treatment ($p = 0.0002$). Rate of relaxation (min dP/dt) increased significantly from baseline after ISO treatment ($p = 0.004$) and significantly declined in the wash phase compared to ISO treatment ($p = 0.001$) (Figure 5.9B). PTI was unaffected by ISO perfusion in KO hearts (Figure 5.10).

Arrhythmic events and arrhythmia scores were quantified in the KO hearts (see Figure 5.11A for representative trace). The number of arrhythmic events was not altered during ISO treatment compared to baseline ($p = 0.54$) (Figure 5.11B). Surprisingly, the wash phase significantly reduced the number of arrhythmic events compared to ISO treatment ($p = 0.04$) and baseline ($p = 0.01$). There was no significant difference in severity of arrhythmias measured by arrhythmia score in KO hearts across all groups ($p = 0.34$) (Figure 5.11C).

Taken together, these data show that response of KO mouse hearts to β-AR stimulation was not impaired with loss of CaMKIIδ. However, and critically, ISO treatment did not promote arrhythmias in the KO hearts as it did in the WT hearts.

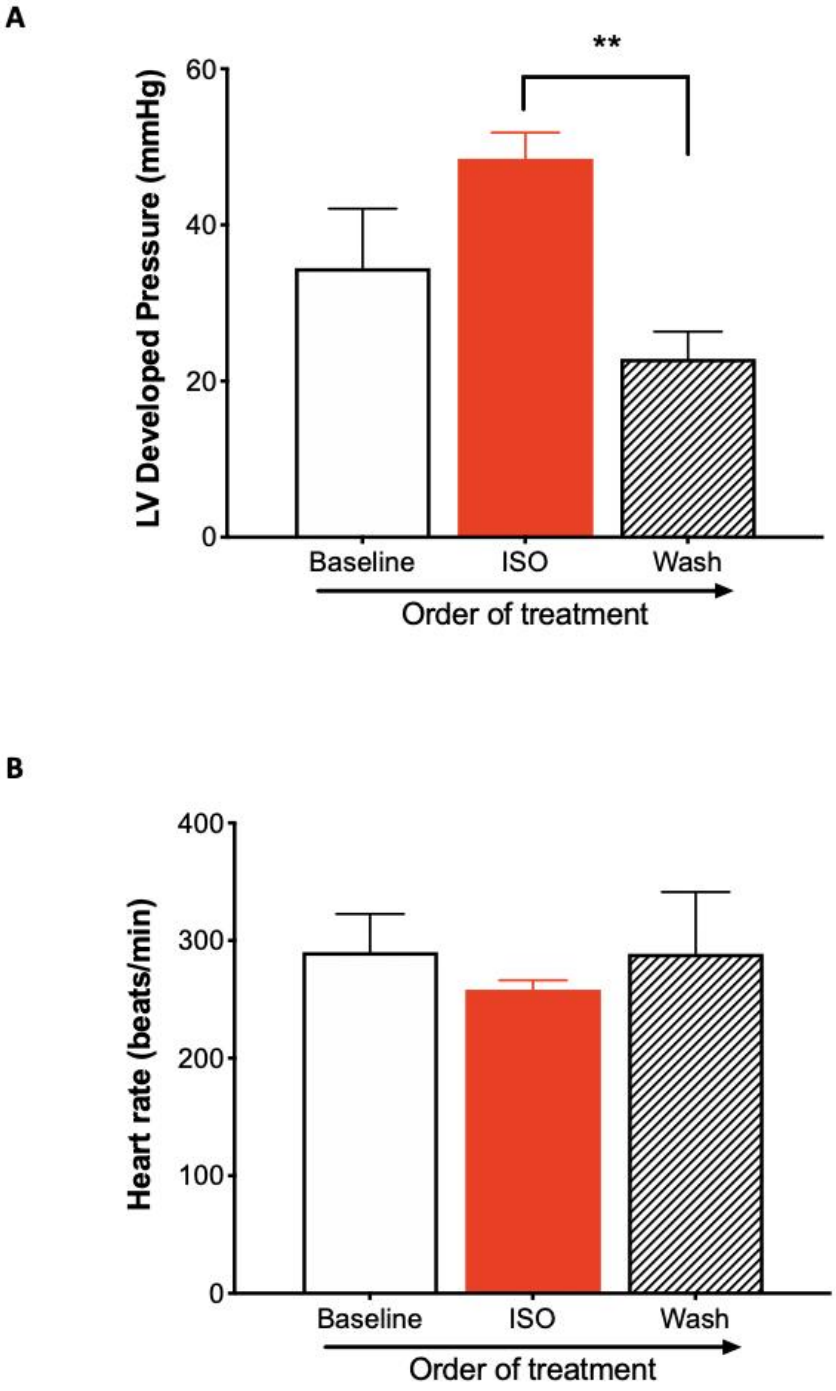

Figure 5.8 LV developed pressure and heart rate in KO hearts with ISO (100 nM) treatment A, LV developed pressure B, Heart rate. Data are means ± SEM. Order of treatment; baseline, ISO, wash, n = 4 hearts. One-way ANOVA (uncorrected Fisher's LSD test) was used to compare across conditions * = $P < 0.05$.

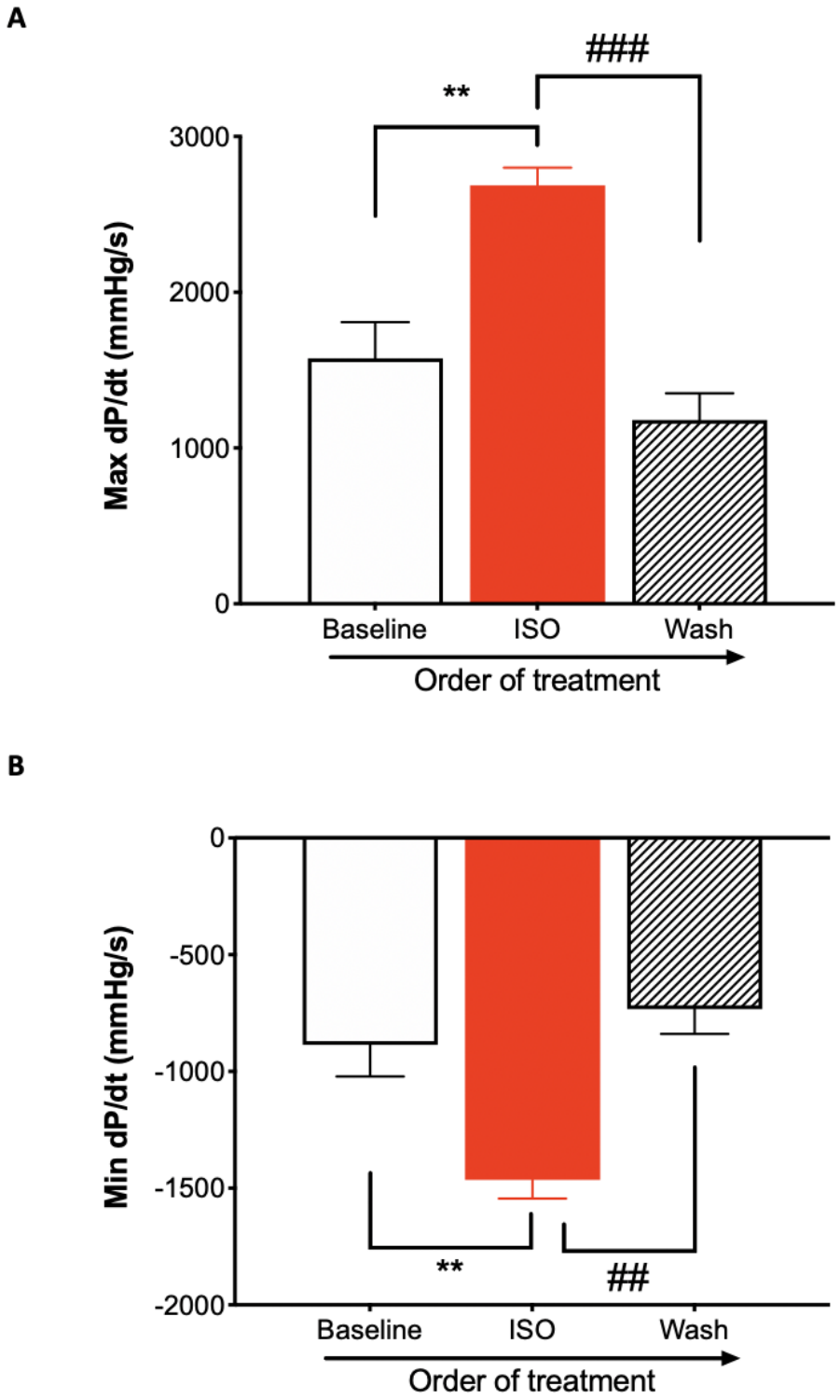

Figure 5.9 Rates of contraction and relaxation in KO hearts with ISO (100 nM) treatment A, Max dP/dt B, Min dP/dt. Data are means ± SEM. Order of treatment; baseline, ISO, wash, n = 4 hearts. One-way ANOVA (uncorrected Fisher's LSD test) was used to compare across conditions ** = P < 0.01 vs baseline, ## = P < 0.01 ### = P < 0.001 vs ISO.

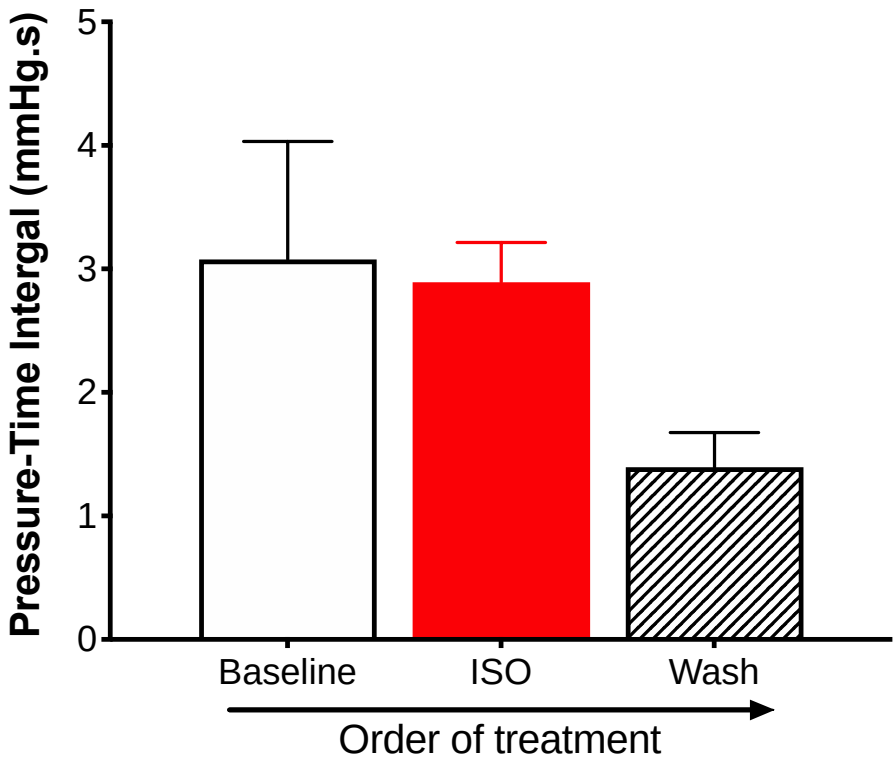

Figure 5.10 Pressure-Time Integral in KO hearts with ISO (100 nM) treatment. Data are means ± SEM Order of treatment; baseline, ISO, wash, n = 4 hearts. One-way ANOVA (uncorrected Fisher's LSD test) was used to compare across conditions.

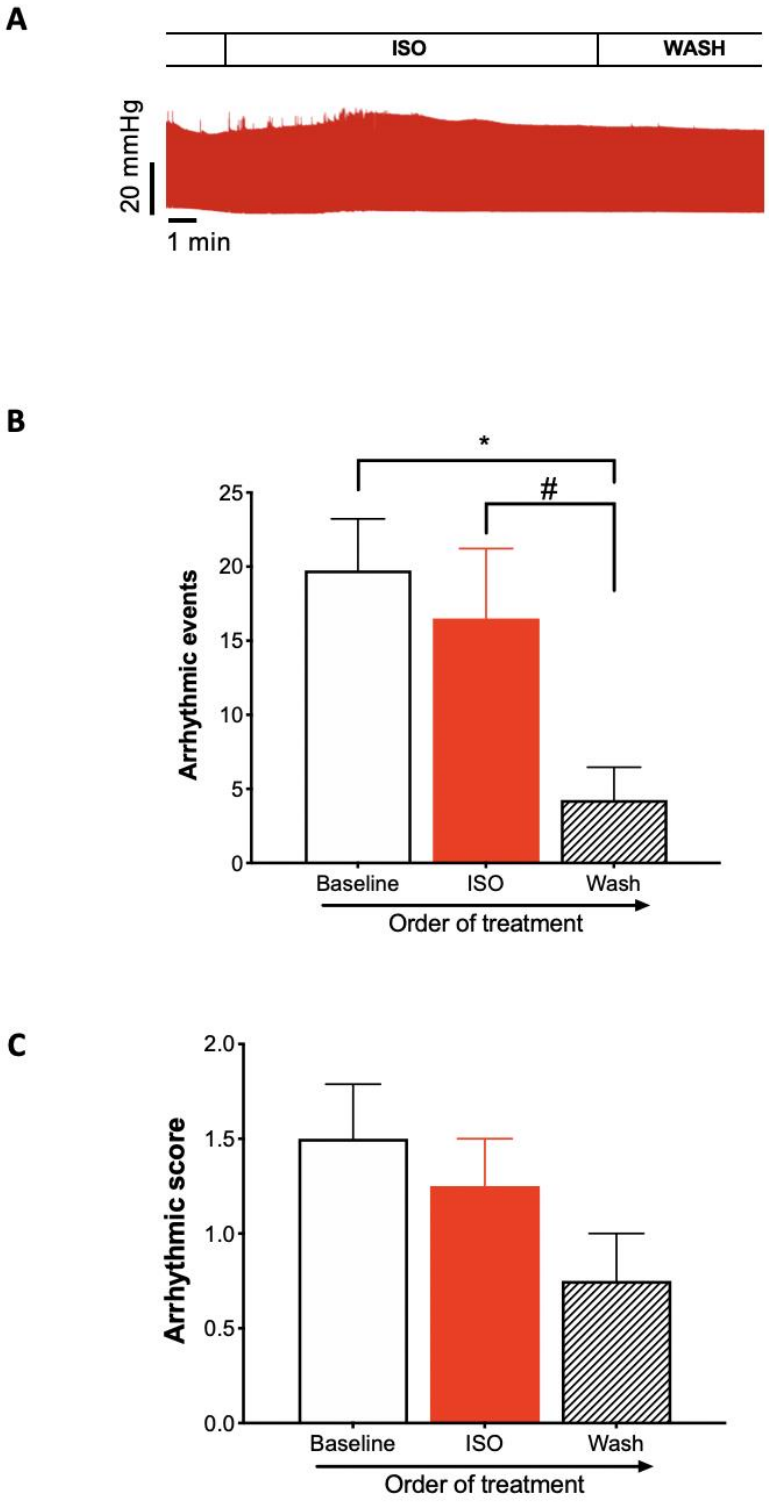

Figure 5.11 Quantification of arrhythmias in KO hearts with ISO (100 nM) treatment A, Representative trace of LV contractions showing arrhythmic events in WT hearts in ISO and WASH phases B, Arrhythmic events C, Arrhythmia score. Data are means ± SEM. Order of treatment; baseline, ISO, wash, n = 4 hearts. One-way ANOVA (uncorrected Fisher's LSD test for arrhythmic events and Kruskal-Wallis test for arrhythmia score) was used to compare across conditions * = $P < 0.01$, vs baseline.

5.3.8 Effect of GSNO treatment on cardiac contraction and relaxation before and after ß-adrenergic stimulation in isolated WT mouse hearts.

Data from the previous sections established that KO hearts were protected from ISO-induced arrhythmias compared to WT hearts when exposed to ISO. The next step was to investigate the effect of ISO and GSNO treatment together on isolated WT hearts.

Treatment of the isolated hearts with ISO prior to GSNO did not alter LVDP compared to baseline ($p = 0.25$) and GSNO ($p = 0.43$) (Figure 5.12A). There was also no significant difference between baseline LVDP and LVDP during GSNO infusion ($p = 0.80$). In the GSNO-ISO group, which involved pre-treatment with GSNO, there was no significant difference between LVDP after GSNO perfusion ($p = 0.91$) and baseline. Upon addition of ISO, there was a trend towards increasing LVDP compared to GSNO ($p = 0.05$) and baseline ($p = 0.07$). The data show that β-adrenergic stimulation did not have any significant effect on the force-frequency relationship, and GSNO failed to alter pressure development in the hearts.

In the ISO-GSNO group, ISO perfusion significantly increased heart rate ($p = 0.007$) from baseline (Figure 5.12B). This increased chronotropy was persistent even after GSNO application and was significantly different from baseline ($p = 0.003$), but there was no difference in heart rate between the ISO challenge and GSNO treatment ($p = 0.71$). When the hearts were perfused with GSNO before ISO (as seen in the GSNO-ISO group), GSNO did not cause any change in heart rate compared to baseline ($p = 0.94$). However, after GSNO perfusion, ISO significantly increased heart rate ($p = 0.002$) and this was also significant compared to baseline ($p = 0.002$).

Figure 5.13A reports the rate of contraction, max dP/dt, for the different groups. Perfusion of the heart with ISO before GSNO (ISO-GSNO group), significantly increased max dP/dt compared to baseline ($p = 0.02$). There was no significant change in the max dP/dt with GSNO infusion proceeded by ISO, compared to ISO perfusion ($p = 0.71$) or baseline ($p = 0.09$). In the GSNO-ISO group, GSNO did not alter max dP/dt compared to baseline ($p = 0.94$). However, ISO perfusion after GSNO treatment, significantly elevated max dP/dt compared to GSNO ($p = 0.001$) and baseline ($p = 0.001$).

As seen in Figure 5.13B, when ISO was perfused in the hearts before GSNO (ISO-GSNO group), min dP/dt significantly increased compared to baseline ($p = 0.001$). In this experimental group, GSNO treatment maintained high min dP/dt which was significant compared to baseline ($p = 0.001$) but not to ISO perfusion ($p = 0.88$). The min dP/dt during GSNO perfusion in the GSNO-ISO group did not significantly change when compared to baseline ($p = 0.91$); however, it significantly increased during ISO perfusion compared to GSNO perfusion ($p = 0.0003$) and baseline ($p = 0.0003$).

PTI was altered following ISO and GSNO perfusion in WT hearts (Figure 5.14). ISO perfusion led to a decline in PTI compared to baseline in ISO-GSNO group ($p = 0.03$). This decrease was sustained after GSNO perfusion, and significantly lower compared to baseline ($p = 0.01$). In the GSNO-ISO group, GSNO pre-treatment had no effect on PTI compared to baseline ($p = 0.75$). ISO induced a significant decrease in PTI compared to GSNO ($p = 0.02$) and baseline ($p = 0.01$).

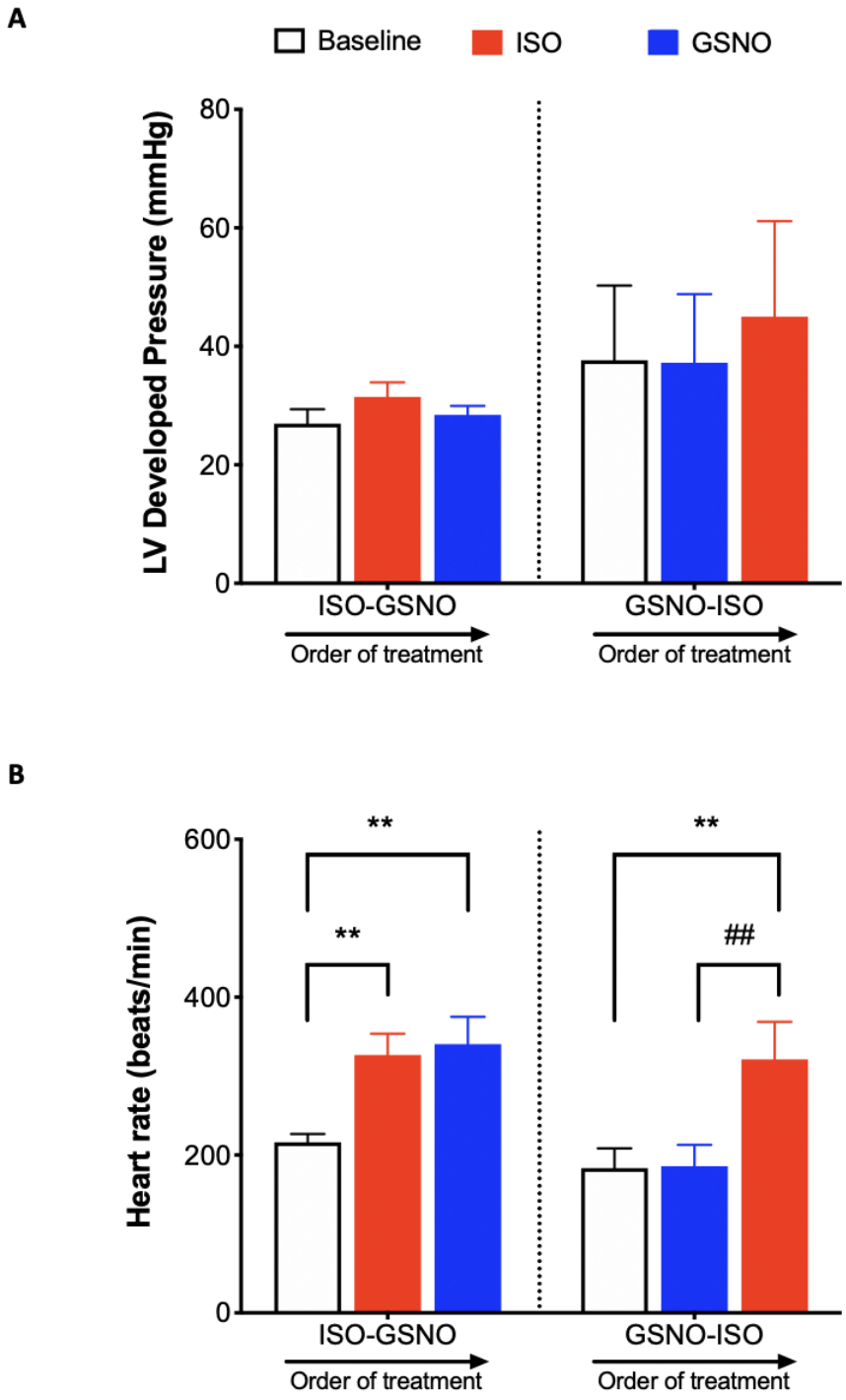

Figure 5.12 LV Developed Pressure and Heart rate in WT mouse hearts under ISO (100 nM) and GSNO (150 µM) treatment conditions A, LVDP B, Heart rate. Data are means ± SEM. Order of treatment; left to right. ISO-GSNO, n = 5, GSNO-ISO, n = 5. White bar = baseline, Red bar = ISO, Blue bar = GSNO. Two-way ANOVA (uncorrected Fisher's LSD test) was used to compare between groups: ** = $p < 0.01$, ## = $p < 0.01$ * = Drug vs baseline, # = drug 1 vs drug 2.

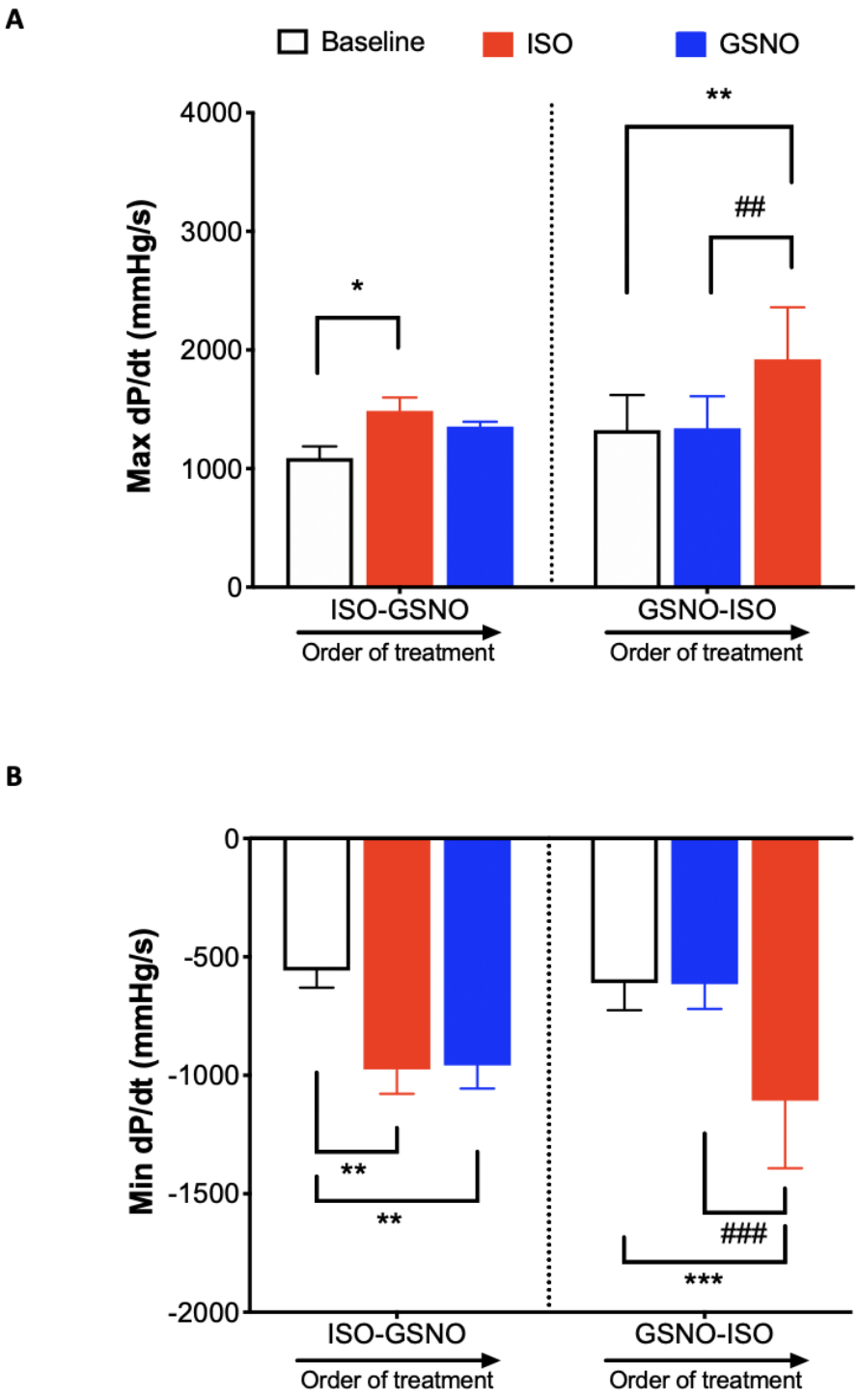

Figure 5.13 Contraction and relaxation parameters in WT mouse hearts before and after treatment with ISO (100 nM) and GSNO (150 µM) A, Rate of Contraction (Max dP/dt) B, Rate of Relaxation (Min dP/dt). Data are means ± SEM. Order of treatment; left to right. ISO-GSNO, n = 5, GSNO-ISO, n = 5. Two-way ANOVA (uncorrected Fisher's LSD test) was used to compare between groups: * = $p < 0.05$, ** = $p < 0.01$, *** = $p < 0.001$, ## = $p < 0.01$### = $p < 0.001$, * = Drug vs baseline, # = drug 1 vs drug 2.

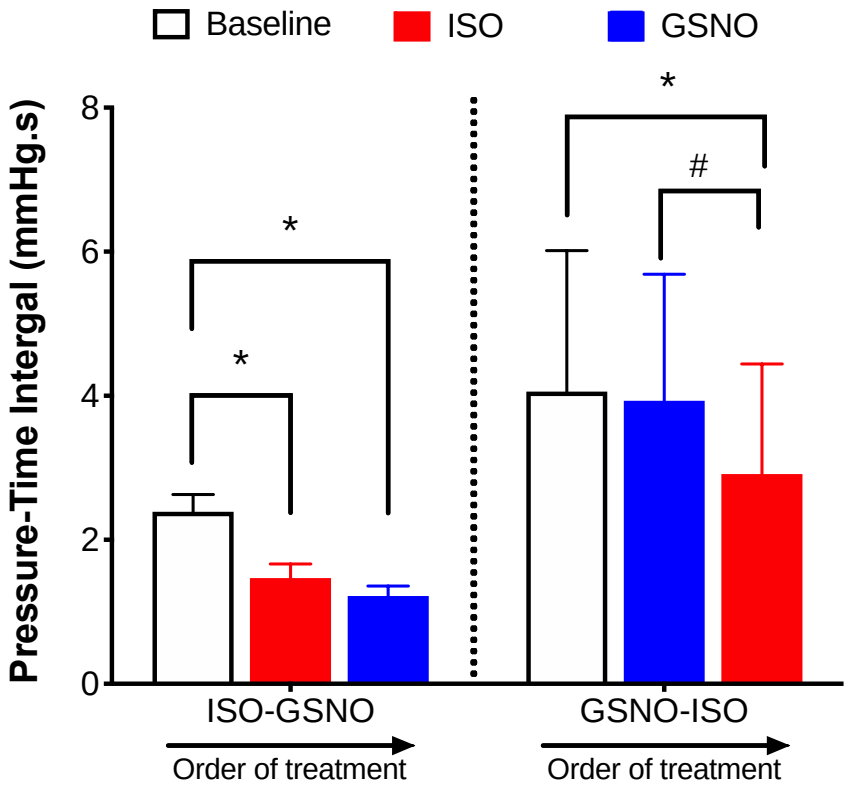

Figure 5.14 Pressure-Time Integral in WT mouse hearts before and after treatment with ISO (100 nM) and GSNO (150 µM). Data are means ± SEM. Order of treatment; left to right. ISO-GSNO, n = 5, GSNO-ISO, n = 5. White bar = baseline, Red bar = ISO, Blue bar = GSNO. Two-way ANOVA (uncorrected Fisher's LSD test) was used to compare between groups: * = $p < 0.05$, # = $p < 0.05$ * = Drug vs baseline, # = drug 1 vs drug 2.

5.3.9 Effect of GSNO treatment and ß-adrenergic stimulation on arrhythmias in isolated mouse hearts.

In Chapter 3, results showed that GSNO could induce arrhythmias with increasing concentration. I analysed arrhythmia count and severity in WT hearts treated with ISO and GSNO. I hypothesised that β-AR stimulation and exogenous NO perfusion would increase the number of arrhythmic events in WT hearts.

As shown in Figure 5.15, there was a clear difference in the arrhythmia patterns in the different groups. In the ISO-GSNO group, ISO perfusion significantly increased the number of arrhythmias from baseline by 8-fold ($p = 0.03$) (Figure 5.16A). Infusion of GSNO after ISO, further increased the number of arrhythmias compared to baseline ($p = 0.002$) but it was not significantly different compared to ISO ($p = 0.20$). In contrast to this finding, when GSNO was perfused through the hearts before ISO in the GSNO-ISO group, there was no significant increase in the number of arrhythmias compared to baseline ($p = 0.50$). Infusion of ISO after GSNO, also failed to induce arrhythmias compared to GSNO ($p = 0.88$) and baseline ($p = 0.40$) in the same group.

Since the number of arrhythmias varied between hearts, I also determined the severity of arrhythmias in each group using arrhythmia scores. There was a significant difference in arrhythmia scores between ISO perfusion and baseline ($p = 0.03$) in the ISO-GSNO group (Figure 5.16B). However, the arrhythmia score with GSNO perfusion after ISO application did not increase as seen with arrhythmia count; instead, it was similar to baseline ($p = 0.10$) and ISO ($p = 0.21$). In the GSNO-ISO group, there was no significant change in arrhythmia severity with GSNO treatment compared to baseline ($p > 0.99$). ISO infusion also did not alter arrhythmia severity compared to GSNO treatment ($p = 0.39$) or baseline ($p = 0.39$).

These data suggest that β-AR stimulation before GSNO infusion induces arrhythmogenesis. However, if GSNO infusion precedes β-AR stimulation, the arrhythmogenic effect of ISO is attenuated.

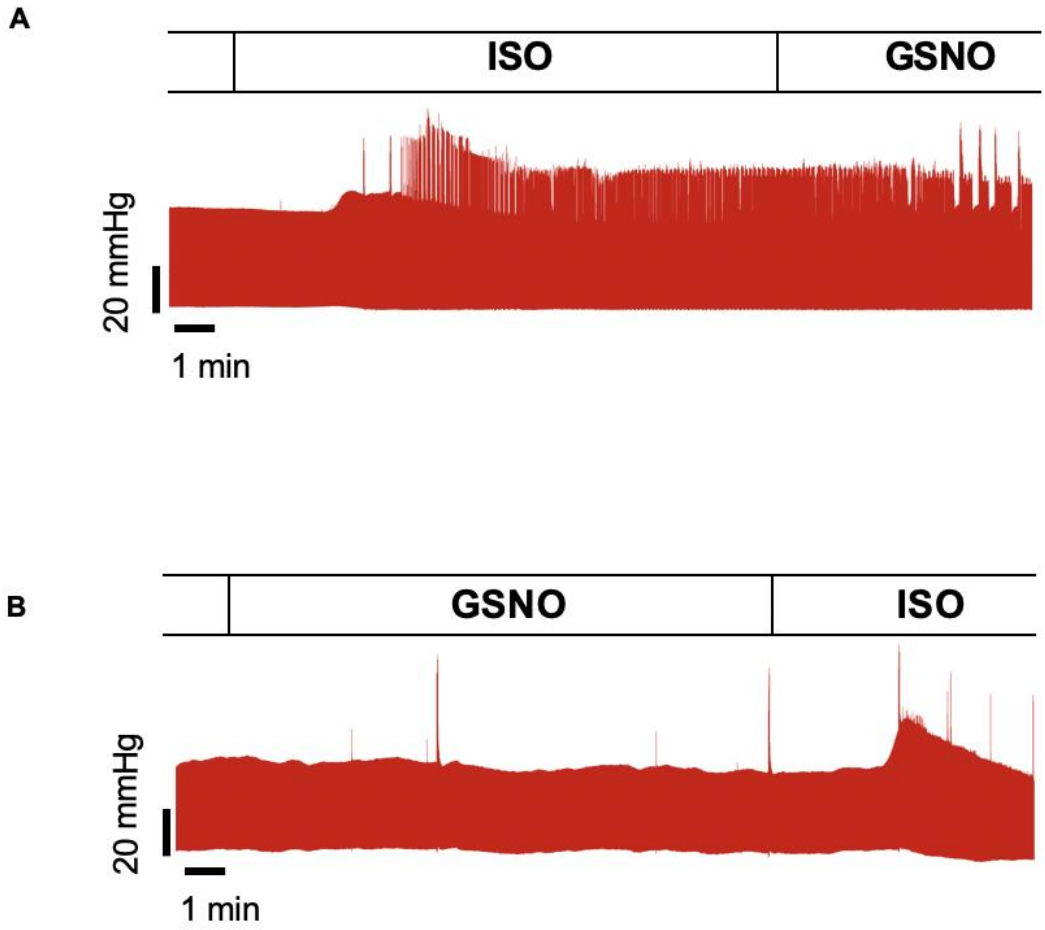

Figure 5.15 Representative trace of LV contractions showing arrhythmic events in WT hearts under ISO and GSNO conditions A, ISO followed by a wash with Krebs-Henseleit buffer; B, ISO followed by GSNO; C, GSNO followed by ISO.

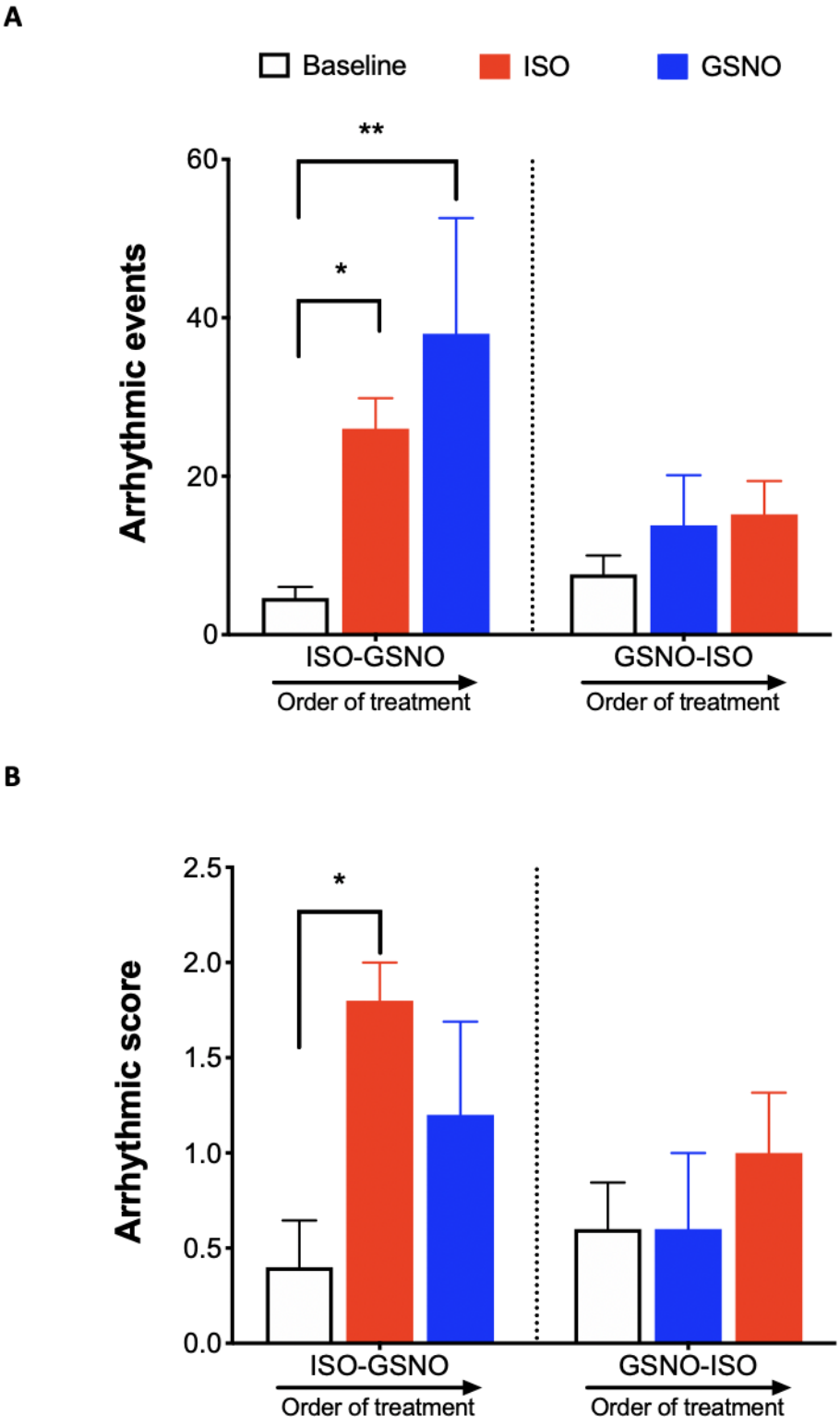

Figure 5.16 Quantification of arrhythmias in WT hearts under ISO (100 nM) and GSNO (150 µM) treatment conditions A, Arrhythmic events B, Arrhythmia score. Data are means ± SEM. Order of treatment; left to right. ISO-GSNO, n = 5, GSNO-ISO, n = 5. Two-way ANOVA (uncorrected Fisher's LSD test) was used to compare between groups: * = $p < 0.05$, ** = $p < 0.01$, * = Drug vs baseline.

5.4 Discussion

It has been reported that CaMKII can induce SR Ca^{2+} leak in cardiomyocytes through the S-nitrosylation pathway during β-adrenergic stress (Gutierrez et al., 2013; Curran et al., 2014) which suggests a complex role of NO in the heart. This chapter investigated the effect of NO donor GSNO and β-AR agonist ISO in isolated WT and KO hearts to understand the role of CaMKII in arrhythmogenesis. I examined the cardiac function of WT and KO mouse hearts during ISO treatment (100 nM). I also investigated cardiac function of WT mouse hearts with exogenous NO donor treatment before and after β-AR stimulation, using 150 µM GSNO and 100 nM ISO. I hypothesised that absence of CaMKIIδ would prevent stress-induced arrhythmias whereas GSNO and ISO would alter heart rate, cardiac contraction and relaxation and induce cardiac arrhythmias in mice with intact CaMKIIδ. The summary of the findings in this chapter is as follows; (a) Loss of CaMKIIδ does not ablate cardiac response to acute β-adrenergic stimulation (b) ISO induces cardiac arrhythmias in WT hearts and not KO hearts (c) ISO induced cardiac inotropy and chronotropy in WT hearts (d) β-AR stimulation prior to GSNO treatment induced and prolonged arrhythmias in WT hearts (e) GSNO treatment prior to β-AR stimulation prevented cardiac arrhythmias in WT hearts (f) GSNO and ISO induce CaMKII phosphorylation and nitrosylation in cardiac tissues.

5.4.1 Loss of CaMKII does not affect response of KO hearts to acute β-AR stimulation

Data from my studies show that β-AR stimulation affected cardiac contractility and this effect was attenuated by the wash phase (Figure 5.8 – 5.10). This result was consistent with that of Grimm et al. (2015), their study showed that acute β-AR stimulation can increase cardiac inotropy in isolated KO mouse hearts. In terms of arrhythmias, it was not surprising that ISO did not affect the number of arrhythmic events in KO hearts (Figure 5.11). Previous studies have shown that CaMKII is one of the primary candidates responsible for arrhythmias, and inhibition of CaMKII is cardioprotective during β-adrenergic stress (Wu et al., 2002; Feng et al., 2017). Surprisingly, the wash phase reduced arrhythmias to below the baseline. The reason for this is not clear. However, it is possible that recovery of the heart from ISO-induced stress and perfusion with KH buffer led to further reduction in arrhythmic events in the wash phase. Taken together, these data

suggest that loss of CaMKII does not affect cardiac response to β-AR stimulation, however it reduces cardiac arrhythmias in isolated mouse hearts.

5.4.2 S-Nitrosylation levels are altered in WT mouse hearts treated with ISO and GSNO

CaMKII undergoes S-nitrosylation at a pair of cysteine residues, and therefore the protein activity can be modified by NO (Erickson et al., 2015). Results from my study show that ISO and GSNO can enhance S-nitrosylation in WT hearts (Figure 5.3B). There was an increase in S-nitrosylation of proteins in the ISO-GSNO group but not in the GSNO-ISO treatment group. CaMKII expression relative to the total protein nitrosylation showed a trend towards increase CaMKII SNO in the ISO-GSNO group. Surprisingly, the CaMKII SNO in the GSNO-ISO group remained similar to control. Previous studies have linked pro-arrhythmic signaling associated with NO exposure to CaMKII S-nitrosylation (Gutierrez et al., 2013; Curran et al., 2014). My hypothesis was that a high level of nitrosylation would be observed in both GSNO-ISO and ISO-GSNO groups due to NO exposure, and this would correspond to the incidence of cardiac arrhythmias (Figure 5.13A). Even though, CaMKII S-nitrosylation levels in the experimental groups were not significant, the data reflected a nearly significant NO-mediated CaMKII activity in the ISO-GSNO and which suggests that effects of GSNO and ISO could be partly mediated via CaMKII.

5.4.3 Acute β-adrenergic stimulation and GSNO treatment alter cardiac contractility in WT hearts

One of the aims of this chapter was to examine the inotropic and chronotropic response of WT hearts during acute β-AR stimulation. Using echocardiography, I measured baseline in vivo cardiac function parameters to ensure similar function in all WT mouse groups (Table 5.7). To measure CaMKII activity, I investigated the presence of CaMKII phosphorylation at Thr 287 after ISO treatment. I found that neither the presence nor timing of GSNO affected either CaMKII expression or phosphorylation (Figure 5.2). Previous literature has shown that ISO does activate CaMKII (Yoo et al., 2009; Feng et al., 2017; Li et al., 2020), but ours is the first study to show that ISO-induced CaMKII activation is not influenced by NO availability.

The next aim was to investigate the effect of β-adrenergic stress and NO on the contractility of the heart. I hypothesised that ISO would enhance cardiac contractility as a response to β-AR stimulation. In contrast to other studies which have shown positive pressure development in WT hearts with exposure to ISO, I observed that ISO did not increase pressure development across all experimental groups. Developed pressure is a measure of the contractility of the ventricles, and it is determined by the difference between maximum and minimum pressure. A study by Grimm et al. (2015) using isolated hearts from WT and CaMKIIδ-KO mice, confirmed that 1 μM ISO increased LV developed pressure in the presence and absence of CaMKIIδ. In my study, the perfusion of ISO through the heart was done for 10 minutes, which is identical to that of Grimm et al. (2015). It is possible that the reason for the contrast in findings could be the difference in the dose, as my study used 100 nM ISO. However, this dose has been shown to be sufficient to increase SR Ca^{2+} in WT cardiomyocytes (Curran et al., 2007; Grimm et al., 2015).

In the ISO-GSNO and GSNO-ISO groups, GSNO also did not alter LV pressure development (Figure 5.12A). This was similar to the observation in Chapter 3 that there was no significant change in LVDP regardless of GSNO concentration. There is no study that has used 150 μM GSNO to measure LV developed pressure in isolated hearts. However, there are studies that have investigated the effect of other NO donors (Kojda et al., 1996; Mohan et al., 1996; Vila-Petroff et al., 1999; González et al., 2008). A common finding is that low concentrations of NO (< 10 μM) increase inotropy and high concentrations (> 10 μM) lead to negative inotropy, and the mechanisms for this effect could be cGMP-dependent or independent. A previous study exploring different NO donors on contractility has shown evidence in frog heart ventricular fibres that active tension, which is a measure of contractility, reduced with increased concentrations of SNP and SNAP (Chesnais et al., 1999).

Despite no change in pressure development with β-AR stimulation, ISO induced a faster rate of contraction and relaxation in all experimental groups compared to baseline. A similar finding has been observed in WT cardiomyocytes treated with 4 nM ISO (Neef et al., 2013). The data in this study showed that positive inotropic effects were associated with ISO and only sustained with GSNO infusion, while GSNO prior to ISO did not induce any increase in rates of contraction (max dP/dt) and relaxation (min dP/dt) (Figure

5.13). Petroff et al. (1994) suggested that the mechanism for the positive lusitropic effect of ISO is via an increase in intracellular cAMP as seen in amphibian hearts. The effect of ISO on rates of contraction and relaxation is consistent with previous studies that have shown that β-AR stimulation increases inotropy and lusitropy in the heart (Kaumann et al., 1999; Freestone et al., 2000). Studies have shown that NOS plays a role in SR Ca^{2+} cycling which determines force frequency response in the heart (Cotton et al., 2001; Khan et al., 2003). The variability between results on the effect of NO donors is quite wide and requires a form of standardization, which is difficult due to the complex role of NO and the dependence of its resultant effects on many factors. In HF patients with normal LV function, it was found that NOS inhibition using L-NMMA, reduced baseline LV max dP/dt but had no effect on basal HR and basal min dP/dt, suggesting that endogenous NO may have little or no inotropic effect in normal human hearts (Cotton et al., 2001). With exogenous NO, there is evidence of augmented or depressed contractility with low or high levels of NO (González et al., 2008). In adult rat cardiomyocytes, 100 µM SNAP reduced contraction amplitude while 1 µM SNAP enhanced contraction amplitude (Vila-Petroff et al., 1999).

Despite perfusing the WT hearts in this study with 150 µM GSNO, it was unclear why there was no change in max dP/dt and min dP/dt from baseline, except when pre-treated with ISO in the ISO-WASH and ISO-GSNO groups. After treatment with ISO, GSNO seemed to sustain the increase in max dP/dt and min dP/dt, but not increase it further, as observed in Figure 5.13. This observation suggests that the effect of exogenous NO could be dependent on β-AR stimulation. It is known that β-AR stimulation activates adenylyl cyclase and induces large increase in cGMP, which activates PKA to increase cardiac contractility (Grimm & Brown, 2010), also high levels of NO stimulates the same pathway, but independent of PKA, and leads to a decrease in cardiac contraction (Vila-Petroff et al., 1999). It is unclear how this sustained inotropic response after ISO application is mediated, as levels of intracellular cGMP before and after ISO were not measured. Taken together, it appears that the inotropic and lusitropic effect of NO is dependent on β-AR stimulation as observed in the ISO-GSNO and GSNO-ISO groups.

ISO application induced faster heart rate in the ISO-GSNO and GSNO-ISO groups (Figure 5.10B), but not in the ISO-WASH group (Figure 5.4B). In the ISO-WASH group, the heart rate only increased during the wash phase which was after ISO infusion was

terminated. Even though the reason for this is unclear, the mechanism of β-AR stimulation and chronotropy involves cGMP production and PKA activation; therefore, one of the possible reasons could be sustained PKA activity during the ISO treatment or an incomplete washout of ISO from the isolated hearts. The duration of ISO application was the same in all groups. In the ISO-GSNO group, it was observed that subsequent infusion of GSNO after ISO did not further enhance chronotropy but maintained it within the 10 minutes of perfusion. In the GSNO-ISO group, HR during GSNO perfusion was equivalent to baseline but increased with ISO perfusion. CaMKII has previously been shown to mediate increased HR associated with β-AR stimulation with ISO infusion in isolated WT hearts (Grimm et al., 2015). Since CaMKII is downstream of β-adrenergic signaling, there is the possibility that this protein mediated the chronotropic effect of ISO in this study. I earlier showed evidence of CaMKII phosphorylation in the WT hearts. This finding is consistent with other studies that have shown increased chronotropy and increased CaMKII activity are associated with β-adrenergic stress (Yoo et al., 2009; Grimm et al., 2015; Zhang, 2017).

Similarly, NO did not independently induce chronotropy except after ISO infusion. This could either be due to the role of β-adrenergic stress or inadequate washout of ISO prior to NO release in the heart. Studies have shown that NO can independently induce increased HR through stimulation of the hyperpolarization-activated inward current I_f, preceded by cGMP activation (Musialek et al., 1997). There are contrasting findings that low levels of NO donor SIN 1 (< 300 µM) induced no change in rat atrial beating rate (Kennedy et al., 1994) and low levels of SNP (10 µM) induced faster heart rate in isolated rat hearts after ischemia and reperfusion (Pabla & Curtis, 1995). Since there is a link between the NO-cGMP pathway, PKA and β-AR stimulation (Pereira et al., 2017), it is possible that this is the mechanism responsible for the chronotropic effect of GSNO seen in the ISO-GSNO group. Currently, there is no data to show if GSNO does increase HR in isolated hearts, but according to data from this study, GSNO had no direct effect on HR, which refutes my hypothesis that GSNO can independently induce cardiac chronotropy. Moreover, it appears that the decrease in PTI during ISO perfusion was due to the increase in heart rate (Figure 5.14).

5.4.4 NO can promote or prevent arrhythmogenic response to β-adrenergic receptor stimulation in WT hearts

Another aim was to investigate the effect of NO on arrhythmias in isolated WT hearts. Previous studies show that excessive β-adrenergic stress can trigger arrhythmias in the heart by spontaneous Ca^{2+} release in cardiomyocytes through a CaMKII-mediated signaling pathway (Wu et al., 2002; Curran et al., 2014; Grimm et al., 2015). Data from this study showed that ISO infusion in WT hearts led to an increased number and severity of triggered arrhythmias (Figure 5.7). This effect was ablated when the hearts were in the wash phase, confirming the arrhythmogenic effect of β-AR stimulation. Sag et al. (2009) showed that CaMKII inhibition abolished ISO-induced arrhythmic events in mouse hearts overexpressing CaMKIIδ_C. They also observed that ISO treatment induced delayed afterdepolarization and spontaneous action potentials in cardiomyocytes from WT mice and in mice that overexpressed CaMKIIδ_C, with the latter having higher incidence of DADs. These data suggest that CaMKII plays a key role in determining the frequency and severity of cardiac arrhythmogenesis during β-AR stimulation.

Recent studies show that NO does activate CaMKII through β-AR signaling and also induces SR Ca^{2+} leak measured as an increase in Ca^{2+} spark frequency (Gutierrez et al., 2013; Curran et al., 2014). I found differences in the response of the heart to ISO and GSNO depending on the order of drug treatment and arrhythmias. ISO application prior to GSNO increased cardiac arrhythmias, and subsequent treatment with GSNO prolonged the arrhythmias (Figure 5.13A). Strikingly, the opposite was observed when the hearts were treated with GSNO before ISO. GSNO treatment did not induce cardiac arrhythmias and, when followed by ISO, there was no further increase in the number of arrhythmia events. ISO increased arrhythmia score in ISO-GSNO, whereas in the GSNO-ISO groups, arrhythmia score was similar across treatments (Figure 5.13B), suggesting that the severity of arrhythmias is also influenced by β-adrenergic stimulation. Thus, for the first time, I have demonstrated a dual role for NO in the whole heart, where NO prolongs cardiac arrhythmias after β-AR stimulation and prevent arrhythmias prior to β-AR stimulation.

The findings from this study suggest that arrhythmogenesis induced by NO is dependent on β-AR stimulation. This is in contrast to the finding by Gutierrez et al. (2013), that NO

treatment in guinea pig cardiomyocytes can increase Ca^{2+} spark frequency directly by CaMKII activation, even in the absence of β-adrenergic signaling. Nevertheless, the role of other Ca^{2+} handling proteins in terms of β-AR and NO signaling have been investigated. In the heart, it has been found that ISO did not significantly modify SERCA2 or LTCC but significantly enhanced RyR2 nitrosylation (Vielma et al., 2016). Studies have suggested that SR Ca^{2+} leak in cardiomyocytes caused by exogenous NO could be due to CaMKII nitrosylation and consequent phosphorylation of RyR2 to increase the opening probability of the channel (Curran et al., 2014), rather than direct RyR2 nitrosylation.

5.4.5 Possible dual role of NO in the heart

It has been previously shown that CaMKIIδ nitrosylation induced by GSNO treatment in cardiomyocytes led to Ca^{2+} mishandling and triggered calcium sparks (Gutierrez et al., 2013; Erickson et al., 2015). Thus, active CaMKII and NO can trigger arrhythmias. Even though the CaMKII-SNO levels observed in my study does not correlate with the incidence of arrhythmic events, Erickson et al. (2015) have shown that NO can modify CaMKIIδ by inhibiting or enhancing its activity. Their study led to the discovery that CaMKIIδ has two nitrosylation sites. During NO signaling, the C273 site which is inhibitory and prevents the deleterious effect of CaMKII while the C290 site is known to be the accelerator of arrhythmias. When CaMKII is in its inactive state, the C273 site is readily available for nitrosylation in the presence of a NO donor and this prevents CaMKII activation. However, upon activation of CaMKII, the C290 site becomes available for nitrosylation, this leads to autonomous activation of CaMKII. This relates to my finding in isolated WT hearts that NO release followed by β-AR stimulation prevents arrhythmias while β-AR stimulation which activates CaMKIIδ, followed by NO release, triggers arrhythmias. It is possible that prior to β-AR stimulation, nitrosylation of C273 acts a brake on CaMKII activity, hence the reduced number of arrhythmic events. Conversely, β-AR stimulation could enhance nitrosylation of the C290 and act as an accelerator of CaMKII activity, thereby increasing the number of arrhythmic events. This means that the activity state is important when it comes to the ability of CaMKIIδ to cause arrhythmias in the presence of exogenous NO donors.

5.4.6 Limitations

One of the technical limitations in this chapter was that NO release during the GSNO perfusion could not be measured in real time due to the complexity of the setup. To address this and to confirm NO release, NO concentration in the buffer solution was determined in a separate experiment by using a sensor to measure NO released from GSNO in KH buffer (Appendix A.2). Levels of cGMP, cAMP and expression of other calcium handling proteins aside from CaMKII were not measured; therefore, it cannot be concluded that the resultant effects were solely due to CaMKII activity. The dose of ISO and GSNO used in this chapter was based on previous experiments done in cardiomyocytes. There is a possibility that the dose was not sufficient to cause marked increase in LV developed pressure in the isolated hearts. One of the aims of this Chapter was to determine the level of arrhythmias in the presence of CaMKII and there was no significant elevation in arrhythmias in the KO mouse hearts during β-adrenergic stress. Therefore, further experiments with ISO and GSNO were not performed in KO hearts which lacked CaMKII.

5.4.7 Conclusion

In summary, the aim of this chapter was to determine the role of NO and CaMKII in cardiac arrhythmias during β-adrenergic stress. β-AR activation of CaMKII is known to contribute to arrhythmogenesis in pathological heart conditions by inducing abnormal calcium cycling. Although NO has many downstream targets which include other calcium handling proteins, CaMKII has been implicated as the key protein responsible for SR Ca^{2+} leak (Gutierrez et al., 2013; Curran et al., 2014). The effect of CaMKII nitrosylation has been established in cardiac cells and is only being investigated in the whole heart for the first time. From these series of experiments, results from this study show that CaMKII can be phosphorylated at Thr 287 in response to increased acute β-AR stimulation and NO signaling in the heart. Even though ISO does not enhance pressure development, it does increase rates of contraction and relaxation, as well as increase heart rate. The data from this study raises the question as to how NO can modulate CaMKII activity and induce cardiac arrhythmias. The different responses observed depending on treatment order might be explained by the NO-CaMKII signaling pathway. CaMKII can be activated by NO at two nitrosylation sites, C273 and C290. These sites have opposing

roles of inhibiting or accelerating CaMKII activity during nitrosylation. Further study will require the use of transgenic mice lacking either C290 or C273 nitrosylation sites to understand the role of each nitrosylation site in the heart. This could explain the dual role of NO in preventing or prolonging arrhythmias. This will be a promising approach towards preventing CaMKII-mediated arrhythmias during NO signaling in cardiac pathology such as heart failure, where there is persistent β-AR stimulation.

CHAPTER 6: GENERAL DISCUSSION

6.1 Summary of key findings

The main objective of this thesis was to investigate the effect of NO treatment on cardiac function. To determine the role of CaMKII in promoting arrhythmias during NO treatment, I used CaMKIIδ-KO mice and WT mice. This thesis describes, for the first time, that the NO donor S-nitrosoglutathione (GSNO) contributes to cardiac arrhythmias by mediating CaMKII activity through S-nitrosylation. S-nitrosylation is one of the mechanisms that mediates biological activity of NO in the cardiovascular system. In the heart, S-nitrosylation of Ca^{2+} handling proteins can be cardioprotective, promoting cardiac contractility and inotropy (Khan et al., 2003; Gonzalez et al., 2007; Murphy et al., 2012). However, a complex role of NO has been discovered which shows that NO plays a role in cardiac arrhythmias. Recent studies have suggested that acute NO exposure contributes to pro-arrhythmic Ca^{2+} handling in cardiomyocytes, possibly through CaMKII S-nitrosylation (Gutierrez et al., 2013; Curran et al., 2014).

To my knowledge, there is limited literature on the effect of CaMKII S-nitrosylation on cardiac function. Previous findings have shown that modification of CaMKII by NO contributes to an increase in Ca^{2+} spark frequency which is an indicator of proarrhythmic remodeling (Curran et al., 2014). However, the effect of CaMKII S-nitrosylation in the whole heart has not been studied prior to the findings in this thesis. The first aim of this thesis was to investigate the effect of loss of CaMKIIδ on basal cardiac function. One of the major findings from this thesis was that knocking out CaMKIIδ does not alter basal cardiac function. Acute GSNO treatment did not alter cardiac contractility in isolated WT and KO hearts; however, heart rate was increased with GSNO in WT hearts only. GSNO also induced arrhythmias with increasing GSNO concentrations in WT hearts; however, KO mouse hearts did not exhibit any change in number of arrhythmic events despite increasing GSNO concentration. With an increase in duration of GSNO treatment, there was evidence of trend towards altered susceptibility of KO mouse hearts to arrhythmias. The results also showed that chronic GSNO treatment reduced cardiac contractility in both WT and KO mouse hearts. In addition, GSNO elevated cardiac arrhythmias in WT and KO mice. KO hearts were responsive to β-adrenergic stimulation, however, they were not susceptible to stress-induced arrhythmias. Whereas, WT hearts with intact CaMKIIδ

were susceptible to stress-induced arrhythmias. This thesis also determined the effect of GSNO and β-adrenergic stimulation on cardiac function in WT hearts. Surprisingly, pre-treating the isolated hearts with GSNO before β-adrenergic stimulation prevented arrhythmias whereas β-adrenergic stimulation before GSNO promoted arrhythmias. This differential role of NO during stress suggested a new mechanism of NO in mediating activity in the whole heart.

6.1.1 Loss of CaMKII prevents arrhythmias during acute GSNO treatment (Chapter 3)

Western blot analysis revealed a reduced expression of CaMKIIδ in CaMKIIδ-KO mice compared to WT mice (Figure 3.2). This was not surprising because CaMKIIδ is the primary cardiac isoform which makes up about 80% of CaMKII expression in the heart. Furthermore, echocardiographic assessment showed that reduced expression of CaMKIIδ did not affect basal cardiac function, this finding is consistent with previous studies (Ling et al., 2009; Grimm et al., 2015). This was due to the fact that CaMKII is mostly inactive at baseline and only activated during stress. I found that isolated WT hearts treated with GSNO exhibited reduced cardiac contractility (Chapter 3, section 3.2.6). GSNO reduced LV developed pressure, increased heart rate and promoted arrhythmias with increasing concentrations in WT hearts. The decreased contraction in the WT hearts could be a result of S-nitrosylation and the activation of cGMP pathway which plays a role in mediating the contractility depending on NO concentration (González et al., 2008). The reason for increase in heart rate increase is not well understood but may be linked to CaMKII activation which in turn promotes Ca^{2+} flux in cardiomyocytes (Wu et al., 2009; Yaniv et al., 2013). In addition, GSNO could be activation of hyperpolarisation-activated inward current via the cGMP pathway (Müller-Strahl et al., 2000). No change in cardiac contractility was observed in the KO mouse hearts following acute GSNO treatment. Also, KO mouse hearts were less susceptible to arrhythmias during acute GSNO treatment compared to WT mouse hearts. There is a possibility that loss of CaMKIIδ in the heart prevented the arrhythmogenic effect associated with presence of CaMKII during NO treatment, therefore the KO hearts did not exhibit any change in arrhythmic events with increasing GSNO concentration. This thesis provides evidence to suggest that the presence of CaMKII contributes to the deleterious effect observed during increased NO

bioavailability. This corresponds to data from cardiomyocytes that show that GSNO promotes proarrhythmic signaling (Gutierrez et al., 2013).

6.1.2 Chronic GSNO treatment does not promote cardiac arrhythmias (Chapter 4)

In acute condition, several effects of NO modulated by CaMKII presence were observed. The main aim of Chapter 4 was to determine the effect of chronic NO treatment on cardiac function. There was no change in in vivo cardiac function in WT and KO hearts after 5-week GSNO treatment. I performed subsequent GSNO treatment on the isolated hearts after GSNO supplementation to WT and KO animals. Results showed there was reduced contractility in both the WT and KO hearts with increasing GSNO concentration compared to baseline. This finding was similar to studies that have shown the effect of increasing GSNO concentration in the heart (Sarkar et al., 2000; González et al., 2008). My hypothesis was that isolated WT hearts would exhibit increase susceptibility to arrhythmias after chronic administration of GSNO and KO hearts would have reduced number of arrhythmic events due to absence of CaMKIIδ. Surprising, there was a trend towards increased cardiac arrhythmias in both WT and KO hearts with increased GSNO concentration following chronic GSNO treatment. Since this observation did not reach a level of significance, a conclusion on the effect of CaMKIIδ can only be drawn by measuring CaMKIIδ nitrosylation levels. My findings do suggest that loss of CaMKIIδ does not prevent cardiac arrhythmias during chronic GSNO treatment, unlike during acute treatment. During acute GSNO treatment, NO-induced arrhythmias occur through a CaMKII-dependent pathway, but during chronic treatment there is the possibility that other signaling pathways influence the occurrence of arrhythmic events. Therefore, knocking out CaMKIIδ is no longer sufficient to protect the heart resulting in the trend of increased arrhythmias observed in WT and KO hearts in the chronic treatment phase compared to the acute treatment phase.

6.1.3 NO promotes stress-induced cardiac arrhythmias (Chapter 5)

β-adrenergic stimulation contributes to upregulation of NO production. Since upregulation of NO has been observed to contribute to arrhythmogenesis in WT hearts, it was necessary to determine how β-adrenergic stress and NO would modulate cardiac

function. To investigate the effect of loss of CaMKII on cardiac function during β-adrenergic stress on cardiac function, KO mouse hearts were treated with the β-adrenergic receptor agonist isoproterenol (ISO). Results showed that KO hearts were protected from ISO-induced arrhythmias. The next step was to perform same investigation in WT mouse hearts. My results suggested that hearts from WT mice were susceptible to arrhythmias during β-adrenergic stress. Echocardiographic data showed similar in vivo cardiac function in all groups of WT hearts prior to drug treatment. β-adrenergic stimulation enhanced cardiac contractility in all groups regardless of treatment order. GSNO did not affect contractility except in the ISO-GSNO group pre-treated with ISO. The ISO-GSNO group developed cardiac arrhythmias during ISO treatment, which were prolonged by GSNO treatment. However, GSNO treatment followed by ISO prevented β-adrenergic stress. In terms of arrhythmias, the mechanism for this is not well understood and requires further studies but this defines a dual role of NO in the heart during stress. Western blot analysis showed CaMKII S-nitrosylation was upregulated in the ISO-GSNO group suggesting that CaMKII nitrosylation contributed to the effect seen in these hearts. Since nitrosylation of CaMKII is suggested to be responsible for arrhythmogenesis, this raises a question as to how NO modifies CaMKII during stress to induce the opposing effects of NO in the isolated hearts. It has been previously documented that CaMKII has two nitrosylation sites which influence its activity during NO signaling. This finding by Erickson et al. (2015) provided specific details for the nitrosylation sites of the cardiac isoform, CaMKIIδ. Their study also showed that exposure of CaMKIIδ to GSNO resulted in autonomous kinase activation via S-nitrosylation on Cys290 site, in contrast, the S-nitrosylation on Cys273 site prevented activation of CaMKII. This led to the identification of a dual pathway of CaMKII activation by NO. This thesis proposes that the nitrosylation sites of CaMKII could mediate the response of the heart to increase in NO production during ß-adrenergic stress.

6.2 Limitations

One of the greatest challenges was working with small hearts and cannulation of these hearts required very steady hands, because the aorta would tear easily without extreme care. The aorta of the mouse is small, however it can be visualised with the naked eye. The cannulation time had to be kept under 5 minutes. This was a difficult task because after excision and arresting of the heart, the vessels around the heart had to be trimmed to

access the aortic root, and this had to be done quickly to avoid ischaemia in the arrested heart. Cutting the aorta too short or cannulating too deep would affect perfusion rate and thereby affect heart function. Hearts with ripped aorta were excluded from final analysis.

The LV balloon for the heart had to be handmade and with this came the challenge of making balloon the right size for a mouse ventricle. This balloon had to be free of leaks, air bubbles which could in turn alter the LV pressure slightly. The LV balloons were made out of saran wrap, as they had to be thin enough to allow compliance and for pressure to be transmitted to the transducer, making them really susceptible to leakage. These balloons had to be made often, so the balloons used in the different sets of the experiments varied. The minimum pressure for every heart had to be > 20 mmHg to be included in analysis. Another reason for low pressure was due to the fact that the hearts were unpaced, because pacing would mask the effect of the drug treatment and the ability to detect arrhythmias. Despite the low baseline pressure (< 100 mmHg), the fluid volume in the balloon was kept constant, 10 µl to yield 5 – 10 mmHg end diastolic pressure. The final data was presented as fold change to present a clearer picture of the pressure change across each protocol. I also had time-matched controls to account for any changes in pressure unrelated to drug treatment.

During my experiment, the flow probe malfunctioned therefore I could not obtain coronary flow for some of my Langendorff experiments. The other option was to measure the volume of perfusate effluent over a given time. However, the mouse heart is very tiny and has to remain in temperature-controlled buffer to protect the integrity of the heart throughout the protocol, so coronary effluent could not be obtained during that period.

Due to the limitations mentioned, and exclusion of hearts that did not meet the criteria of hearts required for my data analysis, my sample size was smaller than anticipated. Some of my data showed trends which could have been as a result of the small sample size. For future studies, an increment in sample size would definitely be necessary.

Using the biotin switch assay to measure S-nitrosylation required a lot of optimisation. While I was able to measure global nitrosylation, I was unable to detect nitrosylated CaMKII levels. It is unclear if this is due to low expression of nitrosylated CaMKII or a technical problem. As an alternative, the samples had to shipped for the experiment had

to be done by our collaborators which finally produced results. Mass spectrometry should have been done to measure nitrosylation at the different sites of CaMKII, however, the lock down due to the pandemic affected the services of the facility and that part of the investigation had to be suspended. Recently, I was able to probe for global protein nitrosylation in the heart tissues, but I am yet to obtain results from nitrosylated CaMKII.

6.3 The role of gamma isoform of CaMKII

As mentioned earlier in the introduction, CaMKIIγ is also expressed in the heart as a secondary isoform. The unique role of CaMKIIγ in cardiac dysfunction has not been fully explored. It is known to contributes to apoptosis of macrophages and plays a role in upregulation of atherosclerotic plaque which could potentially contribute to myocardial infarction (Timmins et al., 2009; Kreusser & Backs, 2014; Doran et al., 2017). Some studies have shown evidence that there is no upregulation of CaMKIIγ to compensate for loss of CaMKIIδ in unstressed KO mice (Backs et al., 2009) and KO mice after aorto-caval shunt (Mohamed et al., 2019). However, a study by Kreusser et al. (2014) showed that CaMKIIγ and CaMKIIγ can compensate for each other in KO mice without cardiac dysfunction. Ling et al. (2009) showed that CaMKIIγ increased in WT and KO mice only after 2-week transverse aortic constriction (TAC)-induced pressure overload of the LV, suggesting that CaMKIIγ can be upregulated in stress conditions to compensate for loss of CaMKIIδ. In Chapter 3, Western blot results obtained in LV tissues of isolated heart after acute GSNO treatment showed that there was reduction in CaMKII expression due to deletion of CaMKIIδ compared to WT heart tissues. There was no evidence of upregulation of CaMKIIγ in the LV tissues. In the chronic study (Chapter 4), deletion of CaMKIIδ had no effect on cardiac arrhythmias, suggesting a possibility that some of the effects in the chronic experiments could be due to the compensatory role of CaMKIIγ. Further studies can be performed to determine the specific role of CaMKIIγ activation during NO exposure.

6.4 S-Nitrosylation of Ca^{2+} handling proteins and cardioprotection

An increase in S-nitrosylation of cardiac proteins is known to be cardioprotective (Murphy et al., 2012). Interestingly, S-nitrosylation also regulates redox signaling during oxidative stress where thiol groups of cysteine residues are shielded by S-nitrosylation

and this prevents irreversible oxidation (Sun et al., 2006b; Kohr et al., 2011). S-nitrosylation of Ca^{2+} handling proteins has also been found to be beneficial. Reduced RyR2 nitrosylation promoted SR Ca^{2+} leak in cardiomyocytes (Gonzalez et al., 2007). S-nitrosylation of L-type Ca^{2+} channel reduced Ca^{2+} entry by reducing channel activity after β-adrenergic stimulation (Sun et al., 2006a). S-nitrosylation of SERCA2a after GSNO treatment in cardiomyocytes enhances SR Ca^{2+} uptake (Sun et al., 2007). The evidence surrounding S-nitrosylation of CaMKII is still developing and the current observation is that CaMKII contributes to pro-arrhythmic signaling in cardiomyocytes (Gutierrez et al., 2013; Curran et al., 2014; Erickson et al., 2015). CaMKII S-nitrosylation has been found to promote arrhythmias during NO treatment, which was one of the findings in this thesis. Another finding was that CaMKII S-nitrosylation could also be cardioprotective if S-nitrosylation precedes β-adrenergic receptor stimulation. The mechanism for this may be explained by the role of the nitrosylation sites.

6.5 Clinical relevance of CaMKII S-nitrosylation

Consistent with previous studies, this thesis contributes to the growing body of knowledge that NO can modulate CaMKII activity (Gutierrez et al., 2013; Curran et al., 2014). Studies have shown that NO is cardioprotective and decreased NO production is associated with cardiac decompensation in heart failure (Recchia et al., 1998; Katz et al., 1999). Data from this thesis has shown that increase NO production can modulate cardiac arrhythmias through a CaMKII-dependent pathway and β-adrenergic stimulation. On the other hand, excessive β-adrenergic stimulation and increased CaMKII activity is associated with heart failure (Hoch et al., 1999; Zhang et al., 2003). In clinical settings, β-adrenergic receptor blockers and NO donors are administered to heart failure patients to suppress sympathetic activity and improve vascular flow. Since my study shows that NO production can contribute to pro-arrhythmic signaling independent of β-adrenergic stimulation, it will be necessary to investigate whether administration of NO donors will promote arrhythmias in heart failure patients. With evidence showing that NO promotes arrhythmogenesis through CaMKII in cardiomyocytes and in the whole heart, CaMKII S-nitrosylation may contribute to the enhancement of SR Ca^{2+} leak and cardiac arrhythmias in heart failure patients. To prevent NO-induced arrhythmias, CaMKII inhibitors could be a potential therapeutic target for clinical use. The findings in this thesis

provide initial evidence of the impact of S-nitrosylation of CaMKII on heart function which can serve as a foundation for further studies using human tissues.

6.6 Future directions

This study has provided insight on the role of NO in modifying CaMKII activity in the heart. Even though there were certain limitations with measurement of NO levels and CaMKII nitrosylation, the use of CaMKIIδ-KO mice helped to ascertain the impact of S-nitrosylation on cardiac arrhythmias.

One of the indicators of cardiac dysfunction is excessive sympathetic activity and in conditions such as diabetic heart disease or heart failure, upregulation of CaMKII expression has also been implicated (Zhang et al., 2005; Erickson et al., 2013). Data from this thesis showed that CaMKIIδ-KO mice become susceptible to arrhythmias after prolonged GSNO treatment but are protected from arrhythmias in the acute phase. In order to understand how this evidence is relevant to the role of CaMKII and NO in heart, it will be necessary to investigate the long-term effect of NO treatment combined with adrenergic stress on cardiac function using WT and KO mice.

According to (Erickson et al., 2015), the order of binding of NO-related species at the Cys273 and Cys290 sites determines the function of CaMKII during NO exposure. Pre-treatment with NO prior to Ca^{2+}/CaM binding caused Cys273 modification while treatment with NO after Ca^{2+}/CaM activation of CaMKII modified the Cys290 site. Nitrosylation of Cys273 reduced Ca^{2+}/CaM binding while nitrosylation of Cys290 fostered Ca^{2+}/CaM binding. This study also showed that there was persistent and significant increase in Ca^{2+} spark frequency when myocytes were treated in an order, with Ca^{2+}/CaM, GSNO and egtazic acid (EGTA) (Erickson et al., 2015). These results were consistent with other studies in showing that autonomous activation of CaMKII by NO induced more frequent and spontaneous SR Ca^{2+} release (Ca^{2+} sparks) which is a predictor of arrhythmias. Furthermore, my study has shown that possible activation of CaMKII during β-adrenergic stimulation prior to GSNO treatment promoted arrhythmias while the reverse of treatment order prevented arrhythmias. This finding in the whole heart can provide a proposed mechanism for mediation of CaMKII activity by NO (Figure 6.1). It would be interesting to determine if there is difference in the level of nitrosylation at these

two sites in mice treated with GSNO. Furthermore, development of mice which lack either nitrosylation sites of CaMKII could provide an understanding of how NO regulates CaMKII activity in the whole heart.

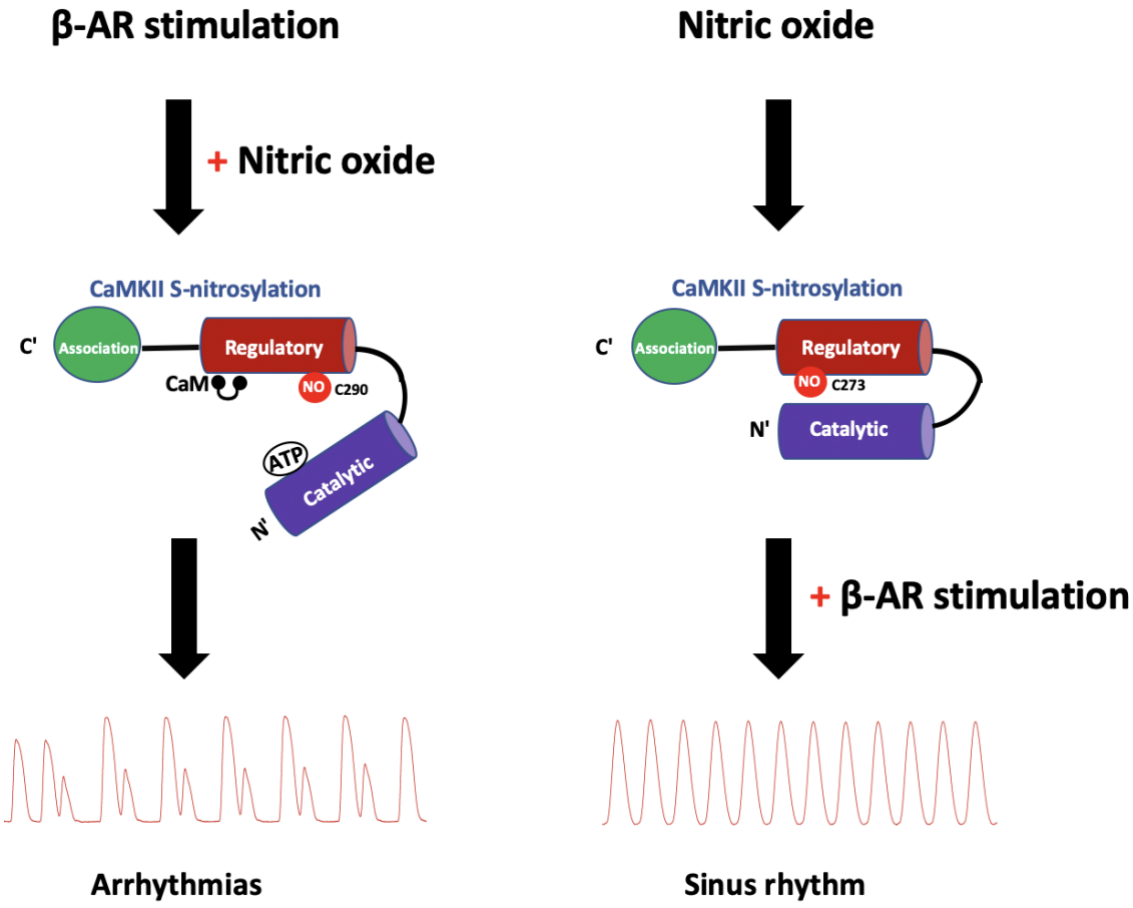

Figure 6.1 CaMKII nitrosylation enhances arrhythmia depending on the nitrosylation site. β-adrenergic receptor (β-AR) stimulation (which promotes Ca^{2+}/CaM binding and activation), followed by NO treatment, promotes S-nitrosylation of Cys290 site and accelerates arrhythmias. NO treatment promotes S-nitrosylation of Cys273 site followed by β-adrenergic stimulation and prevents arrhythmias. Original schematic by Esther Asamudo

6.7 Concluding Remarks

This thesis provides first evidence to show that S-nitrosylation of CaMKII contributes to arrhythmias in isolated hearts while knocking out CaMKIIδ protected against acute GSNO-induced arrhythmias. Duration of GSNO exposure also determined the effect of CaMKII on arrhythmias. Since this concept is new, the findings from this thesis can serve as a foundation for further studies to investigate the mechanisms of CaMKII S-nitrosylation and the role of CaMKII S-nitrosylation sites in cardiac arrhythmias.

REFERENCES

Abiria SA & Colbran RJ. (2010). CaMKII associates with $Ca_{(V)}1.2$ L-type calcium channels via selected β subunits to enhance regulatory phosphorylation. *J Neurochem* **112,** 150.

Aggarwal A, Singh I & Sandhir R. (2018). Protective effect of S-nitrosoglutathione administration against hyperglycemia induced disruption of blood brain barrier is mediated by modulation of tight junction proteins and cell adhesion molecules. *Neurochemistry International* **118,** 205-216.

Ai X, Curran JW, Shannon TR, Bers DM & Pogwizd SM. (2005). Ca^{2+}/Calmodulin–Dependent Protein Kinase Modulates Cardiac Ryanodine Receptor Phosphorylation and Sarcoplasmic Reticulum Ca^{2+} Leak in Heart Failure. *Circulation Research* **97,** 1314-1322.

Anaya-Prado R, Toledo-Pereyra LH, Guo R, Reuben J, Ward PA & Walsh J. (2003). The attenuation of hemorrhage-induced liver injury by exogenous nitric oxide, L-arginine, and inhibition of inducible nitric oxide synthase. *Journal of Investigative Surgery* **16,** 247-261.

Anderson ME, Braun AP, Wu Y, Lu T, Wu Y, Schulman H & Sung RJ. (1998). KN-93, an inhibitor of multifunctional Ca^{++}/calmodulin-dependent protein kinase, decreases early afterdepolarizations in rabbit heart. *Journal of Pharmacology and Experimental Therapeutics* **287,** 996-1006.

Ashpole NM, Herren AW, Ginsburg KS, Brogan JD, Johnson DE, Cummins TR, Bers DM & Hudmon A. (2012). Ca^{2+}/Calmodulin-dependent Protein Kinase II (CaMKII) Regulates Cardiac Sodium Channel NaV1.5 Gating by Multiple Phosphorylation Sites. *Journal of Biological Chemistry* **287,** 19856-19869.

Backs J, Backs T, Neef S, Kreusser MM, Lehmann LH, Patrick DM, Grueter CE, Qi X, Richardson JA & Hill JA. (2009). The δ isoform of CaM kinase II is required for pathological cardiac hypertrophy and remodeling after pressure overload. *Proceedings of the National Academy of Sciences* **106,** 2342-2347.

Balligand J-L, Ungureanu-Longrois D, Simmons WW, Pimental D, Malinski TA, Kapturczak M, Taha Z, Lowenstein CJ, Davidoff AJ & Kelly RA. (1994). Cytokine-inducible nitric oxide synthase (iNOS) expression in cardiac myocytes. Characterization and regulation of iNOS expression and detection of iNOS activity in single cardiac myocytes in vitro. *Journal of Biological Chemistry* **269,** 27580-27588.

Barouch LA, Harrison RW, Skaf MW, Rosas GO, Cappola TP, Kobeissi ZA, Hobai IA, Lemmon CA, Burnett AL & O'Rourke B. (2002). Nitric oxide regulates the heart by spatial confinement of nitric oxide synthase isoforms. *Nature* **416,** 337-339.

Bassani RA, Bassani J & Bers DM. (1994). Relaxation in ferret ventricular myocytes: unusual interplay among calcium transport systems. *The Journal of Physiology* **476,** 295-308.

Bayer KU & Schulman H. (2001). Regulation of signal transduction by protein targeting: the case for CaMKII. *Biochemical and Biophysical Research Communications* **289,** 917-923.

Beckendorf J, van den Hoogenhof MM & Backs J. (2018). Physiological and unappreciated roles of CaMKII in the heart. *Basic Research in Cardiology* **113,** 29.

Bell RM, Mocanu MM & Yellon DM. (2011). Retrograde heart perfusion: The Langendorff technique of isolated heart perfusion. *Journal of Molecular and Cellular Cardiology* **50,** 940-950.

Bers DM. (2002). Cardiac excitation–contraction coupling. *Nature* **415,** 198.

Bers DM. (2014). Cardiac sarcoplasmic reticulum calcium leak: basis and roles in cardiac dysfunction. *Annual Review of Physiology* **76,** 107-127.

Bers DM & Grandi E. (2009). CaMKII regulation of cardiac ion channels. *Journal of Cardiovascular Pharmacology* **54,** 180.

Bers DM & Guo T. (2005). Calcium signaling in cardiac ventricular myocytes. *Annals of the New York Academy of Sciences* **1047,** 86-98.

Betteridge DJ. (2000). What is oxidative stress? *Metabolism* **49,** 3-8.

Bishop CM. (2012). Development of a nitric oxide measurement method in tissue media. *2000-2019-CSU Theses and Dissertations*.

Bouma P, Ferdinandy P, Sipkema P, Allaart C & Westerhof N. (1992). Nitric oxide is an important determinant of coronary flow in the isolated blood perfused rat heart. *Basic Research in Cardiology* **87,** 570-584.

Bovo E, Lipsius SL & Zima AV. (2012). Reactive oxygen species contribute to the development of arrhythmogenic Ca2+ waves during β-adrenergic receptor stimulation in rabbit cardiomyocytes. *The Journal of Physiology* **590,** 3291-3304.

Bradley SA & Steinert JR. (2016). Nitric Oxide-Mediated Posttranslational Modifications: Impacts at the Synapse. *Oxidative Medicine and Cellular Longevity* **2016,** 9.

Braun AP & Schulman H. (1995). The multifunctional calcium/calmodulin-dependent protein kinase: from form to function. *Annual Review of Physiology* **57,** 417-445.

Brunner F, Andrew P, Wölkart G, Zechner R & Mayer B. (2001). Myocardial contractile function and heart rate in mice with myocyte-specific overexpression of endothelial nitric oxide synthase. *Circulation* **104,** 3097-3102.

Burger DE, Lu X, Lei M, Xiang F-L, Hammoud L, Jiang M, Wang H, Jones DL, Sims SM & Feng Q. (2009). CLINICAL PERSPECTIVE. *Circulation* **120,** 1345-1354.

Calvert JW & Lefer DJ. (2013). Role of β-adrenergic receptors and nitric oxide signaling in exercise-mediated cardioprotection. *Physiology* **28,** 216-224.

Campbell DL, Stamler JS & Strauss HC. (1996). Redox modulation of L-type calcium channels in ferret ventricular myocytes. Dual mechanism regulation by nitric oxide and S-nitrosothiols. *The Journal of General Physiology* **108,** 277-293.

Chander V & Chopra K. (2005). Renal protective effect of molsidomine and L-arginine in ischemia-reperfusion induced injury in rats. *Journal of Surgical Research* **128,** 132-139.

Chattopadhyay P, Verma N, Verma A, Kamboj T, Khan NA & Wahi AK. (2008). L-arginine protects from pringle manoeuvere of ischemia-reperfusion induced liver injury. *Biological and Pharmaceutical Bulletin* **31,** 890-892.

Chesnais J-M, Fischmeister R & Mery P-F. (1999). Positive and negative inotropic effects of NO donors in atrial and ventricular fibres of the frog heart. *The Journal of Physiology* **518,** 449.

Chirinos JA, Akers SR, Trieu L, Ischiropoulos H, Doulias PT, Tariq A, Vasim I, Koppula MR, Syed AA & Soto-Calderon H. (2016). Heart failure, left ventricular remodeling, and circulating nitric oxide metabolites. *Journal of the American Heart Association* **5,** e004133.

Chruscinski AJ, Rohrer DK, Schauble E, Desai KH, Bernstein D & Kobilka BK. (1999). Targeted disruption of the β2 adrenergic receptor gene. *Journal of Biological Chemistry* **274,** 16694-16700.

Clancy R, Leszczynska-Piziak J & Abramson S. (1992). Nitric oxide, an endothelial cell relaxation factor, inhibits neutrophil superoxide anion production via a direct

action on the NADPH oxidase. *The Journal of Clinical Investigation* **90,** 1116-1121.

Cotton J, Kearney M & Shah A. (2002). Nitric oxide and myocardial function in heart failure: friend or foe? *Heart* **88,** 564.

Cotton JM, Kearney MT, MacCarthy PA, Grocott-Mason RM, McClean DR, Heymes C, Richardson PJ & Shah AM. (2001). Effects of nitric oxide synthase inhibition on basal function and the force-frequency relationship in the normal and failing human heart in vivo. *Circulation* **104,** 2318-2323.

Curran J, Hinton MJ, Ríos E, Bers DM & Shannon TR. (2007). β-Adrenergic enhancement of sarcoplasmic reticulum calcium leak in cardiac myocytes is mediated by calcium/calmodulin-dependent protein kinase. *Circulation Research* **100,** 391-398.

Curran J, Tang L, Roof SR, Velmurugan S, Millard A, Shonts S, Wang H, Santiago D, Ahmad U, Perryman M, Bers DM, Mohler PJ, Ziolo MT & Shannon TR. (2014). Nitric Oxide-Dependent Activation of CaMKII Increases Diastolic Sarcoplasmic Reticulum Calcium Release in Cardiac Myocytes in Response to Adrenergic Stimulation. *PLoS ONE* **9**.

Currie S, Loughrey CM, Craig M-A & Smith GL. (2004). Calcium/calmodulin-dependent protein kinase IIdelta associates with the ryanodine receptor complex and regulates channel function in rabbit heart. *Biochemical Journal* **377,** 357-366.

Curtis MJ & Walker MJ. (1988). Quantification of arrhythmias using scoring systems: an examination of seven scores in an in vivo model of regional myocardial ischaemia. *Cardiovascular research* **22,** 656-665.

Cutler MJ, Plummer BN, Wan X, Sun Q-A, Hess D, Liu H, Deschenes I, Rosenbaum DS, Stamler JS & Laurita KR. (2012). Aberrant S-nitrosylation mediates calcium-triggered ventricular arrhythmia in the intact heart. *Proceedings of the National Academy of Sciences* **109,** 18186-18191.

D'Andrea E, Nagyova I & Villari P. (2015). Cardiovascular Disease (CVD). In *A Systematic Review of Key Issues in Public Health*, ed. Boccia S, Villari P & Ricciardi W, pp. 33-64. Springer International Publishing, Cham.

Daniels L, Bell JR, Delbridge LMD, McDonald FJ, Lamberts RR & Erickson JR. (2015). The role of CaMKII in diabetic heart dysfunction. *Heart Failure Reviews* **20,** 589-600.

Daniels LJ. (2017). The role of calcium calmodulin dependent protein kinase II in type 2 diabetic heart dysfunction (Thesis, Doctor of Philosophy). University of Otago. Retrieved from http://hdl.handle.net/10523/7492

Daniels LJ, Wallace RS, Nicholson OM, Wilson GA, McDonald FJ, Jones PP, Baldi JC, Lamberts RR & Erickson JR. (2018). Inhibition of calcium/calmodulin-dependent kinase II restores contraction and relaxation in isolated cardiac muscle from type 2 diabetic rats. *Cardiovascular Diabetology* **17,** 1-15.

Dewenter M, Neef S, Vettel C, Lämmle S, Beushausen C, Zelarayan LC, Katz S, von der Lieth A, Meyer-Roxlau S & Weber S. (2017). Calcium/calmodulin-dependent protein kinase II activity persists during chronic β-adrenoceptor blockade in experimental and human heart failure. *Circulation: Heart Failure* **10,** e003840.

Dibb K, Graham H, Venetucci L, Eisner D & Trafford A. (2007). Analysis of cellular calcium fluxes in cardiac muscle to understand calcium homeostasis in the heart. *Cell Calcium* **42,** 503-512.

Dietz NM, Rivera JM, Eggener SE, Fix RT, Warner DO & Joyner MJ. (1994). Nitric oxide contributes to the rise in forearm blood flow during mental stress in humans. *The Journal of Physiology* **480,** 361-368.

Dobrev D & Wehrens XHT. (2014). Role of RyR2 Phosphorylation in Heart Failure and Arrhythmias. *Controversies Around Ryanodine Receptor Phosphorylation in Cardiac Disease* **114,** 1311-1319.

Doran AC, Ozcan L, Cai B, Zheng Z, Fredman G, Rymond CC, Dorweiler B, Sluimer JC, Hsieh J & Kuriakose G. (2017). CAMKIIγ suppresses an efferocytosis pathway in macrophages and promotes atherosclerotic plaque necrosis. *The Journal of Clinical Investigation* **127,** 4075-4089.

Đorđević VB, Stojanović I, Kundalić S, Ristić T, Pavlović R, Ćosić V & Cvetković T. (2012). Pathophysiological importance of nitric oxide in coronary heart disease/Patofiziološki značaj azot-monoksida u koronarnoj bolesti srca. *Journal of Medical Biochemistry* **31,** 287-294.

Edman CF & Schulman H. (1994). Identification and characterization of δB-CaM kinase and δC-CaM kinase from rat heart, two new multifunctional Ca2+/calmodulin-dependent protein kinase isoforms. *Biochimica et Biophysica Acta (BBA)-Molecular Cell Research* **1221,** 89-101.

Edwards AG, Grandi E, Hake JE, Patel S, Li P, Miyamoto S, Omens JH, Brown JH, Bers DM & McCulloch AD. (2014). Nonequilibrium Reactivation of Na⁺ Current Drives Early Afterdepolarizations in Mouse Ventricle. *Circulation: Arrhythmia and Electrophysiology* **7,** 1205-1213.

Erickson J. (2014). Mechanisms of CaMKII Activation in the Heart. *Frontiers in Pharmacology* **5**.

Erickson JR, Joiner MA, Guan X, Kutschke W, Yang J, Oddis CV, Bartlett RK, Lowe JS, O'Donnell S, Aykin-Burns N, Zimmerman MC, Zimmerman K, Ham AJL, Weiss RM, Spitz DR, Shea MA, Colbran RJ, Mohler PJ & Anderson ME. (2008). A dynamic pathway for calcium-independent activation of CaMKII by methionine oxidation. *Cell* **133,** 462-474.

Erickson JR, Nichols CB, Uchinoumi H, Stein ML, Bossuyt J & Bers DM. (2015). S-Nitrosylation induces both autonomous activation and inhibition of calcium/calmodulin-dependent protein kinase II δ. *Journal of Biological Chemistry* **290,** 25646-25656.

Erickson JR, Patel R, Ferguson A, Bossuyt J & Bers DM. (2011). FRET-based sensor Camui provides new insight into mechanisms of CaMKII activation in intact cardiomyocytes. *Circulation Research* **109,** 729.

Erickson JR, Pereira L, Wang L, Han G, Ferguson A, Dao K, Copeland RJ, Despa F, Hart GW, Ripplinger CM & Bers DM. (2013). Diabetic Hyperglycemia activates CaMKII and Arrhythmias by O linked Glycosylation. *Nature* **502,** 372-376.

Fabiato A & Fabiato F. (1978). Calcium-induced release of calcium from the sarcoplasmic reticulum of skinned cells from adult human, dog, cat, rabbit, rat, and frog hearts and from fetal and new-born rat ventricles. *Annals of the New York Academy of Sciences* **307,** 491-522.

Federico M, Portiansky EL, Sommese L, Alvarado FJ, Blanco PG, Zanuzzi CN, Dedman J, Kaetzel M, Wehrens XH & Mattiazzi A. (2017). Calcium-calmodulin-dependent protein kinase mediates the intracellular signalling pathways of cardiac apoptosis in mice with impaired glucose tolerance. *The Journal of Physiology* **595,** 4089-4108.

Fei L, Baron AD, Henry DP & Zipes DP. (1997). Intrapericardial delivery of L-arginine reduces the increased severity of ventricular arrhythmias during sympathetic stimulation in dogs with acute coronary occlusion: nitric oxide modulates sympathetic effects on ventricular electrophysiological properties. *Circulation* **96,** 4044-4049.

Feng Y, Cheng J, Wei B & Wang Y. (2017). CaMKII inhibition reduces isoproterenol-induced ischemia and arrhythmias in hypertrophic mice. *Oncotarget* **8,** 17504.

Ferrero P, Said M, Sánchez G, Vittone L, Valverde C, Donoso P, Mattiazzi A & Mundiña-Weilenmann C. (2007). Ca^{2+}/calmodulin kinase II increases ryanodine binding and Ca2+-induced sarcoplasmic reticulum Ca^{2+} release kinetics during β-adrenergic stimulation. *Journal of Molecular and Cellular Cardiology* **43,** 281-291.

Floras JS. (2009). Sympathetic nervous system activation in human heart failure: clinical implications of an updated model. *Journal of the American College of Cardiology* **54,** 375-385.

Freestone N, Ribaric S, Scheuermann M, Mauser U, Paul M & Vetter R. (2000). Differential lusitropic responsiveness to β-adrenergic stimulation in rat atrial and ventricular cardiac myocytes. *Pflügers Archiv* **441,** 78-87.

Gao S, Ho D, Vatner DE & Vatner SF. (2011). Echocardiography in mice. *Current Protocols in Mouse Biology* **1,** 71-83.

Gao XM, Dart AM, Dewar E, Jennings G & Du XJ. (2000). Serial echocardiographic assessment of left ventricular dimensions and function after myocardial infarction in mice. *Cardiovasc Res* **45**.

Garreffa AM, Woodman OL, Cao AH & Ritchie RH. (2006). Sodium nitroprusside protects adult rat cardiac myocytes from cellular injury induced by simulated ischemia: role for a non-cGMP-dependent mechanism of nitric oxide protection. *Journal of Cardiovascular Pharmacology* **47,** 1-8.

Gaztañaga L, Marchlinski FE & Betensky BP. (2012). Mechanisms of cardiac arrhythmias. *Revista Española de Cardiología (English Edition)* **65,** 174-185.

Giri S, Rattan R, Deshpande M, Maguire JL, Johnson Z, Graham RP & Shridhar V. (2014). Preclinical therapeutic potential of a nitrosylating agent in the treatment of ovarian cancer. *PLoS ONE* **9,** e97897.

Gonano LA, Sepúlveda M, Rico Y, Kaetzel M, Valverde CA, Dedman J, Mattiazzi A & Petroff MV. (2011). Calcium-Calmodulin Kinase II Mediates Digitalis-Induced Arrhythmias. *Circulation: Arrhythmia and Electrophysiology* **4,** 947-957.

Gonzalez DR, Beigi F, Treuer AV & Hare JM. (2007). Deficient ryanodine receptor S-nitrosylation increases sarcoplasmic reticulum calcium leak and arrhythmogenesis in cardiomyocytes. *Proceedings of the National Academy of Sciences* **104,** 20612-20617.

González DR, Fernández IC, Ordenes PP, Treuer AV, Eller G & Boric MP. (2008). Differential role of S-nitrosylation and the NO–cGMP–PKG pathway in cardiac contractility. *Nitric Oxide* **18,** 157-167.

Gonzalez DR, Treuer A, Sun Q-A, Stamler JS & Hare JM. (2009). S-Nitrosylation of cardiac ion channels. *Journal of Cardiovascular Pharmacology* **54,** 188.

Gordan R, Gwathmey JK & Xie L-H. (2015). Autonomic and endocrine control of cardiovascular function. *World Journal of Cardiology* **7,** 204.

Grandi E & Herren A. (2014). CaMKII-dependent regulation of cardiac Na+ homeostasis. *Frontiers in Pharmacology* **5**.

Gray CB & Brown JH. (2014). CaMKIIdelta subtypes: localization and function. *Frontiers in Pharmacology* **5**.

Grievink H, Zeltcer G, Drenger B, Berenshtein E & Chevion M. (2016). Protection by nitric oxide donors of isolated rat hearts is associated with activation of redox metabolism and ferritin accumulation. *PLoS ONE* **11,** e0159951.

Grimm M & Brown JH. (2010). β-Adrenergic receptor signaling in the heart: role of CaMKII. *Journal of Molecular and Cellular Cardiology* **48,** 322-330.

Grimm M, Ling H, Pereira L, Willeford A, Gray CBB, Erickson JR, Sarma S, Respress JL, Wehrens XHT, Bers DM & Brown JH. (2015). CaMKIIδ mediates β-adrenergic effects on RyR2 phosphorylation and SR $Ca(^{2+})$ leak and the pathophysiological response to chronic β-adrenergic stimulation. *Journal of Molecular and Cellular Cardiology* **85,** 282-291.

Grueter CE, Abiria SA, Wu Y, Anderson ME & Colbran RJ. (2008). Differential regulated interactions of calcium/calmodulin-dependent protein kinase II with isoforms of voltage-gated calcium channel β subunits. *Biochemistry* **47,** 1760-1767.

Gutierrez DA, Fernandez-Tenorio M, Ogrodnik J & Niggli E. (2013). NO-dependent CaMKII activation during β-adrenergic stimulation of cardiac muscle. *Cardiovascular Research* **100,** 392-401.

Hancock DB, Martin ER, Vance JM & Scott WK. (2008). Nitric oxide synthase genes and their interactions with environmental factors in Parkinson's disease. *Neurogenetics* **9,** 249-262.

Haynes WG, Noon JP, Walker BR & Webb DJ. (1993). Inhibition of nitric oxide synthesis increases blood pressure in healthy humans. *Journal of Hypertension* **11,** 1375-1380.

He BJ, Joiner MLA, Singh MV, Luczak ED, Swaminathan PD, Koval OM, Kutschke W, Allamargot C, Yang J, Guan X, Zimmerman K, Grumbach IM, Weiss RM, Spitz DR, Sigmund CD, Blankesteijn WM, Heymans S, Mohler PJ & Anderson ME. (2011). Oxidation of CaMKII determines cardiotoxic effects of aldosterone. *Nat Med* **17,** 1610-1618.

He F. (2011). Bradford protein assay. *Bio-protocol***,** e45-e45.

Hegyi B, Chen-Izu Y, Jian Z, Shimkunas R, Izu LT & Banyasz T. (2015). KN-93 inhibits I_{Kr} in mammalian cardiomyocytes. *Journal of Molecular and Cellular Cardiology* **89,** 173-176.

Herman AG & Moncada S. (2005). Therapeutic potential of nitric oxide donors in the prevention and treatment of atherosclerosis. *European Heart Journal* **26,** 1945-1955.

Herren AW, Bers DM & Grandi E. (2013). Post-translational modifications of the cardiac Na channel: contribution of CaMKII-dependent phosphorylation to acquired arrhythmias. *American Journal of Physiology - Heart and Circulatory Physiology* **305,** H431-445.

Hoch B, Meyer R, Hetzer R, Krause E-G & Karczewski P. (1999). Identification and Expression of δ-Isoforms of the Multifunctional Ca^{2+}/Calmodulin-Dependent Protein Kinase in Failing and Nonfailing Human Myocardium. *Circulation Research* **84,** 713-721.

Hoelz A, Nairn AC & Kuriyan J. (2003). Crystal Structure of a Tetradecameric Assembly of the Association Domain of Ca^{2+}/Calmodulin-Dependent Kinase II. *Molecular Cell* **11,** 1241-1251.

Hogan N, Casadei B & Paterson DJ. (1999). Nitric oxide donors can increase heart rate independent of autonomic activation. *Journal of Applied Physiology* **87,** 97-103.

Houston M & Hays L. (2014). Acute effects of an oral nitric oxide supplement on blood pressure, endothelial function, and vascular compliance in hypertensive patients. *The Journal of Clinical Hypertension* **16,** 524-529.

Hu H, Chiamvimonvat N, Yamagishi T & Marban E. (1997). Direct inhibition of expressed cardiac L-type Ca^{2+} channels by S-nitrosothiol nitric oxide donors. *Circulation Research* **81,** 742.

Huang X, Song Z & Qu Z. (2018). Determinants of early afterdepolarization properties in ventricular myocyte models. *PLoS Computational Biology* **14,** e1006382.

Hudmon A, Schulman H, Kim J, Maltez JM, Tsien RW & Pitt GS. (2005). CaMKII tethers to L-type Ca^{2+} channels, establishing a local and dedicated integrator of Ca^{2+} signals for facilitation. *The Journal of Cell Biology* **171,** 537-547.

Huggins CE, Bell JR, Pepe S & Delbridge LM. (2008). Benchmarking ventricular arrhythmias in the Mouse—revisiting the 'Lambeth Conventions' 20 years on. Elsevier.

Hund TJ & Mohler PJ. (2015). Role of CaMKII in cardiac arrhythmias. *Trends Cardiovasc Med* **25,** 392-397.

Ignarro LJ, Napoli C & Loscalzo J. (2002). Nitric oxide donors and cardiovascular agents modulating the bioactivity of nitric oxide: an overview. *Circulation Research* **90,** 21-28.

Irie T, Sips PY, Kai S, Kida K, Ikeda K, Hirai S, Moazzami K, Jiramongkolchai P, Bloch DB, Doulias PT, Armoundas AA, Kaneki M, Ischiropoulos H, Kranias E, Bloch KD, Stamler JS & Ichinose F. (2015). S-Nitrosylation of Calcium-Handling Proteins in Cardiac Adrenergic Signaling and Hypertrophy. *Circ Res* **117,** 793-803.

Ishida A, Kameshita I, Okuno S, Kitani T & Fujisawa H. (1995). A novel highly specific and potent inhibitor of calmodulin-dependent protein kinase II. *Biochemical and Biophysical Research Communications* **212,** 806-812.

Iwai-Kanai E, Hasegawa K, Araki M, Kakita T, Morimoto T & Sasayama S. (1999). α- and β-Adrenergic pathways differentially regulate cell type–specific apoptosis in rat cardiac myocytes. *Circulation* **100,** 305-311.

Jiang H, Torregrossa AC, Potts A, Pierini D, Aranke M, Garg HK & Bryan NS. (2014). Dietary nitrite improves insulin signaling through GLUT4 translocation. *Free Radical Biology and Medicine* **67,** 51-57.

Joca HC, Santos-Miranda A, Joviano-Santos JV, Maia-Joca RP, Brum PC, Williams GS & Cruz JS. (2020). Chronic sympathetic hyperactivity triggers electrophysiological remodeling and disrupts excitation-contraction coupling in heart. *Scientific Reports* **10,** 1-13.

Johnson CN, Pattanayek R, Potet F, Rebbeck RT, Blackwell DJ, Nikolaienko R, Sequeira V, Le Meur R, Radwański PB, Davis JP, Zima AV, Cornea RL, Damo SM, Györke S, George AL & Knollmann BC. (2019). The CaMKII inhibitor KN93-calmodulin interaction and implications for calmodulin tuning of $Na_V1.5$ and RyR2 function. *Cell Calcium* **82,** 102063.

Jones SP, Greer JJ, van Haperen R, Duncker DJ, de Crom R & Lefer DJ. (2003). Endothelial nitric oxide synthase overexpression attenuates congestive heart failure in mice. *Proceedings of the National Academy of Sciences* **100,** 4891-4896.

Kalogeris T, Baines CP, Krenz M & Korthuis RJ. (2012). Cell biology of ischemia/reperfusion injury. In *International Review of Cell and Molecular Biology*, pp. 229-317. Elsevier.

Katz SD, Khan T, Zeballos GA, Mathew L, Potharlanka P, Knecht M & Whelan J. (1999). Decreased activity of the L-arginine–nitric oxide metabolic pathway in patients with congestive heart failure. *Circulation* **99,** 2113-2117.

Kaumann A, Bartel S, Molenaar P, Sanders L, Burrell K, Vetter D, Hempel P, Karczewski P & Krause E-G. (1999). Activation of β_2-adrenergic receptors hastens relaxation and mediates phosphorylation of phospholamban, troponin I, and C-protein in ventricular myocardium from patients with terminal heart failure. *Circulation* **99,** 65-72.

Kennedy RH, Hicks KK, Brian Jr JE & Seifen E. (1994). Nitric oxide has no chronotropic effect in right atria isolated from rat heart. *European Journal of Pharmacology* **255,** 149-156.

Khalifi S, Rahimipour A, Jeddi S, Ghanbari M, Kazerouni F & Ghasemi A. (2015). Dietary nitrate improves glucose tolerance and lipid profile in an animal model of hyperglycemia. *Nitric Oxide* **44,** 24-30.

Khan M, Dhammu TS, Qiao F, Kumar P, Singh AK & Singh I. (2019). S-Nitrosoglutathione Mimics the Beneficial Activity of Endothelial Nitric Oxide Synthase-Derived Nitric Oxide in a Mouse Model of Stroke. *Journal of Stroke and Cerebrovascular Diseases* **28,** 104470.

Khan M & Singh I. (2019). Therapeutic exploitation of the S-nitrosoglutathione/S-nitrosylation mechanism for the treatment of contusion spinal cord injury. *Neural Regeneration Research* **14,** 973.

Khan SA, Skaf MW, Harrison RW, Lee K, Minhas KM, Kumar A, Fradley M, Shoukas AA, Berkowitz DE & Hare JM. (2003). Nitric Oxide Regulation of Myocardial Contractility and Calcium Cycling. *Independent Impact of Neuronal and Endothelial Nitric Oxide Synthases* **92,** 1322-1329.

Khoo MS, Li J, Singh MV, Yang Y, Kannankeril P, Wu Y, Grueter CE, Guan X, Oddis CV & Zhang R. (2006). CLINICAL PERSPECTIVE. *Circulation* **114,** 1352-1359.

Kim Y-M, Bergonia H & Lancaster Jr JR. (1995). Nitrogen oxide-induced autoprotection in isolated rat hepatocytes. *FEBS letters* **374,** 228-232.

Kirchhefer U, Schmitz W, Scholz H & Neumann J. (1999). Activity of cAMP-dependent protein kinase and Ca2+/calmodulin-dependent protein kinase in failing and nonfailing human hearts. *Cardiovascular Research* **42,** 254-261.

Kishi T. (2012). Heart failure as an autonomic nervous system dysfunction. *Journal of Cardiology* **59,** 117-122.

Kohlhaas M, Zhang T, Seidler T, Zibrova D, Dybkova N, Steen A, Wagner S, Chen L, Heller Brown J & Bers DM. (2006). Increased sarcoplasmic reticulum calcium leak but unaltered contractility by acute CaMKII overexpression in isolated rabbit cardiac myocytes. *Circulation Research* **98,** 235-244.

Kohr MJ, Sun J, Aponte A, Wang G, Gucek M, Murphy E & Steenbergen C. (2011). Simultaneous measurement of protein oxidation and S-nitrosylation during preconditioning and ischemia/reperfusion injury with resin-assisted capture. *Circulation Research* **108,** 418-426.

Kojda G & Kottenberg K. (1999). Regulation of basal myocardial function by NO. *Cardiovascular Research* **41,** 514-523.

Kojda G, Kottenberg K, Nix P, Schlüter KD, Piper HM & Noack E. (1996). Low increase in cGMP induced by organic nitrates and nitrovasodilators improves contractile response of rat ventricular myocytes. *Circulation Research* **78,** 91-101.

Kojda G, Kottenberg K & Noack E. (1997). Inhibition of nitric oxide synthase and soluble guanylate cyclase induces cardiodepressive effects in normal rat hearts. *European Journal of Pharmacology* **334,** 181-190.

Kojda G, Laursen JB, Ramasamy S, Kent JD, Kurz S, Burchfield J, Shesely EG & Harrison DG. (1999). Protein expression, vascular reactivity and soluble guanylate cyclase activity in mice lacking the endothelial cell nitric oxide synthase: contributions of NOS isoforms to blood pressure and heart rate control. *Cardiovascular Research* **42,** 206-213.

Komukai K, O-Uchi J, Morimoto S, Kawai M, Hongo K, Yoshimura M & Kurihara S. (2010). Role of Ca^{2+}/calmodulin-dependent protein kinase II in the regulation of the cardiac L-type Ca^{2+} current during endothelin-1 stimulation. *American Journal of Physiology-Heart and Circulatory Physiology* **298,** H1902-H1907.

Konorev E, Tarpey M, Joseph J, Baker J & Kalyanaraman B. (1995). S-nitrosoglutathione improves functional recovery in the isolated rat heart after cardioplegic ischemic arrest-evidence for a cardioprotective effect of nitric oxide. *Journal of Pharmacology and Experimental Therapeutics* **274,** 200-206.

Kovács M, Kiss A, Gönczi M, Miskolczi G, Seprényi G, Kaszaki J, Kohr MJ, Murphy E & Végh Á. (2015). Effect of sodium nitrite on ischaemia and reperfusion-induced arrhythmias in anaesthetized dogs: is protein S-nitrosylation involved? *PLoS ONE* **10,** e0122243.

Koval OM, Snyder JS, Wolf RM, Pavlovicz RE, Glynn P, Curran J, Leymaster ND, Dun W, Wright PJ, Cardona N, Qian L, Mitchell CC, Boyden PA, Binkley PF, Li C, Anderson ME, Mohler PJ & Hund TJ. (2012). Ca^{2+}/calmodulin-dependent protein

kinase II-based regulation of voltage-gated Na^+ channel in cardiac disease. *Circulation* **126,** 2084-2094.

Kreusser MM & Backs J. (2014). Integrated mechanisms of CaMKII-dependent ventricular remodeling. *Frontiers in Pharmacology* **5,** 36.

Kreusser MM, Lehmann LH, Keranov S, Hoting M-O, Oehl U, Kohlhaas M, Reil J-C, Neumann K, Schneider MD & Hill JA. (2014). Cardiac CaM Kinase II genes δ and γ contribute to adverse remodeling but redundantly inhibit calcineurin-induced myocardial hypertrophy. *Circulation* **130,** 1262-1273.

Kruzliak P, Pechanova O & Kara T. (2014). New perspectives of nitric oxide donors in cardiac arrest and cardiopulmonary resuscitation treatment. *Heart Failure Reviews* **19,** 383-390.

Kubota I, Han X, Opel DJ, Zhao Y-Y, Baliga R, Huang P, Fishman MC, Shannon RP, Michel T & Kelly RA. (2000). Increased susceptibility to development of triggered activity in myocytes from mice with targeted disruption of endothelial nitric oxide synthase. *Journal of Molecular and Cellular Cardiology* **32,** 1239-1248.

Landstrom AP, Dobrev D & Wehrens XH. (2017). Calcium signaling and cardiac arrhythmias. *Circulation Research* **120,** 1969-1993.

Layland J, Li JM & Shah AM. (2002). Role of cyclic GMP-dependent protein kinase in the contractile response to exogenous nitric oxide in rat cardiac myocytes. *The Journal of Physiology* **540,** 457-467.

Lebek S, Plößl A, Baier M, Mustroph J, Tarnowski D, Lücht C, Schopka S, Flörchinger B, Schmid C & Zausig Y. (2018). The novel CaMKII inhibitor GS-680 reduces diastolic SR Ca leak and prevents CaMKII-dependent pro-arrhythmic activity. *Journal of Molecular and Cellular Cardiology* **118,** 159-168.

Lefer DJ, Jones SP, Girod WG, Baines A, Grisham MB, Cockrell AS, Huang PL & Scalia R. (1999). Leukocyte-endothelial cell interactions in nitric oxide synthase-deficient mice. *American Journal of Physiology-Heart and Circulatory Physiology* **276,** H1943-H1950.

Li C, Cai X, Sun H, Bai T, Zheng X, Zhou XW, Chen X, Gill DL, Li J & Tang XD. (2011). The δA isoform of calmodulin kinase II mediates pathological cardiac hypertrophy by interfering with the HDAC4-MEF2 signaling pathway. *Biochemical and Biophysical Research Communications* **409,** 125-130.

Li J, Gao Q, Wang S, Kang Z, Li Z, Lei S, Sun X, Zhao M, Chen X & Jiao G. (2020). Sustained increased CaMKII phosphorylation is involved in the impaired

regression of isoproterenol-induced cardiac hypertrophy in rats. *Journal of Pharmacological Sciences* **144,** 30-42.

Li L, Chu G, Kranias EG & Bers DM. (1998). Cardiac myocyte calcium transport in phospholamban knockout mouse: relaxation and endogenous CaMKII effects. *American Journal of Physiology-Heart and Circulatory Physiology* **274,** H1335-H1347.

Li L, Satoh H, Ginsburg KS & Bers DM. (1997). The effect of Ca^{2+}–calmodulin-dependent protein kinase II on cardiac excitation–contraction coupling in ferret ventricular myocytes. *The Journal of Physiology* **501,** 17-31.

Liao R, Podesser BK & Lim CC. (2012). The continuing evolution of the Langendorff and ejecting murine heart: new advances in cardiac phenotyping. *American Journal of Physiology-Heart and Circulatory Physiology* **303,** H156-H167.

Lim Y-C, Budin SB, Othman F, Latip J & Zainalabidin S. (2017). Roselle polyphenols exert potent negative inotropic effects via modulation of intracellular calcium regulatory channels in isolated rat heart. *Cardiovascular Toxicology* **17,** 251-259.

Lima B, Forrester MT, Hess DT & Stamler JS. (2010). S-nitrosylation in cardiovascular signaling. *Circulation Research* **106,** 633-646.

Lindberg T. (2017). Arrhythmias in older people: Focusing on atrial fibrillation. *Epidemiology and Impact on Daily Life [dissertation] Lund: Lund University*.

Ling H, Zhang T, Pereira L, Means CK, Cheng H, Gu Y, Dalton ND, Peterson KL, Chen J & Bers D. (2009). Requirement for Ca^{2+}/calmodulin–dependent kinase II in the transition from pressure overload–induced cardiac hypertrophy to heart failure in mice. *The Journal of Clinical Investigation* **119,** 1230-1240.

Ling WC, Mustafa MR, Vanhoutte PM & Murugan DD. (2018). Chronic administration of sodium nitrite prevents hypertension and protects arterial endothelial function by reducing oxidative stress in angiotensin II-infused mice. *Vascular Pharmacology* **102,** 11-20.

Liu Y, Chenhai Xia, Rutao Wang, Jinglong Zhang, Tao Yin, Yanzuo Ma, and Ling Tao. (2017). The opposite effects of nitric oxide donor, S-nitrosoglutathione, on myocardial ischaemia/reperfusion injury in diabetic and non-diabetic mice. *Clinical and Experimental Pharmacology and Physiology* **44,** 854-861.

Liu Y-H, Xu J, Yang X-P, Yang F, Shesely E & Carretero OA. (2002). Effect of ACE inhibitors and angiotensin II type 1 receptor antagonists on endothelial NO synthase knockout mice with heart failure. *Hypertension* **39,** 375-381.

Luo M, Guan X, Luczak ED, Lang D, Kutschke W, Gao Z, Yang J, Glynn P, Sossalla S, Swaminathan PD, Weiss RM, Yang B, Rokita AG, Maier LS, Efimov IR, Hund TJ & Anderson ME. (2013). Diabetes increases mortality after myocardial infarction by oxidizing CaMKII. *The Journal of Clinical Investigation* **123,** 1262-1274.

Maier LS, Zhang T, Chen L, DeSantiago J, Brown JH & Bers DM. (2003). Transgenic CaMKIIδC overexpression uniquely alters cardiac myocyte Ca^{2+} handling: reduced SR Ca^{2+} load and activated SR Ca^{2+} release. *Circulation Research* **92,** 904-911.

Marionneau C, Lichti CF, Lindenbaum P, Charpentier F, Nerbonne JM, Townsend RR & Mérot J. (2012). Mass spectrometry-based identification of native cardiac $Na_V1.5$ channel α subunit phosphorylation sites. *Journal of Proteome Research* **11,** 5994-6007.

Marquez J, Lee SR, Kim N & Han J. (2016). Post-Translational Modifications of Cardiac Mitochondrial Proteins in Cardiovascular Disease: Not Lost in Translation. *Korean Circulation Journal* **46,** 1-12.

Massion P & Balligand JL. (2003). Modulation of cardiac contraction, relaxation and rate by the endothelial nitric oxide synthase (eNOS): lessons from genetically modified mice. *The Journal of Physiology* **546,** 63-75.

Massion P, Feron O, Dessy C & Balligand J-L. (2003). Nitric oxide and cardiac function: ten years after, and continuing. *Circulation Research* **93,** 388-398.

Massoudy P, Zahler S, Freyholdt T, Henze R, Barankay A, Becker BF, Braun SL & Meisner H. (2000). Sodium nitroprusside in patients with compromised left ventricular function undergoing coronary bypass: reduction of cardiac proinflammatory substances. *The Journal of Thoracic and Cardiovascular Surgery* **119,** 566-574.

Mayer P, Möhlig M, Schatz H & Pfeiffer A. (1994). Additional isoforms of multifunctional calcium/calmodulin-dependent protein kinase II in rat heart tissue. *Biochemical Journal* **298,** 757.

Mesubi OO, Rokita AG, Abrol N, Wu Y, Chen B, Wang Q, Granger JM, Tucker-Bartley A, Luczak ED & Murphy KR. (2020). O-GlcNAcylation, oxidation and CaMKII contribute to atrial fibrillation in type 1 and type 2 diabetes by distinct mechanisms. *BioRxiv*.

Ministry of Health. (2017). Mortality and Demographic Data 2015 (provisional) [updated: January 2018].

Mohamed BA, Elkenani M, Jakubiczka-Smorag J, Buchholz E, Koszewa S, Lbik D, Schnelle M, Hasenfuss G & Toischer K. (2019). Genetic deletion of calcium/calmodulin-dependent protein kinase type II delta does not mitigate adverse myocardial remodeling in volume-overloaded hearts. *Scientific Reports* **9,** 1-11.

Mohamed BA, Hartmann N, Tirilomis P, Sekeres K, Li W, Neef S, Richter C, Zeisberg EM, Kattner L, Didié M, Guan K, Schmitto JD, Lehnart SE, Luther S, Voigt N, Seidler T, Sossalla S, Hasenfuss G & Toischer K. (2018). Sarcoplasmic reticulum calcium leak contributes to arrhythmia but not to heart failure progression. *Science Translational Medicine* **10,** eaan0724.

Mohan P, Brutsaert DL, Paulus WJ & Sys SU. (1996). Myocardial contractile response to nitric oxide and cGMP. *Circulation* **93,** 1223-1229.

Mohler PJ & Hund TJ. (2011). Role for CaMKII in cardiovascular health, disease, and arrhythmia. *Heart rhythm : The Official Journal of the Heart Rhythm Society* **8,** 142-144.

Mohri M, Egashira K, Tagawa T, Kuga T, Tagawa H, Harasawa Y, Shimokawa H & Takeshita A. (1997). Basal release of nitric oxide is decreased in the coronary circulation in patients with heart failure. *Hypertension* **30,** 50-56.

Mollova MY, Katus HA & Backs J. (2015). Regulation of CaMKII signaling in cardiovascular disease. *Front Pharmacol* **6**.

Moosavi M, Abbasi L, Zarifkar A & Rastegar K. (2014). The role of nitric oxide in spatial memory stages, hippocampal ERK and CaMKII phosphorylation. *Pharmacology Biochemistry and Behavior* **122,** 164-172.

Müller-Strahl G, Kottenberg K, Zimmer HG, Noack E & Kojda G. (2000). Inhibition of nitric oxide synthase augments the positive inotropic effect of nitric oxide donors in the rat heart. *The Journal of Physiology* **522,** 311-320.

Murphy E, Kohr M, Sun J, Nguyen T & Steenbergen C. (2012). S-nitrosylation: a radical way to protect the heart. *Journal of Molecular and Cellular Cardiology* **52,** 568-577.

Musialek P, Lei M, Brown HF, Paterson DJ & Casadei B. (1997). Nitric oxide can increase heart rate by stimulating the hyperpolarization-activated inward current, If. *Circulation Research* **81,** 60-68.

Neef S, Sag CM, Daut M, Bäumer H, Grefe C, El-Armouche A, DeSantiago J, Pereira L, Bers DM & Backs J. (2013). While systolic cardiomyocyte function is preserved, diastolic myocyte function and recovery from acidosis are impaired in CaMKIIδ-KO mice. *Journal of Molecular and Cellular Cardiology* **59,** 107-116.

Neef S, Steffens A, Pellicena P, Mustroph J, Lebek S, Ort KR, Schulman H & Maier LS. (2018). Improvement of cardiomyocyte function by a novel pyrimidine-based CaMKII-inhibitor. *Journal of molecular and cellular cardiology* **115,** 73-81.

Pabla R & Curtis MJ. (1995). Effects of NO modulation on cardiac arrhythmias in the rat isolated heart. *Circulation Research* **77,** 984-992.

Paolocci N, Ekelund UE, Isoda T, Ozaki M, Vandegaer K, Georgakopoulos D, Harrison RW, Kass DA & Hare JM. (2000). cGMP-independent inotropic effects of nitric oxide and peroxynitrite donors: potential role for nitrosylation. *American Journal of Physiology-Heart and Circulatory Physiology* **279,** H1982-H1988.

Peng W, Zhang Y, Zheng M, Cheng H, Zhu W, Cao C-M & Xiao R-P. (2010). Cardioprotection by CaMKII-δB is mediated by phosphorylation of heat shock factor 1 and subsequent expression of inducible heat shock protein 70. *Circulation Research* **106,** 102-110.

Pereira L, Bare DJ, Galice S, Shannon TR & Bers DM. (2017). β-Adrenergic induced SR Ca^{2+} leak is mediated by an Epac-NOS pathway. *Journal of Molecular and Cellular Cardiology* **108,** 8-16.

Petroff MV, Mundiña-Weilenmann C, Vittone L, de Cingolani GC & Mattiazzi A. (1994). Lusitropic effects of α-and β-adrenergic stimulation in amphibian heart. *Molecular and Cellular Biochemistry* **141,** 87-95.

Phillips L, Toledo AH, Lopez-Neblina F, Anaya-Prado R & Toledo-Pereyra LH. (2009). Nitric oxide mechanism of protection in ischemia and reperfusion injury. *Journal of Investigative Surgery* **22,** 46-55.

Poluektov YM, Petrushanko IY, Undrovinas NA, Lakunina VA, Khapchaev AY, Kapelko VI, Abramov AA, Lakomkin VL, Novikov MS & Shirinsky VP. (2019). Glutathione-related substances maintain cardiomyocyte contractile function in hypoxic conditions. *Scientific Reports* **9,** 1-12.

Preckel B, Kojda G, Schlack W, Ebel D, Kottenberg K, Noack E & Thämer V. (1997). Inotropic effects of glyceryl trinitrate and spontaneous NO donors in the dog heart. *Circulation* **96,** 2675-2682.

Prendergast BD, Sagach VF & Shah AM. (1997). Basal release of nitric oxide augments the Frank-Starling response in the isolated heart. *Circulation* **96,** 1320-1329.

Purohit A, Rokita AG, Guan X, Chen B, Koval OM, Voigt N, Neef S, Sowa T, Gao Z, Luczak ED, Stefansdottir H, Behunin AC, Li N, El-Accaoui RN, Yang B, Swaminathan PD, Weiss RM, Wehrens XHT, Song L-S, Dobrev D, Maier LS &

Anderson ME. (2013). Oxidized Ca^{2+}/Calmodulin-Dependent Protein Kinase II Triggers Atrial Fibrillation. *Circulation* **128,** 1748-1757.

Qu Z, Xie L-H, Olcese R, Karagueuzian HS, Chen P-S, Garfinkel A & Weiss JN. (2013). Early afterdepolarizations in cardiac myocytes: beyond reduced repolarization reserve. *Cardiovascular Research* **99,** 6-15.

Rajtik T, Goncalvesova E, Varga ZV, Leszek P, Kusmierczyk M, Hulman M, Kyselovic J, Ferdinandy P & Adameova A. (2017). Posttranslational modifications of calcium/calmodulin-dependent protein kinase IIδ and its downstream signaling in human failing hearts. *American Journal of Translational Research* **9,** 3573.

Rakhit A, Maguire CT, Wakimoto H, Gehrmann J, Li GK, Kelly RA, Michel T & Berul CI. (2001). In Vivo Electrophysiologic Studies in Endothelial Nitric Oxide Synthase (eNOS)-Deficient Mice. *Journal of Cardiovascular Electrophysiology* **12,** 1295-1301.

Ramanathan C, Ghanem RN, Jia P, Ryu K & Rudy Y. (2004). Noninvasive electrocardiographic imaging for cardiac electrophysiology and arrhythmia. *Nature Medicine* **10,** 422-428.

Rassaf T, Poll LW, Brouzos P, Lauer T, Totzeck M, Kleinbongard P, Gharini P, Andersen K, Schulz R & Heusch G. (2006). Positive effects of nitric oxide on left ventricular function in humans. *European Heart Journal* **27,** 1699-1705.

Rastaldo R, Pagliaro P, Cappello S, Penna C, Mancardi D, Westerhof N & Losano G. (2007). Nitric oxide and cardiac function. *Life Sciences* **81,** 779-793.

Rauhala P, Andoh T & Chiueh CC. (2005). Neuroprotective properties of nitric oxide and S-nitrosoglutathione. *Toxicology and Applied Pharmacology* **207,** 91-95.

Recchia FA, McConnell PI, Bernstein RD, Vogel TR, Xu X & Hintze TH. (1998). Reduced nitric oxide production and altered myocardial metabolism during the decompensation of pacing-induced heart failure in the conscious dog. *Circulation Research* **83,** 969-979.

Rees D, Ben-Ishay D & Moncada S. (1996). Nitric oxide and the regulation of blood pressure in the hypertension-prone and hypertension-resistant Sabra rat. *Hypertension* **28,** 367-371.

Reichelt ME, Willems L, Hack BA, Peart JN & Headrick JP. (2009). Cardiac and coronary function in the Langendorff-perfused mouse heart model. *Experimental Physiology* **94,** 54-70.

Respress JL, van Oort RJ, Li N, Rolim N, Dixit SS, deAlmeida A, Voigt N, Lawrence WS, Skapura DG & Skårdal K. (2012). Role of RyR2 phosphorylation at S2814 during heart failure progression. *Circulation Research* **110,** 1474-1483.

Rodriguez-Peña A, Garcia-Criado FJ, Eleno N, Arevalo M & Lopez-Novoa JM. (2004). Intrarenal Administration of Molsidomine, a Molecule Releasing Nitric Oxide, Reduces Renal Ischemia-Reperfusion Injury in Rats. *American Journal of Transplantation* **4,** 1605-1613.

Rokita AG & Anderson ME. (2012). New therapeutic targets in cardiology: arrhythmias and Ca^{2+}/calmodulin-dependent kinase II (CaMKII). *Circulation* **126,** 2125-2139.

Ruschitzka FT, Wenger RH, Stallmach T, Quaschning T, De Wit C, Wagner K, Labugger R, Kelm M, Noll G & Rülicke T. (2000). Nitric oxide prevents cardiovascular disease and determines survival in polyglobulic mice overexpressing erythropoietin. *Proceedings of the National Academy of Sciences* **97,** 11609-11613.

Sag CM, Wadsack DP, Khabbazzadeh S, Abesser M, Grefe C, Neumann K, Opiela MK, Backs J, Olson EN, Brown JH, Neef S, Maier SKG & Maier LS. (2009). Calcium/Calmodulin-Dependent Protein Kinase II Contributes to Cardiac Arrhythmogenesis in Heart Failure. *Circulation Heart Failure* **2,** 664-675.

Said M, Becerra R, Palomeque J, Rinaldi G, Kaetzel M, Diaz-Sylvester P, Copello JA, Dedman JR, Mundiña-Weilenmann C & Vittone L. (2008). Increased intracellular Ca2+ and SR Ca2+ load contribute to arrhythmias after acidosis in rat heart. Role of Ca2+/calmodulin-dependent protein kinase II. *American Journal of Physiology-Heart and Circulatory Physiology* **295,** H1669-H1683.

Sander M, Chavoshan B & Victor RG. (1999). A large blood pressure–raising effect of nitric oxide synthase inhibition in humans. *Hypertension* **33,** 937-942.

Sandirasegarane L & Diamond J. (1999). The nitric oxide donors, SNAP and DEA/NO, exert a negative inotropic effect in rat cardiomyocytes which is independent of cyclic GMP elevation. *Journal of Molecular and Cellular Cardiology* **31,** 799-808.

Sarkar D, Vallance P, Amirmansour C & Harding SE. (2000). Positive inotropic effects of NO donors in isolated guinea-pig and human cardiomyocytes independent of NO species and cyclic nucleotides. *Cardiovascular Research* **48,** 430-439.

Shesely EG, Maeda N, Kim H-S, Desai KM, Krege JH, Laubach VE, Sherman PA, Sessa WC & Smithies O. (1996). Elevated blood pressures in mice lacking endothelial nitric oxide synthase. *Proceedings of the National Academy of Sciences* **93,** 13176-13181.

Shiferaw Y, Aistrup GL & Wasserstrom JA. (2012). Intracellular Ca^{2+} waves, afterdepolarizations, and triggered arrhythmias. Oxford University Press.

Shizukuda Y, Buttrick PM, Geenen DL, Borczuk AC, Kitsis RN & Sonnenblick EH. (1998). β-Adrenergic stimulation causes cardiocyte apoptosis: influence of tachycardia and hypertrophy. *American Journal of Physiology-Heart and Circulatory Physiology* **275,** H961-H968.

Simonian MH & Smith JA. (2006). Spectrophotometric and colorimetric determination of protein concentration. *Current Protocols in Molecular Biology* **76,** 10.11. 11-10.11 A. 19.

Sindler AL, Cox-York K, Reese L, Bryan NS, Seals DR & Gentile CL. (2015). Oral nitrite therapy improves vascular function in diabetic mice. *Diabetes and Vascular Disease Research* **12,** 221-224.

Sommese L, Valverde CA, Blanco P, Castro MC, Rueda OV, Kaetzel M, Dedman J, Anderson ME, Mattiazzi A & Palomeque J. (2016). Ryanodine receptor phosphorylation by CaMKII promotes spontaneous Ca^{2+} release events in a rodent model of early stage diabetes: the arrhythmogenic substrate. *International journal of cardiology* **202,** 394-406.

Strijdom H, Chamane N & Lochner A. (2009). Nitric oxide in the cardiovascular system: a simple molecule with complex actions. *Cardiovascular Journal of Africa* **20,** 303.

Sun J, Morgan M, Shen R-F, Steenbergen C & Murphy E. (2007). Preconditioning results in S-nitrosylation of proteins involved in regulation of mitochondrial energetics and calcium transport. *Circulation Research* **101,** 1155-1163.

Sun J, Picht E, Ginsburg KS, Bers DM, Steenbergen C & Murphy E. (2006a). Hypercontractile female hearts exhibit increased S-nitrosylation of the L-type Ca^{2+} channel α1 subunit and reduced ischemia/reperfusion injury. *Circulation Research* **98,** 403-411.

Sun J, Steenbergen C & Murphy E. (2006b). S-nitrosylation: NO-related redox signaling to protect against oxidative stress. *Antioxidants & redox signaling* **8,** 1693-1705.

Sun J, Yamaguchi N, Xu L, Eu JP, Stamler JS & Meissner G. (2008). Regulation of the cardiac muscle ryanodine receptor by O2 tension and S-nitrosoglutathione. *Biochemistry* **47,** 13985-13990.

Tessier S, Karczewski P, Krause E-G, Pansard Y, Acar C, Lang-Lazdunski M, Mercadier J-J & Hatem SN. (1999). Regulation of the transient outward K^+ current by Ca^{2+}/calmodulin-dependent protein kinases II in human atrial myocytes. *Circulation Research* **85,** 810-819.

Timmins JM, Ozcan L, Seimon TA, Li G, Malagelada C, Backs J, Backs T, Bassel-Duby R, Olson EN & Anderson ME. (2009). Calcium/calmodulin-dependent protein kinase II links ER stress with Fas and mitochondrial apoptosis pathways. *The Journal of Clinical Investigation* **119,** 2925-2941.

Toischer K, Hartmann N, Wagner S, Fischer TH, Herting J, Danner BC, Sag CM, Hund TJ, Mohler PJ, Belardinelli L, Hasenfuss G, Maier LS & Sossalla S. (2013). Role of late sodium current as a potential arrhythmogenic mechanism in the progression of pressure-induced heart disease. *Journal of Molecular and Cellular Cardiology* **61,** 111-122.

Triposkiadis F, Karayannis G, Giamouzis G, Skoularigis J, Louridas G & Butler J. (2009). The Sympathetic Nervous System in Heart Failure: Physiology, Pathophysiology, and Clinical Implications. *Journal of the American College of Cardiology* **54,** 1747-1762.

Tse G. (2016). Mechanisms of cardiac arrhythmias. *Journal of Arrhythmia* **32,** 75-81.

Vielma AZ, León L, Fernández IC, González DR & Boric MP. (2016). Nitric oxide synthase 1 modulates basal and β-adrenergic-stimulated contractility by rapid and reversible redox-dependent S-nitrosylation of the heart. *PLoS ONE* **11,** e0160813.

Vila-Petroff M, Salas MA, Said M, Valverde CA, Sapia L, Portiansky E, Hajjar RJ, Kranias EG, Mundiña-Weilenmann C & Mattiazzi A. (2007). CaMKII inhibition protects against necrosis and apoptosis in irreversible ischemia–reperfusion injury. *Cardiovascular Research* **73,** 689-698.

Vila-Petroff MG, Younes A, Egan J, Lakatta EG & Sollott SJ. (1999). Activation of distinct cAMP-dependent and cGMP-dependent pathways by nitric oxide in cardiac myocytes. *Circulation Research* **84,** 1020-1031.

Vincent KP, McCulloch AD & Edwards AG. (2014). Toward a hierarchy of mechanisms in CaMKII-mediated arrhythmia. *Frontiers in Pharmacology* **5,** 110.

Wagner S, Dybkova N, Rasenack ECL, Jacobshagen C, Fabritz L, Kirchhof P, Maier SKG, Zhang T, Hasenfuss G, Brown JH, Bers DM & Maier LS. (2006). Ca^{2+}/calmodulin-dependent protein kinase II regulates cardiac Na^{+} channels. *The Journal of Clinical Investigation* **116,** 3127-3138.

Wang H, Kohr MJ, Wheeler DG & Ziolo MT. (2008). Endothelial nitric oxide synthase decreases β-adrenergic responsiveness via inhibition of the L-type Ca^{2+} current. *American Journal of Physiology-Heart and Circulatory Physiology* **294,** H1473-H1480.

Wang H, Viatchenko-Karpinski S, Sun J, Györke I, Benkusky NA, Kohr MJ, Valdivia HH, Murphy E, Györke S & Ziolo MT. (2010). Regulation of myocyte contraction via neuronal nitric oxide synthase: role of ryanodine receptor S-nitrosylation. *The Journal of Physiology* **588,** 2905-2917.

Wang Q, Quick AP, Cao S, Reynolds J, Chiang DY, Beavers D, Li N, Wang G, Rodney GG & Anderson ME. (2018). Oxidized CaMKII (Ca^{2+}/Calmodulin-Dependent Protein Kinase II) Is Essential for Ventricular Arrhythmia in a Mouse Model of Duchenne Muscular Dystrophy. *Circulation: Arrhythmia and Electrophysiology* **11,** e005682.

Wang W, Zhu W, Wang S, Yang D, Crow MT, Xiao R-P & Cheng H. (2004). Sustained β1-adrenergic stimulation modulates cardiac contractility by Ca^{2+}/calmodulin kinase signaling pathway. *Circulation Research* **95,** 798-806.

Wang Y-g, Wagner MB, Joyner RW & Kumar R. (2000). cGMP-dependent protein kinase mediates stimulation of L-type calcium current by cGMP in rabbit atrial cells. *Cardiovascular Research* **48,** 310-322.

Webb A, Bond R, McLean P, Uppal R, Benjamin N & Ahluwalia A. (2004). Reduction of nitrite to nitric oxide during ischemia protects against myocardial ischemia–reperfusion damage. *Proceedings of the National Academy of Sciences* **101,** 13683-13688.

Wehrens XHT, Lehnart SE, Reiken SR & Marks AR. (2004). Ca^{2+}/Calmodulin-Dependent Protein Kinase II Phosphorylation Regulates the Cardiac Ryanodine Receptor. *Circulation Research* **94,** e61-e70.

Weiss JN, Garfinkel A, Karagueuzian HS, Chen P-S & Qu Z. (2010). Early afterdepolarizations and cardiac arrhythmias. *Heart rhythm : The Official Journal of the Heart Rhythm Society* **7,** 1891-1899.

Wiemer G, Itter G, Malinski T & Linz W. (2001). Decreased nitric oxide availability in normotensive and hypertensive rats with failing hearts after myocardial infarction. *Hypertension* **38,** 1367-1371.

Wildhirt SM, Weismueller S, Schulze C, Conrad N, Kornberg A & Reichart B. (1999). Inducible nitric oxide synthase activation after ischemia/reperfusion contributes to myocardial dysfunction and extent of infarct size in rabbits: evidence for a late phase of nitric oxide-mediated reperfusion injury. *Cardiovascular Research* **43,** 698-711.

Wink DA, Miranda KM, Espey MG, Pluta RM, Hewett SJ, Colton C, Vitek M, Feelisch M & Grisham MB. (2001). Mechanisms of the antioxidant effects of nitric oxide. *Antioxidants and redox signaling* **3,** 203-213.

Wit AL & Boyden PA. (2007). Triggered activity and atrial fibrillation. *Heart rhythm : the official journal of the Heart Rhythm Society* **4,** S17-S23.

Wong MH, Samal AB, Lee M, Vlach J, Novikov N, Niedziela-Majka A, Feng JY, Koltun DO, Brendza KM & Kwon HJ. (2019). The KN-93 molecule inhibits calcium/calmodulin-dependent protein kinase II (CaMKII) activity by binding to Ca^{2+}/CaM. *Journal of molecular biology* **431,** 1440-1459.

World Health Organisation. (2017). Cardiovascular Disease Fact Sheet: World Health Organisation [online]

Wu Y & Anderson ME. (2014). CaMKII in sinoatrial node physiology and dysfunction. *Frontiers in Pharmacology* **5,** 48.

Wu Y, Gao Z, Chen B, Koval OM, Singh MV, Guan X, Hund TJ, Kutschke W, Sarma S & Grumbach IM. (2009). Calmodulin kinase II is required for fight or flight sinoatrial node physiology. *Proceedings of the National Academy of Sciences* **106,** 5972-5977.

Wu Y, MacMillan LB, McNeill RB, Colbran RJ & Anderson ME. (1999). CaM kinase augments cardiac L-type Ca^{2+} current: a cellular mechanism for long QT arrhythmias. *American Journal of Physiology-Heart and Circulatory Physiology* **276,** H2168-H2178.

Wu Y, Temple J, Zhang R, Dzhura I, Zhang W, Trimble R, Roden DM, Passier R, Olson EN, Colbran RJ & Anderson ME. (2002). Calmodulin Kinase II and Arrhythmias in a Mouse Model of Cardiac Hypertrophy. *Circulation* **106,** 1288-1293.

Wyeth RP, Temma K, Seifen E & Kennedy RH. (1996). Negative inotropic actions of nitric oxide require high closes in rat cardiac muscle. *Pflügers Archiv-European Journal of Physiology* **432,** 678-684.

Xiao R-P, Cheng H, Lederer W, Suzuki T & Lakatta EG. (1994). Dual regulation of Ca^{2+}/calmodulin-dependent kinase II activity by membrane voltage and by calcium influx. *Proceedings of the National Academy of Sciences* **91,** 9659-9663.

Xu L, Lai D, Cheng J, Lim HJ, Keskanokwong T, Backs J, Olson EN & Wang Y. (2010). Alterations of L-type calcium current and cardiac function in CaMKIIδ knockout mice. *Circulation Research* **107,** 398-407.

Xu X, Yang D, Ding J-H, Wang W, Chu P-H, Dalton ND, Wang H-Y, Bermingham Jr JR, Ye Z & Liu F. (2005). ASF/SF2-regulated CaMKIIδ alternative splicing temporally reprograms excitation-contraction coupling in cardiac muscle. *Cell* **120,** 59-72.

Yang XP, Liu YH, Rhaleb NE, Kurihara N, Kim HE & Carretero OA. (1999). Echocardiographic assessment of cardiac function in conscious and anesthetized mice. *Am J Physiol* **277**.

Yaniv Y, Spurgeon HA, Ziman BD & Lakatta EG. (2013). Ca $^{2+}$/calmodulin-dependent protein kinase II (CaMKII) activity and sinoatrial nodal pacemaker cell energetics. *PLoS ONE* **8,** e57079.

Yoo BS, Lemaire A, Mangmool S, Wolf MJ, Curcio A, Mao L & Rockman HA. (2009). β(1)-Adrenergic receptors stimulate cardiac contractility and CaMKII activation in vivo and enhance cardiac dysfunction following myocardial infarction. *American Journal of Physiology - Heart and Circulatory Physiology* **297,** H1377-1386.

Zhang P. (2017). CaMKII: The molecular villain that aggravates cardiovascular disease. *Experimental and therapeutic medicine* **13,** 815-820.

Zhang R, Khoo MSC, Wu Y, Yang Y, Grueter CE, Ni G, Price Jr EE, Thiel W, Guatimosim S, Song L-S, Madu EC, Shah AN, Vishnivetskaya TA, Atkinson JB, Gurevich VV, Salama G, Lederer WJ, Colbran RJ & Anderson ME. (2005). Calmodulin kinase II inhibition protects against structural heart disease. *Nature Medicine* **11,** 409.

Zhang T & Brown JH. (2004). Role of Ca^{2+}/calmodulin-dependent protein kinase II in cardiac hypertrophy and heart failure. *Cardiovascular Research* **63,** 476-486.

Zhang T, Guo T, Mishra S, Dalton ND, Kranias EG, Peterson KL, Bers DM & Brown JH. (2010). Phospholamban ablation rescues SR Ca^{2+} handling but exacerbates cardiac dysfunction in CaMKIIδC transgenic mice. *Circulation research* **106,** 354.

Zhang T, Johnson EN, Gu Y, Morissette MR, Sah VP, Gigena MS, Belke DD, Dillmann WH, Rogers TB & Schulman H. (2002). The cardiac-specific nuclear δB isoform of Ca^{2+}/calmodulin-dependent protein kinase II induces hypertrophy and dilated cardiomyopathy associated with increased protein phosphatase 2A activity. *Journal of Biological Chemistry* **277,** 1261-1267.

Zhang T, Maier LS, Dalton ND, Miyamoto S, Ross J, Bers DM & Brown JH. (2003). The δC Isoform of CaMKII Is Activated in Cardiac Hypertrophy and Induces Dilated Cardiomyopathy and Heart Failure. *Circulation Research* **92,** 912-919.

Zhang X, Cardosa L, Broderick M, Fein H & Davies IR. (2000). Novel calibration method for nitric oxide microsensors by stoichiometrical generation of nitric oxide from SNAP. *Electroanalysis: An International Journal Devoted to Fundamental and Practical Aspects of Electroanalysis* **12,** 425-428.

Zhong P, Quan D, Huang Y & Huang H. (2017). CaMKII Activation Promotes Cardiac Electrical Remodeling and Increases the Susceptibility to Arrhythmia Induction in High-fat Diet–Fed Mice With Hyperlipidemia Conditions. *Journal of Cardiovascular Pharmacology* **70,** 245-254.

Zima AV, Bovo E, Bers DM & Blatter LA. (2010). Ca^{2+} spark-dependent and-independent sarcoplasmic reticulum Ca^{2+} leak in normal and failing rabbit ventricular myocytes. *The Journal of Physiology* **588,** 4743-4757.

Ziolo MT & Bers DM. (2003). The real estate of NOS signaling: location, location, location. *Am Heart Assoc.*

Ziolo MT, Kohr MJ & Wang H. (2008). Nitric oxide signaling and the regulation of myocardial function. *Journal of Molecular and Cellular Cardiology* **45,** 625-632.

Ziolo MT, Maier LS, Piacentino III V, Bossuyt J, Houser SR & Bers DM. (2004). Myocyte nitric oxide synthase 2 contributes to blunted β-adrenergic response in failing human hearts by decreasing Ca^{2+} transients. *Circulation* **109,** 1886-1891.

APPENDIX A

A.1 Nitric oxide analysis

The nitric oxide (NO) donors used were S-nitroso-N-acetylpenicillamine (SNAP, Sapphire biosciences) and S-nitrosoglutathione (GSNO, Cayman chemicals). The Apollo 1000 Free Radical analyser and the ISO-NOPF100 NO microsensor (1 mm) (WPI Florida, USA) were used to measure the concentration of NO released in water samples and plasma. Data was recorded using Powerlab 2/25 (ADInstruments, Australia).

The microsensor was immersed in copper (II) chloride solution (0.1 M $CuCl_2$, Merck Millipore) to allow for polarisation. The aim of polarisation was to create a potential difference between recording electrode relative to the reference electrode, which is amplified and recorded when NO is oxidised on the membrane of the probe (Bradley & Steinert, 2015). Poise voltage on the Apollo 100 was set at 865 mV, the current range was < 8000nA and the data was sampled at 5 Hz. The polarisation time for the microsensor was 1 – 2 hrs until a stable baseline was observed. The probe was immersed in a beaker containing 20 ml of $CuCl_2$ (0.1 M) and a stirring bar for continuous mixing of the solution. For calibration, a stock solution of 100 µM SNAP and 44 µM EDTA (Merck Millipore) was prepared on the day. Once the microsensor was polarised and the voltage reached a stable baseline, different volumes (64 µl, 128 µl, 256 µl, 512 µl, 1024 µl) of SNAP + EDTA solution was added to the CuCl2 solution. After each volume was added, the voltage increased and reached a plateau, before the decay, the next volume of SNAP was added. The concentration of NO released from the SNAP solution was calculated considering the conversion efficiency of SNAP to NO in $CuCl_2$ which is 60% (Bradley & Steinert, 2015). For every mole of SNAP, 0.6 mole of NO is liberated. A calibration curve of probe voltage against NO concentration was constructed.

A.

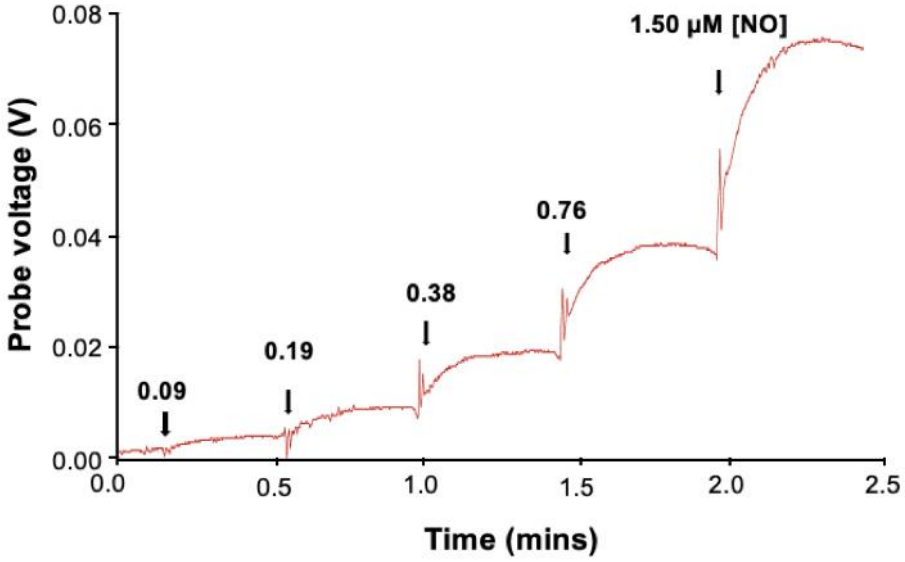

B.

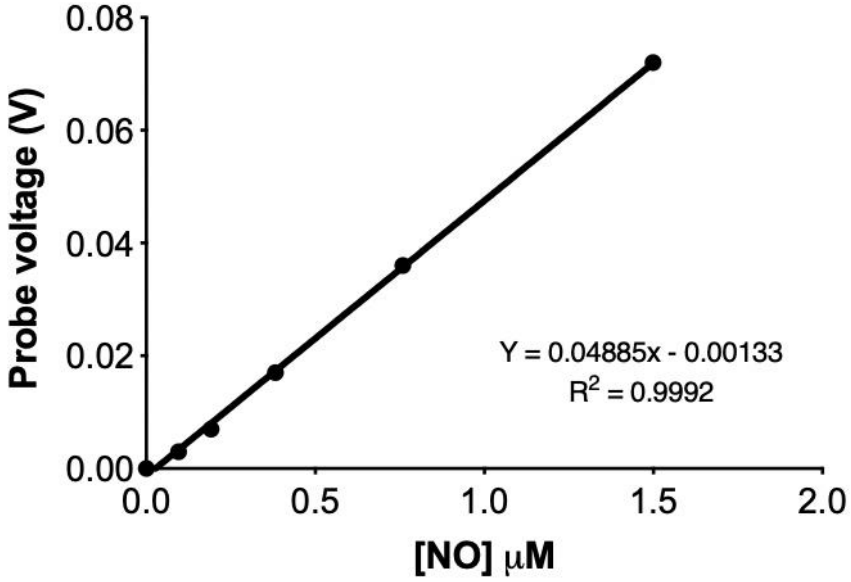

Figure A.1 Calibration of NO microsensor with SNAP (a) Representative graph showing change in probe voltage with addition of SNAP in increasing concentrations. (b) Calibration curve for SNAP calibration.

A.2 Measurement of nitric oxide release from GSNO

After calibration, the micro sensor was immersed in a beaker containing Krebs-Henseleit (KH) buffer. A baseline current measurement was taken. Thereafter, increasing concentrations of GSNO (100 µM, 150 µM, 600 µM, 1600 µM) were added to the buffer. Change in current was recorded and used to calculate the concentration of NO released from GSNO. The presence of NO was confirmed using a NO scavenger, 100 µM 2-(4-carboxyphenyl)-4,4,5,5-tetramethylimidazoline-1-oxyl-3-oxide potassium salt (c-PTIO, Cayman Chemical Company). These experiments were repeated three times (Sample 1, Sample 2, Sample 3) and performed at room temperature.

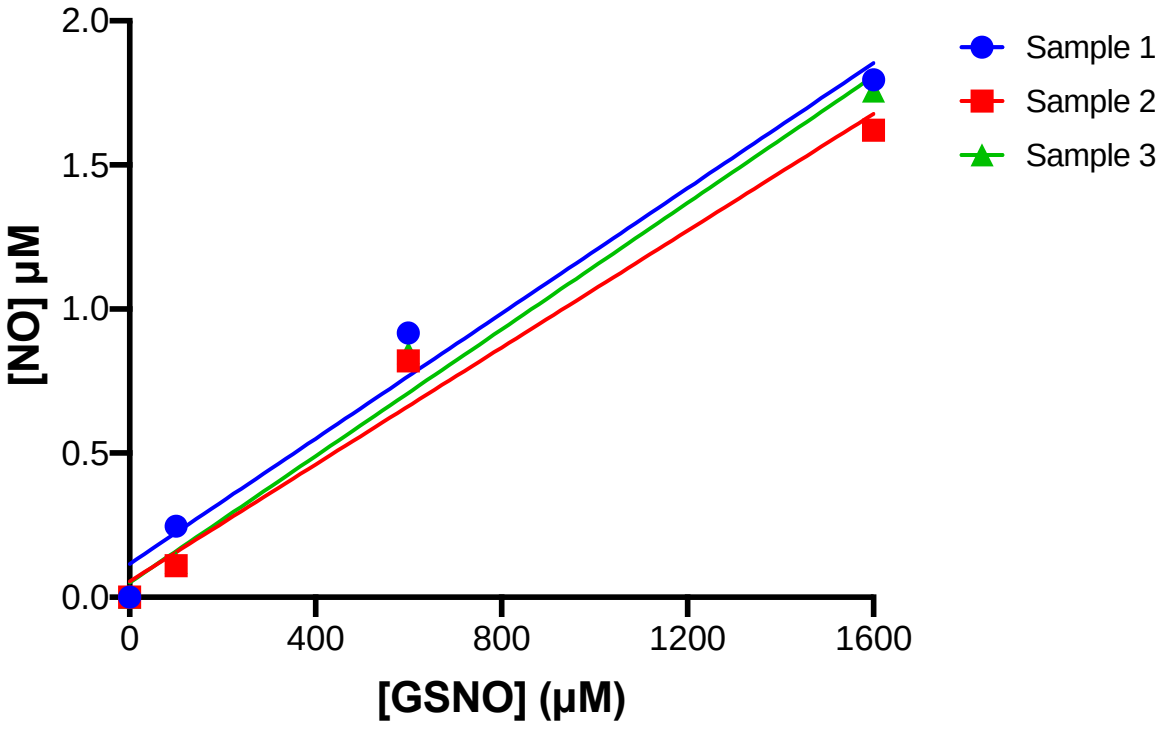

Figure A.2 Measurement of NO release in buffer. Results were obtained from three samples and NO release in KH buffer was consistent across all samples. Two-way ANOVA (uncorrected Fisher's LSD test) was used to compare between groups.

A.3 Contraction and relaxation in WT and KO hearts with acute GSNO treatment

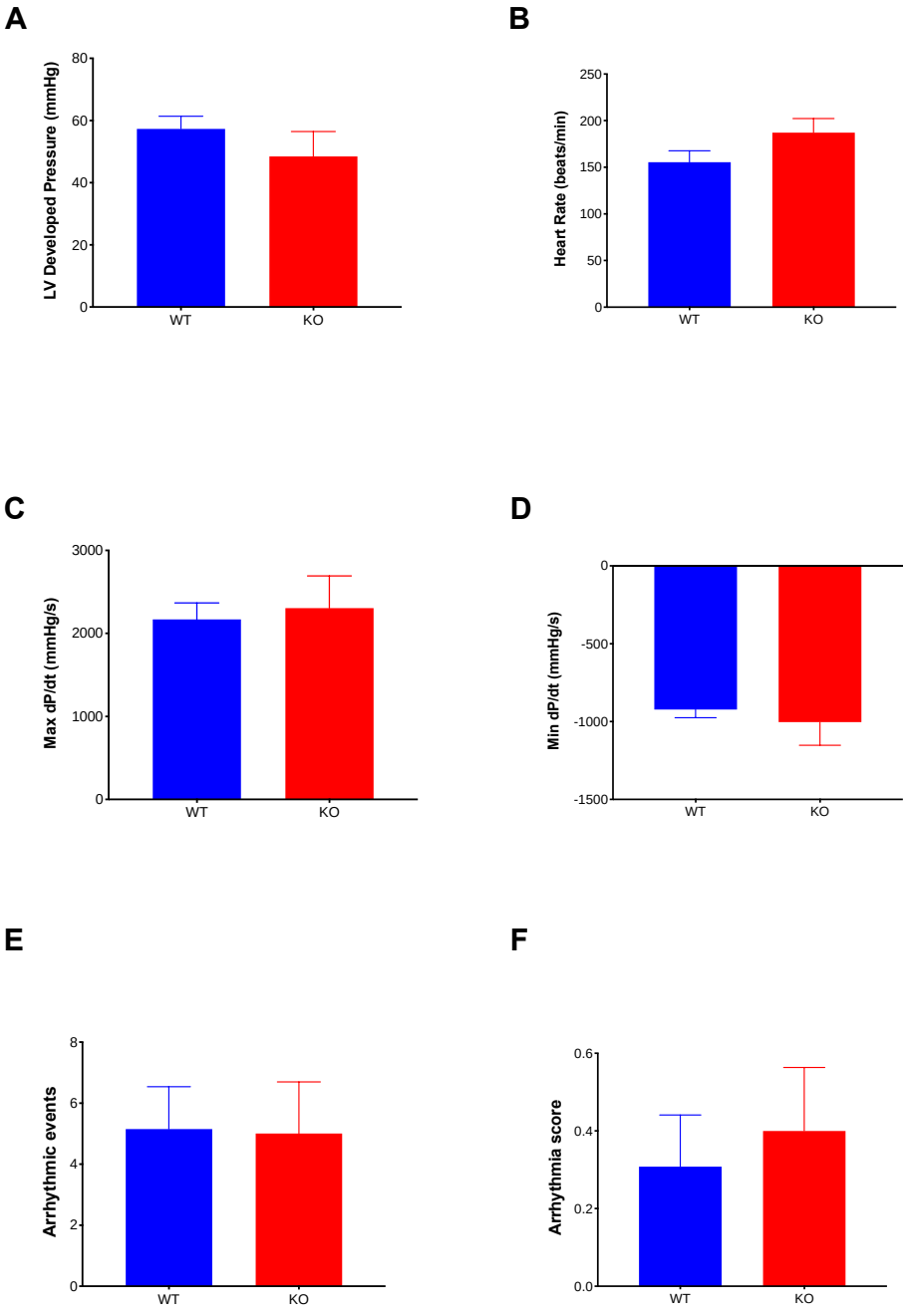

Figure A.3 Basal contraction and relaxation parameters in WT and KO mouse hearts prior to acute GSNO treatment A, LV Developed Pressure. B, Heart rate. C, Maximum rate of contraction (Max dP/dt). D, Minimum rate of relaxation (Min dP/dt). E, Arrhythmic events F, Arrhythmia scores. Data are means ± SEM. WT, blue bar, n = 13 hearts; KO, red bar, n = 10 hearts. Two-way ANOVA (uncorrected Fisher's LSD test) was used to compare between animal models.

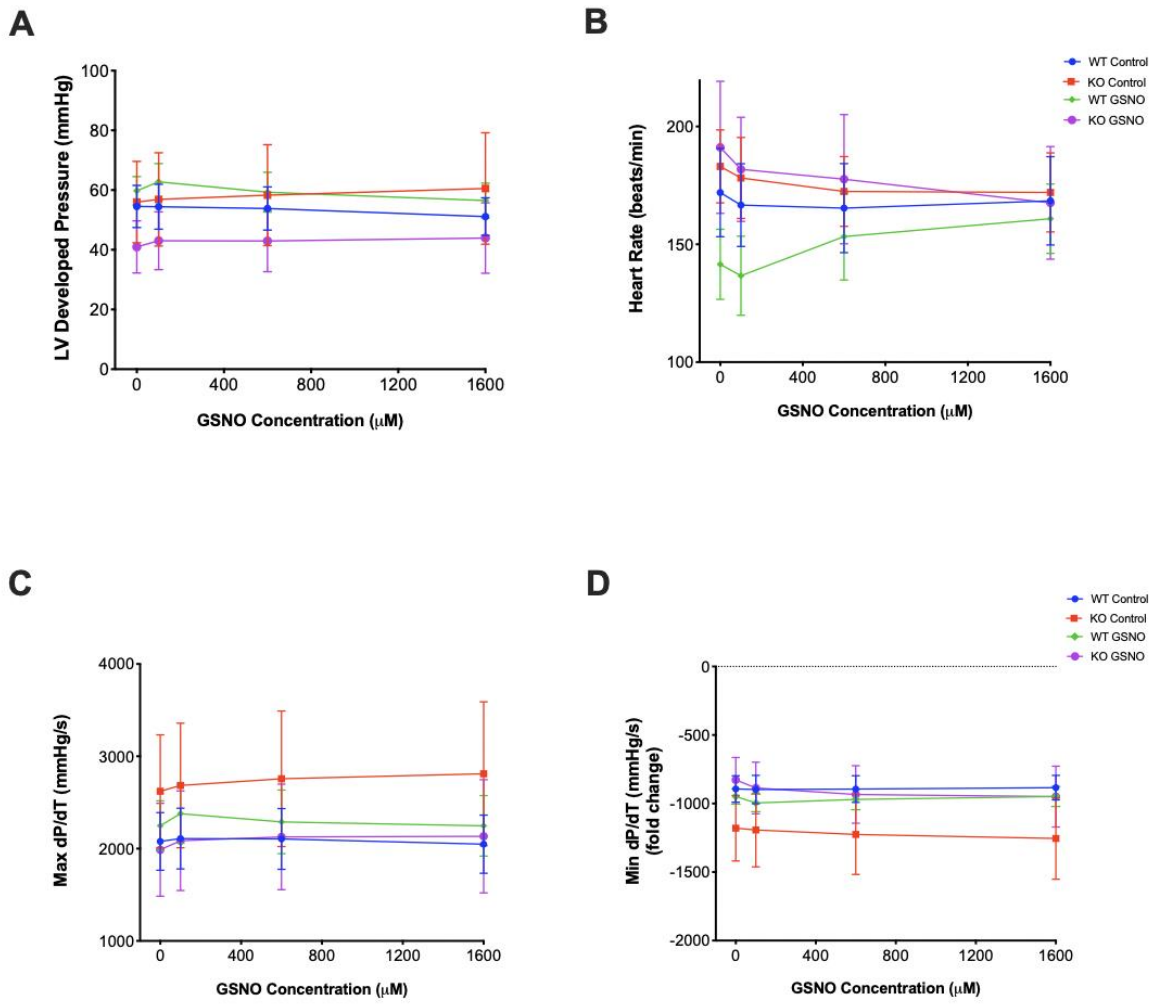

Figure A.4 Contraction and relaxation parameters in WT and KO mouse hearts with GSNO treatment (100 µM, 600 µM and 1600 µM) A, LV developed pressure B, Heart rate, C, Max dP/dt, D, Min dP/dt. Data are means ± SEM. WT Control, blue line, n = 6 hearts; WT GSNO, green, line, n = 7 hearts; KO Control, red line, n = 5 hearts; KO GSNO, purple line, n = 5 hearts. Two-way ANOVA (uncorrected Fisher's LSD test) was used to compare between groups.

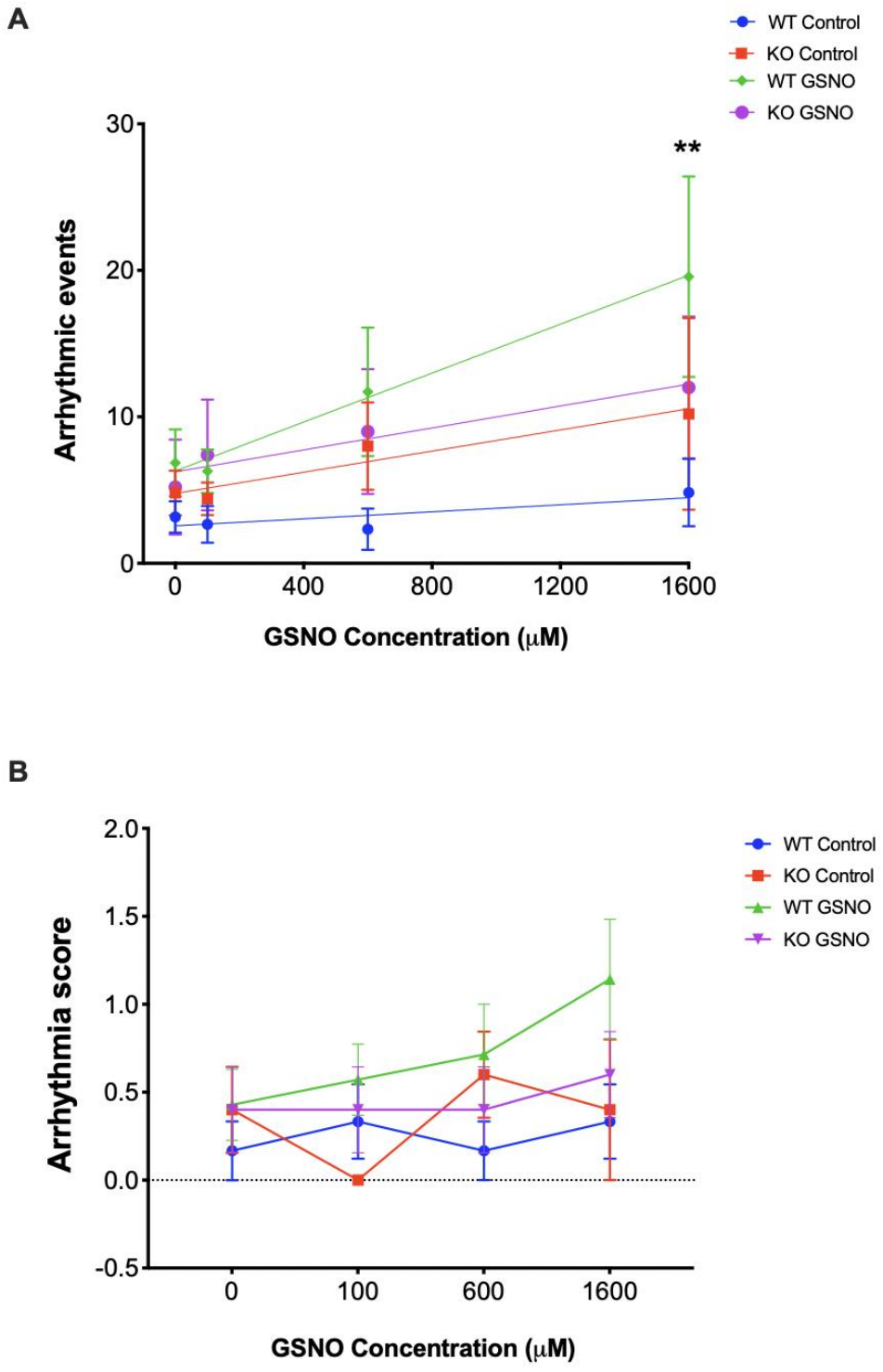

Figure A.5 Arrhythmias during GSNO treatment (100 µM, 600 µM and 1600 µM) in in WT and KO mouse hearts A, Arrhythmic events B, Arrhythmia scores. Data are means ± SEM. WT Control, blue line, n = 6 hearts; WT GSNO, green, line, n = 7 hearts; KO Control, red line, n = 5 hearts; KO GSNO, purple line, n = 5 hearts. Two-way ANOVA (uncorrected Fisher's LSD test) was used to compare between groups. ** = P < 0.01 treatment effect (0 vs 1600 µM)

A.4 Coronary flow in WT and KO hearts during acute GSNO treatment

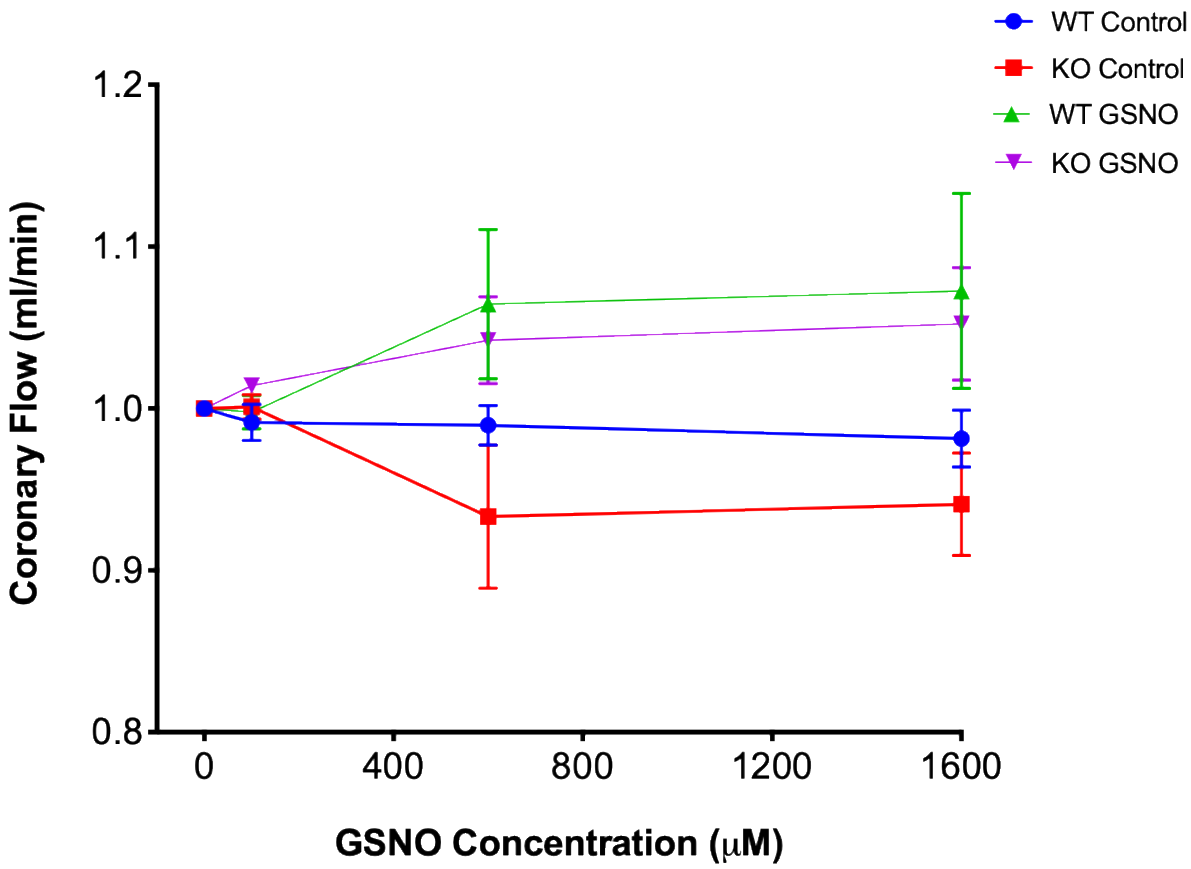

Figure A.6 Coronary flow during GSNO treatment (100 µM, 600 µM and 1600 µM) in WT and KO mouse hearts. Data are means ± SEM. WT Control, blue line, n = 6 hearts; WT GSNO, green, line, n = 7 hearts; KO Control, red line, n = 5 hearts; KO GSNO, purple line, n = 5 hearts. Two-way ANOVA (uncorrected Fisher's LSD test) was used to compare between groups.

APPENDIX B

B.1 NO stability in drinking water

Water bottles were filled with ~ 300 ml of tap water and different concentrations of GSNO. The bottles were wrapped with aluminium foil to protect from light and placed in the animal cage. 50 ml of each concentration was obtained from each bottle after 1 hour and further after 24 and 48 hours, to measure the stability of GSNO in water.

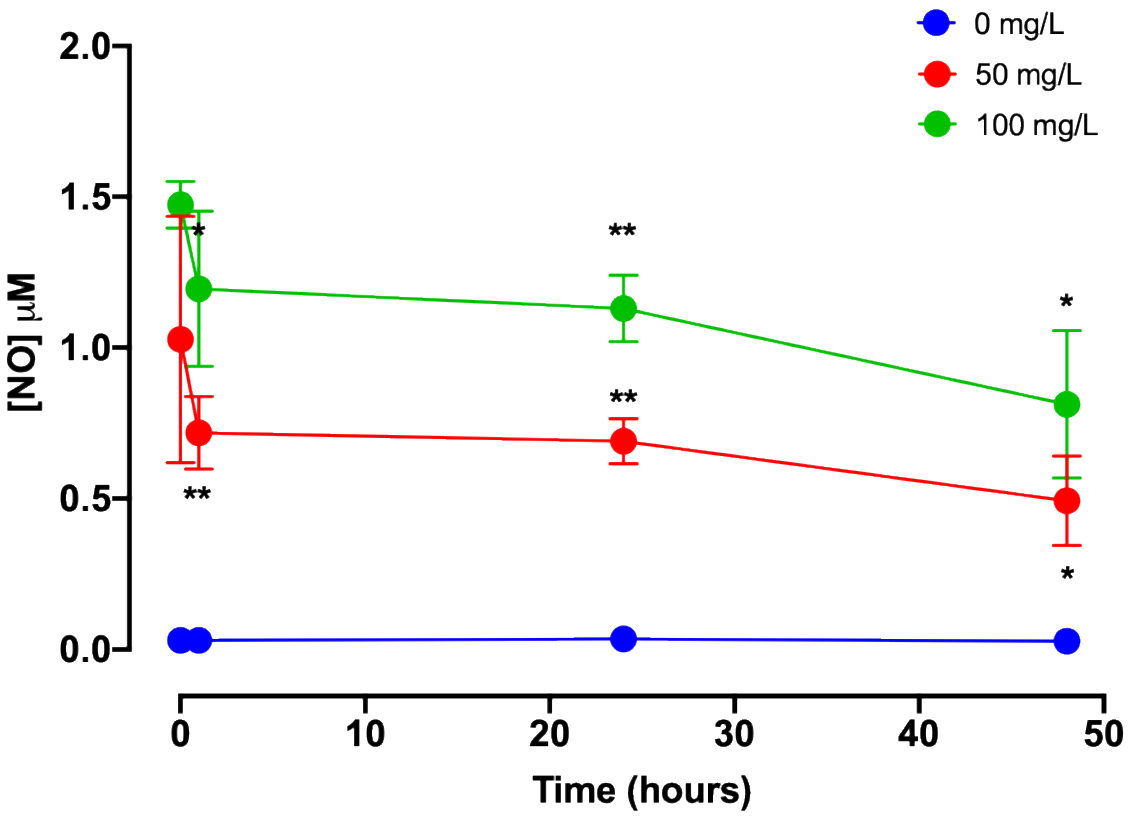

Figure B.1 NO stability in water after 1, 24 and 48 hours. Results were obtained from three samples and NO release in KH buffer was consistent across all samples. Two-way ANOVA (uncorrected Fisher's LSD test) was used to compare between groups. * = $P < 0.05$, ** = $P < 0.01$ concentration effect (vs 0 mg/L)

B.2 Detection of NO levels in plasma

To assess NO levels, plasma was obtained after 5 weeks of GSNO treatment. It was expected that NO supplementation in drinking water would increase the level of plasma NO in the treatment groups. Blood samples (400 – 500 µl) were obtained from the chest cavity of the mouse after heart excision using a 1 ml syringe previously washed with heparin and collected in a tube. Plasma was obtained after centrifugation at 3000 rcf at 4oC for 10 min by removing 200 – 250 µl of the supernatant using a Pasteur pipette. NO content was detected using a NO sensor which was placed into the tube containing the plasma. The current depicting the presence of NO was recorded for 30 minutes and the peak value was obtained and calculated as NO concentration, according to the manufacturer's instructions.

There was no significant change in plasma NO levels between WT and KO ($p = 0.23$). In addition, there was no significant change between the control or treatment group after 5 weeks of chronic GSNO treatment ($p = 0.55$) (Figure 4.6B). This result suggested that there was no increase in circulating NO in plasma as expected despite the 5-week GSNO treatment.

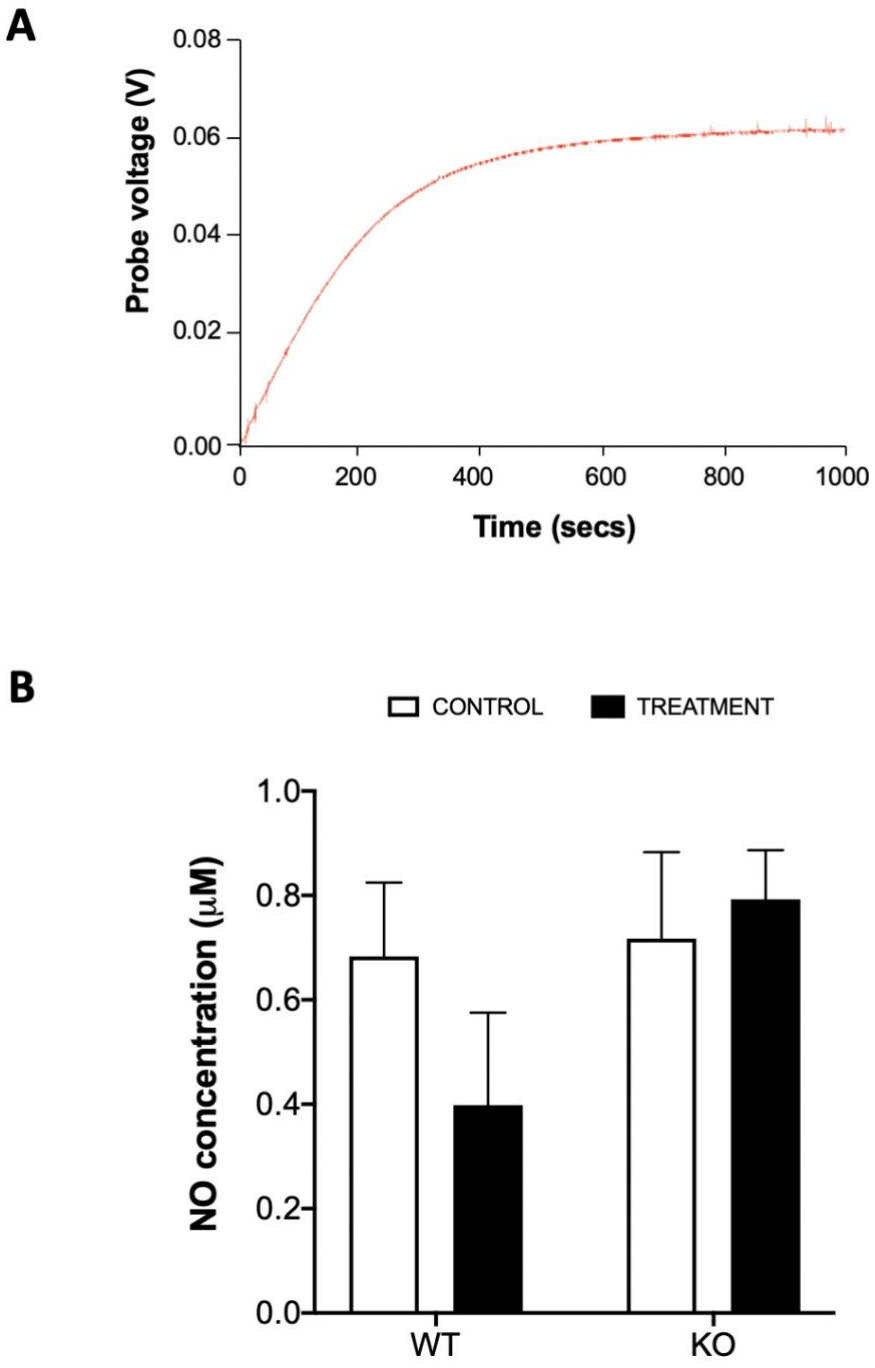

Figure B.2 Quantification of Plasma NO levels with GSNO pretreatment A, Representative trace of NO release in plasma B, NO concentration in WT and KO mice treated with GSNO. Data are means ± SEM. WT control, white bar, n = 4 hearts; WT treatment, black bar, n = 3 hearts; KO control, white bar, n = 7 hearts KO treatment, black bar, n = 4 hearts. Two-way ANOVA (uncorrected Fisher's LSD test) was used to compare between animal models and treatment effect.

B.3 Contraction and relaxation in WT and KO hearts with chronic GSNO treatment

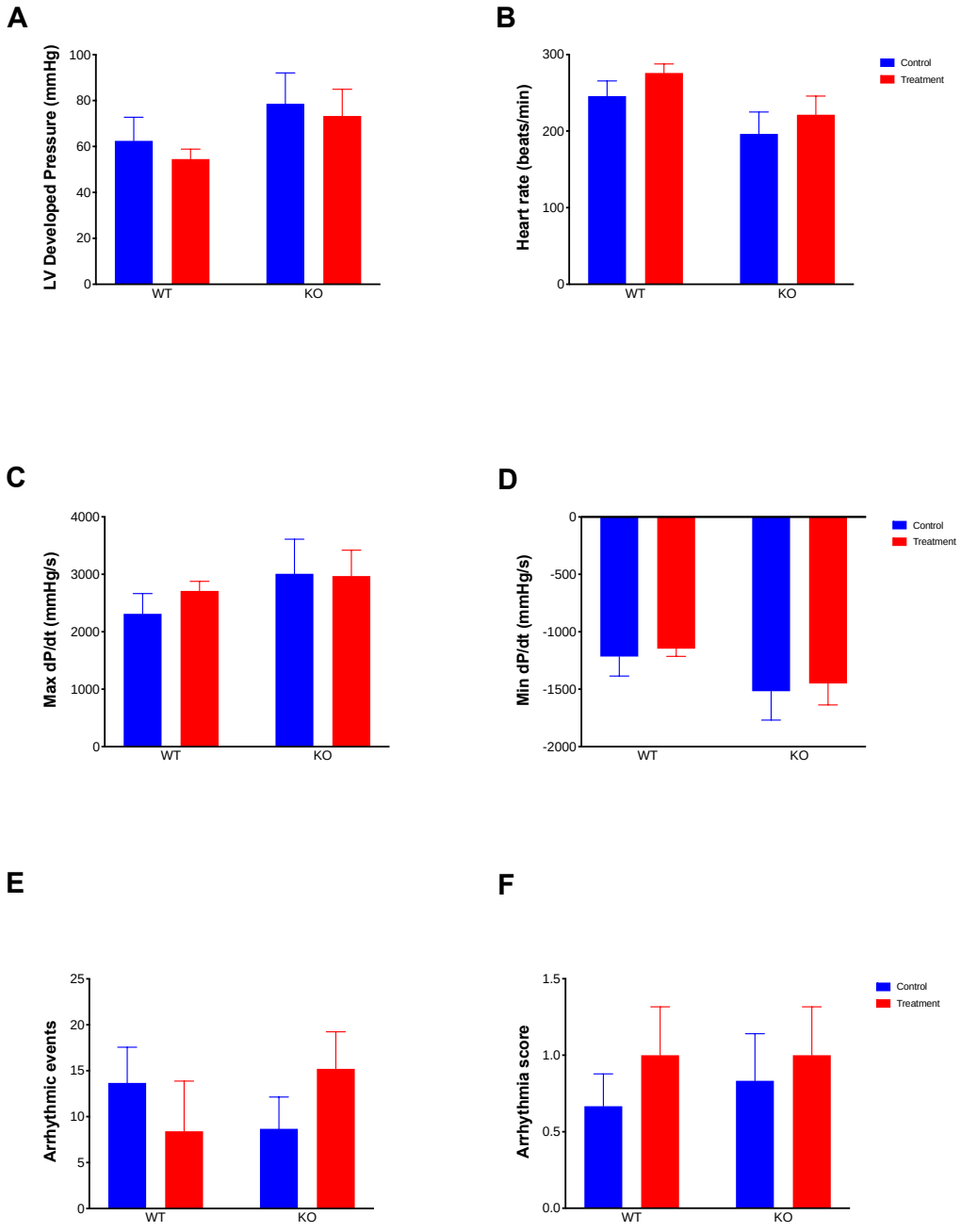

Figure B.3 Basal contraction and relaxation parameters in WT and KO mouse hearts after in vivo GSNO supplementation A, LV Developed Pressure. B, Heart rate. C, Maximum rate of contraction (Max dP/dt). D, Minimum rate of relaxation (Min dP/dt). E, Arrhythmic events F, Arrhythmia scores. Data are means ± SEM. WT Control, n = 6 hearts; WT GSNO, n = 5 hearts; KO Control, n = 6 hearts; KO GSNO, n = 5 hearts. Two-way ANOVA (uncorrected Fisher's LSD test) was used to compare between groups.

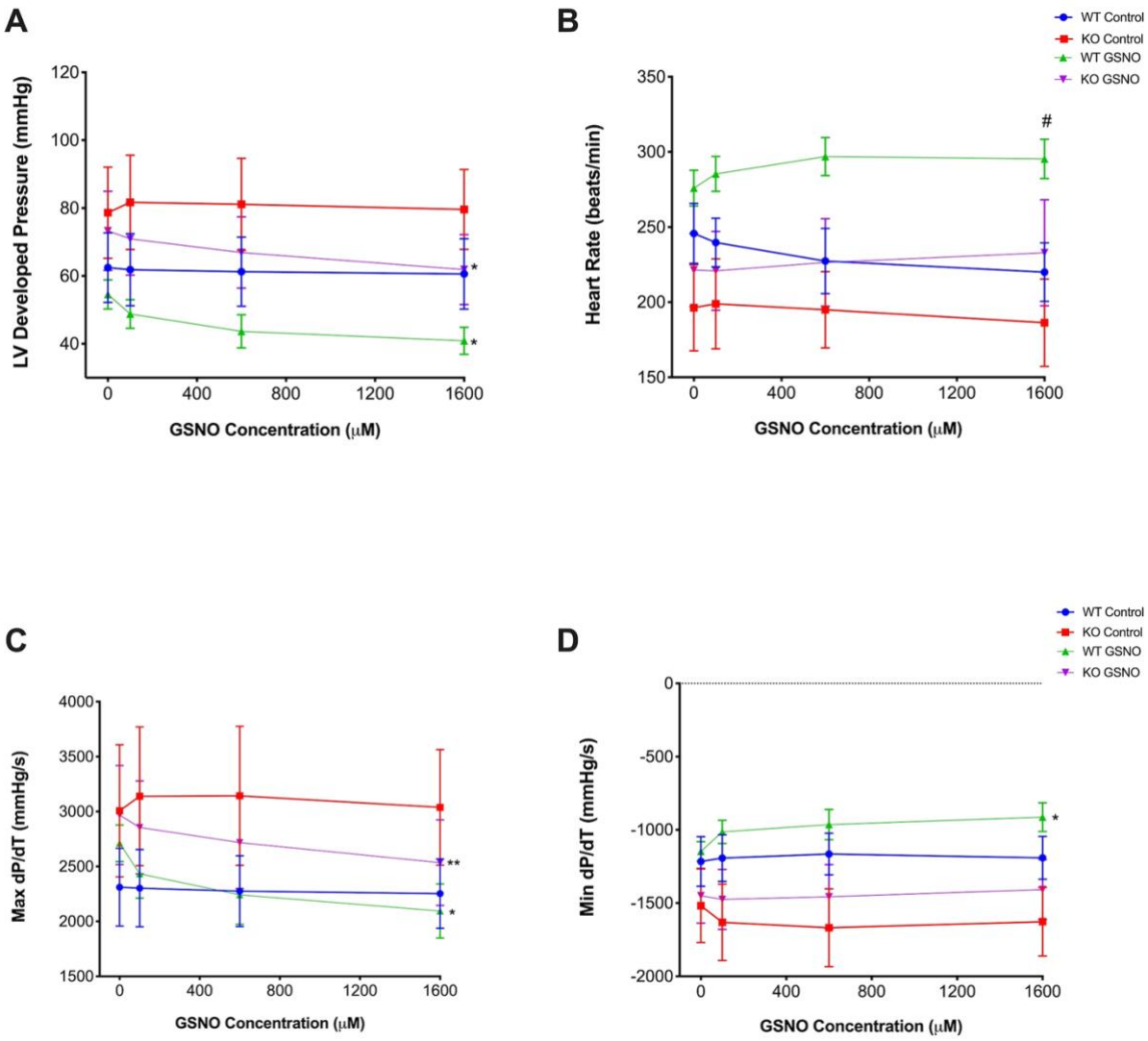

Figure B.4 Contraction and relaxation parameters in WT and KO mouse hearts during ex vivo chronic GSNO treatment (100 µM, 600 µM and 1600 µM) A, LV developed pressure B, Heart rate, C, Max dP/dt, D, Min dP/dt. Data are means ± SEM. WT Control, blue line, n = 6 hearts; WT GSNO, green, line, n = 5 hearts; KO Control, red line, n = 6 hearts; KO GSNO, purple line, n = 5 hearts. Two-way ANOVA (uncorrected Fisher's LSD test) was used to compare between groups. * = P<0.05, ** = P<0.01, treatment effect (0 vs 1600 µM).

B.4 Arrhythmias in WT and KO hearts with chronic GSNO treatment

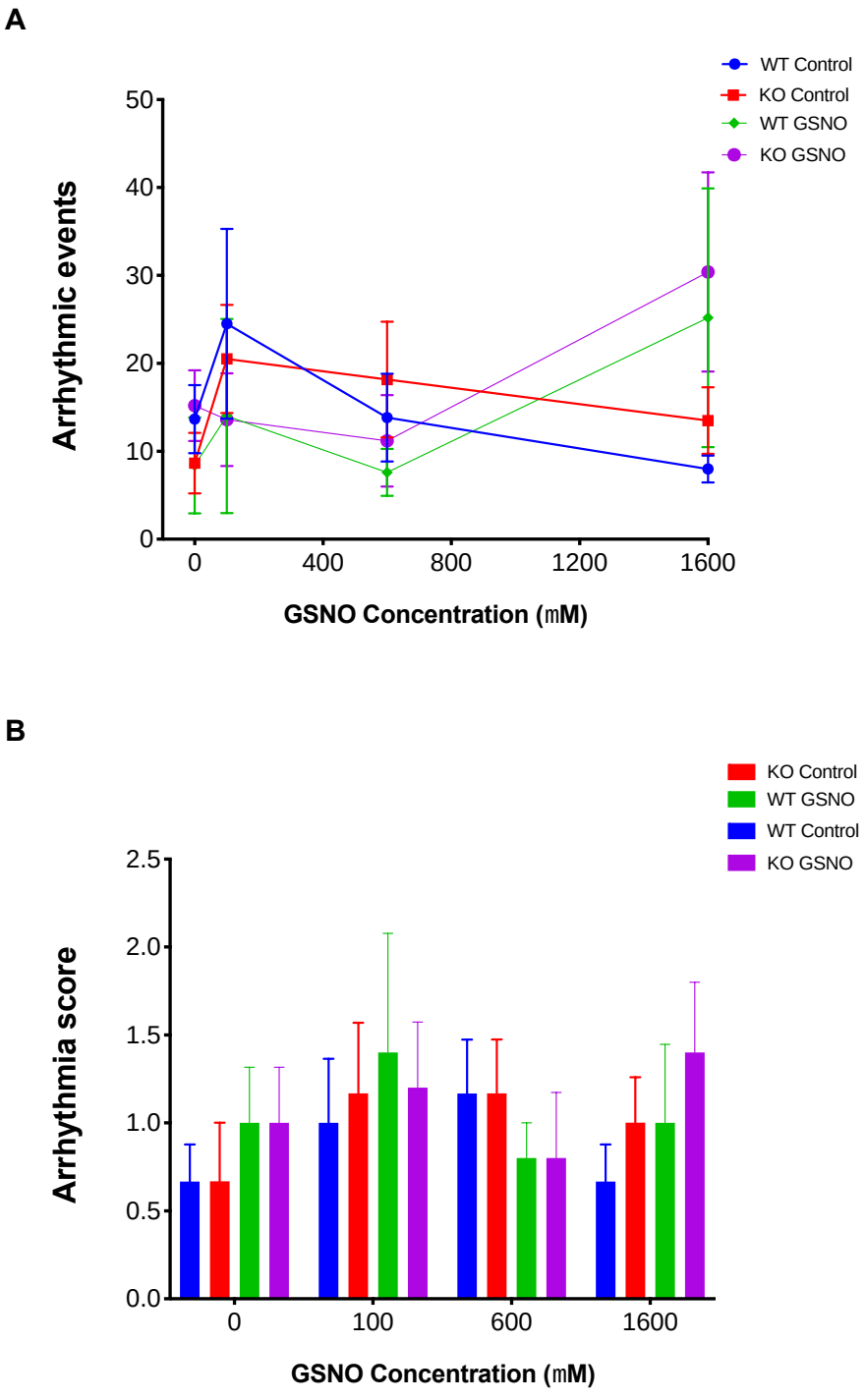

Figure B.5 Arrhythmias during GSNO treatment (100 µM, 600 µM and 1600 µM) in WT and KO mouse hearts A, Arrhythmic events B, Arrhythmia scores. Data are means ± SEM. WT Control, blue line, n = 6 hearts; WT GSNO, green, line, n = 6 hearts; KO Control, red line, n = 6 hearts; KO GSNO, purple line, n = 5 hearts. Two-way ANOVA (uncorrected Fisher's LSD test) was used to compare between groups.

B.5 Coronary flow in WT and KO hearts during chronic GSNO treatment

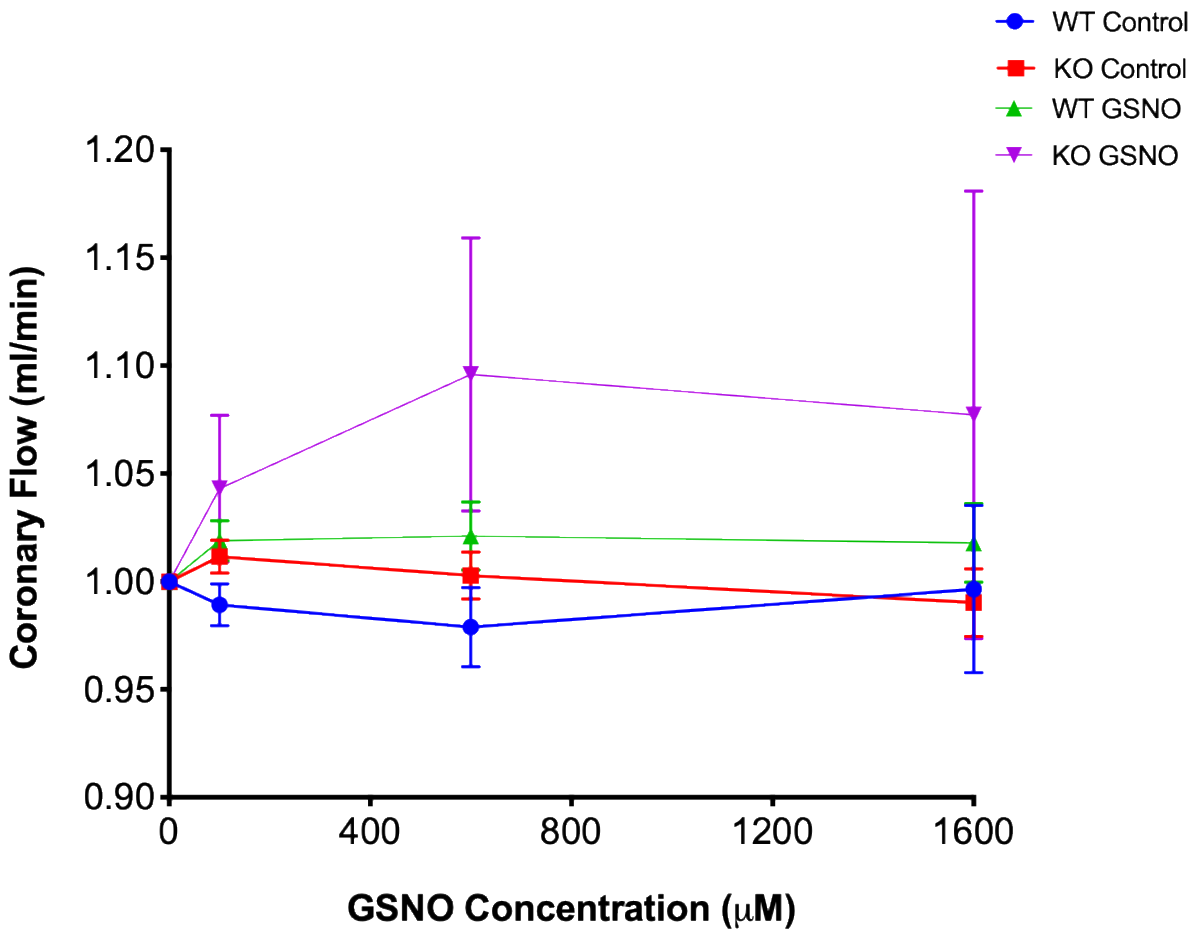

Figure B.6 Coronary flow during chronic GSNO treatment (100 µM, 600 µM and 1600 µM) in WT and KO mouse hearts Data are means ± SEM. WT Control, blue line, n = 6 hearts; WT GSNO, green, line, n = 7 hearts; KO Control, red line, n = 5 hearts; KO GSNO, purple line, n = 5 hearts. Two-way ANOVA (uncorrected Fisher's LSD test) was used to compare between groups.

APPENDIX C

C.1 Coronary flow in WT hearts during ISO treatment

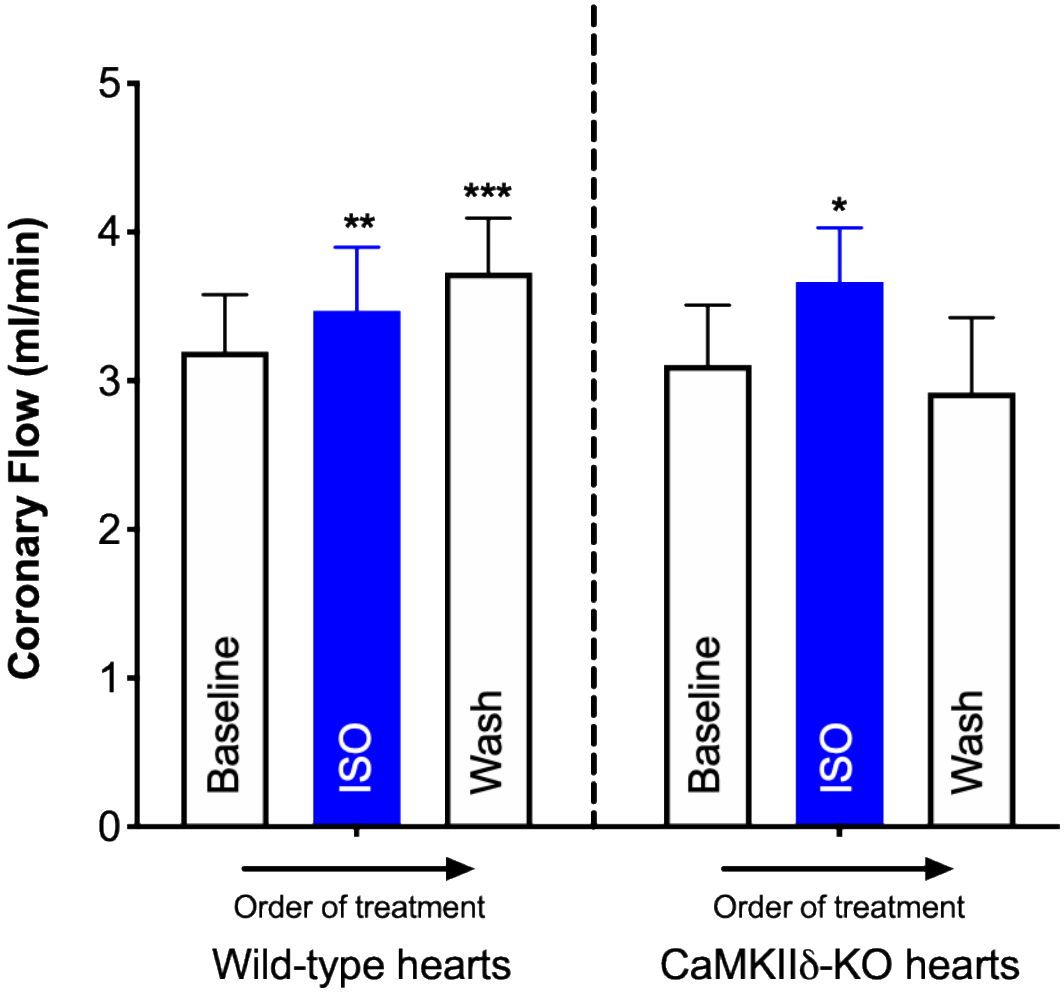

Figure C.1 Coronary flow during acute ISO treatment (100 nM) in WT and KO mouse hearts Data are means ± SEM. Order of treatment; left to right. ISO-GSNO, Wild-type hearts, n = 6, CaMKIIδ-KO hearts, n = 4. Two-way ANOVA (uncorrected Fisher's LSD test) was used to compare between groups: * = $p < 0.05$, ** = $p < 0.01$, *** = $p < 0.001$, * = Drug vs baseline.